

UNIVERSITY COLLEGE LONDON

**Exploiting Aerobic C–H Bond
Activation and the Synthetic Utility of
Acyl Hydrazides**

by

André Shamsabadi

A thesis submitted in partial fulfillment for the
degree of Doctor of Philosophy

in the
Faculty of Mathematical and Physical Sciences
Department of Chemistry

March 2020

Declaration of Authorship

I, André Shamsabadi, confirm that the work presented in this thesis is my own. Where information has been derived from other sources, I confirm that this has been indicated in the thesis.

André Shamsabadi

May 26, 2020

For mama, baba, avó and bibi

In loving memory of vovô and baba bozorg

“boa noite, shab bekheir”

Abstract

Faculty of Mathematical and Physical Sciences

Department of Chemistry

Doctor of Philosophy

by André Shamsabadi

This project is focused on two separate but correlated fields of research. The first segment describes chemical transformations that are initiated by the reaction of organic species with dioxygen in air as means to construct C–N bonds *via* radical addition. The second segment explores the untapped synthetic utility of acyl hydrazides in order to form further desirable moieties. Chapter 1 introduces important fundamental ideas central to the project and covers the background for the structure, generation and behaviour of radical entities and modern methods for C–H bond functionalisation reactions. Furthermore, the reaction behaviour of azodicarboxylate and acyl hydrazide moieties are explored. Chapter 2 describes C–H amination of ethereal compounds using azodicarboxylates as the nitrogen source and fluorinated alcohols as the reaction solvent. Reaction optimisation and mechanistic evaluation through NMR titration and theoretical analysis are discussed. Chapter 3 details the use of acyl hydrazides, obtained from aerobic-based hydroacylation of azodicarboxylates in high yields, in a one-pot synthesis of *N*-acyl carbamates. Reaction optimisation and substrate scope are covered. Chapter 4 reports a direct transformation of acyl hydrazides into 2-hydrazobenzophenones *via* a molecular rearrangement involving an aryne intermediate. The mechanism of the transformation is studied and evaluated. Furthermore, the corresponding products are amenable to further derivatisation to afford both 1*H*- and 2*H*-indazoles.

Impact Statement

The primary aim of this research project is to provide the results to influence a shift in the way aerobic oxidation is typically viewed and applied, *i.e.* from a nuisance reaction that requires the use of an inert atmosphere to suppress/avoid ‘oxidative degradation’ to how it can be utilised as a means to initiate relatively challenging bond formations. Through the trapping of intermediates present in the aerobic oxidation pathway of a particular molecule, a plethora of useful entities can be made in a ‘green’ and sustainable manner. Moreover, as aerobic oxidation of organic compounds is often initiated by a C–H bond breaking process, the development of reactions conditions that allow for effective use of air (or more specifically dioxygen in air) as a reagent concurrently contribute to an important and long-standing goal in organic chemistry — controlled C–H bond activation.

Previously, this method has been applied in the formation of a wide variety of unsymmetrical ketones and acyl hydrazides, both of which have been shown to have broad use in organic synthesis. In this thesis, the protocol is extended for the optimised C–N bond formation at the α -site of ethers. The conditions that were developed are in sharp contrast to previous conditions for established ethereal C–H bond transformations, which tend to use toxic/expensive transition metals, peroxides that require thermal or photochemical degradation, or additives that act as polarity reversal catalysts necessary for efficient reactions. Further to this, acyl hydrazides (readily accessible *via* the aerobically-initiated hydroacylation of azodicarboxylates) represent synthetically versatile scaffolds which have been of particular use in acyl donation reactions for the formation of esters, thioesters, amides and ketones. Herein, protocols have been developed for: (i) the metal-free ionic-rupture of the N–N bond in acyl hydrazides resulting in their facile transformation to *N*-acyl carbamates and (ii) the aryne-based formation of both *1H*- and *2H*-indazoles from acyl hydrazides. These products have significant use in pharmaceuticals and the developed methodologies to form these are achieved without the use of toxic/expensive transition metal species.

Acknowledgements

During my time at UCL I have always counted myself as extremely fortunate to have met so many great and talented people who not only have I had the pleasure to work with, but whom I can call close friends of mine which I cherish greatly. I entertain the idea that choosing my Masters and ultimately PhD project was the best decision of my life so far, and it is in no small part due to the support and friendship of my workmates at the KLB.

First and foremost, I owe an incredible debt of gratitude to my supervisor and mentor Prof. Vijay Chudasama, for allowing me the opportunity to partake in this research project, for the vast wealth of knowledge that he has supplied me with and for his unparalleled guidance with which I have been able to make significant progress as a chemist during my time in the laboratory. He has always been fully supportive of my ideas and has given me every possible opportunity to learn, explore, discover and adapt the project as I see fit. He is a man of pristine talent and ambition, and a force to be reckoned with.

I would also like to accredit many past and present members of The Chudasama Group:

Antoine Maruani is one of the smartest and most naturally-gifted human being I have ever encountered and probably ever will. Never have I met someone who not only has a passion to know and learn, but to excel in and master such a vast array of talents.

Max Lee is genuinely the funniest, most animated and down-to-Earth person I have ever met. His hard-working yet jovial attitude towards science and life is highly admirable and he was indispensable for the upkeep of my morale during his time in the lab.

Dan Richards has acted as a big brother figure and has always made an effort to look after me more than I tend to look after myself. He consistently filled the lab with the most infectious laugh which I could never tire of hearing.

Calise Bahou has stuck it out with me since day 1 and I could not have asked for a more remarkable labmate to have shared many challenges and adventures together. He is a fantastic lab partner and his loyalty and reliability is second to none. I only wish I could work beside him for the rest of my scientific career.

João Nogueira, meu irmão, has consistently encouraged me to break out of my comfort zone and has definitely taught me to enjoy life more. He has an unmatched zest for life and his love for exploration is a mark of not only a good scientist, but an exciting human being.

Marcos Fernández was always a calm and relaxed figure who has shared the undergraduate experience with me since 2012. I thank him for giving me a great many help with difficult NMR and MS assignments.

Faiza Javaid is someone who I can only give my greatest endearments to and I am so glad to have met her. A friend who I could easily share my thoughts with and would only be met with utmost support, empathy and enthusiasm. I cherish our friendship.

Péter Szijj is a person of untold potential. He is a master strategist and has a mind that is perfectly poised to excel in not only all the games I've had the delight to play with him, but to also pursue his goals in science. I also greatly respect his moral compass and truly believe in his ability to judge what is right.

Nehaal Ahmed has the most laid-back and placid demeanour, can seemingly and effortlessly lighten up any atmosphere and is an incredibly worthy adopter of this research project.

Richard Spears is undoubtedly the politest member of the group but nonetheless he is a filthy Peach main and thinks his gun is faster than my knife. He possesses the kindest heart and is a pleasant blend of both sporting and spirited.

Alex Furby has a cheerful, jaunty presence and is one part fun, two parts ruthless in competition. I admire his superior general knowledge and if I need him, I know exactly where to find him: Roots Hall.

Fabien Thoreau may be the newest member of the group, but has seamlessly integrated into the lab. He is incredibly wise and I wish him the very best for the future. I hope he enjoys his time at UCL just as much as I have.

The Chudasama Group has been humbled by some of the smartest, driven and most entertaining set of people I have had the absolute pleasure to work alongside.

I would like to extend my gratitude to all members of the KLB labs who have had no small part in making my PhD life so magical. Special mention has to go to Marco Sabatini, Archie Wall, Nafsika Forte, Rachel Szpara, Lula Salerno, Roshni Malde, Charlotte Coomber, Alina Chrzastek, Dave Chisholm, Muhammed Haque, Usman Shabbir, Yanbo Zhao and Peter Seavill, as well as past Master students: Jack Ren, Diogo da Silva and Andréa Poupard.

Outside of the laboratory, I would like to express my gratitude to my close friends and family for helping me accomplish what I have been able to up to this point. I would like to recognise Maya Rosenwasser, Eisha Jain, Azam Sheikh, Elly Mousley, Nick Shiers, Natan Janner-Klausner, Sina Abdolrazaghi and Faiza Ahmed for over a decade of support

and companionship. I would like to acknowledge my parents for providing me with the strongest of foundations in life and education, and for never failing to love me. And finally my sister Monika, who is without question, my favourite person in the entire world.

Finally, I also wish to extend my gratitude to my examiners, Prof. Stephen Marsden and Prof. Tom Sheppard, who have kindly accepted to read my thesis and carry out my *viva* examination.

"All men dream, but not equally. Those who dream by night in the dusty recesses of their minds, wake in the day to find that it was vanity: but the dreamers of the day are dangerous men, for they may act on their dreams with open eyes, to make them possible"

– T. E. Lawrence

Contents

Declaration of Authorship	i
Abstract	iii
Impact Statement	iv
Acknowledgements	v
Abbreviations	xi
1 Introduction	1
1.1 The Free Radical	1
1.1.1 History	1
1.1.2 Properties	2
1.1.2.1 Structure	2
1.1.2.2 Type & Stability	3
1.1.3 Formation of Free Radicals	5
1.1.3.1 Homolysis	5
1.1.3.2 Single Electron Transfer	5
1.1.4 Radical Processes	6
1.1.4.1 Unimolecular	6
1.1.4.2 Bimolecular	8
1.1.5 Chain Reactions	9
1.1.5.1 Initiation	11
1.1.5.2 Propagation	12
1.1.5.3 Termination	13
1.1.6 The Ethereal Radical	14
1.1.6.1 Generation of Ethereal Radicals	16
1.1.7 The Acyl Radical	16
1.1.7.1 Generation of Acyl Radicals	17
1.2 Dioxygen	20
1.2.1 Auto-oxidation	21
1.2.1.1 Aldehyde Auto-oxidation	23

1.3	C–H Bond Activation	24
1.4	Reactivity of Azodicarboxylates	25
1.4.1	Mitsunobu Reaction	26
1.4.2	Carboxylation Reaction	27
1.4.3	Azodicarboxylate as an Oxidant	28
1.4.4	Azodicarboxylate as an Electrophile	28
1.5	Hydroacylation <i>via</i> Aerobic C–H Bond Activation	31
1.6	Reactivity of Acyl Hydrazides	33
1.6.1	Acyl Donors	33
1.6.2	Functionalisation at the N–H bond	36
1.7	Aims	37
2	Exploiting Auto-oxidation of Ethers for C–N Bond Formation	39
2.1	Introduction	39
2.2	Optimisation	41
2.3	Scope	43
2.3.1	Azodicarboxylates	43
2.3.2	Cyclic Ethers	44
2.3.3	Acetals	46
2.3.4	Acyclic Ethers	47
2.4	Mechanistic Studies	48
2.4.1	NMR Titration	48
2.4.2	Theoretical Investigations	50
2.5	Formation of (protected) α -amino ethers	53
2.6	Further Context	54
2.7	Conclusions	56
3	Formation of <i>N</i>-Acyl Carbamates from Acyl Hydrazides	57
3.1	Introduction	57
3.2	Formation of Acyl Hydrazides	59
3.3	Initial Screening	61
3.4	Optimisation of <i>N</i> -Acyl Carbamate Formation	62
3.5	Substrate Scope	64
3.5.1	Aryl	64
3.5.2	Carbamate Groups	65
3.5.3	Alkyl	66
3.6	Conclusions	68
4	Formation of Indazoles from Acyl Hydrazides	69
4.1	Introduction	69
4.2	Initial Screening	71
4.3	Formation of Acyl Hydrazides	72
4.4	Examination of Carbamate Scope	74
4.5	Formation of 2-hydrazobenzophenones	75
4.6	Formation of 1 <i>H</i> -indazoles	77
4.7	Formation of 2 <i>H</i> -indazoles	79

4.8	Mechanistic Studies	81
4.9	Conclusions	83
5	Summary & Future Work	84
6	Experimental	87
6.1	Experimental for Chapter 2	89
6.2	Experimental for Chapter 3	101
6.3	Experimental for Chapter 4	133
	References	169

Abbreviations

Ac	Acetyl
ACS	American Chemical Society
AIBN	Azobisisobutyronitrile
aq.	Aqueous
BDE	Bond dissociation enthalpy
BHT	Butylated hydroxytoluene
Boc	<i>tert</i> -Butyloxycarbonyl
br.	Broad
Bu	Butyl
calcd	Calculated
CI	Chemical ionisation
cy	Cyclohexyl
d	Doublet
DCM	Dichloromethane
de	Diastereomeric excess
DEAD	Diethyl azodicarboxylate
DIAD	Diisopropyl azodicarboxylate
DMAD	Dimethyl azodicarboxylate
DMA	Dimethylacetamide

DMF	Dimethylformamide
DMSO	Dimethyl sulfoxide
EDG	Electron donating group
EI	Electron ionisation
eq.	Equivalents
ES	Electrospray
Et	Ethyl
EWG	Electron withdrawing group
HFIP	1,1,1,3,3,3-Hexafluoro-2-propanol
HRMS	High resolution mass spectrometry
<i>i</i> Bu	Isobutyl
<i>i</i> Pr	Isopropyl
IR	Infrared
<i>J</i>	Coupling constant
m	Multiplet
Me	Methyl
MO	Molecular orbital
MS	Mass spectrometry
NBS	<i>N</i> -Bromosuccinimide
NMR	Nuclear magnetic resonance
PFP	Pentafluorophenyl
Ph	Phenyl
Pr	Propyl
q	Quartet
s	Singlet

sat.	Saturated
SOMO	Singly occupied molecular orbital
t	Triplet
TBAT	Tetrabutylammonium difluorotriphenylsilicate
<i>t</i> Bu	<i>tert</i> -Butyl
TEMPO	(2,2,6,6-Tetramethylpiperidin-1-yl)oxyl
TFA	Trifluoroacetic acid
TFE	2,2,2-Trifluoroethanol
THF	Tetrahydrofuran
THP	Tetrahydropyran
TLC	Thin layer chromatography
TTMSS	Tris(trimethylsilyl)silane
UCL	University College London
UV	Ultraviolet
VSEPR	Valence shell electron pair repulsion

Chapter 1

Introduction

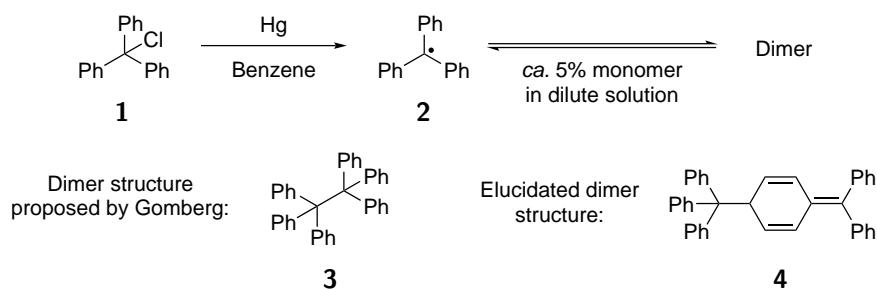
1.1 The Free Radical

The electronic configuration of atomic and molecular entities generally consists of paired electrons, either as bonding pairs or unshared electron pairs. Each pair consists of two electrons existing in opposite spin orientations; $\pm\frac{1}{2}$, in a single orbital as dictated by Pauli's exclusion principle. The term 'free radical' refers to a class of atoms or molecules that do not exhibit an electronic configuration consisting exclusively of electron pairs; as in, free radical species possess at least one unpaired valence electron. Radical entities are inherently paramagnetic and with a few exceptions, are regarded as transient and highly reactive. In contemporary methods of expressing chemical structures, equations and mechanisms, the unpaired electron is portrayed as a dot. In reaction mechanisms, the movement of a single electron is depicted with a single-headed arrow.

1.1.1 History

The modern understanding of the term 'radical' can be traced back to the start of the 20th century and is primarily credited to Moses Gomberg upon observation of the first instance of a trivalent carbon.¹ Gomberg proposed that the yellow colour produced following the introduction of mercury to a solution of chlorotriphenylmethane **1** in benzene was due to the presence of the tertiary triphenylmethyl radical **2**. Gomberg postulated that this

species existed in equilibrium with the desired dimer molecule hexaphenylethane **3**. The radical was indeed in equilibrium with its corresponding dimer species, but it was not until 1968 that the true nature of the triphenylmethyl radical dimer was deduced from NMR studies to be the ‘head-tail’ dimer **4** (Scheme 1.1).²



SCHEME 1.1: Formation of the triphenylmethyl radical **2** and its subsequent dimer.

The idea of trivalent carbon was initially met with scepticism, although more evidence to support Gomberg’s hypothesis arose with further reports of trivalent carbon in the early 20th century. In 1929, Paneth and Hofeditz provided evidence for the existence of the methyl radical³ and in 1934, Donald Hey proposed that the decomposition of benzoyl peroxide gave rise to free phenyl radicals.⁴ Eventually, free radical chemistry became better understood and, particularly in the modern day, has developed into a useful synthetic tool in organic synthesis.⁵

1.1.2 Properties

1.1.2.1 Structure

The structure of the simple methyl radical entity **5** can be rationalised *via* direct comparison to the methyl anion **6** and methyl cation **7** (Figure 1.1). The carbon atom in the methyl anion **6** possesses eight valence electrons, is sp^3 hybridised and in agreement with VSEPR theory, the structure assumes a tetrahedral geometry (bond angle = 109.5°). The methyl cation **7**, however, has six valence electrons, adopts sp^2 hybridisation and is therefore predicted and observed to be trigonal planar (bond angle = 120°).

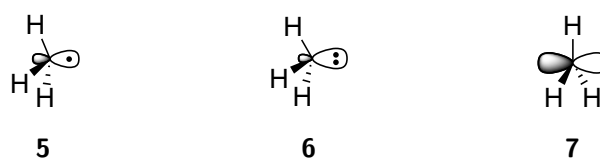


FIGURE 1.1: The shape of the methyl radical **5**, methyl anion **6** and methyl cation **7**.

The methyl radical **5**, consisting of seven valence electrons, can therefore be rationalised as adopting an intermediate structure between the methyl anion **6** and methyl cation **7**, where the structure has been denoted as quasi-trigonal planar.⁶ The barrier to pyramidal inversion of the methyl radical (Figure 1.2) and other carbon-centred radical species is shown to be experimentally minute (*ca.* $2.5 \text{ kJ}\cdot\text{mol}^{-1}$ measured experimentally for the *tert*-butyl radical),⁷ with rapid inversion observed even at extremely low temperatures.⁷ As a result, a radical generated at a chiral centre will normally result in the destruction of that chirality.

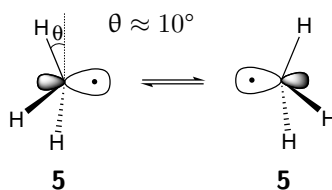


FIGURE 1.2: Inversion of the ‘shallow pyramid’ of the quasi-trigonal planar methyl radical **5**.

1.1.2.2 Type & Stability

There are two kinds of radicals: neutral and charged. Thus, radicals are found to be electronically neutral, anionic or cationic in character. Moreover, radicals can be further subcategorised into σ -type and π -type. This simply refers to the type of orbital the unpaired electron occupies, whether it be a σ -type or π -type orbital. The orbital in which the lone electron (hereby referred to as the ‘radical’) resides is termed the ‘SOMO’ (singly occupied molecular orbital). In a carbon-centred radical, the carbon atom on which the radical resides possesses seven electrons and is therefore one electron short of satisfying the octet rule. As such, the carbon centre can be thought of as electron-deficient. For π -type radicals, the stability of the subvalent entity increases as the radical centre becomes more substituted due to stabilising hyperconjugation interactions. Thus, akin to carbocation chemistry, tertiary radicals are generally more stable than secondary radicals which in

turn are more stable than primary radicals (Figure 1.3). This effect is not typically observed for σ -type radicals due to there being no such stabilising hyperconjugation effect, typically resulting in a comparatively more reactive entity.

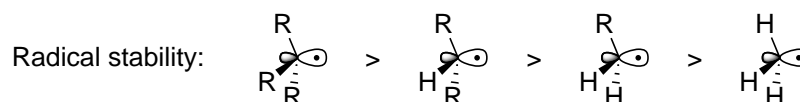


FIGURE 1.3: The relative stability of substituted carbon-centred radicals.

Radical species can also be stabilised by conjugation through electron-withdrawing groups (EWGs) due to the delocalisation of the unpaired electron over multiple atoms, or by neighbouring electron-donating groups (EDGs) where adjacent heteroatoms can donate electron density into the partially empty SOMO. The presence of EDGs and EWGs often has a secondary effect of altering the reactivity behaviour of the radical centre. Molecular orbital (MO) theory describes frontier orbital interactions about the radical and can be used to determine the reactivity behaviour of different radical species (Figure 1.4). EDGs adjacent to the radical centre increase the energy of the SOMO therefore creating a more nucleophilic radical whilst adjacent EWGs decrease the energy of the SOMO thereby generating a radical more electrophilic in nature.

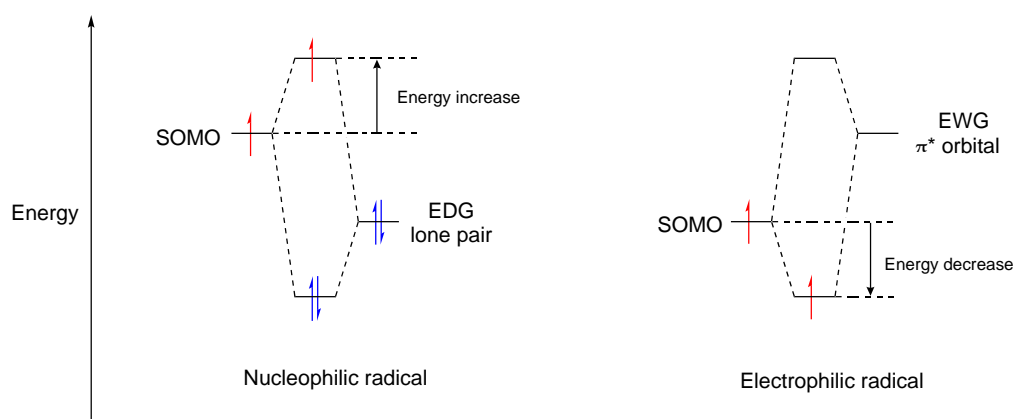
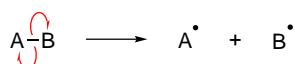


FIGURE 1.4: Molecular orbital diagram showing the electronic representation of a nucleophilic radical and an electrophilic radical.

1.1.3 Formation of Free Radicals

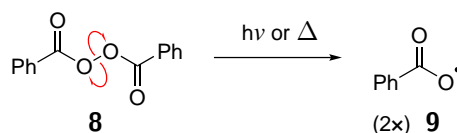
1.1.3.1 Homolysis

The symmetric cleavage of a covalent bond (shared pair of electrons) generates two radical species as one electron is given to each atom that formed the initial covalent bond (Scheme 1.2). An activation energy is required to carry out this bond cleavage and typically this energy is administered *via* thermal or photochemical methods.



SCHEME 1.2: General homolytic process, creating two radical species.

The amount of energy required to carry out covalent bond homolysis is termed the bond dissociation enthalpy (BDE). In stable organic molecules, the BDEs of covalent single bonds typically range from around 200 kJ·mol⁻¹ (C–I bonds) to over 400 kJ·mol⁻¹ (C–H bonds).⁸ Most of these bonds are deemed too strong to undergo homolysis at any appreciable rate at commonly employed reaction temperatures (-78 to 150 °C), though the use of UV light can initiate bond homolysis of relatively weak C–I bonds. As such, only bonds with low BDEs are useful for homolysis at synthetically-appropriate conditions.⁹ An example of a common radical initiator species used in laboratory reactions is benzoyl peroxide **8** where the low BDE of the O–O bond (*ca.* 142 kJ·mol⁻¹) means that homolysis of this bond and therefore the formation of free radical species **9** can be achieved at moderate operational temperatures (half-life of benzoyl peroxide is 1 h at 92 °C, Scheme 1.3).⁹

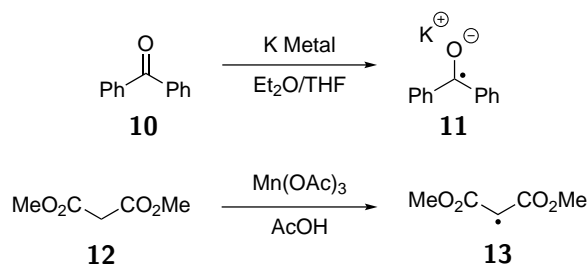


SCHEME 1.3: Homolytic cleavage of the O–O bond in benzoyl peroxide **8** to form radical species **9**.

1.1.3.2 Single Electron Transfer

An alternative method for generation of a radical from a spin-paired molecule is either the addition or removal of a single electron from a spin-paired molecular species (known

as reduction or oxidation respectively). An example of a reductive single electron transfer can be demonstrated *via* the reduction of benzophenone **10** with an alkali metal to form the ‘ketyl’ radical anion **11** (Scheme 1.4).¹⁰ A complementary example of an oxidative single electron transfer can be shown through the treatment of dimethyl malonate **12** with Mn(OAc)₃ salt to form electrophilic radical **13** (Scheme 1.4).¹¹



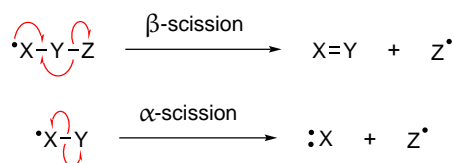
SCHEME 1.4: (Top) The formation of the ‘ketyl’ radical anion **11** from benzophenone **10**.¹⁰ (Bottom) The formation of radical species **13** from dimethyl malonate **12**.¹¹

1.1.4 Radical Processes

Generally, radical processes can be divided into two classes: unimolecular and bimolecular. The latter can be further subdivided into radical-molecule and radical-radical interactions. These will all be discussed in turn below.

1.1.4.1 Unimolecular

Unimolecular radical processes are characterised by the intramolecular fragmentation of a bond influenced by the presence of a lone electron. The two types of bond fragmentation processes are β -scission and α -scission, defined by the bond broken relative to the location of the initial radical (Scheme 1.5).



SCHEME 1.5: (Top) General β -scission process, resulting in formation of a new π -bond. (Bottom) General α -scission process, resulting in a species with a non-bonding lone pair of electrons.

β -Scission

β -Scission describes the cleavage of a σ -bond β - to the radical centre, resulting in the formation of a new π -bond. This step is thermodynamically favourable if the new π -bond is particularly strong and/or the σ -bond being broken is relatively weak. In a β -scission process, the new π -bond is formed from the unpaired electron and one of the electrons in the breaking σ -bond. Therefore, in a π -type radical, the singly occupied π -orbital must be in alignment with the σ -bond being broken. This effect is clearly demonstrated when comparing β -scission in acyclic and cyclic systems. In an acyclic molecule, unhindered rotation about a C–C single bond ensures good alignment of the relevant orbitals (Figure 1.5).

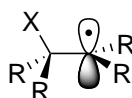
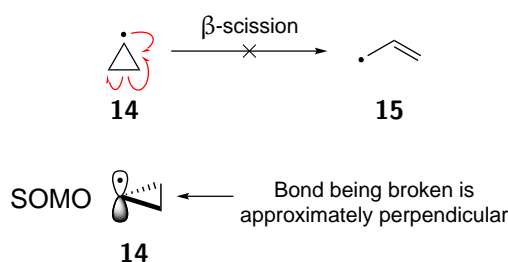


FIGURE 1.5: Example of an acyclic molecule in the ideal conformation for β -scission where the SOMO is aligned with the bond being broken (C–X bond).

In a cyclic system, however, the degree of orbital overlap will influence the feasibility of a β -scission pathway. Whilst the β -scission of cyclopropyl radical **14** to form allyl radical **15** is thermodynamically favourable due to the release of ring strain; the process however, occurs slowly due to the negligible overlap of the SOMO with the C–C σ^* -orbital (Scheme 1.6).



SCHEME 1.6: (Top) Inefficient β -scission of cyclopropyl radical **14**. (Bottom) Negligible overlap between SOMO and bond being broken in cyclopropyl radical **14**.

 α -Scission

α -Scission describes the process where the cleavage of a σ -bond α - to the radical centre is achieved. This is most commonly and significantly observed in the cleavage of acyl radicals **16** in a decarbonylation process, producing an alkyl radical **17** and carbon monoxide **18** as a by-product (Scheme 1.7). The rate of decarbonylation of acyl radicals

is correlated to the stability of the alkyl radical formed. In effect, the α -scission of acyl radical species occurs rapidly in the formation of tertiary radicals when compared to the formation of primary radicals.



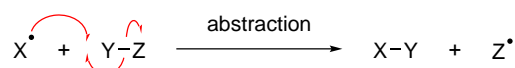
SCHEME 1.7: α -Scission of acyl radical **16** to form alkyl radical species **17** and carbon monoxide **18**.

1.1.4.2 Bimolecular

Bimolecular radical processes can either occur between a free radical and spin-paired molecular species or two free radical species.

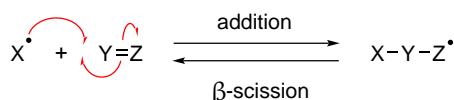
Radical-molecule interactions

The interaction between a free radical and a spin-paired entity can occur through either an abstraction or an addition process. Abstraction describes the process in which an atom (or, less commonly, a group of atoms) is transferred from a molecule to a radical (Scheme 1.8). As these reactions involve the breaking and formation of bonds, the process is normally governed by thermodynamics and proceeds best if the process is exothermic.



SCHEME 1.8: General radical abstraction process.

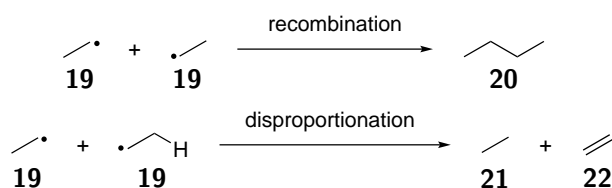
Radical addition reactions typically involve the combination of a radical with an unsaturated bond, thereby forming a new free radical adduct species. Mechanistically, the process is the reverse of β -scission (Scheme 1.9) and is therefore governed by the same stereo-electronic effects: the radical is formed with the SOMO and new σ -bond in the same plane.



SCHEME 1.9: A general radical addition process is the reverse of β -scission.

Radical-radical interactions

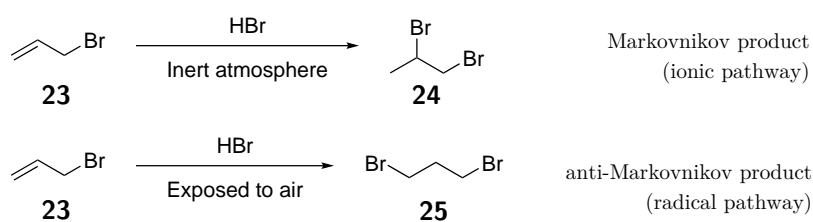
Radical-radical reactions often have very low activation energies and thus are intrinsically very fast – in solution, the rate of reaction is frequently diffusion-controlled. The interaction of two radical species can occur either by a recombination pathway to form a single spin-paired molecule, or *via* a disproportionation process to form two spin-paired species (Scheme 1.10). The two major factors which determine the relative rates of recombination and disproportionation are the number of C–H sites available β - to the radical centre (which governs rate of disproportionation) and the steric hindrance experienced about the radical centres (which governs rate of recombination).^{12,13}



SCHEME 1.10: The two possible termination processes (recombination and disproportionation) shown for the bimolecular reaction of ethyl radicals **19**.

1.1.5 Chain Reactions

Radical chain reaction processes can be a useful tool for the synthetic chemist. These reactions can be complementary to ionic reactions as alternative reaction pathways can be accessed that would not otherwise be achievable *via* an ionic route. In addition, there are several advantages of reactions proceeding through a radical pathway over an ionic pathway. Radicals are neutral species and as such are typically far less solvated than cations and anions and therefore, can operate in polar environments where ionic chemistry tends to fail.¹⁴ Radicals on the whole are also more tolerant of a different category of functional groups and therefore cumbersome protection-deprotection steps are often obviated.¹⁵ The first experimental example demonstrating the differing pathways offered by radical and ionic reactions was shown in 1933 where Kharasch observed the effect of different reaction conditions in the addition of HBr to allyl bromide **23**.¹⁶ Kharasch reported that the addition of HBr to allyl bromide formed both 1,2-dibromopropane **24** (Markovnikov product) and 1,3-dibromopropane **25** (anti-Markovnikov product) in varying quantities with various physical and chemical influences being reported to favour the formation of one product over the other (Scheme 1.11).



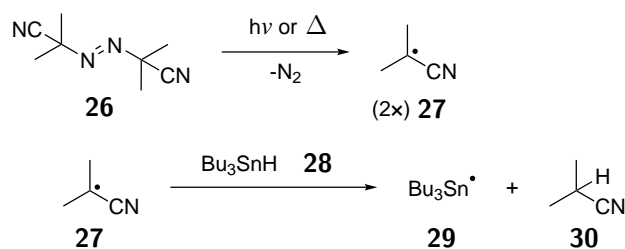
SCHEME 1.11: The addition of HBr to allyl bromide **23** showcasing an example of different reaction pathways that can be accessed by radical transformations compared to ionic transformations.

Kharasch proposed that the formation of the anti-Markovnikov product was due to the reaction proceeding *via* a radical addition chain process brought about by the presence of intervening peroxide species. Kharasch discovered that when the reaction was conducted *in vacuo* in the absence of any peroxide, the Markovnikov product was attained as the major product in a reaction that took 10 days to go to completion. However, when the reaction was exposed to air, under otherwise identical reaction conditions, the anti-Markovnikov product was formed as the major product with only 30 minutes required for complete consumption of alkene. Kharasch proposed that dioxygen in air was responsible for the *in situ* generation of trace amounts of peroxy species in the reaction mixture which would thereby initiate a radical chain reaction process generating the anti-Markovnikov product.¹⁶ He also observed that many other factors affected the yield and selectivity of the reaction such as temperature, solvent or light conditions. It was concluded that these factors had an influence on the properties of the reaction *via* directly effecting peroxides present in the reaction mixture.

The process describing the formation of the anti-Markovnikov product shown above would be described as a radical chain reaction. In a radical chain process, there are three distinct phases: initiation, propagation and termination. The manipulation of these phases can have a significant impact in the efficiency of radical-based reactions and as such, are important points of consideration in the development of efficient radical chain reaction methodologies. These are discussed in detail respectively.

1.1.5.1 Initiation

Radical chain reactions usually start with the formation of a free radical (Chapter 1.1.3). In a chemical reaction, this is commonly achieved by the inclusion of an initiator species where thermal, photochemical or sonochemical degradation of the radical initiator species triggers the formation of radicals and therefore the start of a chain reaction.¹⁷ Radical initiator species come with a temperature dependant half-life and ideally, a radical initiator is used at an operating temperature in which the half-life is of an approximate time of the reaction duration, ensuring a consistent release of free radical species throughout the reaction.¹⁷ Azobisisobutyronitrile **26** (AIBN) is a commonly used radical initiator and exhibits many advantages over other initiators. It can be activated by either thermal or photochemical methods, it is safer to handle than many peroxides (*e.g.* benzoyl peroxide)¹⁸ and it can be activated at relatively low temperatures compared with most peroxides.¹⁷ The major drawback of AIBN is the low reactivity of the produced 2-cyano-2-propyl radical species **27**, which will generally only initiate homolytic cleavage of relatively weak bonds.¹⁷ For this reason, AIBN is commonly used in conjunction with tributyltin hydride **28** (Bu_3SnH) where the cleavage of the weak Sn–H bond is achieved by radical species **27** to form a tin-centred radical **29** (Scheme 1.12), which is used for the selective cleavage of C–X (X= Cl, Br, I) bonds commonly found in organic molecules (Sn–halogen bonds are relatively strong compared to Sn–C bonds, and therefore the tin-centred radical is unlikely to participate in unwanted addition reactions to unsaturated C=C bonds).

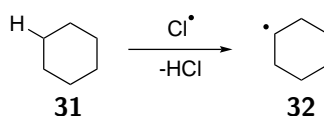


SCHEME 1.12: Photochemical or thermal degradation of AIBN **26** to produce radical species **27** followed by abstraction of an H atom from tributyltin hydride **28** affords tin-centred radical **29** and volatile isobutyronitrile **30**.

Having multiple methods of initiating radical processes is useful as a reaction may be sensitive to certain light or high temperature conditions. In particular, tributyltin hydride can also be used as a standalone radical initiator where it has been observed that sonochemical degradation of the Sn–H bond at room temperature generates the tin-based radical **29**.¹⁹ Whilst tributyltin hydride has established itself as a robust and reliable compound for the initiation of radical chain reactions, it is important to note that tin and organotin compounds typically exhibit high toxicity and require specialised disposal methods. As such, alternative methods of achieving radical initiation that forgo the use of tributyltin hydride are highly desirable and this is a key theme in this thesis.

1.1.5.2 Propagation

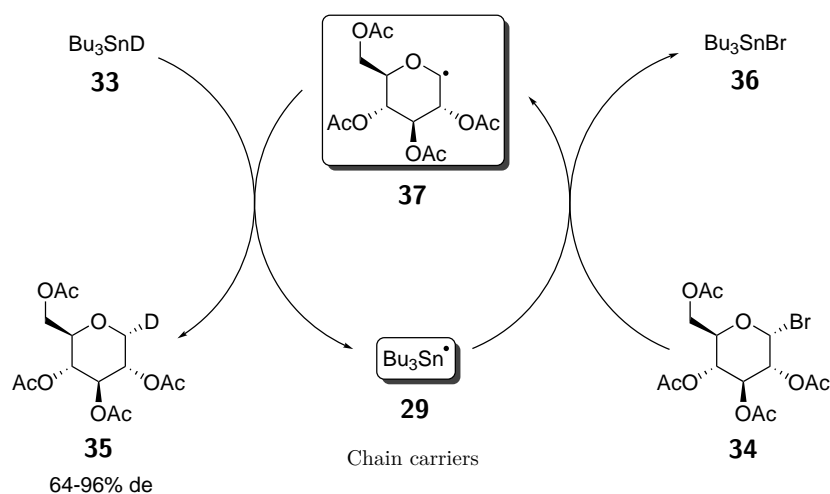
In propagation steps, elementary reactions are repeated numerous times in a cyclic fashion. There is no net increase or decrease in the number of radical species during a propagation step (Scheme 1.13).



SCHEME 1.13: Demonstration of a propagation reaction where abstraction of an H atom from cyclohexane **31** is achieved by a chlorine radical to afford cyclohexyl radical **32**.

Radical chain processes require a propagation cycle. A typical cycle consists of two sets of propagation reactions repeating alternatively until the starting material is exhausted or competing termination pathways prevail. The chain carriers continuously regenerate themselves through reaction with starting materials, driving the formation of the product from starting materials. An example of a propagation cycle is shown below (Scheme 1.14) where tributyltin deuteride **33** is used to dehalogenate D-glucopyranosyl bromide **34** at the anomeric position to form D-glucopyranosyl deuteride **35** and tributyltin bromide **36**.²⁰ In the propagation phase of this reaction, the glucosyl radical **37** and tributyltin radical **29** demonstrate ‘disciplined’ reactivity.²¹ The glucosyl radical **37** will favourably only abstract deuterium from the weak Sn–D bond in tributyltin deuteride **33**, whilst the tributyltin radical **29** will prefer to abstract the halogen atom from glucosyl bromide **34** to form the comparatively strong Sn–Br bond. It is this kind of discriminatory reactivity

that can allow radical chain reactions to exhibit great chemo- and regioselectivity and has contributed significantly to the established use of radical chemistry reactions in modern day synthesis.



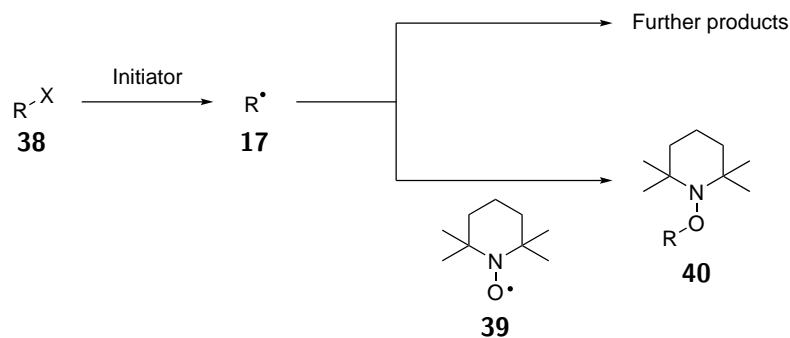
SCHEME 1.14: A propagation cycle for the dehalogenation of D-glucopyranosyl bromide **34** using tributyltin deuteride **33**.

1.1.5.3 Termination

Termination of a radical chain reaction comes about when an alternative reaction pathway involving one of the chain carriers in a propagation cycle occurs, thereby preventing the participation of the radical species in further propagation steps. The most common method of radical termination involves the interaction of two radical species in either a combination or disproportionation pathway (Chapter 1.1.4.2). Radical chain termination is often a diffusion-controlled process in solution. For this reason, to limit undesired radical chain termination, radical chemistry reactions are designed to limit the quantity of free radical species existing at any single time point.^{22,23} To achieve this, factors taking into account radical initiator half-lives, dilute reaction solutions and dropwise addition of the initiator to the reaction mixture are often considered.²³ If a reaction is not conducted under an inert atmosphere, dioxygen in the air may interact with an intermediate radical in a chain reaction, forming a peroxy radical and effectively removing the species from the cycle.

Intentionally-induced radical termination can be utilised to great effect in determining if a reaction mechanism indeed proceeds *via* a radical-mediated pathway. Radical scavengers

such as (2,2,6,6-tetramethylpiperidin-1-yl)oxyl (TEMPO) **39** take advantage of the low energy barrier involving radical-radical interactions to purposely access a recombination pathway where characterisation of TEMPO-adduct species **40** can help determine the identity of any reaction intermediate radical species **17** (Scheme 1.15). The observation of a TEMPO-adduct species or the inhibition of a reaction upon use of radical scavengers are common identifiers of a reaction proceeding *via* a radical pathway.



SCHEME 1.15: The trapping of a radical intermediate **17** using TEMPO **39**.

1.1.6 The Ethereal Radical

The ethereal radical features predominantly in the work presented in this thesis (Chapter 2) and this is discussed in detail below. Broadly, ethereal radicals can refer to any ether species in which there exists a radical centre. Experimentally, however, ethereal radicals refer to species in which a radical exists on a carbon atom α - to the oxygen atom in ethers. This is because the α -ethereal radical is the experimentally viable radical that can be accessed. This is shown theoretically for cyclic ether tetrahydrofuran (THF) **41** in which the bond dissociation energy (BDE) of the α -C-H bond is calculated to be *ca.* 390 kJ·mol⁻¹ whereas the BDE for the β -C-H bond is calculated at *ca.* 410 kJ·mol⁻¹ (Figure 1.6).²⁴ Despite the β -furanly radical **43** existing adjacent to two -CH₂- groups and therefore experiencing a higher degree of hyperconjugation compared to the α -furanly radical **42**, the SOMO is too far away from the oxygen lone pairs to participate in efficient electronic delocalisation over the radical centre. As a consequence, when it comes to logistically forming furanyl radical species, and by extension ethereal radical species, the radical is observed on the carbon atom α - to the oxygen atom.

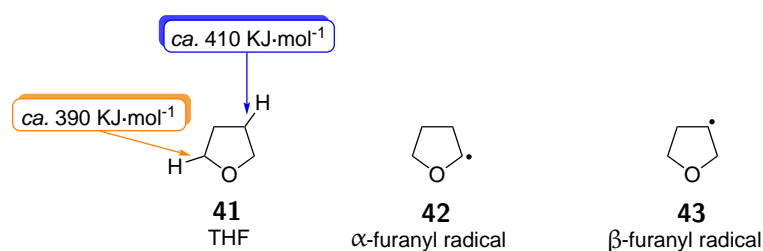


FIGURE 1.6: Structure of THF **41**, α -furanyl radical **42** and β -furanyl radical **43**.

The formation of the α -furanyl radical **42** has been experimentally observed to be consistent with a shortening of the C–O bond length,²⁴ providing evidence for the electronic delocalisation of the oxygen lone pair with the SOMO. According to MO theory, the effect of electronic donation of the oxygen lone pairs to the adjacent SOMO in α -radical species renders these radicals nucleophilic in behaviour and thus α -etheral radicals are excellent candidates for reaction with electrophilic entities.

It is important to note that the BDE of α -C–H bonds can vary significantly between various ethers and acetals (Figure 1.7).²⁵ Tertiary C–H bonds (as present in 2-methyltetrahydrofuran) typically have a lower BDE due to increased stability of the formed radical through hyperconjugation effects. Similarly, the presence of neighbouring phenyl groups (as present in dibenzyl ether) can also stabilise a radical due to conjugation of the radical with the π -system. Also of note is that cyclic ethers typically have a lower BDE compared to acyclic ethers. This is to be expected as the ‘locked’ configuration of the ring system on which an α -etheral radical lies results in a constant maximal overlap of the oxygen lone pair with the SOMO, as opposed to acyclic ethers where there are greater rotational degrees of freedom.

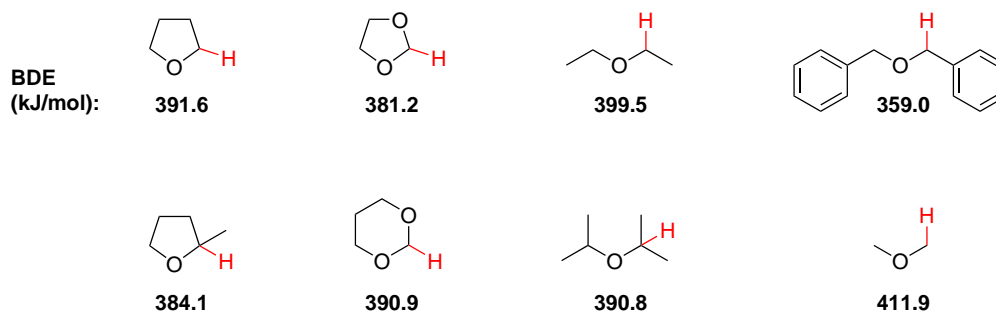


FIGURE 1.7: Mean BDE of α -C–H bonds in common ethers and acetals determined from kinetic data.²⁵

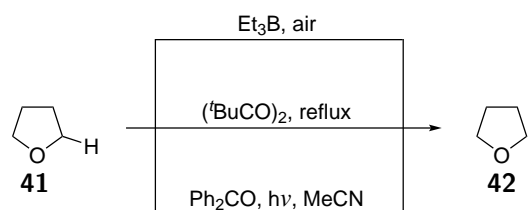
1.1.6.1 Generation of Ethereal Radicals

Ethereal radicals are commonly generated through C–H activation processes. The typical functionality required for efficient radical formation in organic molecules (weak C–X bonds, X = Cl, Br, I) is not observed to be stable α - to the oxygen atom in ethers due to facile elimination to form the oxocarbenium cation (Scheme 1.16).



SCHEME 1.16: Facile elimination of α -halo functionality in ethers to form an oxocarbenium cation **45**.

Thus, C–H abstraction processes are typically employed to access ethereal radicals. The relatively low BDE to access α -ethereal radicals allows the use of many commonly-employed radical initiation methods to access the α -ethereal radical (Scheme 1.17).^{26–28}



SCHEME 1.17: Typically employed methods to access α -ethereal radicals *via* C–H bond homolysis.

1.1.7 The Acyl Radical

Also of significant interest to this thesis, the acyl radical will be discussed in detail below. An acyl radical **16** describes a type of free radical in which the unpaired electron is situated at the carbon atom of a carbonyl group. The geometry of the radical has been theoretically and experimentally established to be bent with the unpaired electron residing in an orbital with significant $2s$ character; it is therefore characterised as a σ -type radical (Figure 1.8).²⁹

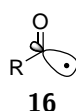


FIGURE 1.8: The acyl radical **16** showing the SOMO with substantial $2s$ character.²⁹

Unlike the varied bond dissociation energies of the α -C–H in ethers, experimental analysis has shown that the RC(O)–H bond dissociation energies for a range of aldehyde motifs (alkyl, vinyl and aryl) are very consistent.^{29–32} This is to be expected considering the proposed σ -type nature of the acyl radical which implies that any delocalisation of the unpaired electron with an adjacent vinyl or aryl system would be insignificant to non-existent. This suggests that the formation of any acyl radical **16** from the corresponding aldehyde should have a similar thermodynamic barrier since the bond dissociation energy is virtually independent of the R group (Figure 1.9).³³

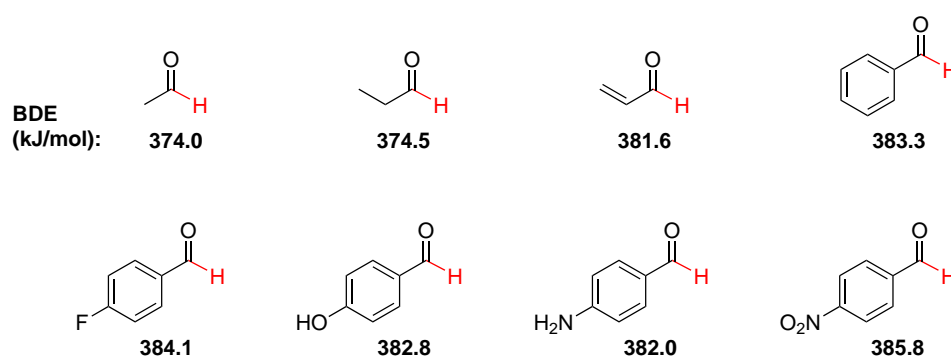


FIGURE 1.9: Theoretical calculations of BDE of aldehydic C–H bonds in common aldehydes.³³

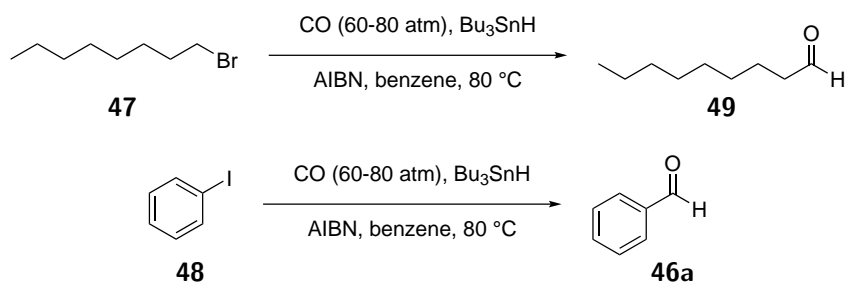
Molecular orbital theory predicts that the presence of the lone pairs on the oxygen atom adjacent to the radical centre would cause the acyl radical to be nucleophilic in nature (Chapter 1.1.3) and will therefore interact favourably with electrophilic entities. Evidence for this interaction between the carbonyl oxygen lone pairs and the SOMO in acyl radicals comes from infrared (IR) spectroscopy. The stretching frequencies of the C=O bond in acyl radicals are larger than that observed in their corresponding aldehydes and this implies some triple bond character between the carbon and oxygen atoms.³⁴

1.1.7.1 Generation of Acyl Radicals

Carbonylation of alkyl and aryl radicals

In 1990, Ryu *et al.* reported the formation of acyl radicals *via* the carbonylation of alkyl or aryl radicals under a high pressure of carbon monoxide.³⁵ Thus, carbonyl functionality could be introduced from aryl and alkyl halide precursors. It was demonstrated that dehalogenation of *n*-octyl bromide **47** and iodobenzene **48** through the use of AIBN/Bu₃SnH

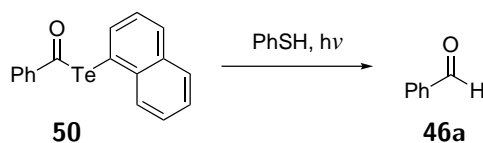
followed by carbonylation through the use of a high pressure (60-80 atm) of carbon monoxide gave access to acyl radical intermediates. A subsequent H-abstraction process would then generate the corresponding aldehydes (Scheme 1.18). Ryu and co-workers established that the administered pressure of carbon monoxide and relative equivalency of tributyltin hydride played a significant role in the success of trapping the alkyl and acyl radicals with carbon monoxide, which was found to compete with the simple dehalogenation of the starting alkyl or aryl halide species. Thus, a higher pressure of CO and higher equivalency of Bu_3SnH was necessary for efficient carbonylation. Subsequent radical carbonylation studies found that substituting Bu_3SnH with TTMSS (tris(trimethylsilyl)silane) resulted in a slower generation of alkyl radicals, thus resulting in efficient carbonylation of alkyl radicals at even lower reaction pressures of CO (15-30 atm).³⁶ Furthermore, catalytic Ph_3GeH has also been employed as an alternative radical initiator to Bu_3SnH , although both high pressures of CO (*ca.* 95 atm) and high temperatures (105 °C) were required.³⁷



SCHEME 1.18: The formation of aldehydes **49** & **46a** by trapping acyl radicals formed from the carbonylation of alkyl halide **47** (top) or aryl halide **48** (bottom), respectively.

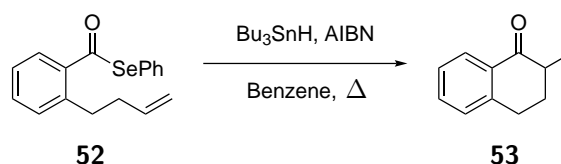
Acyl radicals from chalcogen-esters

Chalcogen (*viz.* tellurium, selenium & sulfur) carboxylate compounds have also been successfully employed as precursors to acyl radicals. Telluroesters have been recognised as an excellent source of acyl radicals upon photolysis with a 250 W tungsten lamp, or *via* thermal decomposition (refluxing benzene).³⁸ Evidence for the formation of acyl radicals is shown in the efficient trapping of the supposed radical species with TEMPO, diphenyl disulfide and diphenyl diselenide resulting in their respective adduct-species. Similarly, benzaldehyde **46a** can be formed on photolysis of aryl acyl telluride species **50** in the presence of thiophenol for efficient H abstraction (Scheme 1.19).³⁸



SCHEME 1.19: The formation of benzaldehyde **51** by trapping the acyl radical formed from the photolytic cleavage of telluroester **50**.

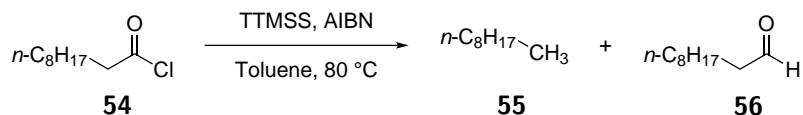
Similarly, selenoesters and thioesters can also be used as acyl radical precursors.³⁹ Selenoesters are typically preferred due to the weaker carbon-selenium bond allowing for a more efficient generation of acyl radicals.⁴⁰ Boger *et al.* have exploited this chemistry to achieve intramolecular cyclisation *via* acyl radical intermediates to generate ring structures of various sizes. As an example, the acyl radical formed when selenoester **52** is treated with AIBN and Bu₃SnH undergoes an intramolecular radical cyclisation to form tetralone **53** (Scheme 1.20).⁴¹



SCHEME 1.20: The intramolecular cyclisation of selenoester **52** *via* an acyl radical intermediate to form tetralone **53**.

Acyl radicals from acyl chlorides

In 1992, Chatgililoglu *et al.* reported the generation of acyl radicals from common acyl chloride starting materials upon subjection to TTMSS and AIBN at elevated temperatures.⁴² The group observed that treatment of acid chloride **54** to TTMSS and AIBN at 80 °C in the absence of a radical trap led to a mixture of fully reduced alkane **55** and aldehyde **56** (Scheme 1.21). This indicates the formation of an intermediate acyl radical, which either undergoes an intermolecular abstraction of an H atom to give aldehyde **56**, or an α -scission process to form an alkyl radical where subsequent H-abstraction gives alkane **55**. In a control reaction, no transformation of the acyl chloride was observed in the absence of AIBN.



SCHEME 1.21: The formation of acyl radical reaction intermediate upon treatment of acyl chloride **54** with TTMSS and AIBN at high temperatures.

1.2 Dioxygen

Understanding the radical characteristics of dioxygen is important for this research project where dioxygen (molecular oxygen) will feature significantly. It is well understood that the composition of air consists of 20.94% dioxygen (by volume).⁴³ Dioxygen can exist in either the singlet ($^1\text{O}_2$) or triplet ($^3\text{O}_2$) spectroscopic state. The triplet state is the ground energy state of dioxygen and its electronic configuration consists of two unpaired electrons (Figure 1.10).⁴⁴ As a consequence, triplet dioxygen is termed a 'biradical' and the unpaired electrons inhabit two degenerate SOMOs.

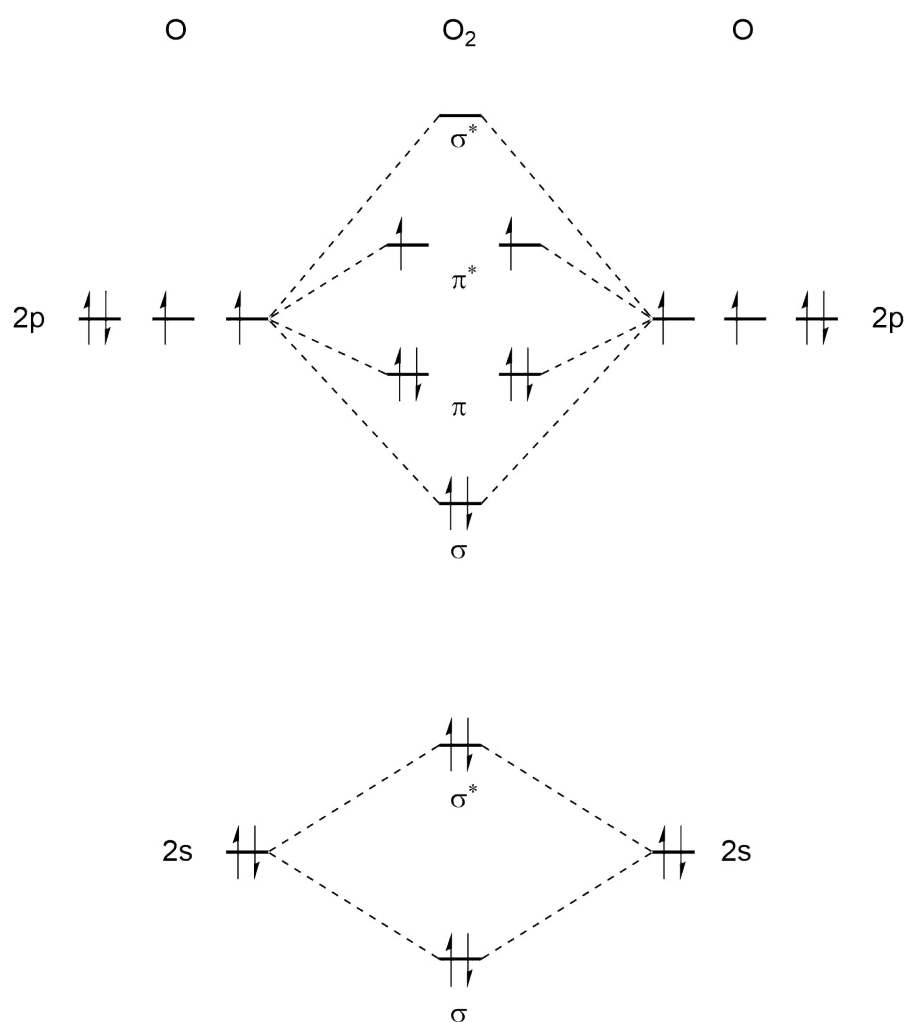


FIGURE 1.10: Molecular orbital diagram depicting the biradical nature of triplet dioxygen ($^3\text{O}_2$).

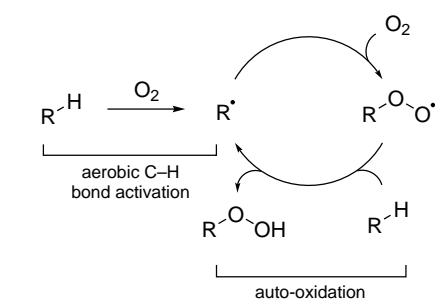
The singlet state of dioxygen is of a higher energy state with all its electrons paired (electron repulsion experienced by electrons occupying the same orbital is termed 'spin

pairing energy' and is responsible for the higher energy on the singlet state), meaning there is no SOMO present. As such, singlet dioxygen exhibits a different reactivity profile when compared to triplet dioxygen and can participate in reactions that triplet dioxygen cannot, *e.g.* Diels-Alder type reactions where singlet dioxygen acts as an excellent dieneophile.^{44,45} This type of reactivity is a primary cause for the oxidative degradation of lipids in food ('ene'-type reactivity involving unsaturated C=C bonds) where singlet oxygen is shown to be at least 1450 times more effective than triplet oxygen in the oxidation of linoleic acid.⁴⁶ It is therefore important to note that whilst atmospheric dioxygen is primarily composed of triplet oxygen (triplet oxygen is *ca.* 95 kJ·mol⁻¹ lower in energy than singlet oxygen),⁴⁷ singlet oxygen is consistently produced through photosensitisation with atmospheric pollutants (typically polycyclic aromatic hydrocarbons such as anthracene and chrysene) and UV photon absorption.^{47,48}

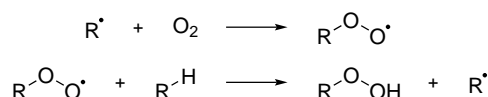
Dioxygen can also interact with a carbon-centred radical to give a peroxy radical.⁴⁵ As hypothesised in experiments conducted by Kharasch (Chapter 1.1.5),¹⁶ abstraction of a H atom by a peroxy radical can bring about the start of a chain reaction. In the same principle, the addition of dioxygen to a carbon-centred radical acting as a chain carrier in a propagation cycle is likely to terminate the reaction sequence as the peroxy radical formed will not participate in the desired reaction sequence and may participate in alternative reaction pathways (Chapter 1.1.5.3). As such, many radical reactions are conducted under an inert atmosphere to prevent the interference of atmospheric dioxygen with intermediates in radical pathways.

1.2.1 Auto-oxidation

The auto-oxidation process describes the autocatalytic oxidation of organic or inorganic systems. For organic systems, it is usually used to describe the propagation reactions in a chain reaction cycle in which carbon radicals couple with dioxygen to form peroxy radical species, which in turn can then abstract H atoms to form a peroxide product and regenerate further carbon radicals (Scheme 1.22). In these radical chain oxidation reactions, the initial activation of a C-H bond is typically achieved through the use of a radical initiator or UV light.



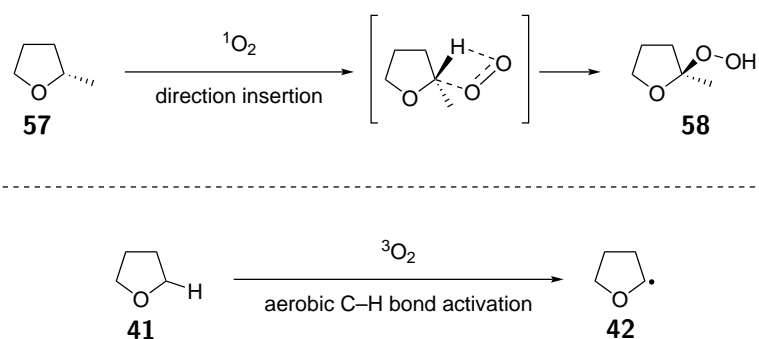
Propagation steps:



SCHEME 1.22: (Top) General radical-based dioxxygen-initiated auto-oxidation pathway. (Bottom) Propagation steps in an auto-oxidation process.

A rare but intriguing discussion regarding auto-oxidation events is the observation that dioxxygen can directly interact with certain C–H bonds to generate carbon radicals without the apparent use of any radical initiating species.⁴⁹ The C–H bonds observed to be susceptible to dioxxygen-induced homolysis are often those with low BDE (*e.g.* α -C–H bonds in ethers, aldehydic C–H bonds).

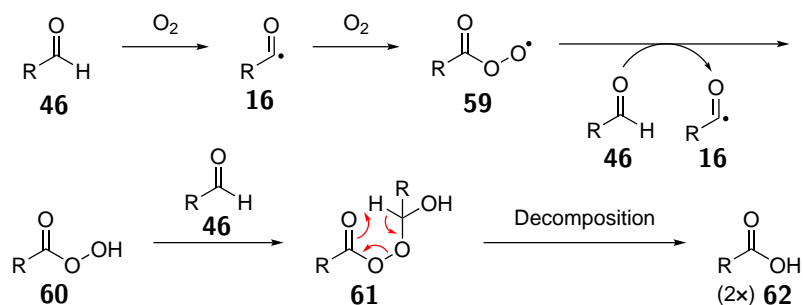
Surprisingly, the mechanism for this aerobic C–H bond activation pathway has been scarcely studied. Whilst a multitude of research groups have specifically analysed the auto-oxidation propagation reactions of organic radicals with dioxxygen, investigations into the initial interaction of a C–H bond with dioxxygen to form a radical species has generally been viewed as an afterthought. In 2017, pioneering work by Hwang and Su investigated specifically the interaction of singlet oxygen with α -C–H bonds in ethers.⁵⁰ A mechanistic study utilising enantiopure (*S*)-2-methyltetrahydrofuran **57** resulted in the formation of hydroperoxide product **58** with minimal loss of enantiomeric purity. This led the authors to suggest a direct insertion pathway of singlet oxygen into the C–H bond (Scheme 1.23), with no formation of any intermediate species. This was intriguing as, up to this point, the direct interaction of C–H bonds with dioxxygen was assumed to always occur *via* a radical pathway. Owing to the fact that no radical intermediates was observed in the direct insertion pathway of singlet oxygen into C–H bonds, it was therefore suggested that triplet oxygen is likely to be responsible for the formation of organic radical species observed in the alternative auto-oxidation pathway (Scheme 1.22),⁵⁰ initiated *via* a H-abstraction process (Scheme 1.23).



SCHEME 1.23: (Top) Proposed pathway for the direction insertion of singlet dioxygen into the (*S*)-2-methyltetrahydrofuran **57** to form (*R*)-2-hydroperoxy-2-methyltetrahydrofuran **58**.⁵⁰ (Bottom) Suggested pathway for ethereal radical formation *via* interaction of C–H bond with triplet dioxygen.

1.2.1.1 Aldehyde Auto-oxidation

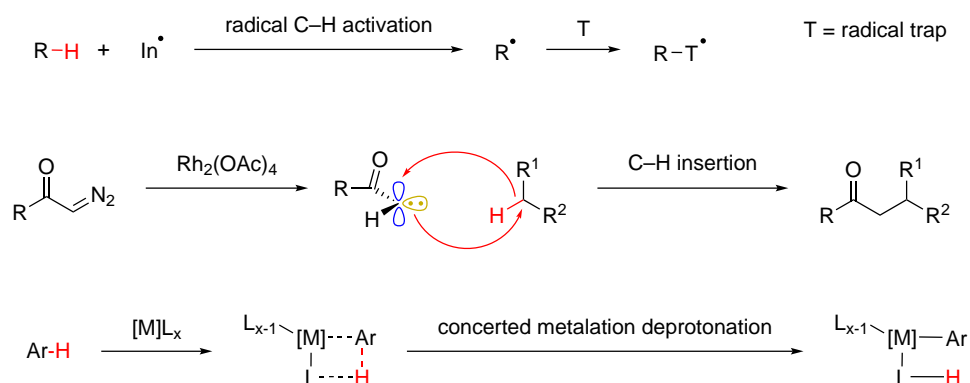
The aldehyde auto-oxidation process differs from typical auto-oxidation pathways (in which the final product is a peroxy species) as the final product observed is in fact the stable corresponding carboxylic acid. Mechanistically, dioxygen triggers homolysis of the aldehydic C–H bond. This generates an acyl radical **16** intermediate which in the absence of alternative reaction pathways will interact with another molecule of dioxygen to form a peracyl radical **59**. This peracyl radical will then abstract an aldehydic hydrogen atom from another aldehyde species **46** forming the peroxy acid **60** and generating another acyl radical **16**, thereby providing the auto-catalytic nature of this process. The formed peroxy acid will subsequently interact with another instance of aldehyde **46** to form an unstable intermediate **61** (known as the Criegee intermediate), which will fragment to generate two molecules of carboxylic acid **62** (Scheme 1.24).⁵¹



SCHEME 1.24: The proposed mechanism for the aldehyde auto-oxidation process.

1.3 C–H Bond Activation

Direct C–H bond activation has long been credited as the ‘holy grail’ of organic chemistry.⁵² The concept of discriminatively activating what is typically an inert C–H bond is a fundamentally powerful tool in synthesis for a number of reasons: (i) C–H bonds are ubiquitous in organic molecules, (ii) C–H bond functionalisation processes typically reduce the amount of transformations in multi-step syntheses which can consist of long and laborious protection-deprotection sequences, (iii) it establishes an ideal transformation regarding atom economy and waste minimisation when compared to classic cross-coupling reactions (*e.g.* Negishi coupling, Suzuki coupling, etc.). Over the past few decades, great strides have been made in the development of elegant C–H bond activation methodologies which has seen the process turn from being an aspirational idea to a commonplace reaction that is now heavily studied⁵³ and used in both academia and industry.^{54,55} Modern C–H functionalisation reactions are carried out through (i) C–H bond homolysis *via* SET (single electron transfer) processes normally involving radical initiators or first-row transition metal species followed by radical functionalisation, (ii) C–H insertion through use of singlet carbenes or nitrenes, or (iii) metallic C–H activation *via* a C–metal intermediate by way of σ -bond metathesis, concerted metalation deprotonation, and oxidative addition (Scheme 1.25).



SCHEME 1.25: General methods for the activation of C–H bonds.

Unfortunately, each protocol often utilises harsh reagents or additives to activate what is otherwise a typically unreactive C–H bond. Owing to the ever-increasing popularity and widespread usage of C–H activation processes, there is significant pressure to improve the sustainability of C–H reactions from an environmental standpoint: radical initiators are generally toxic or shock sensitive, nitrenes and carbenes are high-energy materials that

require intricate and heavily-monitored reaction conditions and organometallic C–H bond activation often requires the use of precious metals and stoichiometric amounts of oxidants (*e.g.* MnO₂). Indeed, it has been highlighted recently by the ACS Green Chemistry Institute® Pharmaceutical Roundtable that C–H activation processes utilising green oxidants whilst giving predictable site-selectivities is one of the top three research areas that would benefit from improvements in process ‘greenness’.⁵⁶ To achieve this, chemists have created increasingly elegant and boundary-pushing ideas for organometallic C–H bond activation including catalysis by Earth-abundant metals (*e.g.* iron,⁵⁷ copper⁵⁸) or forgoing the use of metals altogether.⁵⁹ In the goal for effectively using greener and milder oxidants, recent advances have been achieved in using arguably the most sustainable oxidant: dioxygen.⁴⁹ As discussed earlier (Chapter 1.2.1), dioxygen (especially pertaining to atmospheric dioxygen) is abundant, freely accessible and has been under-exploited in its ability to initiate C–H bond homolysis. Whilst process chemists have previously utilised an essentially free reagent (air) in the homogenous catalytic oxidation of organic and inorganic compounds, the use of dioxygen has very rarely been used as the focal point for C–H bond activation.

It should be appreciated that this aerobically-based C–H bond activation pathway of organic compounds offers a unique opportunity for the clean and simple access to radical species without the use of any potentially undesirable metal reagents or initiator species. The development of reactions conditions that allow for effective use of air (or more specifically dioxygen in air) as a reagent would therefore contribute to the long-standing goal of achieving controlled C–H bond activation whilst utilising a mild and sustainable oxidant. It is unfortunate that the majority of research exploring auto-oxidation and the interaction of organic molecules with dioxygen has resulted in methods to suppress the process rather than utilise it as a means to achieve discriminate C–H functionalisation.

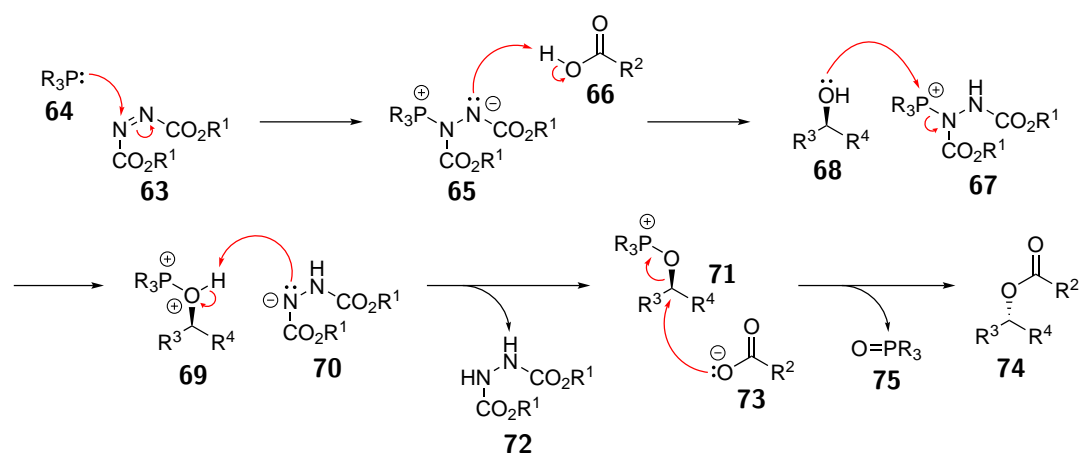
1.4 Reactivity of Azodicarboxylates

Azodicarboxylates are compounds consisting of an unsaturated N=N bond in which each N atom is directly bonded to a carboxylate group. These azo species exhibit unique structural and electronic properties which have allowed them to find use as reagents in many desirable transformations (*vide supra*).⁶⁰ Azodicarboxylates feature heavily in the

work presented in this thesis and their current established use in organic synthesis is described below.

1.4.1 Mitsunobu Reaction

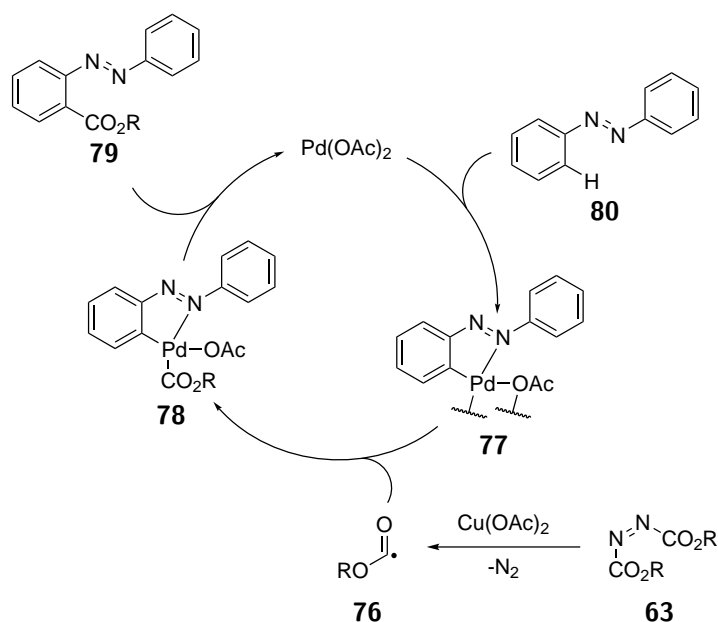
Perhaps the most famous and widespread use of azodicarboxylates is in the Mitsunobu reaction, named after Oyo Mitsunobu who developed the process in 1967.⁶¹ The classic transformation involves reaction of primary or secondary alcohols with an acidic pronucleophile (*e.g.* carboxylic acids, phenols, succinimides, phthalimides) to generate a variety of functional groups mediated by stoichiometric amounts of azodicarboxylate and tri-alkyl- or tri-arylphosphine (Scheme 1.26). The azodicarboxylate **63** employed reacts with the phosphine **64** to form the zwitterionic Mitsunobu intermediate **65**. This is then protonated by the acidic pronucleophile **66** to form phosphonium species **67**. This cationic intermediate **67** then binds to the alcohol starting material **68** to form protonated activated alcohol **69** and deprotonated hydrazine dicarboxylate **70**. Intermolecular proton transfer then forms activated alcohol **71** and hydrazine dicarboxylate **72** as by-product. The activated alcohol **71** is susceptible to nucleophilic attack from the formed nucleophile **73** to afford desired product **74** and stoichiometric amount of tri-substituted phosphine oxide **75**. Any stereochemistry about the alcohol group in the starting material is inverted during the reaction.



SCHEME 1.26: General Mitsunobu reaction mechanism.

1.4.2 Carboxylation Reaction

Whilst the utilisation of azodicarboxylates as carboxylating reagents is much less explored, these reagents have the ability to donate their carboxylate groups for the carboxylation of aromatic C(*sp*²)-H bonds. The use of azodicarboxylates is a complement to other carboxylation reagents, such as CO and CO₂, which avoids the requisites of harsh reaction conditions such as high pressure and temperature. Mechanistic investigations indicates that the reaction proceeds *via* a free radical mechanism.⁶²⁻⁶⁴ It is proposed that C-N bond homolysis on both sides of the N=N bond would result in two instances of alkoxyacyl radical **76** and is entropically favoured due to release of N₂ gas. Different research groups have employed various methods for generating the alkoxyacyl radical from azodicarboxylates, such as thermal decomposition (reaction temperature of 100 °C)⁶² or use of additives that aid SET such as (NH₄)₂S₂O₈⁶³ or Cu(OAc)₂.⁶⁴ The alkoxyacyl radicals can coordinate to Pd intermediates **77** formed following cyclopalladation of C-H bonds in aromatic substrates. Reductive elimination of the Pd complex **78** affords the carboxylated product **79**. The mechanistic cycle proposed for the *ortho*-carboxylation of azobenzene **80** in work conducted by Wang *et al.* is shown *vide infra* (Scheme 1.27).⁶⁴ This mechanism suggests the formation of an intermediate Pd(III) complex **78** prior to

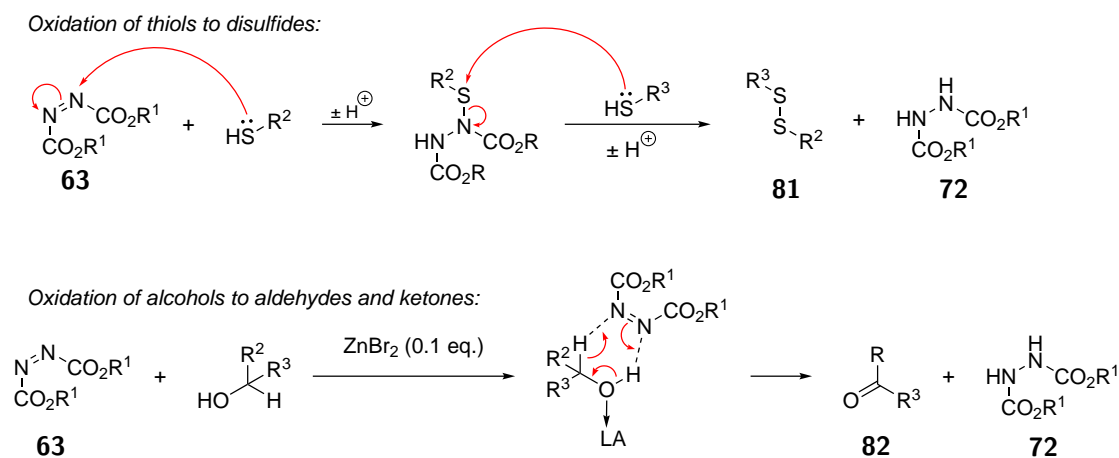


SCHEME 1.27: Mechanism proposed by Wang *et al.* for aromatic C-H carboxylation using azodicarboxylates **63** as an alkoxyacyl radical **76** source.⁶⁴

reductive elimination. It is therefore assumed that an unrepresented disproportionation step takes place to access a Pd(IV) species before a reductive elimination takes place to form the desired product and produce Pd(II) to continue the catalytic cycle.

1.4.3 Azodicarboxylate as an Oxidant

Azodicarboxylates can be effectively used in the oxidation of many protic functionalities such as alcohols, amines, hydrazines, thiols and hydroxylamines. As azodicarboxylates can be readily reduced to its corresponding hydrazine-dicarboxylate **72**, they are effective reagents for dehydrogenation reactions. As such, reactions utilising azodicarboxylate as an oxidant result in the formation of a stoichiometric amount of hydrazine-dicarboxylate **72**. Examples for the use of azodicarboxylates for the dehydrogenation of thiols to symmetrical or unsymmetrical disulfides **81**⁶⁵ and the for Lewis-acid assisted oxidation of alcohols to aldehydes and ketones **82**⁶⁶ is provided (Scheme 1.28).



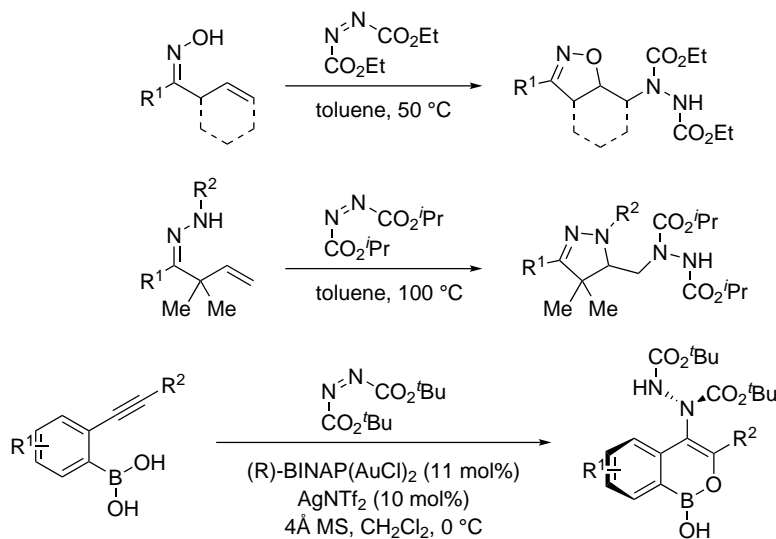
SCHEME 1.28: (Top) The use of azodicarboxylates for the dehydrogenation of thiols to symmetrical or unsymmetrical disulfides.⁶⁵ (Bottom) The use of azodicarboxylates for Lewis-acid assisted oxidation of alcohols to aldehydes and ketones.⁶⁶

1.4.4 Azodicarboxylate as an Electrophile

The strong electrophilic nature and possession of a vacant bonding orbital renders azodicarboxylates excellent candidates for attack by nucleophiles.⁶⁷ Whilst it is commonly stated that the presence of the adjacent carboxylate groups is a principle reason for the electrophilic nature of azodicarboxylates, crystallographic and theoretical studies have

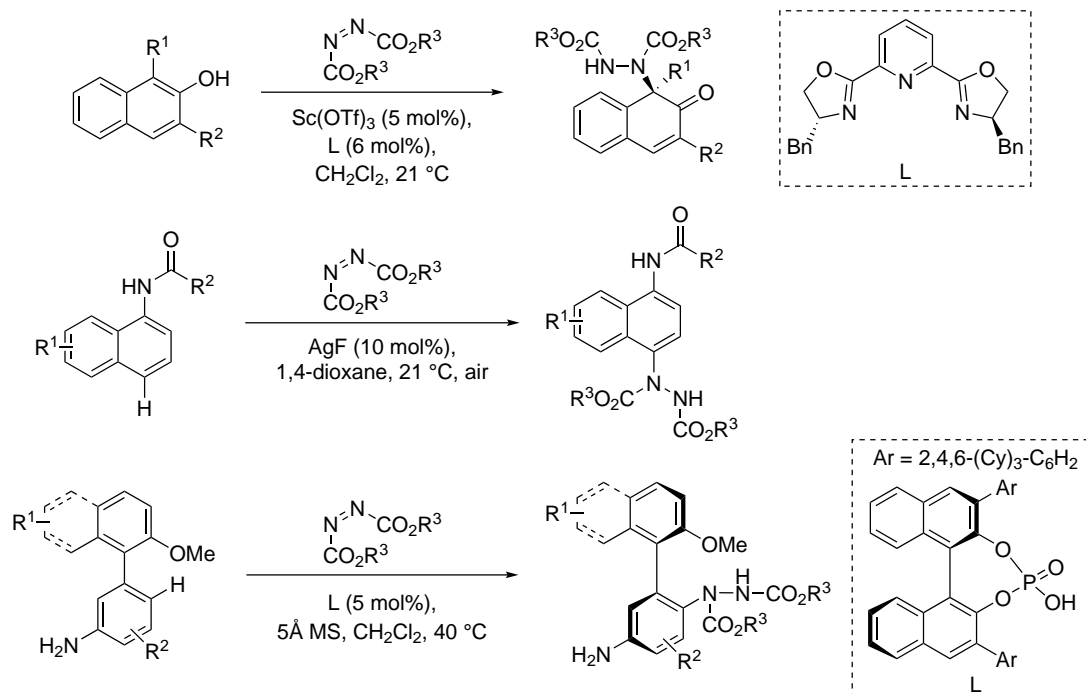
shown that these groups exist orthogonal to the N=N double bond, suggesting minimal interaction between the N=N and C=O π -systems.⁶⁸ The assumption that these species adopt a planar geometry that is analogous to those of carbon-based α,β -unsaturated esters is not correct.

Nonetheless, the use of azodicarboxylates as electrophiles has led to a multitude of amination reactions. Amination in this context describes the formation of an X–N bond. This has been used extensively in the formation of heterocycles (Scheme 1.29).^{69–71} Of particular note is the use of a chiral gold catalyst in the cycloisomerisation-amination of 2-(alkynyl)phenyl boronic acids, where it is proposed that complexation of the azodicarboxylate to the chiral catalyst enabled the effective asymmetric synthesis of heteroaryl atropisomers.



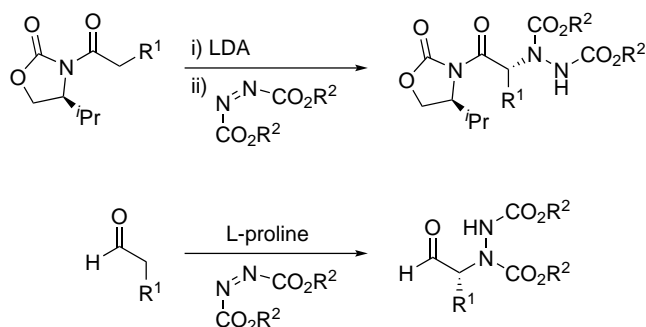
SCHEME 1.29: (Top) Amination of alkenes for the synthesis of isoxazolines.⁶⁹ (Middle) Amination of alkenes for the synthesis of pyrazolines.⁷⁰ (Bottom) Cycloisomerisation-amination of 2-(alkynyl)phenyl boronic acids.⁷¹

Azodicarboxylates also find frequent use as amination reagents in the formation of C(*sp*²)–N bonds upon nucleophilic attack by electron-rich aryl rings. Again, chiral catalysts have been demonstrated to be effective in asymmetric protocols involving azodicarboxylates for the formation of tetra-substituted stereogenic carbon centres and atroposelective formation of biaryl systems (Scheme 1.30).^{72–74}



SCHEME 1.30: (Top) Amination of alkenes for the synthesis of isoxazolines.⁷² (Middle) Amination of alkenes for the synthesis of pyrazolines.⁷³ (Bottom) Cycloisomerisation-amination of 2-(alkynyl)phenyl boronic acids.⁷⁴

Finally, azodicarboxylates get frequent use in the α -amination of carbonyl functionalities. This has particular use in asymmetric synthesis through either the employment of a chiral auxiliary⁷⁵ or asymmetric organocatalyst⁷⁶ and is a principle method of introducing chiral $\text{C}(sp^3)\text{-N}$ bonds into molecules (Scheme 1.31). The use of more bulky azodicarboxylates (*i.e.* dibenzyl and di-*t*-butyl derivatives) have been observed to enhance the diastereoselectivity provided by the chiral auxiliary or asymmetric organocatalyst when compared to less sterically-hindered azodicarboxylates (*i.e.* dimethyl and diethyl).



SCHEME 1.31: (Top) Use of a chiral auxiliary to create a stereogenic centre through the formation of a C-N bond.⁷⁵ (Bottom) Use of an asymmetric organocatalyst to create a stereogenic centre through the formation of a C-N bond.⁷⁶

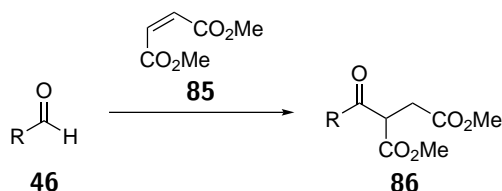
1.5 Hydroacylation *via* Aerobic C–H Bond Activation

In 2008, a hydroacylation reaction utilising an acyl radical formed *via* the aerobic aldehyde oxidation process was achieved by the Caddick group.⁷⁷ The reaction of aldehydes **46** with several vinyl sulfonates **83** under aerobic conditions afforded various unsymmetrical ketones **84** in respectable yields (*ca.* 70%) and all at room temperature (Scheme 1.32). Following on from this, the group found that the use of water as a solvent, the ideal ‘green’ solvent, produced similar if not better yields of the ketones.⁷⁸



SCHEME 1.32: Metal-free hydroacylation of vinyl sulfonates.

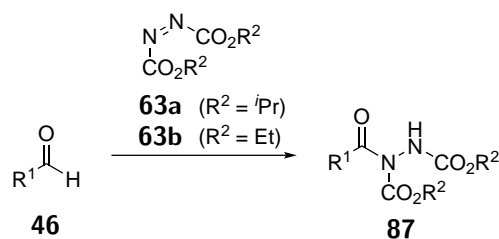
The group suspected that this transformation occurred *via* a radical pathway and supported this theory by showing that the reactions were completely inhibited in the presence of radical scavenger butylated hydroxytoluene (BHT).⁷⁷ Upon confirmation of a radical pathway, the group postulated that the reaction is initiated by reaction of the aldehyde with dioxygen in air. Following the hydroacylation of vinyl sulfonates **83**, the Caddick group then expanded the scope of this hydroacylation method to include α,β -unsaturated ester **85** where aliphatic aldehydes were once again found to give respectable yields of up to 89%, thereby expanding the possible radical acceptors available for this process (Scheme 1.33).⁷⁹



SCHEME 1.33: Metal-free hydroacylation of α,β -unsaturated esters **85**.

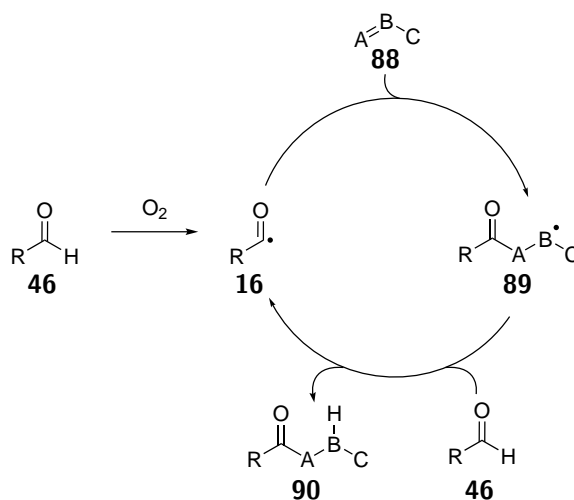
Indeed, the group then extended the scope of the protocol to include vinyl phosphonates, which were successfully utilised as acyl radical acceptors.⁸⁰ In 2011, acyl hydrazides **87** were synthesised particularly efficiently using azodicarboxylates **63** as radical acceptors (Scheme 1.34).⁸¹ Both diethyl azodicarboxylate (DEAD) and diisopropyl azodicarboxylate (DIAD) were shown to be compatible with both aliphatic and aromatic aldehydes for

hydroacylation *via* aerobic C–H activation. The efficiency of the reaction was clearly demonstrated with excellent yields being attained even when utilising aldehydes as the limiting reagent.⁸¹



SCHEME 1.34: Metal-free hydroacylation of azodicarboxylates **63** to form acyl hydrazides **87**.

The group also found that the reaction was tolerant of different functionalities displayed on the aldehyde motif, as well as retaining any stereochemistry throughout the reaction pathway,^{81,82} which widened the scope of the reaction for the synthesis of complex molecules where a large number of functional groups are likely to be present.^{81,82}



SCHEME 1.35: The general mechanism for hydroacylation *via* aerobic C–H activation.⁸²

The mechanism for the aerobic hydroacylation reactions achieved by the Caddick group is initiated by the interaction of aldehyde **46** with dioxygen in air to form an acyl radical **16** (Scheme 1.35). The acyl radical is nucleophilic in nature and can efficiently participate in radical addition to electron-deficient unsaturated bonds **88** to form an electrophilic radical-adduct species **89**. This species then abstracts a proton from the starting aldehyde, giving the process an autocatalytic nature and driving the formation of product **90** from starting material. The conditions that were developed are in sharp contrast to previous conditions for hydroacylation, which tend to use expensive transition

metals, peroxides that require thermal or photochemical degradation, or *N*-heterocyclic carbenes.

1.6 Reactivity of Acyl Hydrazides

The acyl hydrazide moiety displays a number of interesting chemical properties (*e.g.* acidic proton, relatively weak N–N bond, acyl group, carbamate functionality) and is often a stable crystalline solid (Figure 1.11), which can be exploited for transformation into important and desirable chemical functionalities; these will be discussed in turn.

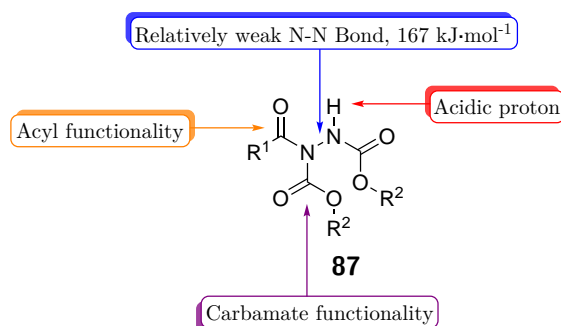
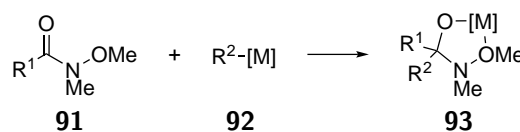


FIGURE 1.11: Structural and chemical characteristics of acyl hydrazides **87**.

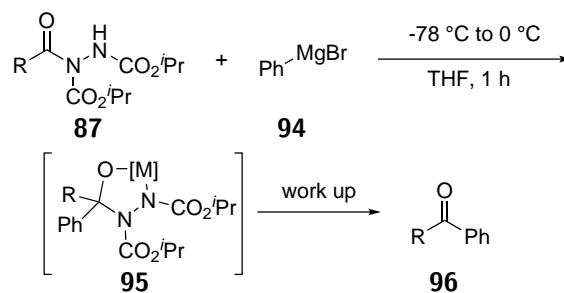
1.6.1 Acyl Donors

To date, the most common use of acyl hydrazides has been their application as acyl donors. Primarily, acyl hydrazides have been successfully shown to react with Grignard reagents in a controlled manner for the synthesis of diaryl and aryl alkyl ketones. Typically, the use of organometallics to form ketones from acyl equivalents has been inefficient due to the potential for over-addition due to the formed ketone being susceptible to further attack.⁸³ Historically, this has led to the use of Weinreb amides to be utilised in the synthesis of ketones where the synthesis of a stable metal complex **93** prevents over-addition from occurring (Scheme 1.36).⁸⁴



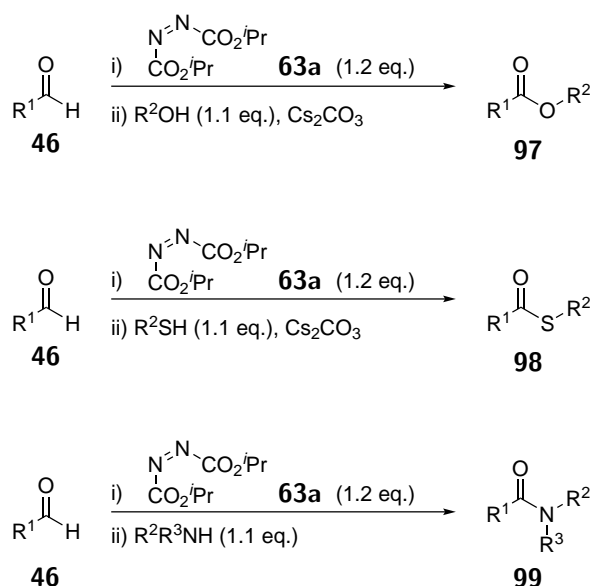
SCHEME 1.36: Attack of organometallic species **92** to Weinreb Amides **91** results in stable metal complex **93**.

Acyl hydrazides **87** have been found to mimic these properties where efficient mono-addition of Grignard reagents **94** were found to afford ketones **96** in good to excellent yields (Scheme 1.37).⁸⁵ The synthesis of Weinreb amide analogues in multiple one-step procedures from aldehyde starting materials represents a useful complementary reaction as Weinreb amides are typically formed from the coupling of O-alkylated hydroxylamines with acyl halides or activated carboxylic acids.⁸⁴



SCHEME 1.37: Attack of Grignard reagent **94** on acyl hydrazides **87** results in stable metal complex **95** which collapses upon work to form ketone **96**.

In a similar vein, although without the need for the aforementioned complexation intermediate, the Chudasama group later achieved the formation of esters **97**, thioesters **98** and amides **99** from aldehydes **46** *via* an acyl hydrazide reaction intermediate that was formed *in situ*.⁸⁶ The acyl hydrazide was initially formed *via* aerobic activation of a stoichiometric amount of aldehyde and reaction with 1.2 equivalents of DIAD **63a**. After 24 h, 1.1 equivalents of an alcohol, or amine (Scheme 1.38) was introduced into the reaction mixture. This resulted in the formation of an ester, a thioester or an amide respectively. The use of base (Cs_2CO_3) was necessary for the formation of esters and thioesters only; it was redundant in the formation of amides.

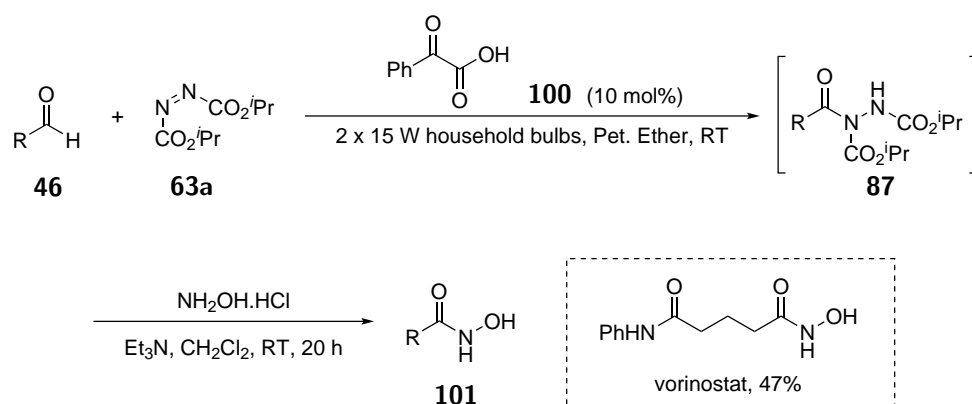


SCHEME 1.38: One-pot conversion of aldehydes **46** to either esters **97**, thioesters **98** and amides **99** using DIAD **63a** and alcohols, thiols or amines respectively.

The one-pot nature of the procedure and the use of aldehyde as limiting reagent were focal points in the methodology, especially as aldehydes are often oxidised to other functionalities such as esters, thioesters or amides under far harsher conditions and tend to require multiple steps with numerous isolations and purifications.

A similar one-pot approach was utilised by Papadopoulos and Kokotos⁸⁷ in the formation of hydroxamic acids **101** where the *in situ* generation of the acyl hydrazide functionality **87** allowed a nucleophilic addition elimination step of hydroxylamine at the acyl position. The method of choice for the formation of the acyl hydrazide was the author's previously described photoorganocatalytic process utilising phenylglyoxylic acid **100** as photoinitiator (Scheme 1.39).⁸⁸ The group also demonstrated the effectiveness of the reaction in the final step of the total synthesis of the drug vorinostat, where a 47% yield was achieved.

The use of acyl hydrazides as acyl donors also importantly highlights the use of acyl hydrazides as an attractive acyl halide alternative. Whereas acyl halides are often lachrymators and can be extremely reactive with respect to water, alcohol and amines and thus require the use of anhydrous conditions, acyl hydrazides are commonly stable crystalline solids with extremely long shelf-lives and do not require the use of anhydrous conditions or inert atmosphere.

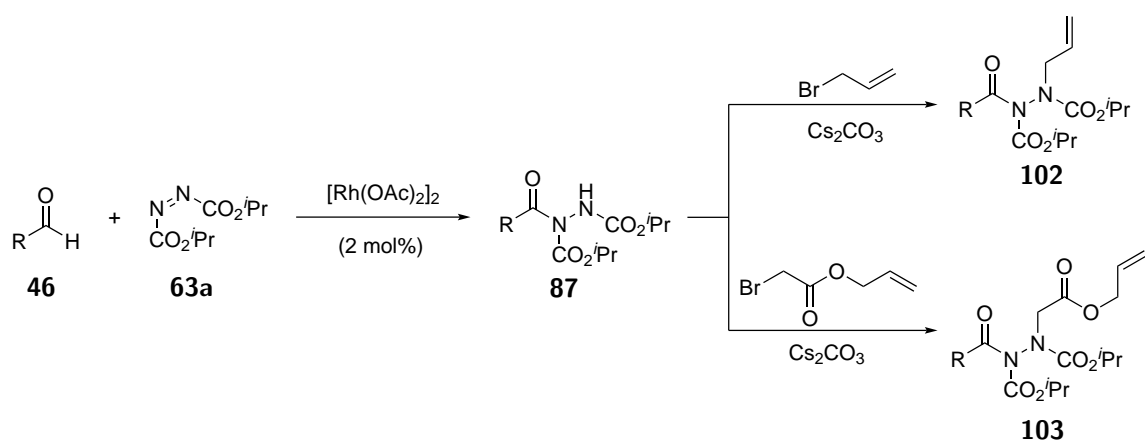


SCHEME 1.39: One-pot synthesis of hydroxamic acids **101** *via* formation of an acyl hydrazone intermediate **87**. (Inset) Structure of drug vorinostat synthesised *via* this method.

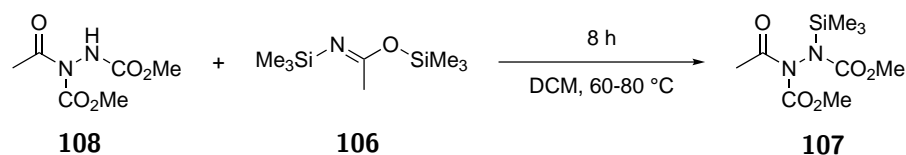
1.6.2 Functionalisation at the N–H bond

In 2004, Kim and Lee⁸⁹ employed a rhodium acetate catalyst to form acyl hydrazides and then either allylated or alkylated at the acidic N–H site by using α -bromoallyl or α -bromoacetate derivatives as electrophiles under basic conditions (Scheme 1.40). The group then took advantage of the stereodynamics of the substituted acyl hydrazide **104** (restricted N–N bond rotation with CO–N–N–CO dihedral angle of approximately 90°) to achieve a ring-closing metathesis by employment of Grubbs® second generation catalyst (Scheme 1.40).

Very early research into the reactivity of acyl hydrazides by Kalinin and co-workers⁹⁰ also showed that a silicon group can be added to the acidic site. Here, 1.5 equivalents of bis(trimethylsilyl)acetamide (BSA) **106** was used as the silylating agent to achieve an 85% yield of the silylated acyl hydrazide **107** (Scheme 1.41). The authors noted that hydrazine derivatives featuring a trimethylsilyl group on the nitrogen can act as convenient models in the study of conformational transitions in hydrazines.



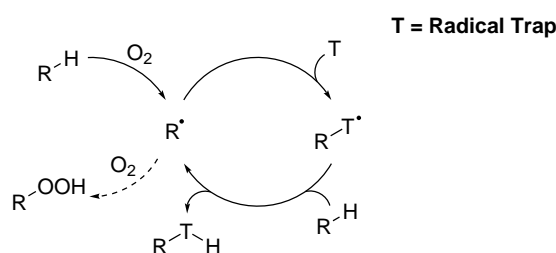
SCHEME 1.40: (Top) Alkylation of the N-H site in acyl hydrazides through use of either an α -bromoallyl or α -bromoacetate alkylating agent and Cs_2CO_3 . (Bottom) Ring-closing metathesis of diene-acyl hydrazide utilising Grubbs® second generation catalyst.



SCHEME 1.41: Silylation of acyl hydrazide **108** through the use of silylating agent BSA **106**.

1.7 Aims

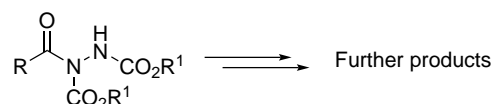
The primary aim of this project was to take advantage of the mechanisms of what is largely viewed as a nuisance reaction in oxidative degradation and how it can be exploited as a pathway to form desirable entities. The aspiration was to develop optimised methodologies for the formation of various entities by using air, or more specifically dioxygen in air, as an activating agent for susceptible C-H bonds. This would be achieved by trapping intermediates that arise in the aerobic oxidation pathway of a particular molecule. As such, the introduction of a radical trapping agent into a medium where radical species are being formed through aerobic C-H bond activation would result in regiospecific C-H bond functionalisation (Scheme 1.42).



SCHEME 1.42: Proposed main goal of project: the trapping of radical intermediates formed from the interaction of organic molecules with dioxygen in air.

Polarity matching rules will be used to rationally select appropriate radical trapping agents (*i.e.* electrophilic trapping agents would be used to trap nucleophilic radicals). A two-pronged approach to develop efficient aerobic C–H bond functionalisation reactions would be employed: (i) the means of controlling/manipulating the interaction of organic species with dioxygen in air (*e.g.* through modification of reaction stirring rate) and (ii) the means of creating more effective trapping agents by increasing their susceptibility to radical attack (*e.g.* through the interaction with additive species).

A secondary goal of this project will take into consideration the efficient synthesis of acyl hydrazides (formed through aerobic hydroacylation of azodicarboxylates) and develop novel methodologies to form other desirable moieties. Acyl hydrazides represent an under-utilised synthetic moiety that has already shown to be of particular use in acyl donation reactions. Expanding the synthetic scope of these products will result in greater desire to incorporate aerobic C–H bond activation in synthesis, thus providing new synthetic routes to complicated molecules that start from otherwise simple, readily available starting materials (Scheme 1.43).



SCHEME 1.43: Proposed secondary goal of project: the formation of further desirable entities from the reaction of aerobic C–H bond activation products.

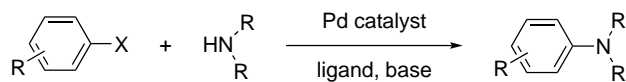
Chapter 2

Exploiting Auto-oxidation of Ethers for C–N Bond Formation

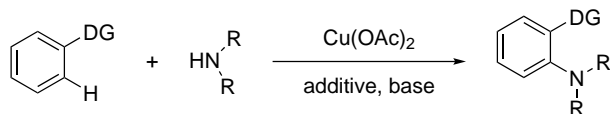
2.1 Introduction

C–H bond aminations are an extremely desirable process due to the plethora of nitrogen containing compounds found in pharmaceuticals.⁹¹ However, there are still many challenges in this area (Scheme 2.1): (i) the amination of C(*sp*³)–H bonds remains difficult despite significant advancements in the field of C(*sp*²)–N bond formation (*e.g.* Buchwald-Hartwig amination),^{92,93} (ii) the over-reliance of directing groups, especially in the case of C(*sp*³)–H bond activation, resulting in synthetic routes requiring additional installation and removal steps of the protecting/directing group,^{94,95} (iii) the current standard of using nitrene insertion reactions as a means of C(*sp*³)–H amination suffers from suboptimal regioselectivity and requires the use of specialised reagents such as organic azides as the nitrogen source,^{96–98} and (iv) the prevalent use of toxic/expensive transition metal reagents in the activation of inert C–H bonds.^{99,100} Despite providing a direct route to C–N bond formation, the existence of these limitations and the current quantity of external additives required for efficient reaction means that there is a need to develop C–H bond activation methodologies that are more attractive from a green chemistry standpoint.⁵⁶

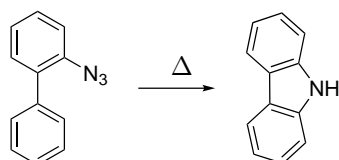
Buchwald-Hartwig amination:



Directing group-assisted amination:

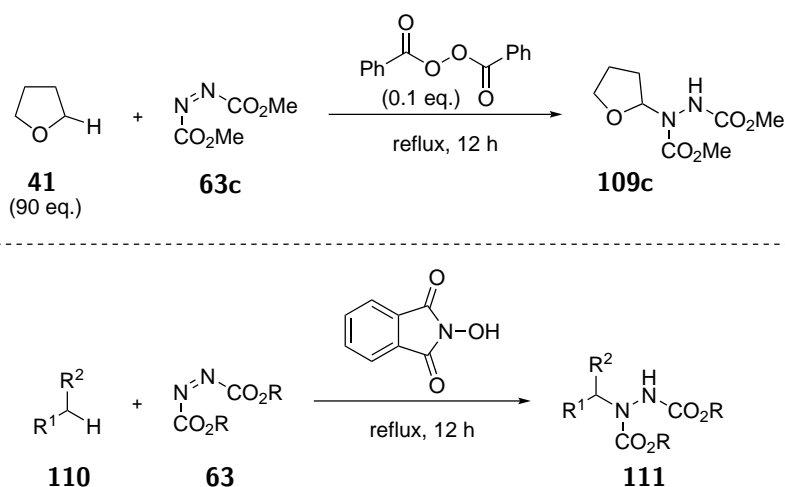


Nitrene C–H insertion:



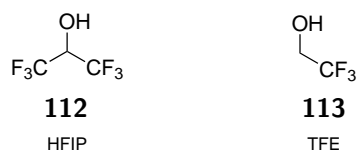
SCHEME 2.1: Modern methods for C–N bond formation.

In modern radical-based C–N bond formation, commercially available azodicarboxylates are the standout class of compounds used as radical acceptors. As previously shown (Chapter 1.4.4), these species are strongly electrophilic and are excellent candidates for attack by nucleophilic radicals and this has been extensively observed when utilising acyl radical chemistry for the formation of C(*sp*²)–N bonds^{81,82,86,88,101} (Chapter 1.5). Unfortunately, translation of these protocols to C(*sp*³)–N formation has been a significant challenge and has required either the substrate to be used in vast excess (*ca.* 90 eq.)¹⁰² or use of a specialised initiator/polarity reversal catalyst.¹⁰³



SCHEME 2.2: (Top) Benzoyl peroxide initiated α -C(*sp*³)–H amination utilising large excess of THF **41**.¹⁰² (Bottom) C(*sp*³)–H bond amination utilising initiator/polarity reversal catalyst *N*-Hydroxyphthalimide (NHPI).¹⁰³

Therefore, a protocol that would substantially increase the efficiency of the process; omitting the requirement of any additional additive whilst utilising molecular dioxygen in air to initiate α -C(sp^3)–H activation was sought-after. In view of this, the use of fluorinated alcohols such as 1,1,1,3,3,3-hexafluoroisopropanol (HFIP) **112** and 2,2,2-trifluoroethanol (TFE) **113** as reaction solvents (Table 2.1) was considered. These moieties exhibit higher relative acidity and substantial H-bond donating ability when compared to traditional solvents (alcoholic and non-alcoholic).¹⁰⁴ It was postulated that H-bonding of fluorinated alcohols to azodicarboxylates could result in a decrease in the energy of the LUMO (lowest unoccupied molecular orbital), thus increasing the susceptibility of these species to nucleophilic attack from ethereal radicals and resulting in an increased efficiency of reaction.



Solvent	Boiling point/°C	p <i>K</i> _a	HBD (α)	HBA (β)
AcOH	118.1	4.8	0.12	0.00
H ₂ O	100.0	14	1.17	0.18
ⁱ PrOH	82.5	17.1	0.76	0.95
EtOH	78.4	15.9	0.83	0.77
HFIP	58.2	9.3	1.96	0.03
TFE	73.8	12.4	1.51	0.18

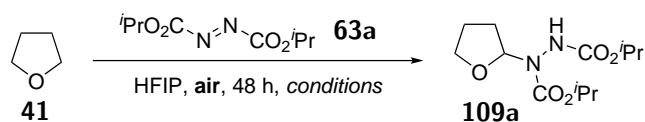
TABLE 2.1: Relevant properties of fluorinated alcohols and common protic solvents.¹⁰⁴ HBD (α) = hydrogen bond donating constant & HBA (β) = hydrogen bond accepting constant based on scale established by Abraham through analysis of experimentally determined association constants for formation of H-bonded complexes in carbon tetrachloride solution.¹⁰⁵

2.2 Optimisation

It was postulated an aerobic protocol could be developed through the formation of the integral ethereal radical intermediate by simple exposure of the reaction mixture to air. Investigations began with optimisation of the reaction between tetrahydrofuran (THF) **41** and commercially available diisopropyl azodicarboxylate (DIAD) **63a** to form desired

ether-hydrazide adduct **109a**. As previous reports for the reaction between ethers and azodicarboxylates utilised the ethereal substrate in vast excess,^{102,106} it was a goal from the offset to develop a protocol that employed a more desirable quantity of substrate.

An initial reaction using 5 equivalents of THF **41** at 21 °C, a stirring rate of 700 rpm and the reaction mixture exposed to air resulted in a trace amount of desired product (2% yield, Table 2.2, Entry 1). Pleasingly, the same reaction conducted with use of 1 mL of HFIP resulted in a four-fold increase in yield (8% yield, Table 2.2, Entry 2). This suggested that use of fluorinated alcohols as solvent for the transformation could improve the reaction. It was observed that when utilising HFIP, increasing the temperature also had a large impact on the efficiency of the reaction (Table 2.2, Entries 2-4), where a reaction temperature of 80 °C afforded a 64% yield of desired product **109a** (Table 2.2, Entry 4).



Entry	Temperature/°C	Stirring rate/rpm	HFIP/mL	109 /% ^a
1	21	700	0	2 (5%)
2	21	700	1	8 (16%)
3	60	700	1	52 (64%)
4	80	700	1	64 (77%)
5	80	1050	1	83 (96%)
6	80	350	1	60 (66%)
7	80	0	1	54 (58%)
8	80	1050	0.5	92 (100%)
9	80	1050	2	78 (92%)
10	80	1050	0	55 (59%)
11 ^b	80	1050	0.5	82 (89%)
12 ^c	80	1050	0.5	68 (75%)
13 ^d	80	1050	0.5	0 (1%)
14 ^e	80	1050	0.5	2 (4%)

TABLE 2.2: Reaction conditions: **41** (5 mmol), **63a** (1 mmol), air, 48 h. ^aIsolated yield, conversion of **63a** given in parenthesis based on amount recovered. ^bUse of TFE instead of HFIP. ^cUse of AcOH instead of HFIP. ^dUse of 10 mol% BHT. ^eSubstrates and solvent degassed and reaction conducted under an argon atmosphere.

As it is well understood that stirring rate can have a significant effect on the rate of aerobic oxidation,⁸² investigations on whether modification of the stirring rate affected reaction efficiency were conducted (Table 2.2, Entries 5-7). Gratifyingly, it was observed that increasing the stirring rate to 1050 rpm resulted in a far more desirable yield of **109a** (83%, Table 2.2, Entry 5), whereas decreasing stirring rate resulted in systematic reductions in reaction yield. (Table 2.2, Entries 6-7). Finally, a decrease in the amount of HFIP solvent to 0.5 mL resulted in a highly desirable 92% yield of **109a** (Table 2.2, Entry 8), whereas increasing the amount of HFIP resulted in a reduction in yield to 78%.

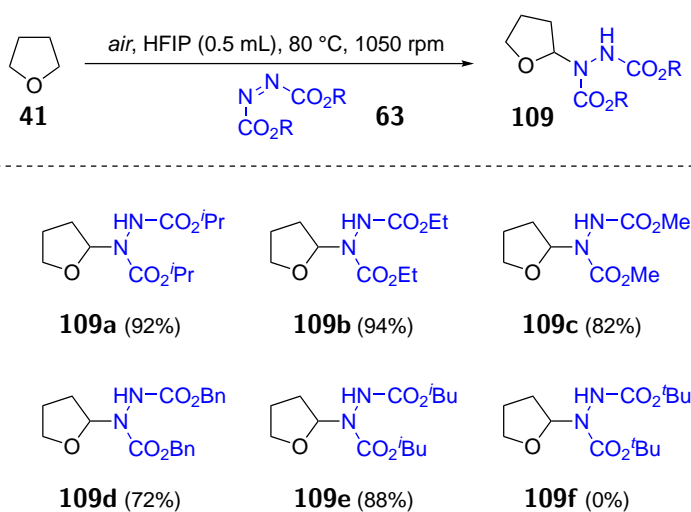
With an efficient reaction using HFIP in hand, investigations into the effect of alternative solvents on reaction efficiency were carried out. Conducting the reaction in the absence of solvent resulted in a 55% yield (Table 2.2, Entry 10). Substitution of HFIP to alternative fluorinated alcohol TFE resulted in only a small reduction in yield to 82% (Table 2.2, Entry 11), whilst use of an alternative acidic solvent AcOH (despite displaying stronger acidity, it is an inferior H-bond donor compared to HFIP¹⁰⁷) resulted in a significant decrease in yield of **109a** (68%, Table 2.2, Entry 12). This provided evidence that the increase in efficiency of the reaction when utilising fluorinated alcohols was mainly due to their substantial H-bonding ability and not their acidity. To confirm the presence of a radical pathway, a reaction was conducted under the optimised conditions with 10 mol% of radical inhibitor BHT (2,6-di-*tert*-butyl-4-methylphenol). It was observed that the use of BHT resulted in minimal conversion of starting material **63a** (Table 2.2, Entry 13). Finally, to demonstrate that the reaction proceeds *via* a dioxygen-initiated pathway, the optimised reaction of **41** and **63a** was conducted under an inert atmosphere (utilising degassed reagents and solvent) and resulted in a modest 2% yield of **109a** (Table 2.2, Entry 14).

2.3 Scope

2.3.1 Azodicarboxylates

With optimised conditions in hand, the generality of the procedure was then appraised (Scheme 2.3). Alongside DIAD, all azodicarboxylates trialled displaying primary and secondary alkyl groups gave their respective desired products in good to excellent yields

(72–94%), resulting in ether-azodicarboxylate adducts with carbamate esters that could be removed under either basic (methyl-, ethyl-carbamate), acidic (isopropyl-carbamate) or hydrogenation (benzyl-carbamate) conditions. Unfortunately, use of di-*tert*-butyl azodicarboxylate did not result in the formation of the desired product **109f**. This is suspected to be due to the incredible steric bulk of the tertiary alkyl Boc-groups preventing ethereal attack on the N=N bond. A similar effect is observed where acyl radicals require extensively long reaction times and higher reaction temperatures to react with di-*t*-butyl azodicarboxylate (Chapter 3.2).

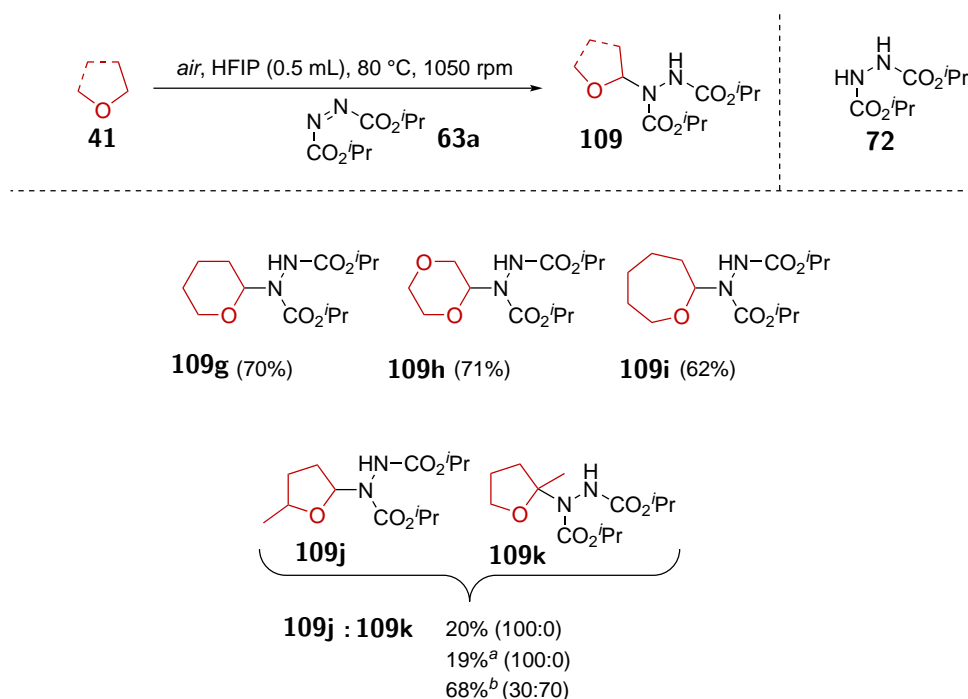


SCHEME 2.3: Reaction conditions: **41** (5 mmol), **63** (1 mmol), HFIP (0.5 mL), air, 1050 rpm, 80 °C, 48 h. Isolated yield.

2.3.2 Cyclic Ethers

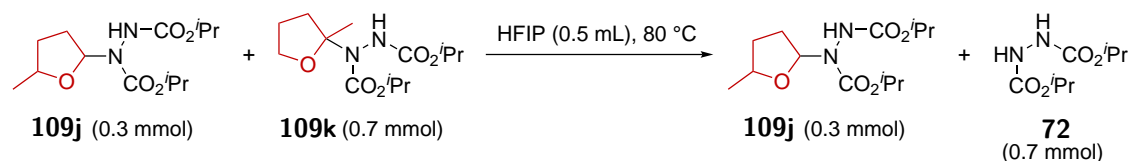
Use of 6- and 7-membered ring cyclic ethers also proved to be compatible under the reaction conditions with desired products isolated in good yields (62–71%, Scheme 2.4). This was particularly pleasing as the BDE of ethereal α -C–H bonds (Chapter 1.1.6) and the rate of auto-oxidation between ethereal species are known to vary quite significantly.¹⁰⁸ However, when employing α -substituted cyclic ether 2-methyltetrahydrofuran, only 20% of the sole regioisomer **109j** was observed, with a significant amount of hydrazine-dicarboxylate **72** recovered. This was intriguing as the appearance of regioisomer **109k** was expected and it was hypothesised that acid-mediated cleavage of the C–N bond in **109k** brought about through the presence of HFIP (pK_a = 9.3) led to the formation of **72**. In an attempt to reduce this pathway, utilisation of the comparatively less acidic fluorinated alcohol TFE

(pKa = 12.4) was explored. Unfortunately, this did not seem to improve the reaction with regards to yield or reducing formation of byproduct **72**. When the reaction was conducted under neat conditions, a 30:70 ratio of **109j** to **109k** in 68% yield was observed.



SCHEME 2.4: Reaction conditions: **41** (5 mmol), **63a** (1 mmol), HFIP (0.5 mL), air, 1050 rpm, 80 °C, 48-96 h (see Supplementary Information). Isolated yield. ^aUse of TFE instead of HFIP. ^bNeat reaction.

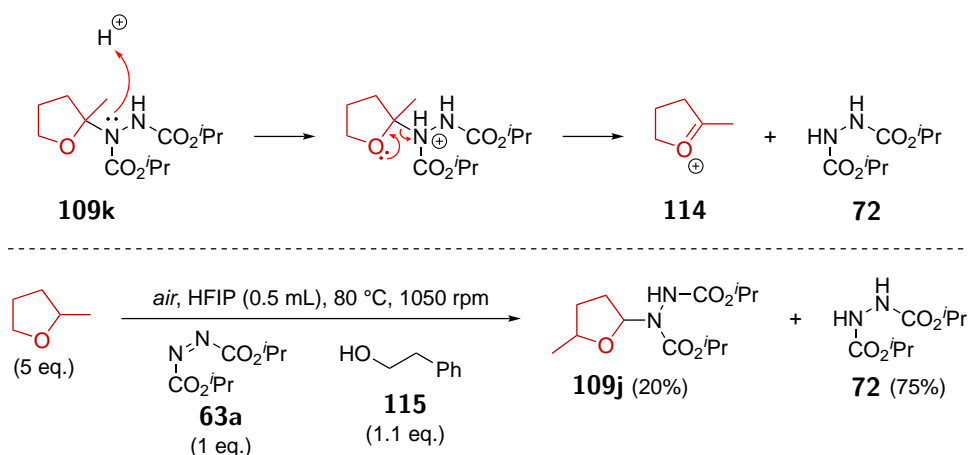
To provide evidence that α -alkylated, α -aminated ethers of the form **109k** are unstable under acidic conditions, the regioisomeric mixture of **109j** and **109k** was subjected to HFIP at 80 °C (Scheme 2.5). This led only to decomposition of the **109k** regioisomer, resulting in full conversion of **109k** to hydrazine-dicarboxylate **72**, whilst **109j** was fully recovered.



SCHEME 2.5: Reaction conditions: **109j** (0.3 mmol), **109k** (0.7 mmol), HFIP (0.5 mL), 80 °C, 24 h.

It was proposed that the acid-mediated cleavage of the C–N bond in **109k** would result in the formation of oxocarbenium cation intermediate **114** (Scheme 2.6). It was postulated that this process was only observed for the tetra-substituted **109k** regioisomer as this will

result in the formation of a fully-substituted oxocarbenium cation. An attempt was made to provide evidence for this mechanism *via* the introduction of alcoholic species **115** into the optimised reaction conditions between 2-methyltetrahydrofuran and DIAD with the idea that the nucleophilic alcohol would be capable of reacting with a transiently formed oxocarbenium cation (Scheme 2.6). Unfortunately, no reaction involving the participation of the alcohol was observed and the nature of the mechanism for acid-mediated cleavage of the C–N bond is still speculated.

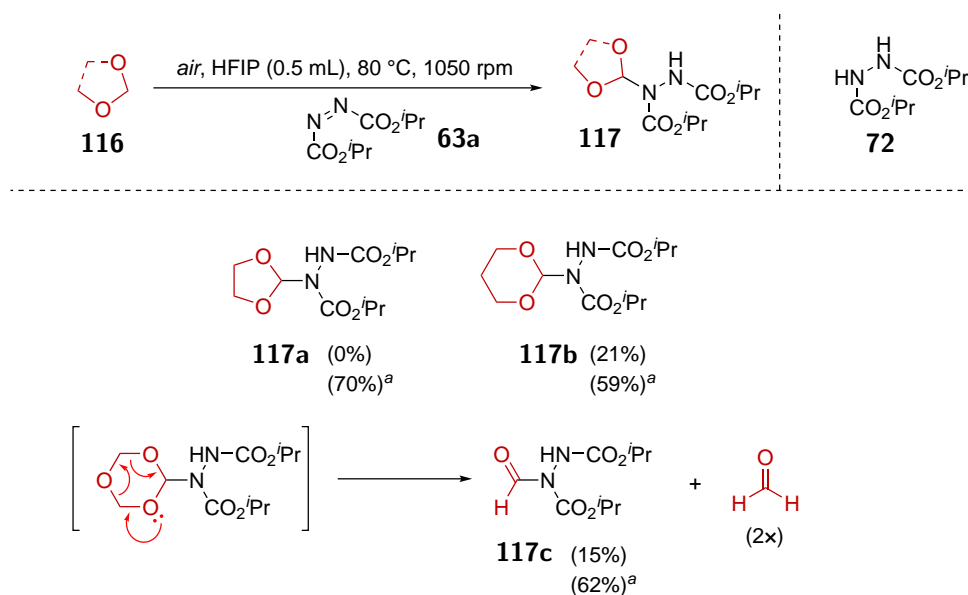


SCHEME 2.6: (Top) Postulated mechanism for the acid-mediated cleavage of the C–N bond in **109k**. (Bottom) *Reaction conditions*: 2-methyltetrahydrofuran (5 mmol), **63a** (1 mmol), **115** (1.1 mmol), HFIP (0.5 mL), air, 1050 rpm, 80 °C, 48 h.

2.3.3 Acetals

Upon the utilisation of cyclic acetals in the optimised conditions of $\text{C}(sp^3)\text{--H}$ amination (Scheme 2.7), it was again observed that the use of HFIP as the reaction solvent resulted in the formation of a large amount of hydrazine-dicarboxylate **72**, thereby resulting in suboptimal reaction yields (0–21%). To reduce this, the comparatively less acidic fluorinated alcohol TFE was again used in place of HFIP. Gratifyingly, minimal quantities of hydrazine-dicarboxylate **72** was observed upon full consumption of azodicarboxylate, resulting in far more efficient reactions (59–70% yield). Fascinatingly, when utilising 1,3,5-trioxane as the ether substrate and TFE as the reaction solvent, 62% of product **117c** was observed (*i.e.* formylation of the azodicarboxylate species). It is suspected this is due to 1,3,5-trioxane being a formaldehyde trimer which is prone to acidic decomposition.¹⁰⁹ Indeed, it was observed that use of HFIP resulted in only 15% yield of **117c**. It is proposed

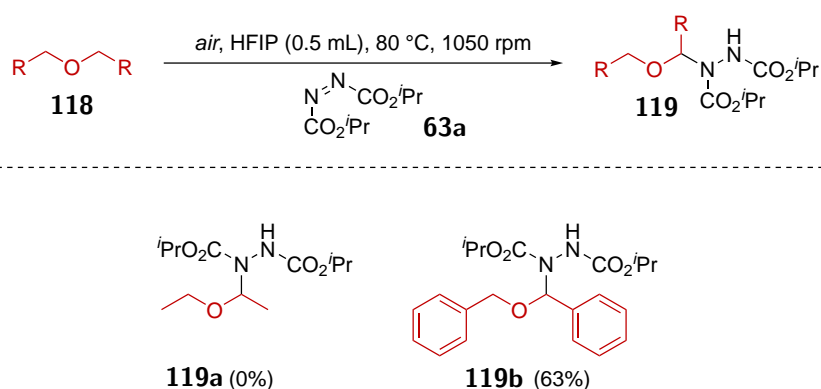
that this is due to rapid decomposition of 1,3,5-trioxane to volatile formaldehyde under the action of the more acidic HFIP prior to significant C–N formation.



SCHEME 2.7: Reaction conditions: **116** (5 mmol), **63a** (1 mmol), HFIP (0.5 mL), air, 1050 rpm, 80 °C, 24 h. Isolated yield. ^aUse of TFE instead of HFIP.

2.3.4 Acyclic Ethers

The scope of acyclic ethers was then appraised (Scheme 2.8). Disappointingly, diethyl ether did not appear to not undergo any transformation under the reaction conditions. It was suspected that this is due to the comparatively larger bond dissociation energy (BDE) about the α -C(sp^3)-H in diethyl ether (*ca.* 400 KJ·mol⁻¹) compared to cyclic ethers (*i.e.* 380-390 KJ·mol⁻¹). To provide evidence for this, acyclic dibenzyl ether (which exhibits a BDE of 359 KJ·mol⁻¹) was trialed and the reaction proceeded efficiently with a 63% of desired adduct **119b** observed.

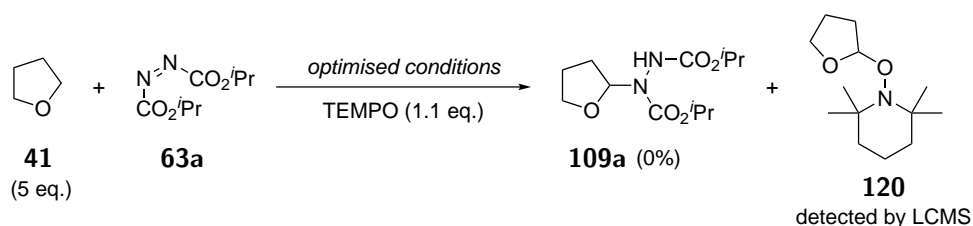


SCHEME 2.8: Reaction conditions: **118** (5 mmol), **63a** (1 mmol), HFIP (0.5 mL), air, 1050 rpm, 80 °C, 72 h. Isolated yield.

2.4 Mechanistic Studies

Note: All calculations pertaining to theoretical investigations (Host:Guest binding constant extracted from a ^1H NMR titration curve, geometry optimisation, frontier molecular orbital analysis and condensed Fukui functions) were carried out by Dr Antoine Maruani.

For initial investigations of the reaction mechanism, a control experiment using 2,2,6,6-tetramethyl-1-piperidinyloxy (TEMPO) as a radical scavenger was conducted under the optimised conditions (Scheme 2.9). As expected, a complete retardation of the reaction was observed and the THF-TEMPO adduct **120** was detected by LC-MS analysis (MS = 228.2 Da), suggesting the mechanism proceeds through the initial formation of a THF radical.



SCHEME 2.9: TEMPO trapping experiment. Reaction conditions: **41** (5 mmol), **63a** (1 mmol), HFIP (0.5 mL), TEMPO (1.1 mmol) air, 1050 rpm, 80 °C.

2.4.1 NMR Titration

It is well understood that fluorinated alcohols such as HFIP and TFE are excellent hydrogen-bond donors and this has been extensively studied in the interaction with

hydrogen-bond accepting ethers.¹⁰⁴ It was thus proposed that fluorinated alcohols can also participate in efficient H-bonding to azodicarboxylates. It was therefore experimentally examined, through ¹H NMR titration, the formation of H-bond complexes of HFIP with DIAD. The titration was conducted through successive additions of DIAD to an NMR sample of a fixed quantity of HFIP in CDCl₃ and the change in the chemical shift (δ) of the hydroxyl proton was recorded. A significant downfield shift of the proton was observed in the ¹H NMR with increasing quantity of DIAD, clearly indicating the formation of a hydrogen-bonded complex (Figure 2.1). The presence of only one hydroxyl proton signal indicates a fast equilibrium on the NMR timescale.

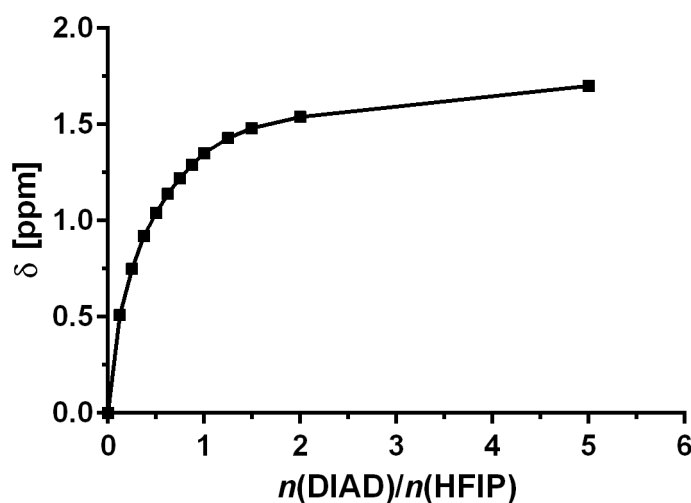


FIGURE 2.1: ¹H NMR titration curve of HFIP with DIAD.

The binding constant values were calculated from ¹H-NMR titration data using Bind-fit^{110,111} for 1:2 (Host:Guest) non-cooperative binding stoichiometry. The following equation was used for calculating the binding constant from titration experiments *via* non-linear fitting method (Nelder–Mead):

$$\Delta\delta = \frac{\delta_{\Delta HG_1} K[G] + \delta_{\Delta HG_2} K^2/4[G]^2}{1 + K[G] + K^2/4[G]^2} \quad (2.1)$$

where K is the binding constant and $\delta_{\Delta HG} = \delta_{HG} - \delta_H$.

NMR data points for DIAD fitted well into this model and yielded a binding constant K of $4.4 \pm 0.5 \text{ M}^{-1}$ (initial H-bonding between HFIP and DIAD), indicating a significant interaction.

2.4.2 Theoretical Investigations

Having experimental support for the hydrogen-bonding effect of HFIP to DIAD **63a**, it was then decided to conduct theoretical studies on the nature and effect such an interaction would have on the mechanism of the overall chemical transformation. First, it was of interest whether DIAD was likely to be accepting a hydrogen-bond through a nitrogen atom on the N=N bond, or the carbonyl oxygen on the carboxylate esters adjacent to the N=N bond (Figure 2.2). Thus, the energy of DIAD **63a**, DIAD-HFIP complex H-bonded through a carbonyl oxygen atom (denoted as **63a^O**) and DIAD-HFIP complex H-bonded through a nitrogen atom (denoted as **63a^N**) were calculated.

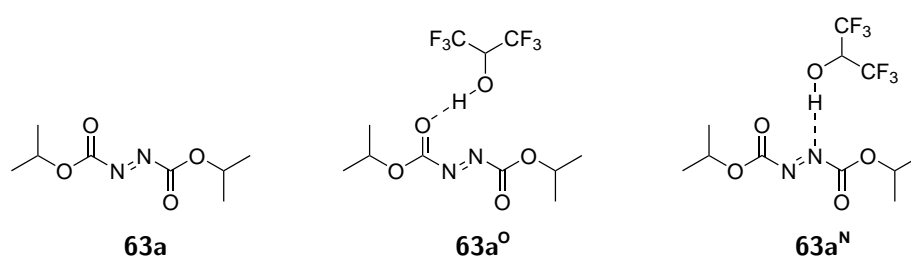


FIGURE 2.2: DIAD **63a**, DIAD-HFIP complex H-bonded through a carbonyl oxygen atom **63a^O** and DIAD-HFIP complex H-bonded through a nitrogen atom **63a^N**.

The molecules were subjected to geometry optimisation at B3LYP/6-311++G(d,p) level; the resulting optimised structure are given in Figure 2.3. Following this, calculations *in vacuo* were performed at M06-2X/6-311++G(d,p) level of theory and the energy difference between **63a^O** and **63a^N** was found to be 1.8 kcal·mol⁻¹, **63a^N** being the lowest in energy. The energy difference being relatively small, both complexes were further investigated to understand the role of HFIP in the reaction.

Frontier molecular orbital analysis (FMO)

As ethereal radicals are nucleophilic in nature and therefore will interact favourably with electrophilic entities such as azodicarboxylates, the LUMO energies of **63a** and **63a^O** and **63a^N** were calculated. They were found to be -2.42 eV for DIAD **63a**, -2.93 eV for DIAD-HFIP complex **63a^O** and -3.25 eV for DIAD-HFIP complex **63a^N**. This suggests that H-bonding to azodicarboxylates does indeed lower the energy of the LUMO, with a significant increase observed upon H-bonding through a nitrogen atom compared to a carbonyl oxygen atom.

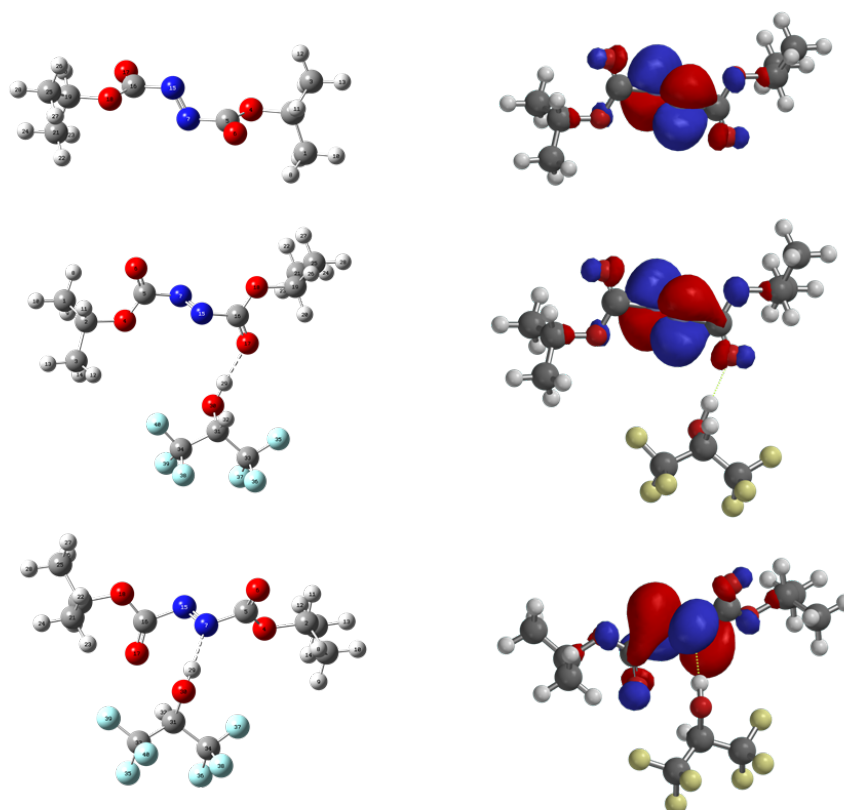


FIGURE 2.3: (Left) Optimised geometry of **63a**, **63a^O** and **63a^N** at M06-2X/6-311++G(d,p) level. (Right) Corresponding calculated LUMO.

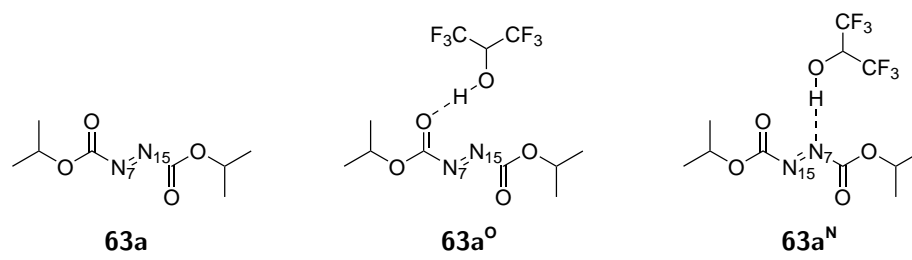
Condensed Fukui function

In computational chemistry, Fukui functions are the reactivity descriptors that enable characterising the relative susceptibility of sites to electrophilic, nucleophilic and radical attack and hence are commonly used for the establishment of the regio- and chemoselectivity observed in reactions. The condensed Fukui function represents the same underlying idea but applied to an atom within a molecule rather than a point in three-dimensional space. The atoms of a molecule, which have the largest Fukui values, are the most feasible sites for the attack. For radical attack, the condensed Fukui function of an atom A is defined as

$$f_A^0 = \frac{q_{N-1}^A - q_{N+1}^A}{2} \quad (2.2)$$

where q_{N-1}^A and q_{N+1}^A are partial charges of atom A in the molecule with $N - 1$ electrons and $N + 1$ electrons, respectively.

Partial charges for both nitrogen atoms were computed using atomic dipole moment-corrected Hirshfeld charges. The condensed Fukui functions for DIAD **63a**, DIAD-HFIP complex **63a^O** and DIAD-HFIP complex **63a^N** were then calculated, the results are presented in Table 2.3.

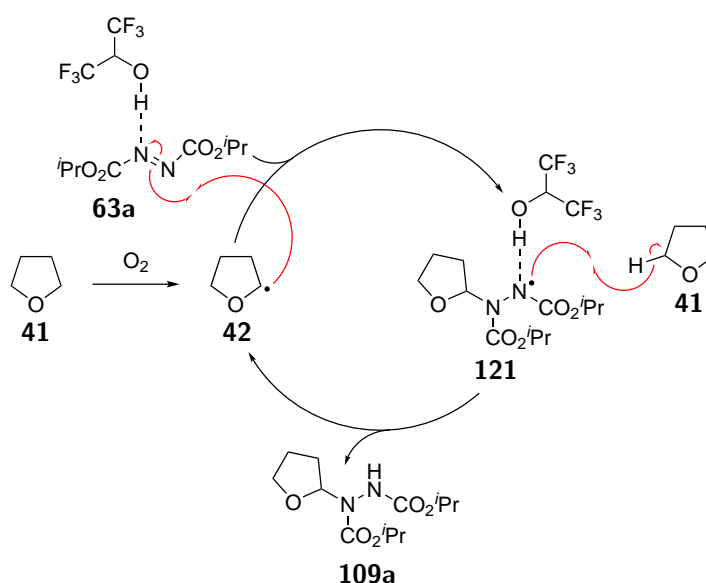


	63a	63a^O	63a^N
N(7)	0.22	0.25	0.11
N(15)	0.21	0.23	0.33

TABLE 2.3: Condensed Fukui function (f^0) values for radical attack on the nitrogen atoms on DIAD **63a**, DIAD-HFIP complex **63a^O** and DIAD-HFIP complex **63a^N** (HFIP H-bonded to N(7) on **63a^N**).

These results highlight the impact of H-bonding through the nitrogen atom where susceptibility of the non-H-bonded nitrogen N(15) on the N=N bond to radical attack is significantly increased. By contrast, H-bonding through a carbonyl oxygen atom did not have a significant effect on the susceptibility of DIAD to radical attack. This fits with the theoretically optimised geometry of azodicarboxylates where the carbonyls of the carboxylate esters adjacent to the N=N bond are shown to be practically orthogonal to the N=N bond,⁶⁸ indicating that the molecule is not conjugated and therefore hydrogen-bonding to the carbonyl oxygen atom should have minimal effect on the reactivity of azodicarboxylates.

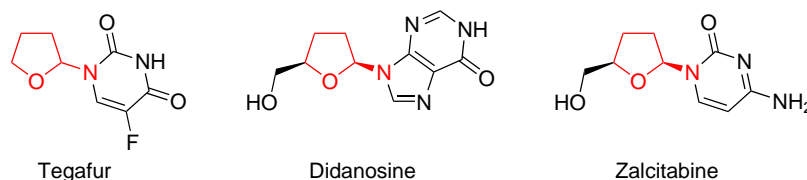
This suggests that the mechanism for radical attack of ethereal radical species **42** on an azodicarboxylate-HFIP complex **63a^N** proceeds *via* H-bonding to the adjacent nitrogen on the N=N bond (Scheme 2.10). The radical adduct species **121** is then expected to abstract a H-atom from the starting material **41**, forming desired product **109a** and reforming ethereal radical **42**.



SCHEME 2.10: Proposed mechanism.

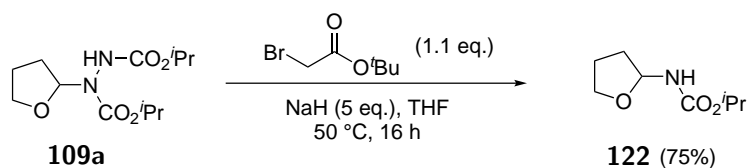
2.5 Formation of (protected) α -amino ethers

The described formation of ethereal α -C–N bonds represents a fundamental advancement that allows for the increase in functionality and complexity of ether substrates in a minimalistic fashion and therefore obviates the need for any undesirable metals, initiators or additives. The use of atmospheric dioxygen represents one of the greenest, most sustainable and freely accessible oxidants to be utilised in synthesis. Furthermore, ethereal α -C–N bonds are present in various bioactive molecules such as Tegafur (chemotherapeutic prodrug) and Crambescin B (voltage-gated sodium channel inhibitor) and are also present in a variety of HIV/AIDS medications (*i.e.* didanosine, zalcitabine, Scheme 2.11).

SCHEME 2.11: Examples of bioactive molecules with α -ethereal C–N bonds.

The formed ether-azodicarboxylates also offer platforms for further synthetic manipulation. As an example, access to (protected) α -amino species is highly desirable and it was demonstrated the formation of these structures through cleavage of the N–N bond (Scheme 2.12).¹¹² A one-pot alkylation-elimination protocol was carried out on compound **42** utilising *tert*-butyl bromoacetate as the alkylating agent and sodium hydride

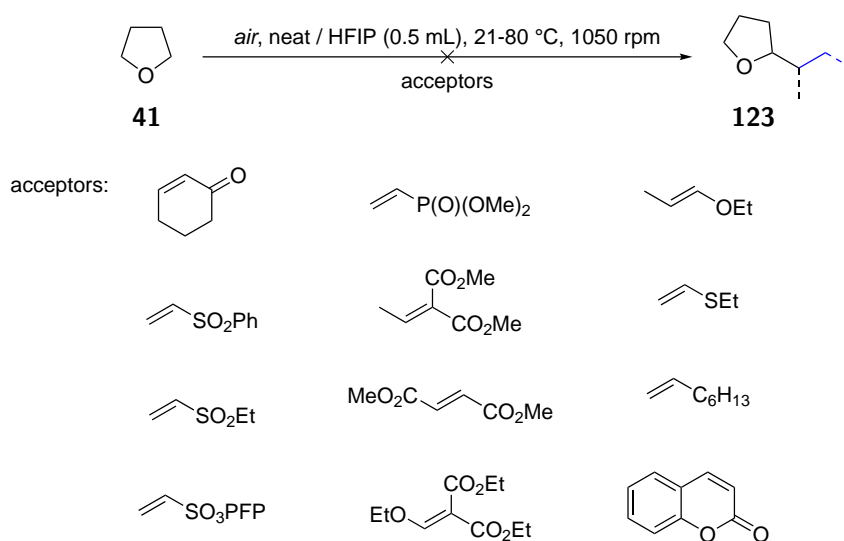
to facilitate base-mediated alkylation and E1cB elimination gave desired product **122** in a 75% yield. This result demonstrates that the amination procedure reported in the study is a powerful tool for the metal-free formation of synthetically useful α -hydrazo and α -amino ethers, as well as being a key step forward in the field of C–H activation.



SCHEME 2.12: Reaction conditions: **109a** (1 mmol), *tert*-butyl bromoacetate (1.1 mmol), THF (2 mL), NaH (60% dispersion in mineral oil, 5 mmol), 50 °C.

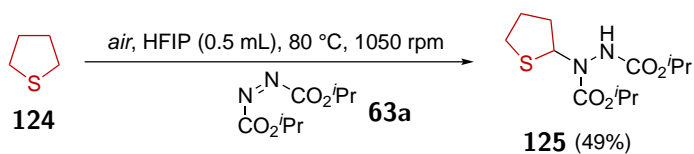
2.6 Further Context

The optimised conditions for efficient α -ethereal C–N bond formation were then trialled for potential α -ethereal C–C bond formation. Several electrophilic moieties containing unsaturated C=C bonds (*e.g.* vinyl sulfones, vinyl sulfonates, vinyl phosphonates, α,β -unsaturated esters) were previously shown in the Chudasama group to be effective acyl radical acceptors^{78–82} and these were trialled in turn with the conditions developed for the reaction of ethers with azodicarboxylates (Scheme 2.13). Unfortunately, none of the acceptors trialled resulted in any desired product formation with no consumption of the acceptor species observed. Any modification in temperature (21–80 °C) or removal of HFIP as the reaction solvent also did not result in any observed reaction. This is postulated to be due to inefficient chain turnover where the radical adduct formed from the addition of THF radical to the acceptor species does not efficiently abstract a H-atom from the starting material, possibly due to the comparatively higher BDE of the α -furanlyl C–H bond (391.6 kJ·mol⁻¹) as compared to aldehydic C–H bonds where efficient chain transfer is observed (*ca.* 380 kJ·mol⁻¹).⁸²



SCHEME 2.13: Reaction Conditions: **41** (5 mmol), acceptor (1 mmol), HFIP (0/0.5 mL), 21–80 °C, 1050 rpm air, 120 h.

Finally, owing to literature describing the oxygen-induced auto-oxidation of organic sulfides,¹¹³ tetrahydrothiophene (sulfur-analogue of THF) was also trialed in the reaction conditions; this resulted in the isolation of the desired product in 49% yield (Scheme 2.14).



SCHEME 2.14: Reaction Conditions: **124** (5 mmol), **63a** (1 mmol), HFIP (0.5 mL), 80 °C, 1050 rpm, air, 48 h.

2.7 Conclusions

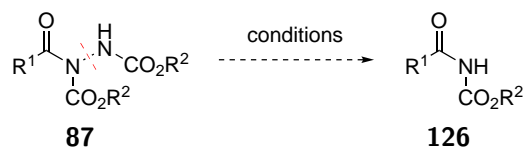
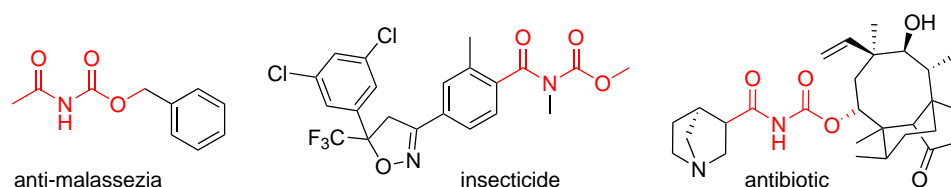
In summary, an aerobic approach for α -C(sp^3)-H amination of ethereal substrates utilising azodicarboxylates has been developed, enabled through the use of fluorinated alcohols. The use of atmospheric oxygen to generate reactive radical species and the dual function of fluorinated alcohols as both reaction solvent and activating agent to increase the susceptibility of azodicarboxylates to radical attack feeds into the sought-after goal of simplification of C–H activation transformations. A broad library of ether- and acetal-azodicarboxylate adducts can be efficiently prepared. Experimental evidence for the H-bonding interaction between HFIP and DIAD and theoretical studies suggests that the H-bonding of HFIP specifically to the nitrogen atom in DIAD results in a substantial lowering of the LUMO energy and increases its susceptibility to radical attack. Moreover, the ether-azodicarboxylate adducts formed offer opportunity for further synthetic manipulation, and in particular, to gain access to α -amino ethers. It is maintained that the use of auto-oxidation to access reactive radical species without the use of any additional reagents is largely unexplored and can be a powerful method in radical-based C–H bond functionalisation. Furthermore, it is hoped that the research conducted into the interaction between fluorinated alcohols and azodicarboxylates will provide new opportunities for X–N bond formations, particularly in radical-based synthesis.

Chapter 3

Formation of *N*-Acyl Carbamates from Acyl Hydrazides

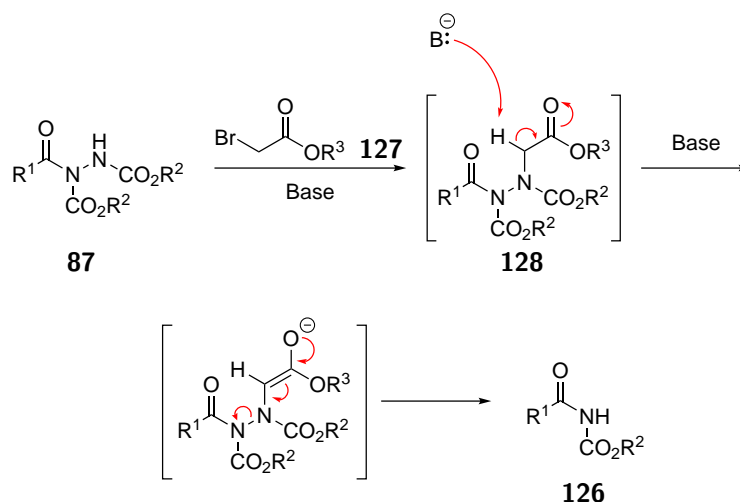
3.1 Introduction

N-Acyl carbamates **126** are prevalent in various bioactive compounds, *e.g.* anti-malassezia agents,¹¹⁴ insecticides,¹¹⁵ antibiotics,¹¹⁶ and pro-drugs.¹¹⁷ The moiety is also present in molecules employed as directing groups in synthesis,^{118,119} and within phototriggers.¹²⁰ It is proposed that this desirable moiety would be accessible upon the cleavage of the N–N bond in readily-formed acyl hydrazides **87** (Scheme 3.1).



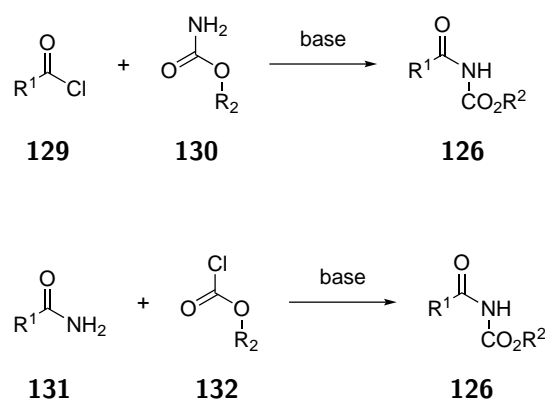
SCHEME 3.1: (Top) Examples of bioactive *N*-acyl carbamates. (Bottom) The proposed synthetic methodology to access *N*-acyl carbamates **126** from acyl hydrazides **87**.

Previous methods for N–N bond cleavage commonly utilise hydrogenation techniques (*i.e.* use of Raney®-Nickel and a reaction atmosphere of H₂).¹²¹ The use of Raney®-Nickel in particular is unfavourable due to the requirement of multiple filtration/purification to remove any residue from the product and the application of high reaction temperature/pressure. Hence, a procedure that efficiently achieves N–N bond cleavage of acyl hydrazides **87** without the employment of any transition metal-based reagents or reductive reaction environments is highly desired. To achieve this, the unique structural composition of acyl hydrazides **87** was utilised. The nucleophilicity of the terminal N atom and presence of an N–H site means that these moieties possess an alkylation site situated on the N–N bond. Therefore, utilisation of a bromoacetate species **127** as the alkylating agent would furnish a tetra-alkylated hydrazine **128** that possesses an α -H that in the presence of base, should facilitate an E1cb mechanism resulting in the cleavage of the N–N bond (Scheme 3.2). As both the alkylation and elimination steps of this synthetic route would require the use of base, it was hoped that the two steps could be carried out subsequently in a one-pot fashion.



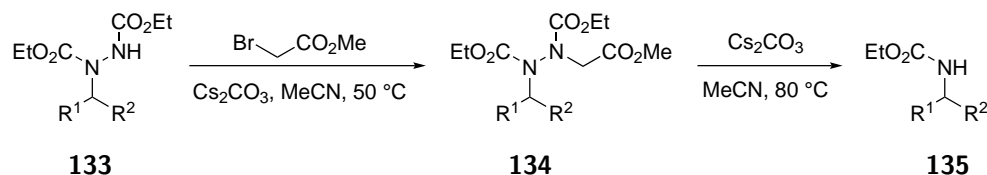
SCHEME 3.2: Proposed two-step, one-pot synthesis of *N*-acyl carbamates **126** from acyl hydrazides **87** through formation of tetra-substituted hydrazine intermediate **128**.

The synthetic route postulated would be complementary to existing traditional approaches for the synthesis of *N*-acyl carbamates, which tend to react acyl halides **129** with carbamates **130** or primary/secondary amides **131** with chloroformates **132** (Scheme 3.3).^{122,123}



SCHEME 3.3: Common synthetic protocols applied for the synthesis of *N*-acyl carbamates **126**.

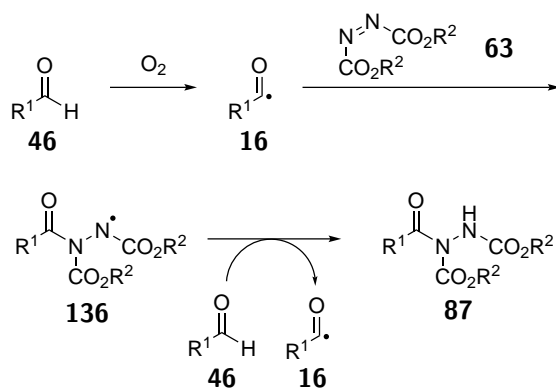
Furthermore, the ability to cleave the N–N bond without the use of hydrogenation, expensive catalysts and/or undesirable metals was seen as a key aspect in itself,^{121,124–128} this is particularly well described in related work by Magnus *et al.* (Scheme 3.4) where conversion of hydrazine dicarboxylates **133** to carbamates **135** was achieved using an elegant alkylation-elimination sequence, albeit in two distinct steps and requiring relatively high temperatures (*ca.* 80 °C).¹²⁷



SCHEME 3.4: The two-step alkylation-elimination sequence developed by Magnus *et al.* for the formation of carbamates **135** from hydrazine dicarboxylates **133**.

3.2 Formation of Acyl Hydrazides

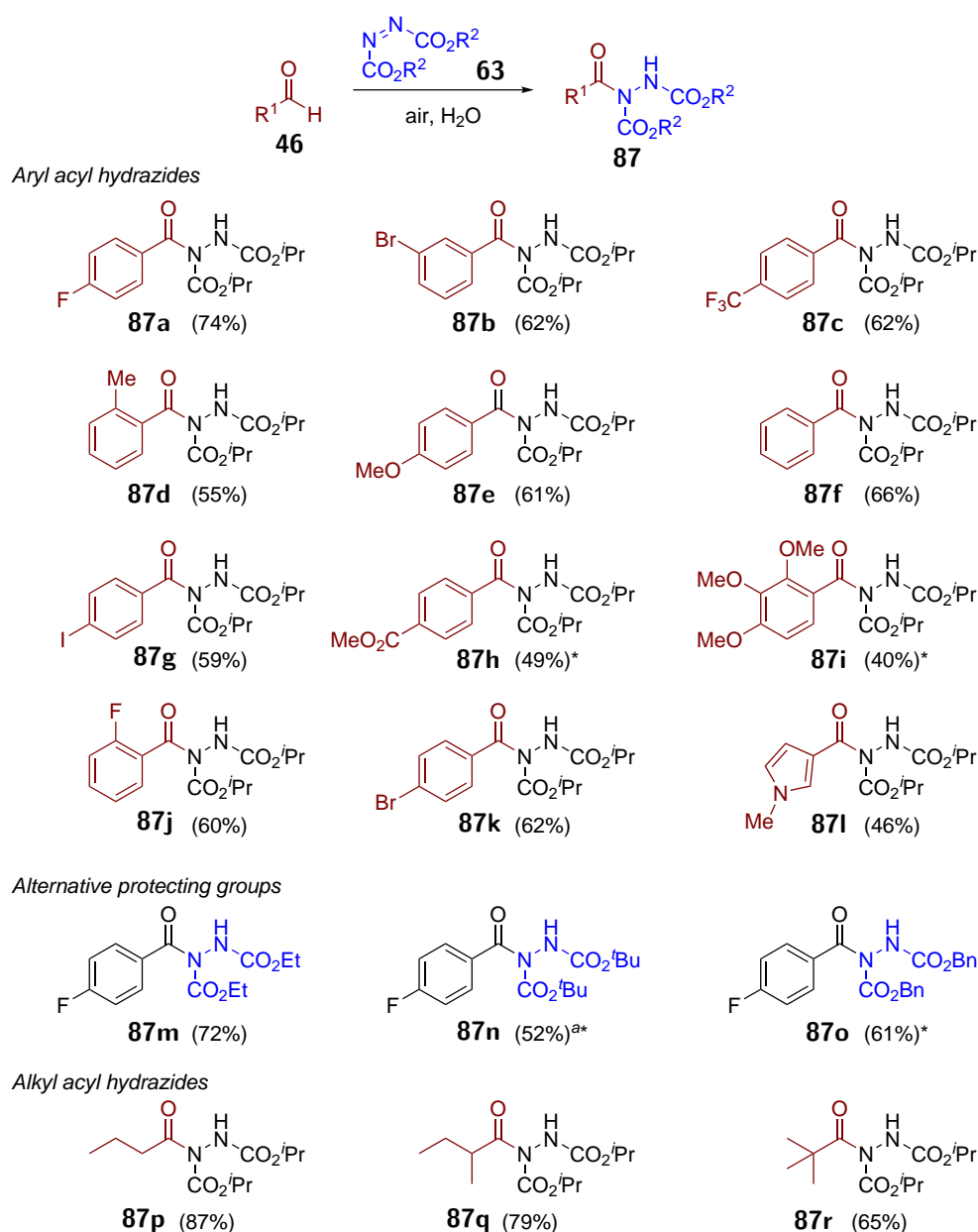
Acyl hydrazides **87** represent synthetically versatile scaffolds that have been successfully utilised for the formation of useful moieties such as thioesters, esters, amides⁸⁶ and ketones⁸⁵ (Chapter 1.6), as well as building blocks for the creation of bioactive molecules such as hydroxamic acids⁸⁷ and macrocyclic enamides.⁸⁹ They have been prepared *via* numerous protocols through the years with a substantial increase in the number of reported methodologies in the past decade.¹⁰¹ Whilst there are some exceptions, the majority of acyl hydrazides are prepared from reaction of an aldehyde and an azodicarboxylate. Previous work in the Chudasama group (Chapter 1.5) has successfully utilised aldehydes



SCHEME 3.5: The synthetic pathway for hydroacylation of azodicarboxylates **63** via aerobic C–H bond activation.

46 (which are viewed as the more valuable of the starting reagents) as the limiting reagent in the synthesis of acyl hydrazides **87** using an aerobic C–H bond activation protocol (Scheme 3.5).

To examine whether a N–N bond cleavage reaction of acyl hydrazides **87** to form *N*-acyl carbamates **126** could be viable, first, a library of acyl hydrazides was synthesised (Scheme 3.6). To test the reagent scope of the subsequent reaction, it was decided to introduce as much structural variation into the acyl hydrazine library as possible. Aryl acyl hydrazides were formed with either electron-deficient or electron-rich groups, as well as with substituents existing on different locations on the aryl ring. Primary, secondary and tertiary alkyl acyl hydrazides were also formed to vary the steric interaction about the amino-carbonyl and number of β-H available.

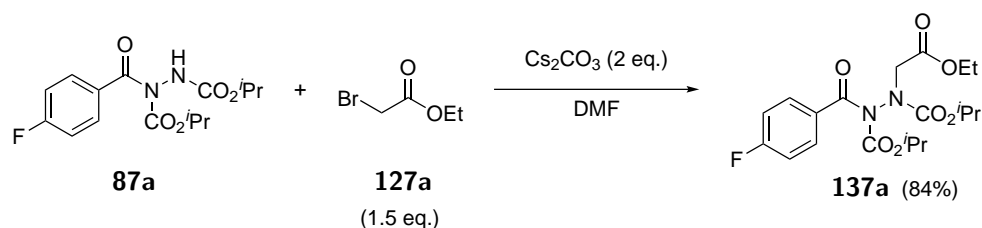


SCHEME 3.6: Aerobic hydroacylation of azodicarboxylates. *Reaction conditions:* azodicarboxylate **63**, (6 mmol, 1.2 eq.), aldehyde **46** (5 mmol, 1 eq.), H₂O (1 mL), 21 °C, 48 h reaction flask exposed to air. ^aReaction time of 120 h. *Novel compound prepared *via* this method.

3.3 Initial Screening

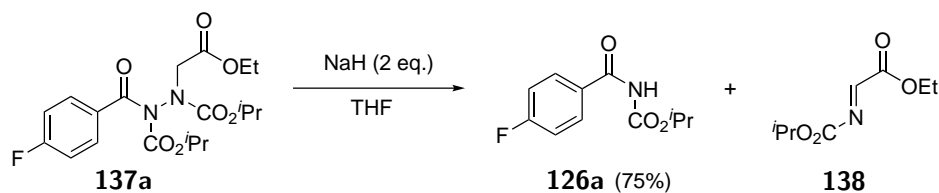
Before the establishment of a two-step, one-pot synthesis, it was important to determine that both reaction steps were feasible. Therefore, the study was initiated with the reaction of acyl hydrazide **87a** and ethyl bromoacetate **127a** in the presence of cesium carbonate, with the aim of forming tetra-alkylated hydrazine **137a** (Scheme 3.7). Gratifyingly, under

the reaction conditions, tetra-alkylated hydrazine **137a** was produced in an efficient yield of 84%. As both the desired alkylation and elimination steps require the use of base, the utilisation of 2 eq. of cesium carbonate is notable as any observation of the *N*-acyl carbamate would imply that the excess cesium carbonate would have been a strong enough base to facilitate the elimination step. As no *N*-acyl carbamate was observed, it was decided that a stronger base was going to be required to facilitate the the elimination step.



SCHEME 3.7: Reaction conditions: **87a** (2 mmol, 1 eq.), **127a** (3 mmol, 1.5 eq.), Cs₂CO₃ (4 mmol, 2 eq.) DMF (6 mL), 21 °C, 24 h.

The tetra-substituted hydrazine was then subjected to strong base NaH with the aim of forming *N*-acyl carbamate **126a**. Pleasingly, the cleavage of the N–N bond was achieved by the use of NaH and afforded the aryl *N*-acyl carbamate product **126a** in a respectable yield (75%). Unfortunately, all efforts to isolate imine **138** were unsuccessful. It is suspected that this electrophilic imine moiety undergoes hydrolysis during an aqueous work-up to form water-soluble byproducts.

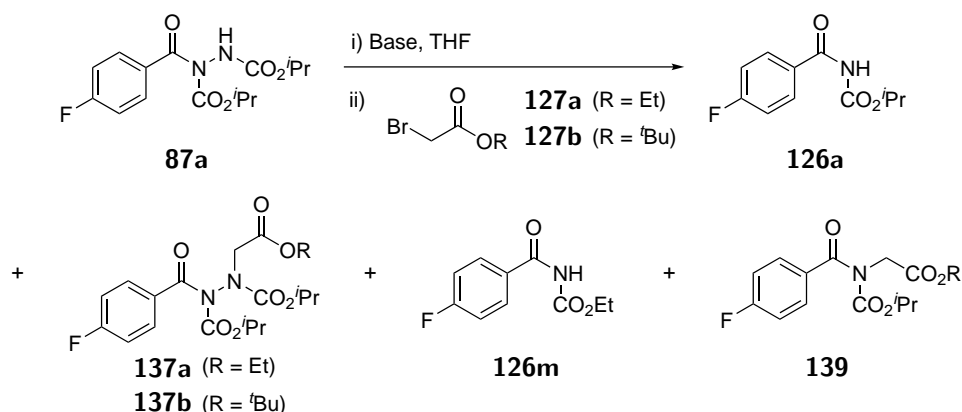


SCHEME 3.8: Reaction conditions: **137a** (1 mmol, 1 eq.), NaH (60% dispersion in mineral oil, 2 eq.) dry THF (2 mL), 21 °C, 24 h.

3.4 Optimisation of *N*-Acyl Carbamate Formation

With good conversions for both alkylation and elimination steps being obtained for the aryl acyl hydrazide **87a**, and the library of acyl hydrazides in hand, it was possible to move onto the optimisation of a one-pot methodology for the reaction. The study began with the reaction of acyl hydrazide **87a** with ethyl bromoacetate **127a** with the aim of

forming acyl carbamate **126a** in a two-step one-pot procedure. Initially, the reaction was carried out under conditions that were developed by Magnus *et al.* for the formation of α -carbamoyl ketals,^{127,128} *i.e.* the use of 1.5 eq. of ethyl bromoacetate and 3 eq. of NaH (although the reaction was conducted at room temperature rather than at 50 °C, Table 3.1, Entry 1). These conditions resulted in the formation of several entities: desired acyl carbamate **126a**; alkylated-hydrazine intermediate **137**; trans-esterified acyl carbamate **126m**; and over-alkylated product **139**.



Entry	R ^a	Base ^b	Base/eq.	126a /%	137 /%	126m /%	139 /%
1	Et (1.5 eq.)	NaH	3	24	38	16	11
2	Et	NaH	3	52	30	6	0
3	Et	NaH	5	69	0	8	0
4	<i>t</i> Bu	NaH	5	83	0	0	0
5	<i>t</i> Bu	NaH	3	58	25	0	0
6	<i>t</i> Bu	Cs ₂ CO ₃	5	0	86	0	0
7 ^c	<i>t</i> Bu	<i>t</i> BuOK	5	0	82	0	0
8	<i>t</i> Bu	NaH (95%)	5	78	0	0	0

TABLE 3.1: Reaction conditions: **87a** (1 mmol), alkyl bromide **127a** or **127b**, 25 °C, 16 h. ^a 1.1 eq. of alkylating agent utilised unless otherwise stated in parenthesis.

^b NaH utilised as a 60% dispersion in mineral oil unless otherwise stated in parenthesis.

^c *t*BuOH utilised as solvent.

Rationally, to limit over-alkylation, the reaction was repeated with 1.1 equivalents of ethyl bromoacetate **127a** (Table 3.1, Entry 2); this completely suppressed formation of over-alkylated product **139**. This also had the additional effect of lowering the yield of trans-esterified acyl carbamate **126m**; suggesting that the ethoxide, which is likely to facilitate the trans-esterification process, may have been liberated from the ethyl

bromoacetate starting material under the basic conditions. Whilst the formation of by-products **139** and **126m** was suppressed by lowering the equivalents of alkylating agent, it was coincident with inadequate conversion of the singly alkylated intermediate **137a** to the desired acyl carbamate **126a**. Most pleasingly, however, simply increasing the equivalents of base from 3 to 5 resulted in full conversion of the intermediate to afford acyl carbamate **126a** in 69% yield (Table 3.1, Entry 3). Whilst the reaction was improved, yields were still limited by the formation of trans-esterified by-product **126m**.

To circumvent the issue, *tert*-butyl bromoacetate **127b** was utilised as the α -bromoacetate source; it was thought that liberation of any free *tert*-butoxide under basic conditions would not result in trans-esterification. Gratifyingly this was the case, with complete suppression of the formation of the trans-esterification product being observed (Table 3.1, Entry 4); this resulted in an 83% yield of the desired product. It also important to note that *tert*-butyl bromoacetate **127b** is more readily obtained and even more economical than its ethyl variant. Lowering the equivalents of base to 3 once again showed incomplete conversion of intermediate, **137b** in this case, to acyl carbamate **127b** (Table 3.1, Entry 5).

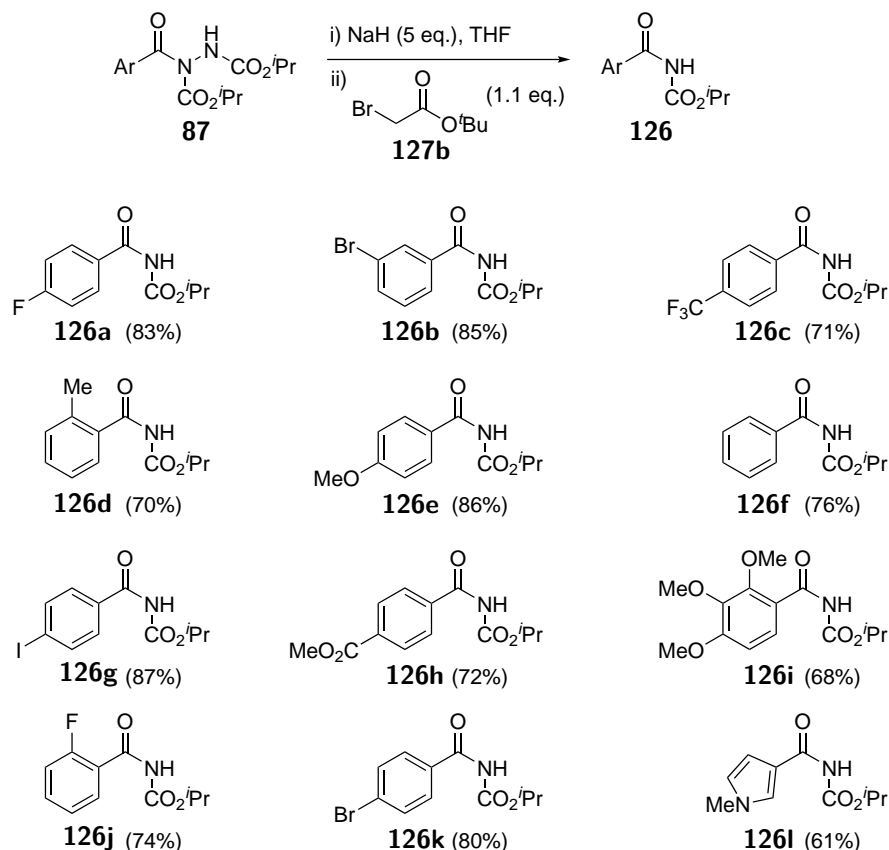
Having established a procedure which led to sole formation of the desired product, the suitability of other bases was appraised (Table 3.1, Entries 6-8). Using Cs_2CO_3 (pKa = 10.3), or *t*BuOK (pKa = 17, reaction in *t*BuOH) only resulted in formation of the alkylated species **137b**, suggesting that at 25 °C for 16 h, these bases were unable to facilitate E1cb elimination. This is perhaps to be expected as the pKa for ester α -H is typically *ca.* 25. Finally, trialling of 95% NaH resulted in a slightly lower yield, 78%, than when using a 60% dispersion in mineral oil.

3.5 Substrate Scope

3.5.1 Aryl

Pleasingly, the reaction was tolerant of various functional groups on the aromatic acyl hydrazide motif, *e.g.* halo, trifluoromethyl, methoxy, ester and methyl functionalities were tolerated with good and consistent yields being observed throughout the series. The

reaction proved to be compatible with electron rich, electron neutral and electron poor moieties, irrespective of the functional groups existing in *ortho*-, *meta*- or *para*-positions on the aryl ring. Gratifyingly, even a sensitive methyl ester functionality was tolerated in the reaction conditions.

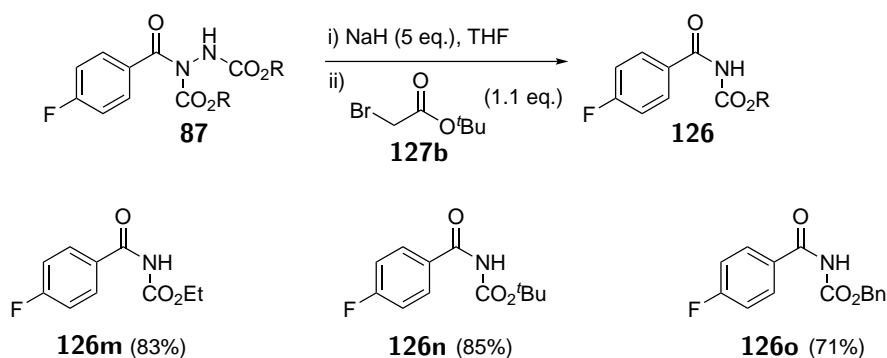


SCHEME 3.9: Reaction conditions: **87** (1 mmol), *tert*-butyl bromoacetate **127b** (1.1 mmol), THF (2 mL), NaH (60% dispersion in mineral oil, 5 mmol), 21 °C.

3.5.2 Carbamate Groups

To further test the scope and attempt to find the limits of the reaction, the tolerance of the reaction with respect to the use of acyl hydrazides that were synthesised from the hydroacylation of azodicarboxylates other than DIAD was then appraised. The optimised reaction conditions allowed for the formation of aryl acyl carbamates with common protecting groups, *e.g.* *tert*-butoxy carbamate (Boc), benzyloxy carbamate (CBz) and ethyl carbamate, in high yields. These acyl carbamates can undergo facile conversion to various species by reaction at the carbamate nitrogen atom before cleavage of the protecting group. It is particularly pleasing that the benzyloxy carbamate (CBz)

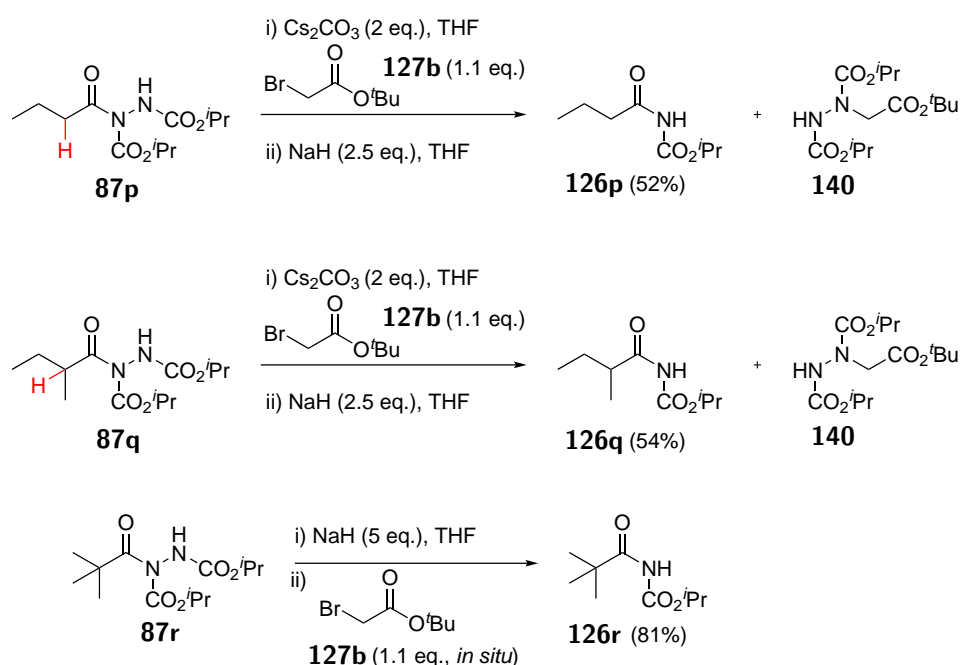
group is unperturbed through the developed methodology as it is not a protecting group that would otherwise survive reductive hydrogenation environments that are typically applied in N–N bond cleavage reactions.



SCHEME 3.10: Reaction conditions: **87** (1 mmol), *tert*-butyl bromoacetate **127b** (1.1 mmol), THF (2 mL), NaH (60% dispersion in mineral oil, 5 mmol), 21 °C.

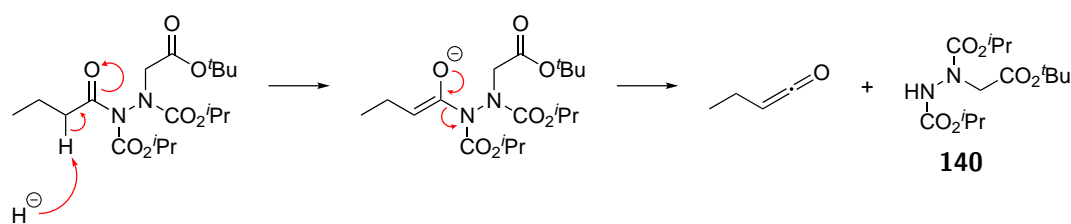
3.5.3 Alkyl

Despite the majority of potent bioactive *N*-acyl carbamates being aryl in their acyl character, the protocol was also tested on alkyl acyl hydrazides. A selection of appropriate acyl hydrazides (*i.e.* primary, secondary and tertiary alkyl examples) prepared using the previously described aerobic C–H activation protocol were trialled under the optimised one-pot procedure. Unfortunately, this only achieved minimal yields of carbamates for the primary and secondary alkyl acyl hydrazides **87p** and **87q**. An alternative step-wise protocol (adapted from the initial step-wise protocol described in Chapter 3.3) provided good yields (Scheme 3.11).



SCHEME 3.11: Conversion of alkyl acyl hydrazides **87p–r** to alkyl acyl carbamates **126p–r**.

The major limitation on yield in all cases was elimination of the hydrazine *via* deprotonation of the α -H (highlighted in red), which was confirmed by isolation of the by-product **140** in a yield that accounted for the mass balance. It is suspected that byproduct **140** is formed through a ketene-formation mechanism (Scheme 3.12). As described in previous work involving acyl hydrazides, the hydrazine-moiety acts as a good leaving group. Consistent with a ketene-formation mechanism (Scheme 3.12), the absence of an α -H acidic proton in tertiary alkyl acyl hydrazide **87r** resulted in a good yield of carbamate **126r**.



SCHEME 3.12: Suspected ketene-formation mechanism for the formation of **140**.

3.6 Conclusions

In conclusion, readily accessed acyl hydrazides are shown to be excellent candidates for the synthesis of *N*-acyl carbamates, which have several applications in terms of their synthetic utility and are often inherently biologically useful (as exemplified by the range of bioactive compounds that bear such a motif). A robust one-pot procedure that is tolerant of a large number of functional groups has been developed; including the synthesis of acyl carbamates with a protecting group on the nitrogen atom – often a key synthetic building block – and adaptability to alkyl & aryl *N*-acyl functionalities. Further to this, the synthetic strategy proposed is complementary to existing traditional approaches for the synthesis of *N*-acyl carbamates, which tend to react acyl halides with carbamates or primary/secondary amides with chloroformates. Furthermore, the ability to cleave the N–N bond without the use of hydrogenation, expensive catalysts and/or undesirable metals was seen as a key aspect in itself.

Chapter 4

Formation of Indazoles from Acyl Hydrazides

4.1 Introduction

The indazole moiety is of great medicinal importance¹²⁹ and compounds containing the indazole nucleus have recently sparked great interest for use as anti-inflammatory,¹³⁰ antitumour^{131,132} and anti-HIV¹³³ agents, and as inhibitors of protein kinase,¹³⁴ HIV-protease,¹³⁵ monoamine oxidase¹³⁶ and *N*-myristoyltransferase,¹³⁷ as well as finding use as a biological probe,¹³⁸ amongst other applications (Figure 4.1). However, most strategies for the synthesis of indazoles are generally limited by their requirement for using complex multi-step syntheses,¹³⁹ and/or using harsh reaction conditions that often promote alternative reaction pathways (*e.g.* undesirable Wolff-Kishner reduction is often observed in hydrazine-based synthesis for the preparation of indazoles)¹⁴⁰ and/or poor functional group tolerance.¹⁴¹ This highlights a general need for synthetic routes that

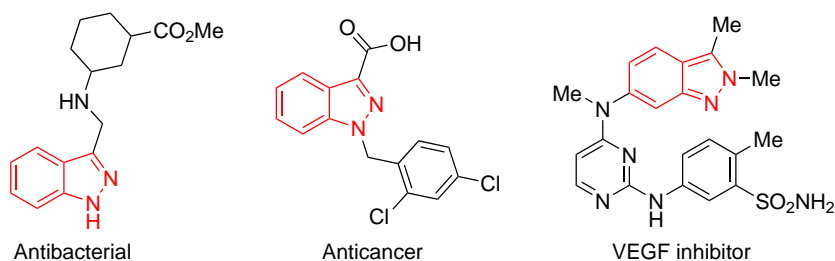
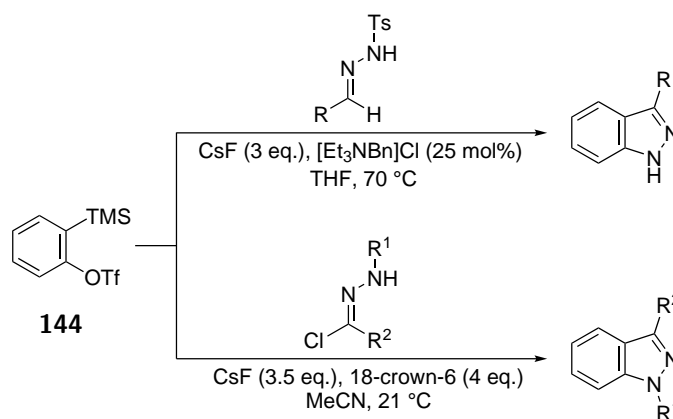


FIGURE 4.1: Examples of bioactive compounds containing the indazole moiety.

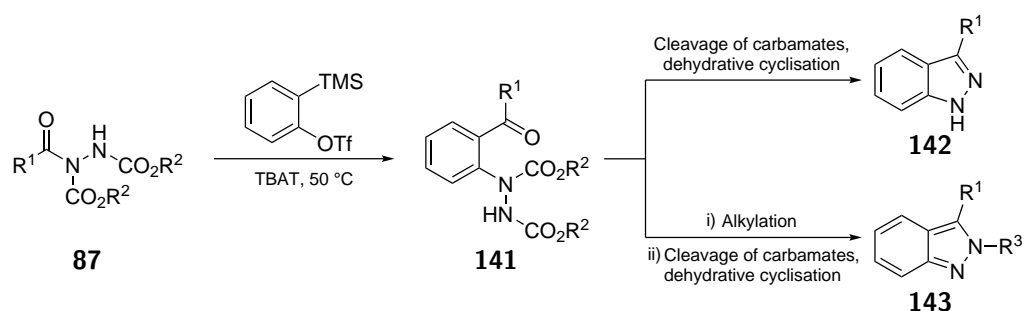
facilitate the synthesis of indazoles, especially those that start from readily accessible starting materials.

Over the past few decades, owing in large part to the plethora of new methodologies that have enabled facile access to arynes,^{142,143} the employment of aryne chemistry in synthesis has seen a major resurgence.^{144–149} A salient feature of aryne chemistry is the possibility for the formation of C–C and C–heteroatom bonds on aryl rings, resulting in the synthesis of various di- and even tri-substituted arenes (*i.e.* if the aryne was already substituted).^{150–152} Owing to this, aryne chemistry has emerged as a very useful method for the synthesis of benzo-fused heterocycles.¹⁵³ Of particular relevance to this thesis is the use of aryne chemistry to synthesise indazoles, *i.e.* through the use of *N*-tosylhydrazones¹⁵⁴ and *in situ* generation of nitrile imines¹⁵⁵ (for *1H*-indazoles, Scheme 4.1) or by using sydnone¹⁵⁶ (for *2H*-indazoles). Whilst these methods have been successfully utilised to selectively afford *1H*- or *2H*-indazoles, the requirement of a phase transfer catalyst additive, limited scope (*i.e.* for the synthesis of 1,3-diarylidindazoles only), and the reliance on the use of precursors that require lengthy/cumbersome syntheses (respectively), highlights several key limitations. Moreover, none of these syntheses provide flexible access to both *1H*- and *2H*-indazoles from a single branch point. As such, despite the inherently favourable nature of aryne chemistry to provide benzo-fused heterocycles, there is still significant scope for development in this area in terms of providing routes to indazoles. This is especially pertinent as currently there is no leading synthetic strategy to synthesise both *1H*- and *2H*-indazoles in a more general sense, *i.e.* outside the scope of aryne-based chemistry.



SCHEME 4.1: Previous aryne-based methods for the synthesis of *1H*-indazoles.^{154,155}

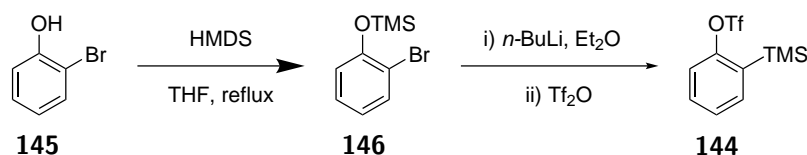
Previous work in the Chudasama group has displayed the utility of acyl hydrazides **87** as acyl halide analogues, where nucleophilic species can attack the acyl group with the protected hydrazine moiety acting as a leaving group (Chapter 1.6.1).^{85,86} The previous chapter also demonstrated the nucleophilic property of the nitrogen lone pair present in acyl hydrazides (Chapter 3).¹¹² In this work, it was envisioned that the reaction of an aryne with an acyl hydrazide would exploit both of these synthetic properties to facilitate a molecular rearrangement reaction pathway that would lead to the synthesis of 2-hydrazobenzophenones **141**. These entities could then act as a single branch point for conversion into 1*H*-indazoles **142** or 2*H*-indazoles **143** by exploiting the removal of the carbamate groups pre- and post-alkylation (Scheme 4.2).



SCHEME 4.2: General method for the synthesis of 2-hydrazobenzophenones **141** from acyl hydrazides **87** *via* benzyne chemistry and how they are proposed for use as a single branch point for the formation of 1*H*- and 2*H*-indazoles (**142** and **143** respectively).

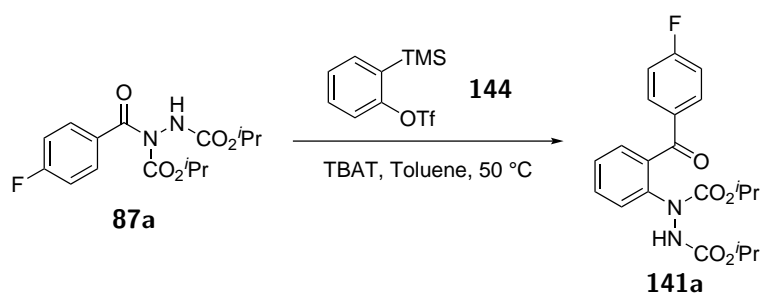
4.2 Initial Screening

Our study began with the reaction of acyl hydrazide **87a** with benzyne precursor **144** in the presence of fluoride source tetrabutylammonium difluorotriphenylsilicate (TBAT), with the aim of forming 2-hydrazobenzophenone **141a** *via* a novel molecular rearrangement pathway (see Scheme 4.13 below for more detail on mechanism studies). Benzyne precursor **144** was prepared *via* a simple route as described in the literature (Scheme 4.3).¹⁵⁷



SCHEME 4.3: Synthesis of benzyne precursor **144**.

Initially, the reaction was carried out under the conditions developed by Pintori *et al.* for the aryl insertion of arynes into amide C(O)–N bonds, *i.e.* the use of 1.5 equivalents of benzyne precursor **144**, 2 equivalents of TBAT and toluene as the reaction solvent at 50 °C. Pleasingly, the reaction proceeded efficiently, resulting in the formation of desired product **141a** in 86% yield (Table 4.1, Entry 1). Moreover, no *N*-arylated starting material was observed, a common issue when utilising primary or secondary amides in the presence of arynes. Lowering the equivalents of fluoride source in the reaction resulted in incomplete conversion of acyl hydrazide **87a** and thus had a negative impact on yield (Table 4.1, Entries 2 & 3).



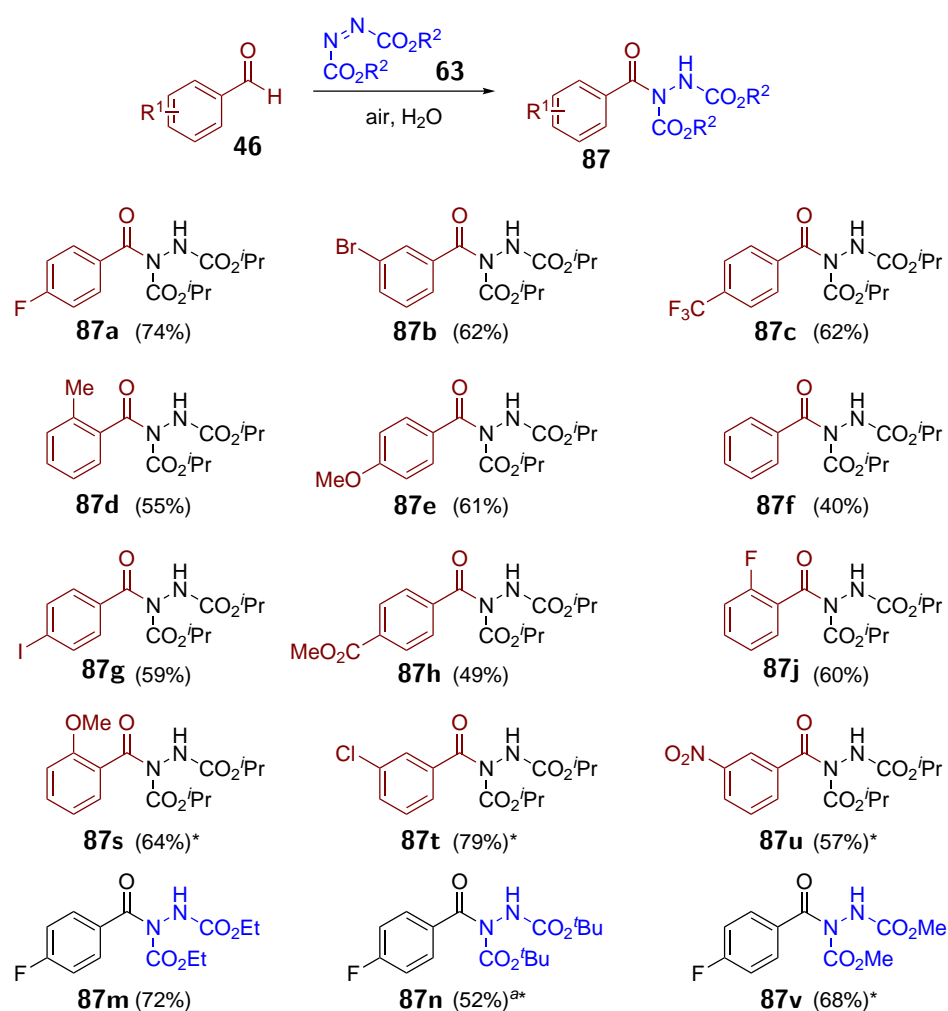
Entry	144 /eq.	TBAT/eq.	Conversion of 87a /%	141a /%
1	1.5	2	100	86
2	1.5	1.5	76	59
3	1.5	1	54	38

TABLE 4.1: Reaction conditions: acyl hydrazide **87a** (0.5 mmol, 1 eq.), benzyne precursor **144** (0.75 mmol, 1.5 eq.) and TBAT in toluene (6 mL); 50 °C for 16 h.

4.3 Formation of Acyl Hydrazides

Following the positive indication for the formation of 2-hydrazobenzophenone **141a** from acyl hydrazide **87a**, a range of acyl hydrazides were thus synthesised (**87a–h,j,s–u**) to trial under the reaction conditions. All starting acyl hydrazides were prepared in good yields using the aerobic hydroacylation pathway in good to excellent yields (Scheme 4.4).

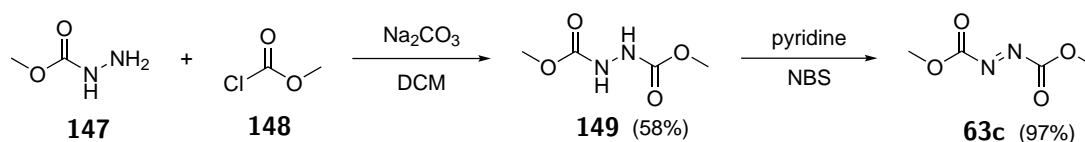
Furthermore, aryl acyl hydrazides with methyl-carbamate, ethyl-carbamate and *tert*-butyl (Boc) protecting groups were synthesised. Since dimethyl azodicarboxylate **63c** is not commercially available, it had to be synthesised prior to aerobic-based hydroacylation



SCHEME 4.4: Aerobic hydroacylation of azodicarboxylates.

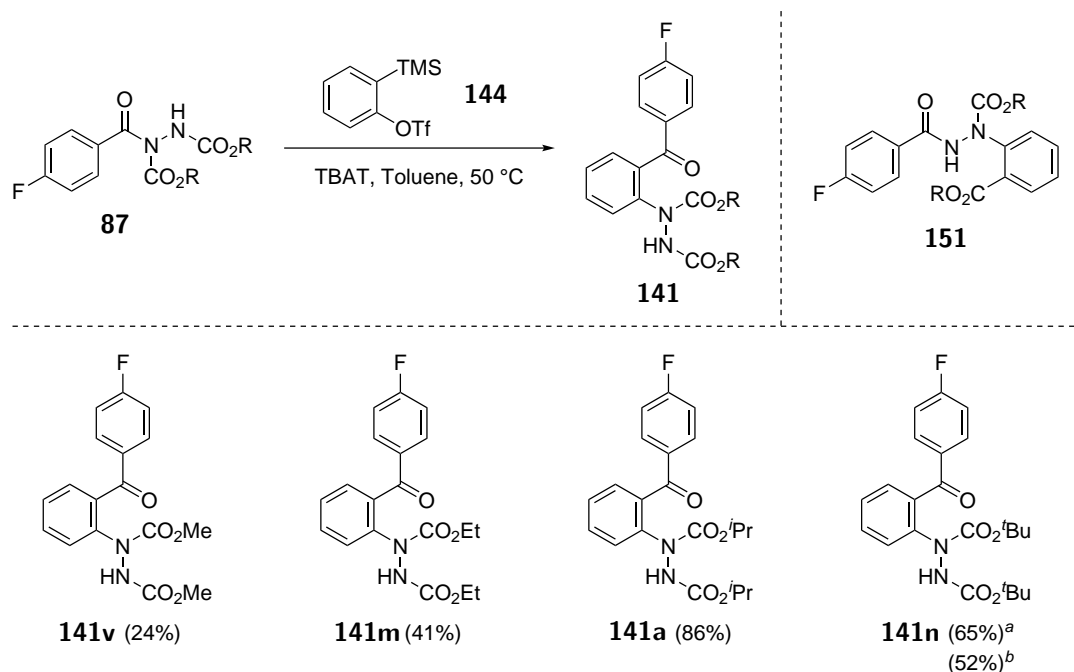
Reaction conditions: azodicarboxylate **63a**, (6 mmol, 1.2 eq.), aldehyde **46** (5 mmol, 1 eq.), H₂O (1 mL), 21 °C, reaction flask exposed to air. ^aReaction time of 120 h. *Novel compound prepared *via* this method.

with 4-fluorobenzaldehyde to form the methyl-carbamate protected acyl hydrazide **87v**. This was achieved in a 2-step process. The first involved acylation of methyl carbamate **147** with methyl chloroformate **148**. Subsequent oxidation of compound **149** using *N*-bromosuccinimide and pyridine yielded product **63c** (Scheme 4.5).

SCHEME 4.5: Preparation of dimethyl azodicarboxylate **63c**.

4.4 Examination of Carbamate Scope

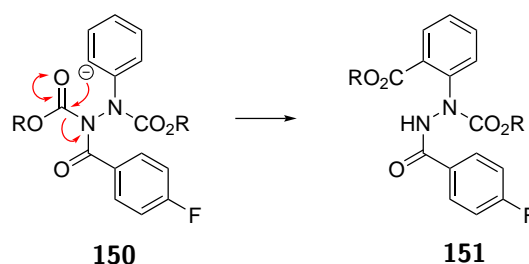
The selection of acyl hydrazides displaying different carbamate groups were then individually subjected to the aryl insertion reaction (1.5 equivalents of benzyne precursor **144** and 2 equivalents of TBAT in toluene at 50 °C for 16 h) to appraise the feasibility of the carbamate protecting groups under the reaction conditions.



SCHEME 4.6: *Reaction conditions:* acyl hydrazide **87**, (0.5 mmol, 1 eq.), benzyne precursor **144** (0.75 mmol, 1.5 eq.) and TBAT (1 mmol, 2 eq.) in toluene (6 mL); 50 °C for 16 h. ^a 80% conversion of starting material. ^b 2 eq. of **144** and 3 eq. of TBAT was added, 82% conversion of starting material.

It was observed that the methyl- and ethyl-carbamate containing acyl hydrazides afforded their respective desired 2-hydrazobenzophenone in low yield (Scheme 4.6). Analysis of the reaction mixture when using methyl-carbamate **87v** revealed the formation of a significant amount, 49% yield, of compound **151** (where R = Me). This accounted for a significant portion of the mass balance as the reaction did show complete conversion of acyl hydrazide starting material. The formation of by-product **151** (where R = Me) can be rationalised by competing attack of the intermediate carbanionic species on the carbamate carbonyl (Scheme 4.7).

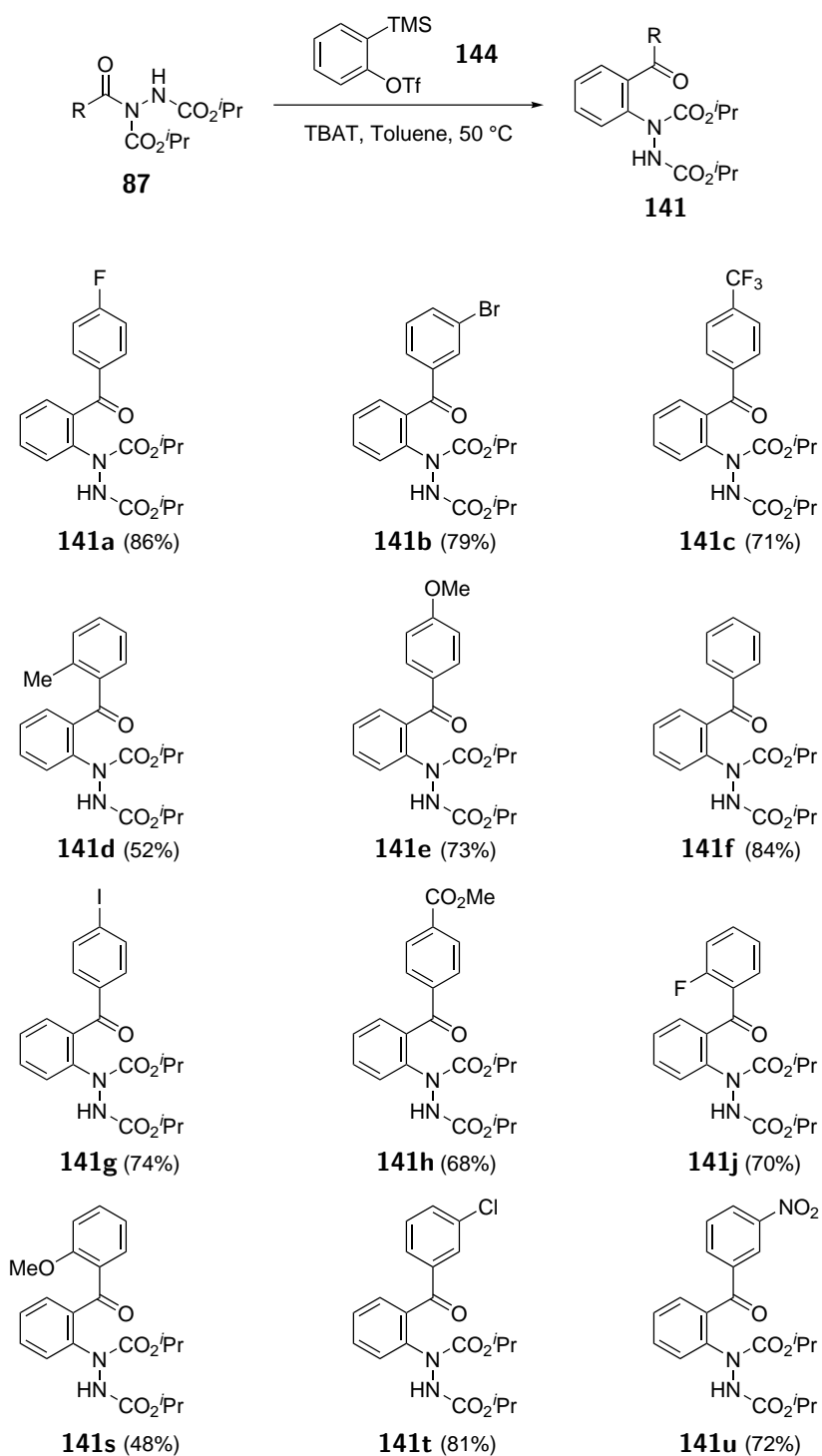
NMR analysis of the crude mixture when employing ethyl-carbamate **87m** as the acyl hydrazide component also showed the presence of a substantial amount of by-product

SCHEME 4.7: Proposed mechanism for the formation of by-product **151**.

species **151** (where R = Et). It was thus rationalised that the high yield observed when using an isopropyl group was due to the increased steric hindrance about the carbamate-carbonyl. In line with this, it was anticipated that the use of a bulkier Boc-protected acyl hydrazide **87n** would result in a more efficient reaction (Scheme 4.6). However, under the reaction conditions, the Boc-protected acyl hydrazide resulted in incomplete conversion of acyl hydrazide **87n**. Increasing the equivalents of benzyne precursor **144** and TBAT, had minimal impact on conversion and resulted in an even lower yield. Analysis of the reaction showed formation of various unidentifiable side-products despite several attempts to isolate each species, but the formation of a by-product of the form of compound **151** was not observed by crude NMR. In conclusion, it appears that the isopropyl groups strike a good balance of offering high conversion of **87a** and yield of **141a** with minimal byproduct formation (Scheme 4.6), and compounds of the form of **141a** were chosen for further studies.

4.5 Formation of 2-hydrazobenzophenones

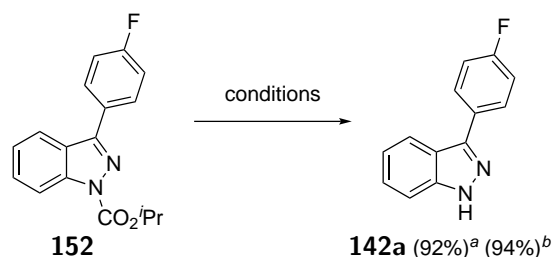
With optimised conditions for the transformation of acyl hydrazides into desired 2-hydrazobenzophenones in-hand, and the isopropyl carbamate group having been established as the optimal group for reaction with benzyne, the opportunity was then taken to investigate the applicability of the protocol for the formation of various 2-hydrazobenzophenones (Scheme 4.8). Gratifyingly, the reaction of acyl hydrazides **87a–h,j,s–u** with benzyne was tolerant of various functional groups on the aromatic acyl hydrazide motif, *e.g.* electron-withdrawing (halo, trifluoromethyl, ester, nitro), electron-rich (methyl, methoxy) and electron-neutral (unsubstituted) functionalities. Unfortunately, the presence of *ortho*-functional groups on the aryl ring resulted in a lower



SCHEME 4.8: Reaction conditions: acyl hydrazide **87a–h,j,s–u** (0.5 mmol, 1 eq.), benzyne precursor **144** (0.75 mmol, 1.5 eq.) and TBAT (1 mmol, 2 eq.) in toluene (6 mL); 50 °C for 16 h.

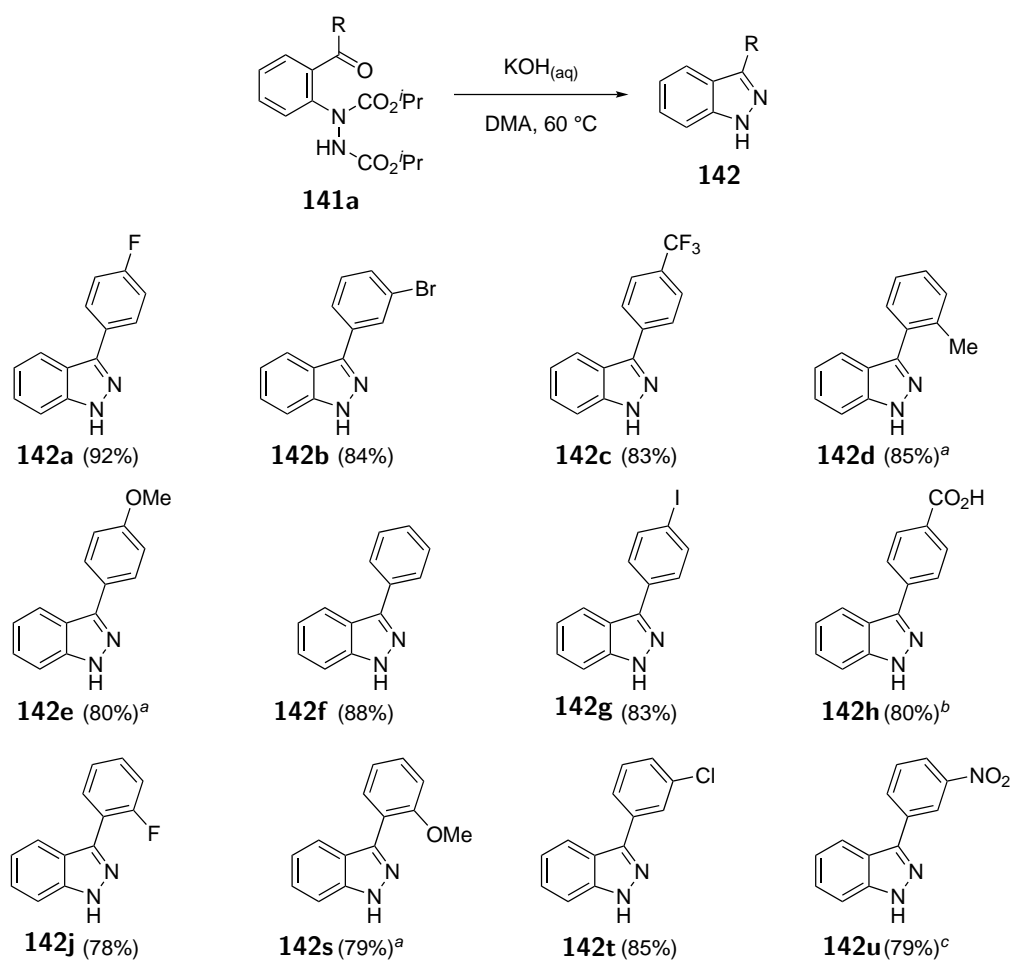
yield of the desired product. This is likely due to increased steric hinderance about the amide-like carbonyl promoting carbanionic attack on the γ -carbamate carbonyl to form compounds of the form of **151**. This hypothesis is further substantiated by the ortho-fluoro

by subjecting it to either the 12 M HCl or KOH reaction conditions (Scheme 4.9). It can be speculated that this could be particularly useful in transformations that require the N–H position of the indazole to be protected, and where both an acidic and a basic option for deprotection is available.



SCHEME 4.9: Deprotection of carbamate-protected 1*H*-indazole. ^aKOH conditions. ^bHCl (12 M) conditions.

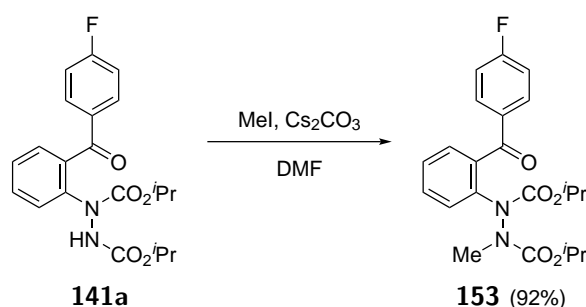
Having established suitable conditions for the removal of the isopropyl carbamate groups and dehydrative cyclisation, the previously formed library of 2-hydrazobenzophenones **141w** were subjected to the relatively mild basic reaction conditions for the formation of various 1*H*-indazoles (Scheme 4.10). Most pleasingly, excellent yields were observed across the series with the exception of the 2-hydrazobenzophenone containing the nitro functionality. Fortunately, and highlighting the advantage of being able to employ either basic or acidic conditions, subjecting nitro 2-hydrazobenzophenone **141x** to the developed acidic reaction conditions resulted in a high yield, 79%. It should also be noted that whilst it is out of the scope of this thesis, 1*H*-indazoles can be readily 1*H*-alkylated *via* several reported procedures.



SCHEME 4.10: Reaction conditions: **141a–h,j,s–u** (0.25 mmol, 1 eq.), KOH (1.00 mmol, 4 eq. in H₂O (3 mL)), DMA (5 mL); 60 °C for 16 h. ^a Reaction was carried out at 100 °C. ^b using **141h** as 2-hydroazobenzophenone, ^c HCl (12 M) conditions.

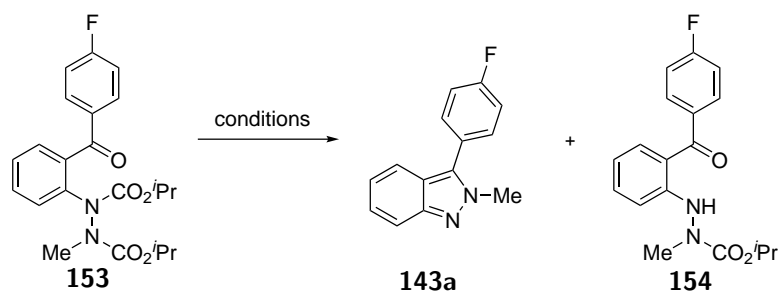
4.7 Formation of 2*H*-indazoles

Compared to 1*H*-indazoles, 2*H*-indazoles have historically been more challenging to prepare. As a result, 2*H*-indazoles have been far less studied. From the outset, the establishment of a method in which the synthesis of *N*-substituted 2*H*-indazoles could be enabled from a common intermediate to that used in the synthesis of the 1*H*-indazoles was a desirable target. It was postulated that alkylation of 2-hydrazobenzophenones prior to carbamate removal (and subsequent dehydrative cyclisation) would result in the selective formation of *N*-substituted 2*H*-indazoles. To appraise this, alkylation of 2-hydrazobenzophenone **141a** was carried out to form alkylated 2-hydrazobenzophenone **153** (Scheme 4.11).



SCHEME 4.11: *Reaction Conditions:* 2-hydrazobenzophenone **141a** (0.50 mmol, 1.0 eq.), iodomethane (0.55 mmol, 1.1 eq.) and Cs₂CO₃ (0.55 mmol, 1.1 eq.) in DMF (5 mL); 21 °C for 16 h.

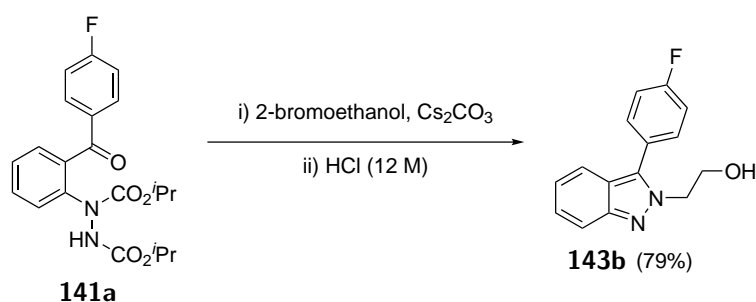
Compound **153** was then subjected to the various deprotection conditions (see Table 4.3) to try and form *N*-methylated 2*H*-indazole **143a**. Fortunately, refluxing HCl (12 M) resulted in the formation of desired *N*-methyl 2*H*-indazole. Use of refluxing AcOH or aqueous KOH in dimethylacetamide only resulted in cleavage of the internal carbamate, forming undesired product **154**; although it should be noted that this product was formed selectively and in good yield.



Entry	Reagent	Solvent	Temperature/°C	Yield/%	Yield/%
1	AcOH	-	Reflux	0	70
2	HCl (12 M)	-	Reflux	91	0
3	KOH (3 M)	DMA	60	0	84

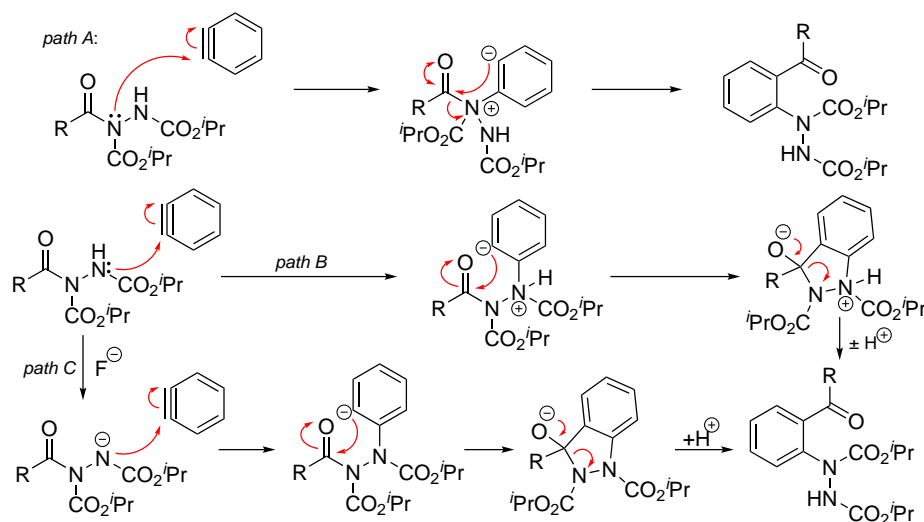
TABLE 4.3: *Reaction conditions:* alkylated 2-hydrazobenzophenone **153** (0.5 mmol) under varying conditions for 16 h. DMA = dimethylacetamide

Having successfully formed 2*H*-indazole **143a** *via* alkylation and subsequent removal of carbamates, the reaction sequence was then applied successfully for the formation of functional 2*H*-indazole **143b** (Scheme 4.12) in 79% yield from 2-hydrazobenzophenone **141a** over 2 steps.

SCHEME 4.12: Formation of functional 2*H*-indazole **143b**.

4.8 Mechanistic Studies

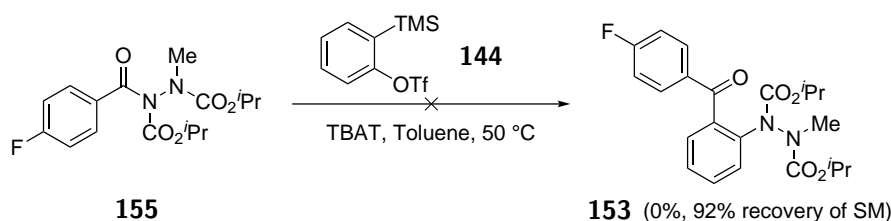
It was then decided to probe the mechanism for the reaction of acyl hydrazide and benzyne. It was important to note, as the starting point, that acyl hydrazides have previously been shown to act as acyl halide analogues, and acyl halides & amides have been shown to react with benzyne *via* an aryl insertion mechanism where the aryne is inserted into the C-halogen σ -bond. Therefore, aryne insertion into the C(O)- α -N bond was considered as a plausible mechanistic pathway (Scheme 4.13, path A). Alternatively, it should be considered that acyl hydrazides can react nucleophilically at the β -N atom and that this position may or may not be deprotonated under the reaction conditions (Scheme 4.13, path B & C, respectively). Therefore, it was necessary to establish whether



SCHEME 4.13: Possible reaction mechanisms.

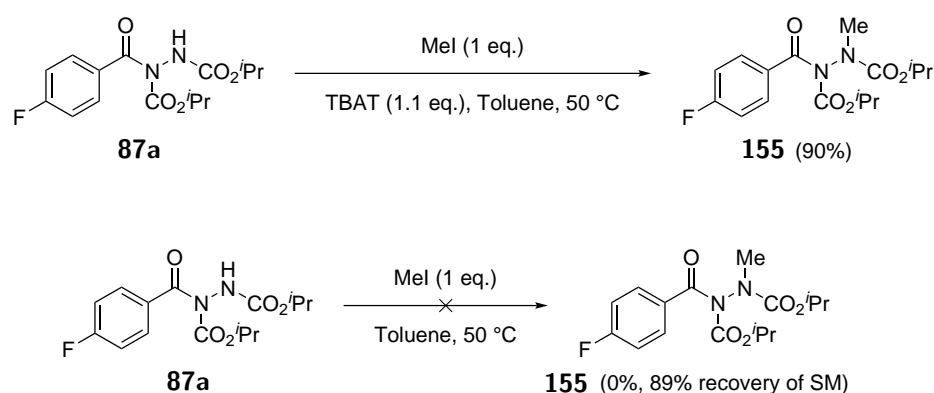
arynes inserts into the C-N σ -bond in acyl hydrazides (Scheme 4.13, path A) or whether it undergoes a novel molecular rearrangement following nucleophilic attack from the more nucleophilic nitrogen atom (Scheme 4.13, paths B & C).

To explore the feasibility of the reaction pathways, methylated acyl hydrazide **155** was synthesised and subject to the aryne functionalisation reaction conditions (Scheme 4.14). Under the reaction conditions, no reaction between the methylated acyl hydrazide **155** and benzyne was observed. If the reaction pathway was proceeding *via* path A, then it would have been expected that methylated 2-hydrazobenzophenone product **153** would have formed under these conditions. The almost quantitative recovery of starting material suggested that the presence of the N–H bond in acyl hydrazides is important for the reaction to proceed.



SCHEME 4.14: Mechanistic evaluation of path A.

Therefore, it was next evaluated whether the acyl hydrazide was deprotonated under the reaction conditions, owing to the acidity of the N–H bond. To do this, acyl hydrazide **87a** was reacted with 1.1 eq. of iodomethane in the presence of 1.1 eq. of TBAT in toluene at 50 °C (Scheme 4.15). A control experiment with the absence of TBAT was conducted in parallel. It was observed that in the presence of TBAT, a significant amount of methylated acyl hydrazide **155**, 90%, was observed (Scheme 4.15). In the absence of TBAT, a near quantitative amount of starting material was recovered. We therefore felt it appropriate to conclude that an acyl hydrazide would be significantly deprotonated under the reaction conditions, and suggest that the reaction proceeds through novel molecular reaction path C (Scheme 4.13).



SCHEME 4.15: Mechanistic evaluation of paths B & C.

4.9 Conclusions

In conclusion, a novel molecular rearrangement pathway involving reaction of readily accessed acyl hydrazides with arynes to provide an intermediate that can be readily converted into either a *1H*- or *2H*-indazole, as desired has been established. The developed reaction conditions enable their synthesis from a single intermediate branch point (*i.e.* providing a highly diverse synthetic route), unveil a novel molecular rearrangement pathway and are tolerant of a range of functional groups enabling the *1H*-indazoles to be formed under either basic or acidic conditions (*i.e.* a highly flexible route). In view of this, the protocols for the facile synthesis of *1H*- and *2H*-indazoles from acyl hydrazides can have wide ranging applications, especially as indazoles are applied in a broad range of medicinal/biological applications. Moreover, the novel reaction pathway that is disclosed may lead to further exploitation of, or inspiration in, aryne-based molecular rearrangements.

Chapter 5

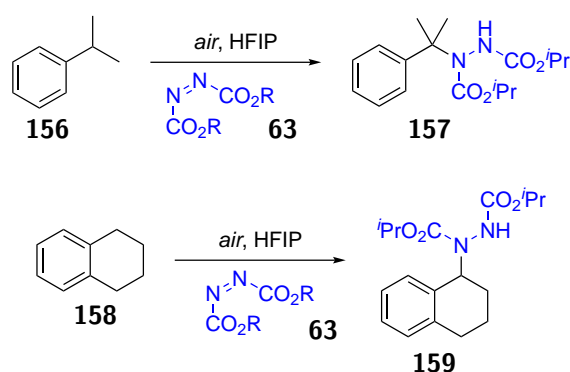
Summary & Future Work

The work conducted out in preparation of this thesis has resulted in the development and optimisation of three synthetic procedures. The first describes aerobically-initiated α -C(sp^3)-H amination of ethers through the use of activated azodicarboxylates (Chapter 2). The procedure is found to work particularly efficiently in the amination of cyclic ethers and acetals and evidence for the activation of azodicarboxylates through a H-bonding interaction with the fluorinated alcohol solvent is provided through experimental and theoretical investigation.

The second developed procedure describes the one-pot conversion of acyl hydrazides into *N*-acyl carbamates *via* metal-free ionic-based rupture of the N–N linkage (Chapter 3). *N*-acyl carbamates have several applications in terms of their synthetic utility and are often inherently biologically useful. The use of readily accessed acyl hydrazides is of great benefit as many analogues bearing various functional groups can be prepared efficiently in an aerobically-mediated manner.

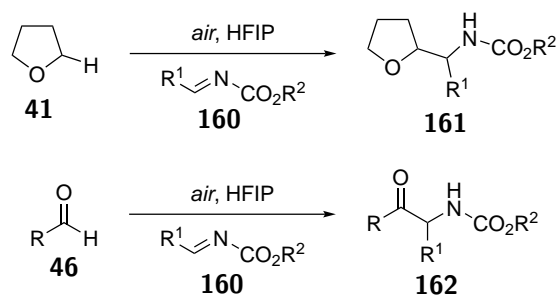
Finally, a synthetic procedure is established to access both pharmaceutically-relevant 1*H*- and 2*H*-indazoles from acyl hydrazides by exploiting a novel aryne-based molecular rearrangement (Chapter 4). The developed methodology forms the initial 2-hydrazobenzophenone intermediate, of which the rearrangement pathway is established through mechanistic analysis. This intermediate acts as a useful branch point for simple access to either indazole tautomer.

Future work in this project will involve the investigation of chemicals which have been reported to undergo auto-oxidation under air with the aim of utilising radical acceptor agents to selectively trap radical species generated by aerobic C–H bond activation. As work in the Chudasama group has primarily focused on exploiting the aerobic C–H bond activation of aldehydes (and has now been extended to ethers and acetals) to form new products, other moieties with a literature precedent for auto-oxidation will be trialled to determine if aerobic C–H bond activation can be further extended. In particular relating to work in this thesis, the use of fluorinated alcohols has been determined to increase the susceptibility of azodicarboxylates to radical attack. It is anticipated that this interaction will provide new opportunities for X–N bond formations (Scheme 5.1).



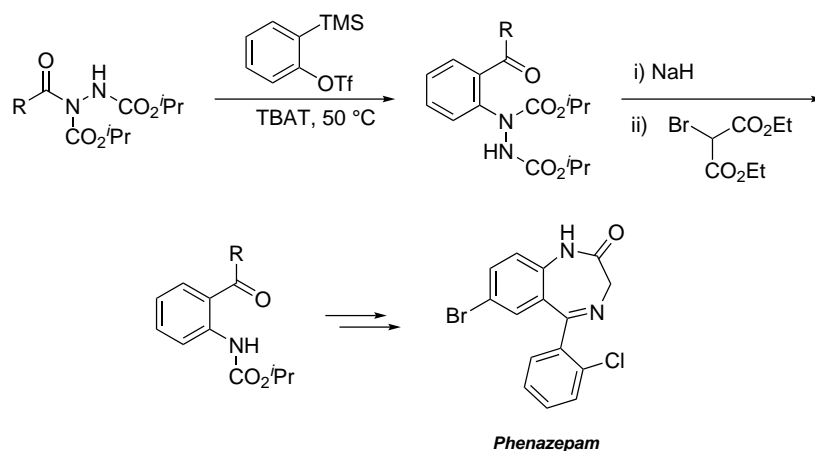
SCHEME 5.1: Potential use of the fluorinated alcohol-azodicarboxylate interaction for aerobic benzylic C–N bond formation.

Furthermore, this interaction could potentially be extended to increasing the ability of molecules with unsaturated C=N bonds to act as efficient radical acceptors (Scheme 5.2). Doing so could potentially lead to novel C–C bond formation pathways.



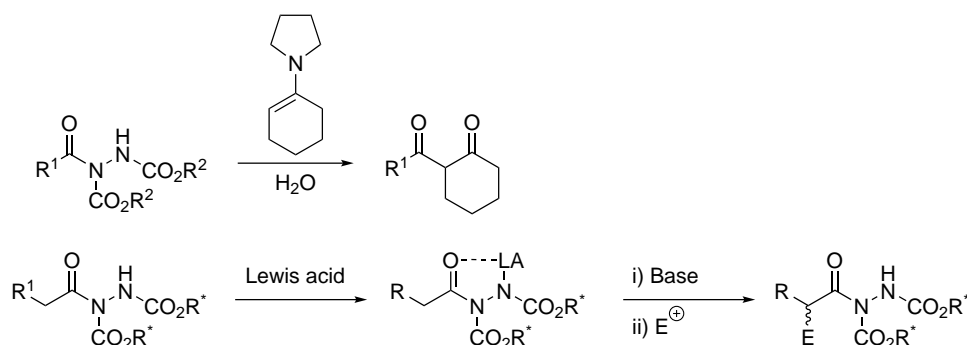
SCHEME 5.2: Potential interaction between fluorinated alcohol and imines for aerobic C–C bond formation.

The ionic based N–N bond cleavage and aryne-based methodologies described in this thesis have already found further use, inspiring a two-step protocol for the formation of 2-aminobenzophenones from acyl hydrazides (Scheme 5.3).¹⁵⁸ These species are paramount in the synthesis of a plethora of pharmaceutically-relevant compounds,¹⁵⁹ and the protocol developed was utilised in the total synthesis of benzodiazepine phenazepam.



SCHEME 5.3: Formation of 2-aminobenzophenones from acyl hydrazides.

Acyl hydrazides still represent an under-utilised functional group and further protocols utilising acyl hydrazides as starting materials could potentially be developed (Scheme 5.4). As acyl hydrazides have been shown to be susceptible to nucleophilic attack, previously untried nucleophiles could potentially be trialled, specifically carbon-based nucleophiles for C–C bond formation. Finally, the reactivity of the N–H bond in acyl hydrazides could potentially be utilised in complex chemistry akin to that of chiral auxiliaries. It could be envisaged that the use of chiral alkyl carbamate groups on acyl hydrazides could bias the stereoselectivity of reactions utilising an enolate-intermediate formed upon removal of an α -H atom.



SCHEME 5.4: Potential further reactions utilising acyl hydrazides as starting materials.

Chapter 6

Experimental

General Experimental

Chemicals

All reagents were purchased from Aldrich or AlfaAesar and were used as received without further purification unless otherwise stated.

Solvents

Where described below, petrol refers to petroleum ether (b.p. 40-60 °C).

Chromatography

All reactions were monitored by thin-layer chromatography (TLC) on pre-coated silica gel plates. Silica gel plates were initially examined under short wave UV light and then developed using aqueous potassium permanganate stain. Flash column chromatography was carried out with pre-loaded GraceResolv™ flash cartridges on a Biotage® Isolera Spektra One flash chromatography system.

Spectroscopy

Quoted yields refer to chromatographically and spectroscopically pure compounds unless otherwise stated. ¹H NMR spectra were recorded at 600 MHz or 700 MHz and ¹³C NMR at 151 MHz or 176 MHz on a Bruker Avance III 600 or Bruker Avance Neo 700 spectrometer. The chemical shifts (δ) for ¹H and ¹³C are quoted

relative to residual signals of the solvent on the parts per million (ppm) scale. Coupling constants (J values) are reported in Hertz (Hz) and are reported as J_{H-H} unless otherwise stated. Signal multiplicities in ^{13}C NMR were determined using the distortionless enhancement by polarisation transfer (DEPT) spectral editing technique.

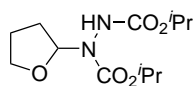
Miscellaneous

Melting points were measured with a Gallenkamp apparatus and are uncorrected.

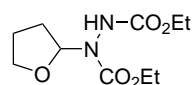
6.1 Experimental for Chapter 2

General experimental for the formation of ether hydrazides

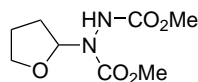
To a solution of azodicarboxylate (1.00 mmol, 1 eq.) in fluorinated alcohol (0.5 mL) was added ether (5.00 mmol, 5 eq.). The reaction mixture was stirred at 80 °C at 1050 rpm for the time specified below and then poured over sat. aq. NaHCO₃ (20 mL). The resulting mixture was extracted with EtOAc (3 × 15 mL). The combined extracts were dried (MgSO₄), filtered and the solvent evaporated *in vacuo*. The resultant crude residue was purified as described below.

Diisopropyl 1-(tetrahydrofuran-2-yl)hydrazine-1,2-dicarboxylate 109a¹⁶⁰

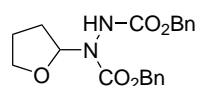
Compound prepared using HFIP as the reaction solvent and a reaction duration of 48 h. Purification by column chromatography (10%-50% EtOAc/Petrol) afforded diisopropyl 1-(tetrahydrofuran-2-yl)hydrazine-1,2-dicarboxylate as a white solid (252 mg, 0.920 mmol, 92%). ¹H NMR (700 MHz, CDCl₃) δ 6.60-6.28 (m, NH, 1H), 6.25-5.83 (m, 1H), 4.98-4.90 (m, 2H), 3.96 (dt, *J* = 7.0 Hz, 1H), 3.73 (dt, *J* = 7.1 Hz, *J* = 7.1 Hz, 1H), 2.10-1.91 (m, 3H), 1.88-1.82 (m, 1H), 1.23 (d, *J* = 6.3 Hz, 12H); ¹³C NMR (151 MHz, CDCl₃) δ 156.5 (C), 155.2 (C), 87.3 (CH), 70.7 (CH), 70.2 (CH), 69.9 (CH), 68.8 (CH₂), 29.8 (CH₂), 29.8 (CH₂), 28.4 (CH₂), 28.1 (CH₂), 25.4 (CH₂), 22.1 (CH₃), 22.1 (CH₃), 22.0 (CH₃); IR (solid) 3261, 2974, 2932, 2856, 1731, 1701 cm⁻¹.

Diethyl 1-(tetrahydrofuran-2-yl)hydrazine-1,2-dicarboxylate 109b¹⁰²

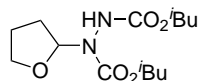
Compound prepared using HFIP as the reaction solvent and a reaction duration of 48 h. Purification by column chromatography (10%-50% EtOAc/Petrol) afforded diethyl 1-(tetrahydrofuran-2-yl)hydrazine-1,2-dicarboxylate as a clear oil (232 mg 0.940 mmol, 94%). ¹H NMR (600 MHz, CDCl₃) δ 6.50-6.18 (m, NH, 1H), 6.12-5.87 (m, 1H), 4.25-4.19 (m, 4H), 3.99 (dt, *J* = 7.1 Hz, *J* = 7.1 Hz, 1H), 3.76 (dt, *J* = 7.1 Hz, *J* = 7.1 Hz, 1H), 2.09-1.94 (m, 3H), 1.91-1.84 (m, 1H), 1.30-1.24 (m, 6H); ¹³C NMR (151 MHz, CDCl₃) δ 156.9 (C), 155.7 (C), 87.7 (CH), 68.8 (CH₂), 63.0 (CH₂), 62.3 (CH₂), 28.4 (CH₂), 25.4 (CH₂), 14.5 (CH₃), 14.5 (CH₃); IR (thin film) 3282, 2982, 2972, 2875, 1718 cm⁻¹.

Dimethyl 1-(tetrahydrofuran-2-yl)hydrazine-1,2-dicarboxylate 109c¹⁰²

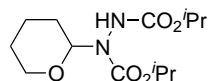
Compound prepared using HFIP as the reaction solvent and a reaction duration of 48 h. Purification by column chromatography (10%-50% EtOAc/Petrol) afforded dimethyl 1-(tetrahydrofuran-2-yl)hydrazine-1,2-dicarboxylate as a clear oil (179 mg, 0.82 mmol, 82%). ¹H NMR (700 MHz, CDCl₃) δ 6.99-6.77 (m, NH, 1H), 5.93 (s, 1H), 3.93 (dd, *J* = 7.1, 6.9 Hz, 1H), 3.71 (s, 6H), 3.71 (app. s, 1H), 2.06-1.89 (m, 3H), 1.86-1.79 (m, 1H); (176 MHz, CDCl₃) δ 157.4 (C), 156.2 (C), 87.7 (CH), 68.7 (CH₂), 53.8 (CH₃), 53.1 (CH₃), 28.2 (CH₂), 25.3 (CH₂); IR (thin film) 3306, 2984, 2939, 1750, 1732 cm⁻¹.

Dibenzyl 1-(tetrahydrofuran-2-yl)hydrazine-1,2-dicarboxylate 109d¹⁰²

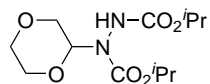
Compound prepared using HFIP as the reaction solvent and a reaction duration of 48 h. Purification by column chromatography (10%-50% EtOAc/Petrol) afforded dibenzyl 1-(tetrahydrofuran-2-yl)hydrazine-1,2-dicarboxylate as a white solid (267 mg, 0.720 mmol, 72%). ¹H NMR (600 MHz, CDCl₃) δ 7.35-7.26 (m, 10H), 7.12 (br s, NH, 1H), 6.02 (s, 1H), 5.20-5.09 (m, 4H), 3.94 (dt, *J* = 7.1 Hz, *J* = 7.1 Hz, 1H), 3.71 (dt, *J* = 7.1 Hz, *J* = 7.1 Hz, 1H), 2.08-1.86 (m, 3H), 1.84-1.75 (m, 1H); ¹³C NMR (151 MHz, CDCl₃) δ 156.8 (C), 155.6 (C), 135.9 (C), 135.8 (C), 128.7 (CH), 128.7 (CH), 128.5 (CH), 128.4 (CH), 128.3 (CH), 128.1 (CH), 87.8 (CH), 68.8 (CH₂), 68.4 (CH₂), 67.9 (CH₂), 28.4 (CH₂), 25.3 (CH₃); IR (solid) 3287, 3067, 3034, 2970, 2894, 1742, 1706, 1686 cm⁻¹.

Diisobutyl 1-(tetrahydrofuran-2-yl)hydrazine-1,2-dicarboxylate 109e

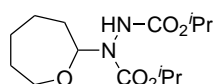
Compound prepared using HFIP as the reaction solvent and a reaction duration of 48 h. Purification by column chromatography (10%-50% EtOAc/Petrol) afforded diisobutyl 1-(tetrahydrofuran-2-yl)hydrazine-1,2-dicarboxylate as a white solid (266 mg, 0.880 mmol, 88%). ^1H NMR (700 MHz, CDCl_3) δ 6.96-6.66 (m, NH, 1H), 6.22-5.65 (m, 1H), 3.93 (dt, $J = 6.6$ Hz, $J = 6.6$ Hz, 1H), 3.91-3.72 (m, 4H), 3.70 (dt, $J = 6.6$ Hz, $J = 6.6$ Hz, 1H), 2.13-1.78 (m, 6H), 0.92-0.78 (m, 12H); ^{13}C NMR (176 MHz, CDCl_3) δ 156.9 (C), 155.5 (C), 87.1 (CH), 72.6 (CH_2), 72.2 (CH_2), 71.9 (CH_2), 68.5 (CH_2), 29.6 (CH_2), 28.1 (CH_2), 27.9 (CH), 27.8 (CH), 25.2 (CH_2), 18.8 (CH_3); IR (solid) 3280, 2972, 2935, 2861, 1738, 1711 cm^{-1} . LRMS (ESI) 303 (100, $[\text{M}+\text{H}]^+$); HRMS (ESI) calcd for $\text{C}_{14}\text{H}_{27}\text{N}_2\text{O}_5$ $[\text{M}+\text{H}]^+$ 303.1915; observed 303.1917.

Diisopropyl 1-(tetrahydro-2H-pyran-2-yl)hydrazine-1,2-dicarboxylate 109g

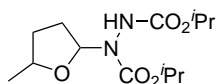
Compound prepared using HFIP as the reaction solvent and a reaction duration of 72 h. Purification by column chromatography (10%-50% EtOAc/Petrol) afforded diisopropyl 1-(tetrahydro-2H-pyran-2-yl)hydrazine-1,2-dicarboxylate as a white solid (202 mg, 0.700 mmol, 70%). ^1H NMR (700 MHz, DMSO-d_6) δ 9.17-8.70 (m, NH, 1H), 5.18-4.95 (m, 1H), 4.81-4.72 (m, 2H), 3.88 (m, 1H), 3.46-3.38 (m, 1H), 1.83-1.75 (m, 1H), 1.59-1.50 (m, 2H), 1.59-1.41 (m, 1H), 1.40-1.28 (m, 2H), 1.26-1.02 (m, 12H); ^{13}C NMR (176 MHz, DMSO-d_6) δ 156.2 (C), 154.5 (C), 83.7 (CH), 83.5 (CH), 69.7 (CH), 69.1 (CH), 68.1 (CH_2), 67.9 (CH), 67.9 (CH), 66.8 (CH_2), 66.8 (CH_2), 28.3 (CH_2), 27.3 (CH_2), 24.8 (CH_2), 22.5 (CH_2), 22.4 (CH_2), 22.3 (CH_2), 22.0 (CH_3), 21.9 (CH_3), 21.8 (CH_3), 21.7 (CH_3), 21.7 (CH_3); IR (solid) 3255, 2983, 2937, 2873, 1740, 1716 cm^{-1} . LRMS (ESI) 289 (100, $[\text{M}+\text{H}]^+$); HRMS (ESI) calcd for $\text{C}_{13}\text{H}_{25}\text{N}_2\text{O}_5$ $[\text{M}+\text{H}]^+$ 289.1938; observed 289.1941.

Diisopropyl 1-(1,4-dioxan-2-yl)hydrazine-1,2-dicarboxylate 109h¹⁶¹

Compound prepared using HFIP as the reaction solvent and a reaction duration of 72 h. Purification by column chromatography (10%-50% EtOAc/Petrol) afforded diisopropyl 1-(1,4-dioxan-2-yl)hydrazine-1,2-dicarboxylate as a white solid (206 mg, 0.710 mmol, 71%). ¹H NMR (600 MHz, CDCl₃) δ 6.75-6.45 (m, NH, 1H), 5.58-5.25 (m, 1H), 4.98-4.90 (m, 2H), 3.92-3.76 (m, 3H), 3.65-3.61 (m, 1H), 3.56-3.47 (m, 2H), 1.28 (d, *J* = 5.8 Hz, 12H); ¹³C NMR (151 MHz, CDCl₃) δ 156.2 (C), 154.7 (C), 81.9 (CH), 80.8 (CH), 71.2 (CH), 70.1 (CH), 67.4 (CH₂), 66.8 (CH₂), 65.6 (CH₂), 22.1 (CH₃), 22.0 (CH₃); IR (solid) 3264, 2980, 2936, 2873, 1735, 1716 cm⁻¹.

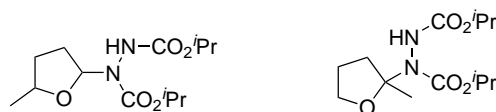
Diisopropyl 1-(oxepan-2-yl)hydrazine-1,2-dicarboxylate 109i

Compound prepared using HFIP as the reaction solvent and a reaction duration of 96 h. Purification by column chromatography (10%-50% EtOAc/Petrol) afforded diisopropyl 1-(oxepan-2-yl)hydrazine-1,2-dicarboxylate as a white solid (187 mg, 0.620 mmol, 62%). ¹H NMR (700 MHz, CDCl₃) δ 6.76-6.40 (m, 1H), 5.60-5.35 (m, 1H), 4.97-4.87 (m, 2H), 3.88-3.82 (m, 1H), 3.71-3.63 (m, 1H), 1.98-1.85 (m, 2H), 1.75-1.65 (m, 3H), 1.51-1.44 (m, 2H), 1.25-1.18 (d, *J* = 5.9 Hz, 12H); ¹³C NMR (151 MHz, CDCl₃) δ 156.4 (C), 86.7 (CH), 86.2 (CH), 70.5 (CH), 69.8 (CH₂), 69.6 (CH), 67.3 (CH₂), 31.5 (CH₂), 31.1 (CH₂), 26.8 (CH₂), 26.8 (CH₂), 24.8 (CH₂), 22.1 (CH₃), 22.1 (CH₃), 22.0 (CH₃); IR (solid) 3293, 2979, 2928, 2863, 1740, 1715 cm⁻¹. LRMS (ESI) 303 (100, [M+H]⁺); HRMS (ESI) calcd for C₁₄H₂₇N₂O₅ [M+H]⁺ 303.1915; observed 303.1918.

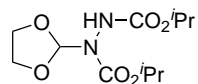
Diisopropyl 1-(5-methyltetrahydrofuran-2-yl)hydrazine-1,2-dicarboxylate
109j

Compound prepared using HFIP as the reaction solvent and a reaction duration of 48 h. Purification by column chromatography (10%-50% EtOAc/Petrol) afforded diisopropyl 1-(5-methyltetrahydrofuran-2-yl)hydrazine-1,2-dicarboxylate as a clear oil (58.0 mg, 0.200 mmol, 20%). ^1H NMR (700 MHz, CDCl_3 , diastereomers (1:1)) δ 6.48-5.85 (m, 2H), 4.98-4.92 (m, 2H), 4.27-4.22 (m, 0.5H), 4.00-3.94 (m, 0.5H), 2.22-1.88 (m, 3H), 1.55-1.41 (m, 1H), 1.30-1.17 (m, 15H); ^{13}C NMR (176 MHz, CDCl_3) δ 156.5 (C), 155.2 (C), 86.8 (CH), 70.6 (CH), 70.1 (CH), 70.0 (CH), 69.9 (CH), 69.8 (CH), 33.1 (CH_2), 32.5 (CH_2), 28.7 (CH_2), 22.2 (CH_3), 22.1 (CH_2), 22.1 (CH_3), 22.1 (CH_3), 22.0 (CH_3), 21.4 (CH_3), 21.0 (CH_3); IR (thin film) 3251, 2986, 2942, 2867, 1732, 1713 cm^{-1} . LRMS (ESI) 303 (100, $[\text{M}+\text{H}]^+$); HRMS (ESI) calcd for $\text{C}_{13}\text{H}_{25}\text{N}_2\text{O}_5$ $[\text{M}+\text{H}]^+$ 303.1915; observed 303.1918.

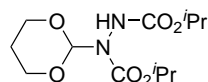
(30:70) Regioisomeric mixture of diisopropyl 1-(5-methyltetrahydrofuran-2-yl)hydrazine-1,2-dicarboxylate **109j and diisopropyl 1-(2-methyltetrahydrofuran-2-yl)hydrazine-1,2-dicarboxylate **109k****



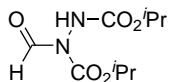
Compounds prepared without the use of fluorinated alcohol as the reaction solvent and a reaction duration of 48 h. Purification by column chromatography (10%-50% EtOAc/Petrol) afforded an inseparable mixture of regioisomers diisopropyl 1-(5-methyltetrahydrofuran-2-yl)hydrazine-1,2-dicarboxylate **109j** and diisopropyl 1-(2-methyltetrahydrofuran-2-yl)hydrazine-1,2-dicarboxylate **109k** as a clear oil (196 mg, 0.68 mmol, 68%). ¹H NMR (700 MHz, DMSO-d₆, regioisomers (3:7) δ 9.14-8.68 (m, NH, 1H), 5.96-5.73 (m, 0.3H), 4.83-4.74 (m, 2H), 3.89-3.72 (m, 1.7H), 2.62-2.50 (m, 1H), 2.10-1.73 (m, 1H), 1.65-1.30 (m, 3H), 1.24-1.10 (m, 12H); ¹³C NMR (176 MHz, CDCl₃) δ 161.2 (C), 161.1 (C), 161.1 (C), 160.8 (C), 159.6 (C), 159.4 (C), 159.0 (C), 103.2 (C), 103.1 (C), 102.8 (C), 102.7 (C), 92.3 (CH), 91.3 (CH), 80.2 (CH), 80.1 (CH), 74.3 (CH₂), 73.6 (CH), 73.5 (CH), 73.4 (CH₂), 73.4 (CH), 73.2 (CH₂), 73.1 (CH₂), 42.9 (CH₂), 42.7 (CH₂), 42.6 (CH₂), 29.7 (CH₂), 29.6 (CH₂), 29.6 (CH₂), 29.6 (CH₂), 29.6 (CH₂), 29.5 (CH₂), 27.3 (CH₂), 27.2 (CH₂), 27.2 (CH₂), 27.2 (CH₂), 27.2 (CH₂), 27.2 (CH₂), 27.1 (CH₂), 27.1 (CH₂), 27.1 (CH₂), 26.9 (CH₂); IR (thin film) 3247, 2986, 2937, 2920, 2863, 1735, 1714 cm⁻¹.

Diisopropyl 1-(1,3-dioxolan-2-yl)hydrazine-1,2-dicarboxylate 117a

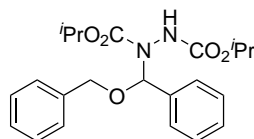
Compound prepared using HFIP as the reaction solvent and a reaction duration of 24 h. Purification by column chromatography (10%-50% EtOAc/Petrol) afforded diisopropyl 1-(1,3-dioxolan-2-yl)hydrazine-1,2-dicarboxylate as a white solid (193 mg, 0.700 mmol, 70%). ^1H NMR (700 MHz, DMSO- d_6) δ 9.10-8.77 (m, NH, 1H), 6.51 (s, 1H), 4.84-4.75 (m, 2H), 4.04-4.01 (m, 1H), 3.94-3.89 (m, 1H) 3.88-3.81 (m, 2H), 1.21-1.10 (m, 12H); ^{13}C NMR (176 MHz, DMSO- d_6) δ 155.4 (C), 153.8 (C), 103.8 (CH), 69.5 (CH), 68.1 (CH), 68.0 (CH), 65.1 (CH_2), 65.0 (CH_2), 64.6 (CH_2), 21.9 (CH_3), 21.8 (CH_3), 21.8 (CH_3), 21.7 (CH_3); IR (solid) 3271, 2986, 2937, 2909, 1748, 1691 cm^{-1} . LRMS (ESI) 277 (100, $[\text{M}+\text{H}]^+$); HRMS (ESI) calcd for $\text{C}_{11}\text{H}_{21}\text{N}_2\text{O}_6$ $[\text{M}+\text{H}]^+$ 277.1394; observed 277.1395.

Diisopropyl 1-(1,3-dioxan-2-yl)hydrazine-1,2-dicarboxylate 117b

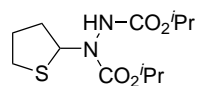
Compound prepared using HFIP as the reaction solvent and a reaction duration of 24 h. Purification by column chromatography (10%-50% EtOAc/Petrol) afforded diisopropyl 1-(1,3-dioxan-2-yl)hydrazine-1,2-dicarboxylate as a white solid (171 mg, 0.590 mmol, 59%). ^1H NMR (700 MHz, DMSO- d_6) δ 9.08-8.72 (m, NH, 1H), 5.95 (s, 1H), 4.82-4.71 (m, 2H), 4.04-4.00 (m, 2H), 3.92-3.84 (m, 2H), 1.81-1.72 (m, 1H), 1.32-1.27 (m, 1H), 1.19-1.08 (m, 12H); ^{13}C NMR (176 MHz, DMSO- d_6) δ 155.4 (C), 153.4 (C), 99.6 (CH), 69.6 (CH), 67.9 (CH_2), 67.8 (CH), 66.1 (CH_2), 66.0 (CH_2), 65.8 (CH_2), 65.7 (CH_2), 24.1 (CH_2), 22.0 (CH_3), 21.8 (CH_3), 21.7 (CH_3), 21.7 (CH_3); IR (solid) 3269, 2982, 2943, 2901, 1740, 1698 cm^{-1} . LRMS (ESI) 291 (100, $[\text{M}+\text{H}]^+$); HRMS (ESI) calcd for $\text{C}_{12}\text{H}_{23}\text{N}_2\text{O}_6$ $[\text{M}+\text{H}]^+$ 291.1551; observed 291.1555.

Diisopropyl 1-benzoylhydrazine-1,2-dicarboxylatedicarboxylate 117c

Compound prepared using TFE as the reaction solvent and a reaction duration of 24 h. Purification by column chromatography (10%-50% EtOAc/Petrol) afforded diisopropyl 1-formylhydrazine-1,2-dicarboxylate as a clear oil (144 mg, 0.620 mmol, 62%). ^1H NMR (700 MHz, DMSO- d_6) δ 9.74-9.35 (m, 1H), 9.20-9.16 (m, NH, 1H), 5.06-4.99 (m, 1H), 4.85-4.77 (m, 1H), 1.32-1.25 (m, 6H), 1.23-1.07 (m, 6H); ^{13}C NMR (176 MHz, DMSO- d_6) δ 166.0 (C), 165.9 (C), 165.9 (C), 165.8 (C), 159.9 (C), 159.2 (C), 157.6 (C), 77.6 (CH), 77.6 (CH), 74.4 (CH), 74.4 (CH), 27.1 (CH_3), 27.0 (CH_3), 26.9 (CH_3), 26.9 (CH_3), 26.7 (CH_3), 26.7 (CH_3), 26.7 (CH_3); IR (solid) 3308, 2981, 2934, 2857, 1730, 1687 cm^{-1} . LRMS (ESI) 233 (100, $[\text{M}+\text{H}]^+$); HRMS (ESI) calcd for $\text{C}_9\text{H}_{17}\text{N}_2\text{O}_5$ $[\text{M}+\text{H}]^+$ 233.1132; observed 233.1134.

Diisopropyl 1-((benzyloxy)(phenyl)methyl)hydrazine-1,2-dicarboxylate
119b

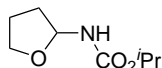
Compound prepared using HFIP as the reaction solvent and a reaction duration of 72 h. Purification by column chromatography (10%-50% EtOAc/Petrol) afforded diisopropyl 1-((benzyloxy)(phenyl)methyl)hydrazine-1,2-dicarboxylate as a white solid (252 mg, 0.630 mmol, 63%). ^1H NMR (700 MHz, DMSO- d_6 , 21 °C) δ 9.29-8.50 (m, NH, 1H), 7.43-7.20 (m, 10H), 6.50-6.25 (m, 1H), 5.10-4.30 (m, 4H), 1.27-0.52 (m, 12H); ^{13}C NMR (176 MHz, DMSO- d_6 , 21 °C) δ 156.4 (C), 155.9 (C), 155.7 (C), 155.5 (C), 155.0 (C), 154.9 (C), 154.5 (C), 138.3 (C), 137.8 (C), 137.6 (C), 137.0 (C), 128.2 (CH), 128.1 (CH), 128.0 (CH), 128.0 (CH), 127.7 (CH), 127.6 (CH), 127.5 (CH), 127.2 (CH), 127.1 (CH), 127.0 (CH), 126.6 (CH), 85.5 (CH), 85.2 (CH), 84.8 (CH), 84.7 (CH), 69.9 (CH), 69.5 (CH), 68.9 (CH), 68.2 (CH), 67.8 (CH), 67.6 (CH), 21.9 (CH₃), 21.9 (CH₃), 21.8 (CH₃), 21.7 (CH₃), 21.7 (CH₃), 20.8 (CH₃); ^1H NMR (400 MHz, DMSO- d_6 , 120 °C) δ 8.43 (br s, NH, 1H), 7.45-7.40 (m, 4H), 7.38-7.27 (m, 6H), 6.44 (s, 1H), 5.00-4.88 (m, 2H), 4.72-4.66 (m, 2H), 1.30-1.22 (m, 6H), 1.15-0.98 (m, 6H); ^{13}C NMR (101 MHz, DMSO- d_6 , 120 °C) δ 156.1 (C), 155.7 (C), 138.7 (C), 137.0 (C), 128.6 (CH), 128.3 (CH), 128.2 (CH), 128.1 (CH), 127.8 (CH), 127.4 (CH), 87.0 (CH), 70.3 (CH), 68.6 (CH), 22.1 (CH₃), 22.0 (CH₃); IR (solid) 3282, 2984, 2937, 1742, 1699, 1681, 1650 cm^{-1} . LRMS (ESI) 401 (100, [M+H]⁺); HRMS (ESI) calcd for C₂₂H₂₉N₂O₅ [M+H]⁺ 401.2071; observed 401.2076.

Diisopropyl 1-(tetrahydrothiophen-2-yl)hydrazine-1,2-dicarboxylate 125

Compound prepared using HFIP as the reaction solvent and a reaction duration of 48 h. Purification by column chromatography (10%-50% EtOAc/Petrol) afforded diisopropyl 1-(tetrahydrothiophen-2-yl)hydrazine-1,2-dicarboxylate as a white solid (142 mg, 0.490 mmol, 49%). ^1H NMR (700 MHz, CDCl_3) δ 6.49-6.25 (m, NH 1H), 6.15-5.90 (s, 1H), 4.99-4.86 (m, 2H), 3.06-2.94 (m, 1H), 2.78-2.68 (m, 1H), 2.14-2.02 (m, 3H), 1.96-1.88 (m, 1H), 1.26-1.19 (m, 12H); ^{13}C NMR (176 MHz, CDCl_3) δ 156.3 (C), 155.0 (C), 70.8 (CH), 70.0 (CH), 69.8 (CH), 67.2 (CH), 66.9 (CH), 34.4 (CH_2), 34.1 (CH_2), 33.3 (CH_2), 30.2 (CH_2), 30.1 (CH_2), 22.1 (CH_3), 22.1 (CH_3), 22.1 (CH_3), 22.0 (CH_3); IR (solid) 3284, 2980, 2934, 1739, 1703 cm^{-1} . LRMS (ESI) 401 (100, $[\text{M}+\text{H}]^+$); HRMS (ESI) calcd for $\text{C}_{12}\text{H}_{23}\text{N}_2\text{O}_4\text{S}$ $[\text{M}+\text{H}]^+$ 291.1373; observed 291.1373.

Formation of protected α -amino ether

Isopropyl (tetrahydrofuran-2-yl)carbamate **122**



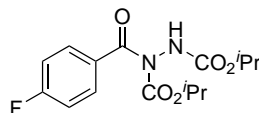
To a stirring solution of sodium hydride (60% mineral oil dispersion, 200 mg, 5.00 mmol, 5 eq.) in anhydrous THF (0.5 mL) was added dropwise a solution of diisopropyl-1-benzoylhydrazine-1,2-dicarboxylate **109** (274 mg, 1.00 mmol, 1 eq.) pre-dissolved in anhydrous THF (1.5 mL) under an atmosphere of argon and the reaction mixture was stirred for 5 minutes. After this time, to the reaction mixture was added dropwise *tert*-butyl bromoacetate (162 μ L, 1.10 mmol, 1.1 eq.) pre-dissolved in anhydrous THF (0.5 mL). The reaction mixture was then stirred at 25 $^{\circ}$ C for 16 h and then poured over saturated aqueous NH_4Cl (10 mL). The resulting solution was extracted with EtOAc (3 \times 15 mL). The combined extracts were dried (MgSO_4), filtered and the solvent evaporated in vacuo. Purification by column chromatography (10%-50% EtOAc/Petrol) afforded isopropyl (tetrahydrofuran-2-yl)carbamate as a white solid (130 mg, 0.75 mmol, 75%). ^1H NMR (700 MHz, CDCl_3) δ 5.53 (br s, NH, 1H), 5.14 (app. s, 1H), 4.91 (septet, $J = 6.2$ Hz, 1H), 3.89 (dt, $J = 7.1$ Hz, $J = 7.1$ Hz, 1H), 3.78 (dt, $J = 7.1$ Hz, $J = 7.1$ Hz, 1H), 2.19-2.12 (m, 1H), 1.96-1.86 (m, 2H), 1.69-1.62 (m, 1H), 1.21 (d, $J = 5.0$ Hz, 6H); ^{13}C NMR (176 MHz, CDCl_3) δ 155.5 (C), 82.2 (CH), 68.5 (CH), 67.1 (CH_2), 31.9 (CH_2), 24.8 (CH_2), 22.2 (CH_3); IR (solid) 3314, 2980, 2933, 2871, 1738, 1683 cm^{-1} . LRMS (ESI) 401 (100, $[\text{M}+\text{H}]^+$); HRMS (ESI) calcd for $\text{C}_8\text{H}_{16}\text{NO}_3$ $[\text{M}+\text{H}]^+$ 174.1125; observed 174.1124.

6.2 Experimental for Chapter 3

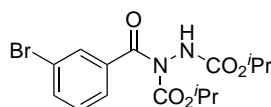
The following molecules were synthesised based on literature procedures described by Caddick *et al.*⁸¹

General experimental for the formation of acyl hydrazides

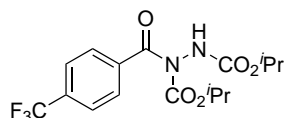
To a solution of azodicarboxylate (6.00 mmol, 1.2 eq.) on H₂O (1 mL) was added aldehyde (5.00 mmol, 1.0 eq.). The reaction mixture stirred at 21 °C for 48 h. The resulting solution was extracted with EtOAc (3 × 15 mL). The combined extracts were dried (MgSO₄), filtered and the solvent was removed *in vacuo*. The resultant crude residue was purified as described below.

Diisopropyl 1-(4-fluorobenzoyl)hydrazine-1,2-dicarboxylate⁸⁶ 87a

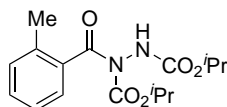
Purification by column chromatography (10%-50% EtOAc/Petrol) afforded diisopropyl 1-(4-fluorobenzoyl)hydrazine-1,2-dicarboxylate as a white solid (1.21 g, 3.70 mmol, 74%). ¹H NMR (600 MHz, CDCl₃) δ 7.80-7.62 (m, 2H), 7.11 (t, *J* = 8.5 Hz, 2H), 6.95-6.70 (m, NH, 1H), 5.02 (septet, *J* = 6.1 Hz, 1H), 4.92 (septet, *J* = 6.1 Hz, 1H), 1.30 (d, *J* = 5.2 Hz, 6H), 1.12 (d, *J* = 5.0 Hz, 6H); ¹³C NMR (150 MHz, CDCl₃) δ 170.3 (C), 165.2 (d, *J*_{C-F} = 253.4 Hz, C), 155.4 (C), 152.9 (C), 131.3 (d, *J*_{C-F} = 2.7 Hz, CH), 131.1 (d, *J*_{C-F} = 9.8 Hz, CH), 115.5 (d, *J*_{C-F} = 22.1 Hz, CH), 72.8 (CH), 70.9 (CH), 22.0 (CH₃), 21.5 (CH₃); IR (solid) 3306, 2984, 2939, 1704, 1602, 1507 cm⁻¹.

Diisopropyl 1-(3-bromobenzoyl)hydrazine-1,2-dicarboxylate⁸⁵ 87b

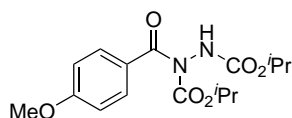
Purification by column chromatography (10%-50% EtOAc/Petrol) afforded diisopropyl 1-(3-bromobenzoyl)hydrazine-1,2-dicarboxylate as a white solid (1.20 g, 3.10 mmol, 62%). ¹H NMR (600 MHz, CDCl₃) δ 7.84-7.73 (m, 1H), 7.67-7.52 (m, 2H), 7.30 (t, *J* = 7.8 Hz, 1H), 6.99-6.80 (m, NH, 1H), 5.01 (septet, *J* = 6.0 Hz, 1H), 4.91 (septet, *J* = 6.0 Hz, 1H), 1.30 (d, *J* = 5.8 Hz, 6H), 1.10 (d, *J* = 5.1 Hz, 6H); ¹³C NMR (150 MHz, CDCl₃) δ 169.8 (C), 155.3 (C), 152.6 (C), 137.2 (C), 134.8 (CH), 131.0 (CH), 129.9 (CH), 126.7 (CH), 122.2 (C), 73.0 (CH), 71.0 (CH), 22.0 (CH₃), 21.5 (CH₃); IR (solid) 3303, 2983, 2938, 1707, 1568 cm⁻¹.

Diisopropyl 1-(4-(trifluoromethyl)benzoyl)hydrazine-1,2-dicarboxylate⁸⁵**87c**

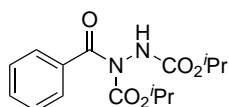
Purification by column chromatography (10%-50% EtOAc/Petrol) afforded diisopropyl 1-(4-(trifluoromethyl)benzoyl)hydrazine-1,2-dicarboxylate as a white solid (1.17 g, 3.10 mmol, 62%). ¹H NMR (600 MHz, CDCl₃) δ 7.82-7.74 (m, 2H), 7.73-7.67 (m, 2H), 6.95-6.70 (m, NH, 1H), 5.03 (septet, *J* = 6.1 Hz, 1H), 4.91 (septet, *J* = 6.1 Hz, 1H), 1.31 (d, *J* = 6.1 Hz, 6H), 1.10 (d, *J* = 6.1 Hz, 6H); ¹³C NMR (150 MHz, CDCl₃) δ 170.2 (C), 155.3 (C), 152.6 (C), 138.8 (C), 133.4 (q, *J*_{C-F} = 31.9 Hz, C), 128.3 (CH), 125.3 (q, *J*_{C-F} = 3.0 Hz, CH), 123.7 (q, *J*_{C-F} = 272.6 Hz, CH), 73.1 (CH), 71.1 (CH), 22.0 (CH₃), 21.5 (CH₃); IR (solid) 3308, 2985, 2941, 1709, 1619, 1514 cm⁻¹.

Diisopropyl 1-(2-methylbenzoyl)hydrazine-1,2-dicarboxylate⁸⁵ **87d**

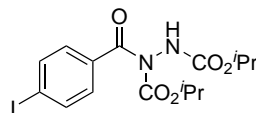
Purification by column chromatography (10%-50% EtOAc/Petrol) afforded diisopropyl 1-(2-methylbenzoyl)hydrazine-1,2-dicarboxylate as a white solid (887 mg, 2.75 mmol, 55%). ¹H NMR (600 MHz, CDCl₃) δ 7.43-7.34 (m, 1H), 7.32 (t, *J* = 7.5 Hz 1H), 7.23-7.16 (m, 2H), 7.06-6.86 (m, NH, 1H), 5.02 (septet, *J* = 5.7 Hz, 1H), 4.82 (septet, *J* = 5.9 Hz, 1H), 2.39 (s, 3H), 1.30 (d, *J* = 5.7 Hz, 6H), 1.05-0.95 (m, 6H); ¹³C NMR (150 MHz, CDCl₃) δ 171.0 (C), 155.3 (C), 152.4 (C), 136.3 (C), 135.4 (C), 130.4 (CH), 130.1 (CH), 126.4 (CH), 125.5 (CH), 72.5 (CH), 70.8 (CH), 22.1 (CH₃), 21.3 (CH₃), 19.3 (CH₃); IR (solid) 3308, 2983, 2938, 1705, 1602 cm⁻¹.

Diisopropyl 1-(4-methoxybenzoyl)hydrazine-1,2-dicarboxylate¹⁶² 87e

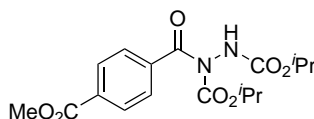
Purification by column chromatography (10%-50% EtOAc/Petrol) afforded diisopropyl 1-(4-methoxybenzoyl)hydrazine-1,2-dicarboxylate as a white solid (1.03 g, 3.05 mmol, 61%). ¹H NMR (600 MHz, CDCl₃) δ 7.76-7.62 (m, 2H), 6.98-6.64 (m, 3H), 5.00 (septet, *J* = 6.2 Hz, 1H), 4.92 (septet, *J* = 6.2 Hz, 1H), 3.86 (s, 3H), 1.29 (d, *J* = 4.5 Hz, 6H), 1.13 (d, *J* = 4.5 Hz, 6H); ¹³C NMR (150 MHz, CDCl₃) δ 170.8 (C), 163.1 (C), 155.5 (C), 153.3 (C), 131.2 (CH), 127.0 (C), 113.5 (CH), 72.4 (CH), 70.7 (CH), 55.6 (CH₃), 22.1 (CH₃), 21.6 (CH₃); IR (solid) 3310, 2982, 2938, 1733, 1699, 1604, 1510 cm⁻¹.

Diisopropyl 1-benzoylhydrazine-1,2-dicarboxylatedicarboxylate¹⁶³ 87f

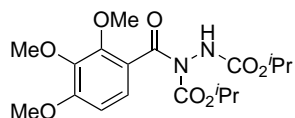
Purification by column chromatography (10%-50% EtOAc/Petrol) afforded diisopropyl 1-benzoylhydrazine-1,2-dicarboxylatedicarboxylate as a white solid (1.02 g, 3.30 mmol, 66%). ¹H NMR (600 MHz, CDCl₃) δ 7.72-7.58 (m, 2H), 7.50 (t, *J* = 7.4 Hz, 1H), 7.40 (t, *J* = 7.6 Hz, 2H), 7.15-6.99 (m, NH, 1H), 5.00 (septet, *J* = 6.3 Hz, 1H), 4.87 (septet, *J* = 5.9 Hz, 1H), 1.28 (d, *J* = 5.5 Hz, 6H), 1.04 (d, *J* = 5.7 Hz, 6H); ¹³C NMR (150 MHz, CDCl₃) δ 171.4 (C), 155.5 (C), 153.0 (C), 135.3 (CH), 132.0 (CH), 128.2 (CH), 72.6 (CH), 70.7 (CH), 22.0 (CH₃), 21.4 (CH₃); IR (solid) 3308, 2983, 2938, 1705, 1601 cm⁻¹.

Diisopropyl 1-(4-iodobenzoyl)hydrazine-1,2-dicarboxylate¹⁶⁴ 87g

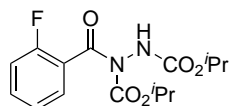
Purification by column chromatography (10%-50% EtOAc/Petrol) afforded diisopropyl 1-(4-iodobenzoyl)hydrazine-1,2-dicarboxylate as a white solid (1.28 g, 2.95 mmol, 59%). ¹H NMR (600 MHz, CDCl₃) δ 7.76 (d, 2H, *J* = 8.2 Hz), 7.43-7.30 (m, 2H), 7.11-7.03 (m, NH, 1H), 4.98 (septet, *J* = 6.2 Hz, 1H), 4.89 (septet, *J* = 6.0 Hz, 1H), 1.30-1.21 (m, 6H), 1.17-1.08 (m, 6H); ¹³C NMR (150 MHz, CDCl₃) δ 170.7 (C), 155.4 (C), 152.8 (C), 137.5 (CH), 134.7 (C), 129.8 (CH), 99.1 (C), 72.9 (CH), 70.9 (CH), 22.0 (CH₃), 21.5 (CH₃); IR (solid) 3302, 2982, 2937, 1705, 1585 cm⁻¹.

Diisopropyl 1-(4-(methoxycarbonyl)benzoyl)hydrazine-1,2-dicarboxylate 87h

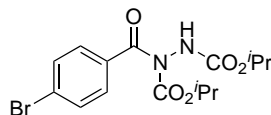
Purification by column chromatography (10%-50% EtOAc/Petrol) afforded diisopropyl 1-(4-(methoxycarbonyl)benzoyl)hydrazine-1,2-dicarboxylate as a white solid (898 mg, 2.45 mmol, 49%). m.p. 106-108 °C; ¹H NMR (600 MHz, CDCl₃) δ 8.08 (d, 2H, *J* = 8.1 Hz), 7.75-7.62 (m, 2H), 7.00-6.76 (m, NH, 1H), 5.03 (septet, *J* = 6.2 Hz, 1H), 4.89 (septet, *J* = 6.0 Hz, 1H), 3.94 (s, 3H), 1.33-1.24 (m, 6H), 1.13-1.05 (m, 6H); ¹³C NMR (150 MHz, CDCl₃) δ 170.6 (C), 166.3 (C), 155.3 (C), 152.6 (C), 139.5 (C), 132.8 (C), 129.5 (CH), 127.9 (CH), 73.0 (CH), 71.0 (CH), 52.6 (CH₃), 22.0 (CH₃), 21.5 (CH₃); IR (solid) 3301, 2980, 2936, 1706, 1571 cm⁻¹; LRMS (ESI) 367 (100, [M+H]⁺), 163 (20, [M-C₈H₁₅N₂O₄+H]⁺); HRMS (ESI) calcd for C₁₇H₂₃N₂O₇ [M+H]⁺ 367.1500; observed 367.1503.

Diisopropyl 1-(2,3,4-trimethoxybenzoyl)hydrazine-1,2-dicarboxylate 87i

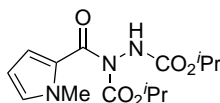
Purification by column chromatography (10%-50% EtOAc/Petrol) afforded diisopropyl 1-(2,3,4-trimethoxybenzoyl)hydrazine-1,2-dicarboxylate as a white solid (797 mg, 2.00 mmol, 40%). m.p. 110-112 °C; ^1H NMR (600 MHz, CDCl_3) δ 7.25-7.08 (m, 1H), 6.88 (s, NH, 1H), 6.69 (d, $J = 8.7$ Hz, 1H), 5.00-4.88 (m, 2H), 3.92 (s, 3H), 3.89 (s, 3H), 3.87 (s, 3H), 1.26 (d, $J = 5.8$ Hz, 6H), 1.20-1.012 (m, 6H); ^{13}C NMR (150 MHz, CDCl_3) δ 168.0 (C), 156.4 (C), 155.1 (C), 152.5 (C), 151.4 (C), 141.7 (C), 124.3 (CH), 122.9 (C), 107.0 (CH), 72.3 (CH), 70.5 (CH), 62.1 (CH_3), 61.1 (CH_3), 56.2 (CH_3), 22.0 (CH_3), 21.6 (CH_3); IR (solid) 3310, 2982, 2940, 1737, 1710, 1596 cm^{-1} ; LRMS (ESI) 399 (30, $[\text{M}+\text{H}]^+$), 195 (100, $[\text{M}-\text{C}_8\text{H}_{15}\text{N}_2\text{O}_4+\text{H}]^+$); HRMS (ESI) calcd for $\text{C}_{18}\text{H}_{27}\text{N}_2\text{O}_8$ $[\text{M}+\text{H}]^+$ 399.1762; observed 399.1760.

Diisopropyl 1-(2-fluorobenzoyl)hydrazine-1,2-dicarboxylate⁸⁵ 87j

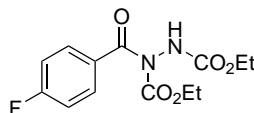
Purification by column chromatography (10%-50% EtOAc/Petrol) afforded diisopropyl 1-(2-fluorobenzoyl)hydrazine-1,2-dicarboxylate as a white solid (979 mg, 3.00 mmol, 60%). ^1H NMR (600 MHz, CDCl_3) δ 7.64-7.50 (m, 1H), 7.48 (m, 1H), 7.22 (t, $J = 7.5$ Hz, 1H), 7.11-7.06 (m, 1H), 6.82-6.52 (m, NH, 1H), 5.04-4.92 (m, 2H), 1.32-1.11 (m, 12H); ^{13}C NMR (150 MHz, CDCl_3) δ 166.2 (C), 159.1 (d, $J_{\text{C}-\text{F}} = 251.1$ Hz, C), 155.1 (C), 152.1 (C), 133.0 (d, $J_{\text{C}-\text{F}} = 7.7$ Hz, CH), 129.9 (CH), 124.4 (d, $J_{\text{C}-\text{F}} = 3.3$ Hz, CH), 124.2 (d, $J_{\text{C}-\text{F}} = 15.6$ Hz, C), 115.6 (d, $J_{\text{C}-\text{F}} = 21.0$ Hz, CH), 72.9 (CH), 70.9 (CH), 22.0 (CH_3), 21.5 (CH_3); IR (solid) 3306, 2984, 2943, 2857, 1739, 1714, 1614, 1581, 1563 cm^{-1} .

Diisopropyl 1-(4-bromobenzoyl)hydrazine-1,2-dicarboxylate¹⁶² 87k

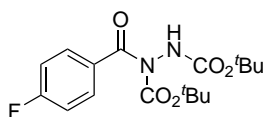
Purification by column chromatography (10%-50% EtOAc/Petrol) afforded diisopropyl 1-(4-bromobenzoyl)hydrazine-1,2-dicarboxylate as a white solid (1.20 g, 3.10 mmol, 62%). ¹H NMR (600 MHz, CDCl₃) δ 7.63-7.48 (m, 4H), 6.88-6.53 (m, NH, 1H), 5.01 (septet, *J* = 6.2 Hz, 1H), 4.92 (septet, *J* = 6.0 Hz, 1H), 1.33-1.24 (m, 6H), 1.18-1.11 (m, 6H); ¹³C NMR (150 MHz, CDCl₃) δ 170.5 (C), 155.3 (C), 152.8 (C), 134.1 (C), 131.6 (CH), 129.9 (CH), 126.9 (C), 72.9 (CH), 71.0 (CH), 22.0 (CH₃), 21.5 (CH₃); IR (solid) 3294, 2979, 2934, 1737, 1711, 1588 cm⁻¹.

Diisopropyl 1-(1-methyl-1*H*-pyrrole-2-carbonyl)hydrazine-1,2-dicarboxylate¹⁶⁵ 87l

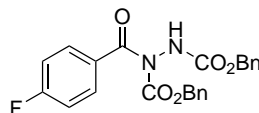
Purification by column chromatography (10%-50% EtOAc/Petrol) afforded diisopropyl 1-(1-methyl-1*H*-pyrrole-2-carbonyl)hydrazine-1,2-dicarboxylate as a pale-yellow solid (716 mg, 2.30 mmol, 46%). ¹H NMR (600 MHz, CDCl₃) δ 7.18-7.10 (m, 1H), 6.88-6.70 (m, 2H), 6.25-6.05 (m, 1H), 4.99-4.91 (m, 2H), 3.84 (s, 3H), 1.25-1.16 (m, 12H); ¹³C NMR (150 MHz, CDCl₃) δ 180.4 (C), 155.6 (C), 153.9 (C), 153.5 (C), 130.8 (CH), 125.4 (C), 120.1 (CH), 108.4 (CH), 72.0 (CH), 70.4 (CH), 36.5 (CH₃), 22.0 (CH₃), 21.7 (CH₃); IR (solid) 3305, 2984, 2939, 1729, 1685, 1528 cm⁻¹.

Diethyl 1-(4-fluorobenzoyl)hydrazine-1,2-dicarboxylate⁸¹ 87m

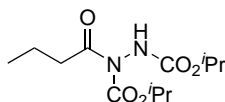
Purification by column chromatography (10%-50% EtOAc/Petrol) afforded diethyl 1-(4-fluorobenzoyl)hydrazine-1,2-dicarboxylate as a white solid (1.07 g, 3.60 mmol, 72%). ¹H NMR (600 MHz, CDCl₃) δ 7.72 (m, 2H), 7.29-7.20 (m, NH, 1H), 7.08 (t, *J* = 8.6 Hz, 2H), 4.22 (q, *J* = 7.1 Hz, 2H), 4.16 (q, *J* = 7.0 Hz, 6H), 1.28 (m, 3H), 1.11 (m, 3H); ¹³C NMR (150 MHz, CDCl₃) δ 170.2 (C), 165.2 (d, *J*_{C-F} = 253.5 Hz, C), 155.8 (C), 153.5 (C), 131.1 (d, *J*_{C-F} = 8.9 Hz, CH), 130.9 (C), 115.5 (d, *J*_{C-F} = 22.2 Hz, CH), 64.2 (CH₂), 62.8 (CH₂), 14.4 (CH₃), 13.9 (CH₃); IR (solid) 3302, 2985, 2940, 1737, 1706, 1603, 1507 cm⁻¹.

Di-*tert*-butyl 1-(4-fluorobenzoyl)hydrazine-1,2-dicarboxylate 87n

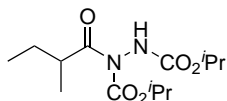
Purification by column chromatography (10%-50% EtOAc/Petrol) afforded di-*tert*-butyl 1-(4-fluorobenzoyl)hydrazine-1,2-dicarboxylate as a white solid (921 mg, 2.60 mmol, 52%). m.p. 104-106 °C; ¹H NMR (600 MHz, CDCl₃) δ 7.78-7.61 (m, 2H), 7.09 (t, *J* = 8.6 Hz, 2H), 6.90-6.60 (s, NH, 1H), 1.48 (s, 9H), 1.34-1.24 (m, 9H); ¹³C NMR (150 MHz, CDCl₃) δ 170.7 (C), 165.0 (d, *J*_{C-F} = 253.1 Hz, C), 154.7 (C), 151.8 (C), 131.9 (C), 131.0 (d, *J*_{C-F} = 8.9 Hz, CH), 115.4 (d, *J*_{C-F} = 22.1 Hz, CH), 84.7 (C), 82.4 (C), 28.2 (CH₃), 27.6 (CH₃); IR (solid) 3335, 3007, 2974, 2937 1756, 1702, 1603, 1506 cm⁻¹. LRMS (ESI) 355 (15, [M+H]⁺), 372 (25, [M+NH₄]⁺); HRMS (ESI) calcd for C₁₇H₂₄FN₂O₅ [M+H]⁺ 355.1666; observed 355.1664.

Dibenzyl 1-(4-fluorobenzoyl)hydrazine-1,2-dicarboxylate 87o

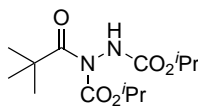
Purification by column chromatography (10%-50% EtOAc/Petrol) afforded dibenzyl 1-(4-fluorobenzoyl)hydrazine-1,2-dicarboxylate as a colourless oil (1.29 g, 3.05 mmol, 61%). m.p. 115-119 °C; ^1H NMR (600 MHz, CDCl_3) δ 7.71-6.90 (m, 14H), 5.26-5.05 (m, 4H); ^{13}C NMR (150 MHz, CDCl_3) δ 170.1 (C), 165.2 (d, $J_{\text{C-F}} = 253.3$ Hz, C), 155.9 (C), 153.5 (C), 135.5 (C), 134.9 (C), 134.4 (C), 131.3 (d, $J_{\text{C-F}} = 8.5$ Hz, CH), 130.7 (C), 128.9 (CH), 128.8 (C), 128.8 (CH), 128.7 (CH), 128.5 (CH), 128.4 (CH), 115.6 (d, $J_{\text{C-F}} = 22.2$ Hz, CH), 69.8 (CH_2), 68.4 (CH_2); IR (solid) 3396, 3067, 2969, 1738, 1707, 1596 cm^{-1} ; LRMS (CI) 440 (100, $[\text{M}+\text{NH}_4]^+$), 423 (15, $[\text{M}+\text{H}]^+$); HRMS (ESI) calcd for $\text{C}_{23}\text{H}_{20}\text{FN}_2\text{O}_5$ $[\text{M}+\text{H}]^+$ 423.1352; observed 423.1351.

Diisopropyl 1-butyrylhydrazine-1,2-dicarboxylate⁸¹ 87p

Purification by column chromatography (10%-50% EtOAc/Petrol) afforded diisopropyl 1-butyrylhydrazine-1,2-dicarboxylate as a colourless oil (1.19 g, 4.35 mmol, 87%). ^1H NMR (600 MHz, CDCl_3) δ 6.79 (br s, NH, 1H), 5.00 (septet, $J = 6.3$ Hz, 1H), 4.94 (septet, $J = 6.3$ Hz, 1H), 2.92-2.67 (m, 2H), 1.66 (sextet, $J = 7.4$ Hz, 2H), 1.30-1.14 (m, 12H), 0.94 (t, $J = 7.4$ Hz, 3H); ^{13}C NMR (150 MHz, CDCl_3) δ 173.9 (C), 155.2 (C), 152.8 (C), 130.9 (C), 72.1 (CH), 70.4 (CH), 39.0 (CH_2), 18.2 (CH_2), 13.7 (CH_3); IR (thin film) 3319, 3022, 2984, 2938 1785, 1729 cm^{-1} .

Diisopropyl 1-(2-methylbutanoyl)hydrazine-1,2-dicarboxylate⁸⁷ 87q

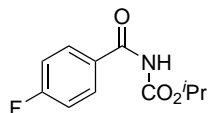
Purification by column chromatography (10%-50% EtOAc/Petrol) afforded diisopropyl 1-(2-methylbutanoyl)hydrazine-1,2-dicarboxylate as a colourless oil (1.14 g, 3.95 mmol, 79%). ¹H NMR (600 MHz, CDCl₃) δ 7.09 (br s, NH, 1H), 4.93 (septet, *J* = 6.2 Hz, 1H), 4.87 (septet, *J* = 6.2 Hz, 1H), 3.43-3.34 (m, 1H), 1.69 (septet, *J* = 6.7 Hz, 1H), 1.35 (septet, *J* = 6.7 Hz, 1H), 1.23-1.05 (m, 15H), 0.82 (t, *J* = 7.3 Hz, 3H); ¹³C NMR (150 MHz, CDCl₃) δ 177.9 (C), 155.3 (C), 152.7 (C), 72.0 (CH), 70.1 (CH), 40.8 (CH), 27.0 (CH₂), 21.9 (CH₃), 21.7 (CH₃), 16.8 (CH₂), 11.6 (CH₃); IR (thin film) 3315, 3023, 2982, 2938, 1784, 1722 cm⁻¹.

Diisopropyl 1-pivaloylhydrazine-1,2-dicarboxylate⁸¹ 87r

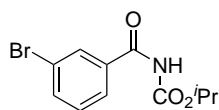
Purification by column chromatography (10%-50% EtOAc/Petrol) afforded diisopropyl 1-pivaloylhydrazine-1,2-dicarboxylate as a colourless oil (937 mg, 3.25 mmol, 65%). ¹H NMR (600 MHz, CDCl₃) δ 7.36-7.14 (m, NH, 1H), 4.93 (septet, *J* = 6.3 Hz, 1H), 4.89 (septet, *J* = 6.3 Hz, 1H), 1.33-1.09 (m, 21H); ¹³C NMR (150 MHz, CDCl₃) δ 179.7 (C), 179.3 (C), 156.3 (C), 155.8 (C), 153.3 (C), 153.1 (C), 72.1 (CH), 70.3 (CH), 42.0 (C), 27.5 (CH₃), 21.9 (CH₃), 21.7 (CH₃); IR (solid) 3295, 2982, 2937, 2876, 1775, 1722, 1506 cm⁻¹.

General experimental for the formation of aryl acyl carbamates

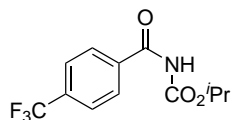
To a stirring solution of sodium hydride (60% mineral oil dispersion, 200 mg, 5.00 mmol, 5 eq.) in anhydrous THF (0.5 mL) was added dropwise a solution of acyl hydrazide (1.00 mmol, 1 eq.) pre-dissolved in anhydrous THF (1.5 mL) under an atmosphere of argon and the reaction mixture stirred for 5 minutes. After this time, to the reaction mixture was added dropwise *tert*-butyl bromoacetate **127b** (162 μ L, 1.10 mmol, 1.1 eq.) pre-dissolved in anhydrous THF (0.5 mL). The reaction mixture was then stirred at 25 °C for 16 h and then poured over saturated aqueous NH₄Cl (10 mL). The resulting solution was extracted with EtOAc (3 \times 15 mL). The combined extracts were dried (MgSO₄), filtered and the solvent evaporated *in vacuo*. The resultant crude residue was purified as described below.

Isopropyl (4-fluorobenzoyl)carbamate 126a

Purification by column chromatography (10%-50% EtOAc/Petrol) yielded isopropyl (4 fluorobenzoyl)carbamate as a white solid (187 mg, 0.83 mmol, 83%). m.p. 112-114 °C; ^1H NMR (600 MHz, CDCl_3) δ 7.97 (br s, NH, 1H), 7.87-7.83 (m, 2H), 7.21-7.10 (m, 2H), 5.09 (septet, $J = 6.3$ Hz, 1H), 1.33 (d, $J = 6.3$ Hz, 6H); ^{13}C NMR (150 MHz, CDCl_3) δ 165.7 (d, $J_{\text{C-F}} = 254.7$ Hz, C), 164.1 (C), 150.5 (C), 130.3 (d, $J_{\text{C-F}} = 9.3$ Hz, CH), 129.5 (d, $J_{\text{C-F}} = 3.1$ Hz, C), 116.1 (d, $J_{\text{C-F}} = 22.1$ Hz, CH), 70.7 (CH), 21.9 (CH_3); IR (solid) 3268, 2979, 2934, 1746, 1682, 1601, 1526 cm^{-1} ; LRMS (CI) 243 (100, $[\text{M}+\text{NH}_4]^+$), 226 (20, $[\text{M}+\text{H}]^+$); HRMS (ESI) calcd for $\text{C}_{11}\text{H}_{13}\text{FNO}_3$ $[\text{M}+\text{H}]^+$ 226.0874; observed 226.0875.

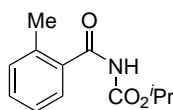
Isopropyl (3-bromobenzoyl)carbamate 126b

Purification by column chromatography (10%-50% EtOAc/Petrol) yielded isopropyl (3 bromobenzoyl)carbamate as a white solid (244 mg, 0.850 mmol, 85%). m.p. 134-135 °C; ^1H NMR (600 MHz, CDCl_3) δ 7.95 (t, $J = 1.7$ Hz, 1H), 7.89 (br s, NH, 1H), 7.79-7.67 (m, 2H), 7.37 (t, $J = 7.9$ Hz, 1H), 5.10 (septet, $J = 6.3$ Hz, 1H), 1.34 (d, $J = 6.3$ Hz, 6H); ^{13}C NMR (150 MHz, CDCl_3) δ 163.8 (C), 150.2 (C), 136.0 (CH), 135.2 (C), 130.8 (CH), 130.5 (CH), 126.2 (CH), 123.2 (C), 70.8 (CH), 21.9 (CH_3); IR (solid) 3250, 3187, 2979, 1764, 1746, 1684, 1594, 1567, 1520 cm^{-1} ; LRMS (ESI) 288 (97, $[\text{M}^{81}\text{Br}+\text{H}]^+$), 286 (100, $[\text{M}^{79}\text{Br}+\text{H}]^+$); HRMS (ESI) calcd for $\text{C}_{11}\text{H}_{13}\text{NO}_3\text{Br}$ $[\text{M}^{79}\text{Br}+\text{H}]^+$ 286.0079; observed 286.0078.

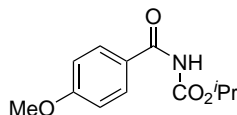
Isopropyl (4-(trifluoromethyl)benzoyl)carbamate 126c

Purification by column chromatography (10%-50% EtOAc/Petrol) yielded isopropyl (4-(trifluoromethyl)benzoyl)

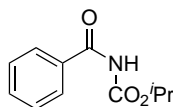
carbamate as a white solid (195 mg, 0.710 mmol, 71%). m.p. 100-102 °C; ^1H NMR (600 MHz, CDCl_3) δ 7.98-7.86 (m, 3H), 7.75 (d, $J = 8.2$ Hz, 2H), 5.10 (septet, $J = 6.3$ Hz, 1H), 1.34 (d, $J = 6.3$ Hz, 6H); ^{13}C NMR (150 MHz, CDCl_3) δ 164.3 (C), 150.2 (C), 136.5 (C), 134.5 (q, $J_{\text{C-F}} = 33.0$ Hz, C), 128.2 (CH), 126.0 (q, $J_{\text{C-F}} = 3.7$ Hz, CH), 123.5 (q, $J_{\text{C-F}} = 272.8$ Hz, C), 71.0 (CH), 21.9 (CH_3); IR (solid) 3273, 2984, 2942, 1753, 1611, 1528 cm^{-1} ; LRMS (ESI) 274 (100, $[\text{M-H}]^-$); HRMS (ESI) calcd for $\text{C}_{12}\text{H}_{11}\text{NO}_3\text{F}_3$ $[\text{M-H}]^-$ 274.0691; observed 274.0696.

Isopropyl (2-methylbenzoyl)carbamate 126d

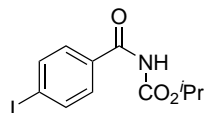
Purification by column chromatography (10%-50% EtOAc/Petrol) yielded isopropyl (2-methylbenzoyl)carbamate as a white solid (155 mg, 0.700 mmol, 70%). m.p. 94-97 °C; ^1H NMR (600 MHz, CDCl_3) δ 8.08 (br s, NH, 1H), 7.36-7.29 (m, 2H), 7.21-7.16 (m, 2H), 4.97 (septet, $J = 6.3$ Hz, 1H), 2.41 (s, 3H), 1.24 (d, $J = 6.3$ Hz, 6H); ^{13}C NMR (150 MHz, CDCl_3) δ 168.5 (C), 150.7 (C), 136.9 (C), 134.5 (C), 131.3 (CH), 131.0 (CH), 126.9 (CH), 125.8 (CH), 70.4 (CH), 21.8 (CH_3), 19.9 (CH_3); IR (solid) 3271, 2981, 2933, 1757, 1696, 1600, 1574 cm^{-1} ; LRMS (ESI) 222 (100, $[\text{M+H}]^+$); HRMS (ESI) calcd for $\text{C}_{12}\text{H}_{16}\text{NO}_3$ $[\text{M+H}]^+$ 222.1125; observed 222.1125.

Isopropyl (4-methoxybenzoyl)carbamate 126e

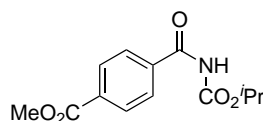
Purification by column chromatography (10%-50% EtOAc/Petrol) yielded isopropyl (4-methoxybenzoyl)carbamate as a white solid (204 mg, 0.860 mmol, 86%). m.p. 120-124 °C; ^1H NMR (600 MHz, CDCl_3) δ 7.90 (br s, 1H), 7.81-7.78 (m, 2H), 6.96-6.94 (m, 2H), 5.09 (septet, $J = 6.3$ Hz, 1H), 3.87 (s, 3H), 1.33 (d, $J = 6.3$ Hz, 6H); ^{13}C NMR (150 MHz, CDCl_3) δ 164.3 (C), 163.5 (C), 150.6 (C), 129.8 (CH), 125.4 (C), 114.2 (CH), 70.3 (CH), 55.6 (CH_3), 22.0 (CH_3); IR (solid) 3314, 2982, 2937, 1738, 1703, 1606, 1579 cm^{-1} ; LRMS (ESI) 238 (100, $[\text{M}+\text{H}]^+$); HRMS (ESI) calcd for $\text{C}_{12}\text{H}_{16}\text{NO}_4$ $[\text{M}+\text{H}]^+$ 238.1079; observed 238.1080.

Isopropyl benzoylcarbamate 126f

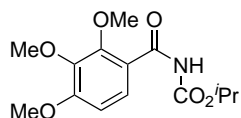
Purification by column chromatography (10%-50% EtOAc/Petrol) yielded isopropyl benzoylcarbamate as a white solid (157 mg, 0.760 mmol, 76%). m.p. 129-133 °C; ^1H NMR (600 MHz, CDCl_3) δ 8.49 (br s, NH, 1H), 7.84 (dd, $J = 7.4$ Hz, 1.1 Hz, 2H), 7.53 (t, $J = 7.4$ Hz, 1H), 7.43 (t, $J = 7.8$ Hz, 2H), 5.03 (septet, $J = 6.3$ Hz, 1H), 1.26 (d, $J = 6.3$ Hz, 6H); ^{13}C NMR (150 MHz, CDCl_3) δ 165.4 (C), 150.9 (C), 133.2 (C), 133.0 (CH), 128.8 (CH), 127.8 (CH), 70.3 (CH), 21.9 (CH_3); IR (solid) 3272, 2979, 2934, 1743, 1682, 1600, 1582, 1510 cm^{-1} ; LRMS (ESI) 206 (100, $[\text{M}+\text{H}]^+$); HRMS (ESI) calcd for $\text{C}_{11}\text{H}_{14}\text{NO}_3$ $[\text{M}+\text{H}]^+$ 206.0968; observed 206.0967.

Isopropyl (4-iodobenzoyl)carbamate 126g

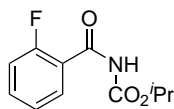
Purification by column chromatography (10%-50% EtOAc/Petrol) yielded isopropyl (4-iodobenzoyl)carbamate as a white solid (290 mg, 0.870 mmol, 87%). m.p. 119-122 °C; ^1H NMR (600 MHz, CDCl_3) δ 8.25 (br s, NH, 1H), 7.82 (d, $J = 8.2$ Hz, 2H), 7.57 (d, $J = 8.2$ Hz, 2H), 5.06 (septet, $J = 6.3$ Hz, 1H), 1.30 (d, $J = 6.3$ Hz, 6H); ^{13}C NMR (150 MHz, CDCl_3) δ 164.8 (C), 150.6 (C), 138.2 (CH), 132.6 (C), 129.3 (CH), 100.6 (C), 70.6 (CH), 21.9 (CH_3); IR (solid) 3266, 2980, 2935, 1746, 1685, 1586, 1517 cm^{-1} ; LRMS (ESI) 334 (100, $[\text{M}+\text{H}]^+$), 292 (60, $[\text{M}+\text{H}]^+$), 231 (20, $[\text{M}-\text{C}_4\text{H}_8\text{NO}_2+\text{H}]^+$); HRMS (ESI) calcd for $\text{C}_{11}\text{H}_{13}\text{INO}_3$ $[\text{M}+\text{H}]^+$ 333.9935; observed 333.9934.

Methyl 4-((isopropoxycarbonyl)carbamoyl)benzoate 126h

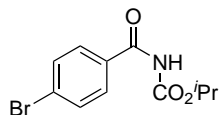
Purification by column chromatography (10%-50% EtOAc/Petrol) yielded methyl 4-((isopropoxycarbonyl)carbamoyl)benzoate as a white solid (191 mg, 0.720 mmol, 72%). m.p. 112-125 °C; ^1H NMR (600 MHz, CDCl_3) δ 8.82 (br s, NH, 1H), 8.05 (d, $J = 8.5$ Hz, 2H), 7.93 (d, $J = 8.5$ Hz, 2H), 5.00 (septet, $J = 6.3$ Hz, 1H), 3.89 (s, 3H), 1.23 (d, $J = 6.3$ Hz, 6H); ^{13}C NMR (150 MHz, CDCl_3) δ 166.2 (C), 165.0 (C), 150.8 (C), 137.1 (C), 133.8 (C), 129.9 (CH), 128.0 (CH), 70.4 (CH), 52.6 (CH_3), 21.9 (CH_3); IR (solid) 3272, 2980, 2943, 1757, 1715, 1677, 1613, 1572, 1515 cm^{-1} ; LRMS (ESI) 266 (100, $[\text{M}+\text{H}]^+$); HRMS (ESI) calcd for $\text{C}_{13}\text{H}_{16}\text{NO}_5$ $[\text{M}+\text{H}]^+$ 266.1023; observed 266.1025.

Isopropyl (2,3,4-trimethoxybenzoyl)carbamate 126i

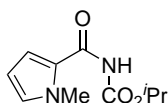
Purification by column chromatography (10%-50% EtOAc/Petrol) yielded isopropyl (2,3,4-trimethoxybenzoyl)carbamate as a white solid (202 mg, 0.680 mmol, 68%). m.p. 122-124 °C; ^1H NMR (600 MHz, CDCl_3) δ 10.06 (br s, NH, 1H), 7.92 (d, $J = 9.0$ Hz, 1H), 6.79 (d, $J = 9.0$ Hz, 2H), 5.07 (septet, $J = 6.3$ Hz, 1H), 4.03 (s, 3H), 3.91 (s, 3H), 3.86 (s, 3H), 1.31 (d, $J = 6.3$ Hz, 6H); ^{13}C NMR (150 MHz, CDCl_3) δ 162.5 (C), 157.9 (C), 152.6 (C), 150.8 (C), 141.7 (C), 127.9 (CH), 117.7 (C), 108.1 (CH), 67.9 (CH), 62.2 (CH_3), 61.1 (CH_3), 56.3 (CH_3), 22.0 (CH_3); IR (solid) 3537, 2982, 2940, 1776, 1705, 1595 cm^{-1} ; LRMS (ESI) 914 (20, $[\text{3M}+\text{Na}]^+$), 617 (50, $[\text{2M}+\text{Na}]^+$), 298 (100, $[\text{M}+\text{H}]^+$); HRMS (ESI) calcd for $\text{C}_{14}\text{H}_{20}\text{NO}_6$ $[\text{M}+\text{H}]^+$ 298.1291; observed 298.1293.

Isopropyl (2-fluorobenzoyl)carbamate 126j

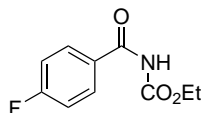
Purification by column chromatography (10%-50% EtOAc/Petrol) yielded isopropyl (2-fluorobenzoyl)carbamate as a white solid (235 mg, 0.740 mmol, 74%). m.p. 129-131 °C; ^1H NMR (600 MHz, CDCl_3) δ 8.53 (br s, NH, 1H), 7.93 (td, $J = 7.8$, 1.7 Hz, 1H), 7.50-7.45 (m, 1H), 7.21 (t, $J = 7.6$ Hz, 1H), 7.10-7.06 (m, 1H), 4.99 (septet, $J = 6.3$ Hz, 1H), 1.24 (d, $J = 6.3$ Hz, 6H); ^{13}C NMR (150 MHz, CDCl_3) δ 161.7 (C), 160.3 (d, $J_{\text{C-F}} = 248.8$ Hz, C), 150.2 (C), 134.8 (d, $J_{\text{C-F}} = 9.4$ Hz, CH), 132.1 (d, $J_{\text{C-F}} = 1.3$ Hz, CH), 125.2 (d, $J_{\text{C-F}} = 3.2$ Hz, CH), 120.6 (d, $J_{\text{C-F}} = 11.4$ Hz, C), 116.3 (d, $J_{\text{C-F}} = 24.2$ Hz, CH), 70.4 (CH), 21.8 (CH_3); IR (solid) 3266, 2980, 2935, 1760, 1691, 1612, 1581 cm^{-1} ; LRMS (ESI) 226 (100, $[\text{M}+\text{H}]^+$); HRMS (ESI) calcd for $\text{C}_{11}\text{H}_{13}\text{FNO}_3$ $[\text{M}+\text{H}]^+$ 226.0874; observed 226.0872.

Isopropyl (4-bromobenzoyl)carbamate 126k

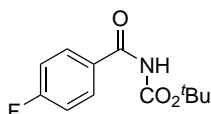
Purification by column chromatography (10%-50% EtOAc/Petrol) yielded isopropyl (4-bromobenzoyl)carbamate as a white solid (229 mg, 0.800 mmol, 80%). m.p. 125-127 °C; ^1H NMR (600 MHz, CDCl_3) δ 8.85 (br s, NH, 1H), 7.79 (d, $J = 8.6$ Hz, 2H), 7.56 (d, $J = 8.6$ Hz, 2H), 5.00 (septet, $J = 6.3$ Hz, 1H), 1.23 (d, $J = 6.3$ Hz, 6H); ^{13}C NMR (150 MHz, CDCl_3) δ 164.9 (C), 151.0 (C), 132.1 (CH), 132.0 (C), 129.7 (CH), 128.0 (C), 70.3 (CH), 21.9 (CH_3); IR (solid) 3274, 2981, 2946, 1760, 1716, 1677, 1613, 1572, 1517 cm^{-1} ; LRMS (ESI) 288 (95, $[\text{M}^{81}\text{Br}+\text{H}]^+$), 286 (100, $[\text{M}^{79}\text{Br}+\text{H}]^+$); HRMS (ESI) calcd for $\text{C}_{11}\text{H}_{13}\text{BrNO}_3$ $[\text{M}+\text{H}]^+$ 286.0078; observed 286.0073.

Isopropyl (1-methyl-1*H*-pyrrole-2-carbonyl)carbamate 126l

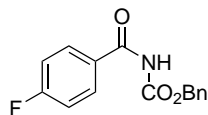
Purification by column chromatography (10%-50% EtOAc/Petrol) yielded isopropyl (1-methyl-1*H*-pyrrole-2-carbonyl)carbamate as a brown solid (128 mg, 0.610 mmol, 61%). m.p. 105-109 °C; ^1H NMR (600 MHz, CDCl_3) δ 7.80 (br s, NH, 1H), 6.88-6.82 (m, 1H), 6.73 (dd, $J = 4.1, 1.6$ Hz, 1H), 6.12 (dd, $J = 4.1, 2.5$ Hz, 1H), 5.08 (septet, $J = 6.3$ Hz, 1H), 3.95 (s, 3H), 1.32 (d, $J = 6.3$ Hz, 6H); ^{13}C NMR (150 MHz, CDCl_3) δ 158.0 (C), 150.7 (C), 130.8 (CH), 124.1 (C), 114.5 (CH), 108.0 (CH), 70.0 (CH), 22.0 (CH_3); IR (solid) 3273, 3119, 2980, 2938, 1921, 1897, 1869, 1741, 1673, 1567, 1531 cm^{-1} . LRMS (ESI) 211 (95, $[\text{M}+\text{H}]^+$), 233 (100, $[\text{M}+\text{Na}]^+$); HRMS (ESI) calcd for $\text{C}_{10}\text{H}_{15}\text{N}_2\text{O}_3$ $[\text{M}+\text{H}]^+$ 211.1077; observed 211.1077.

Ethyl (4-fluorobenzoyl)carbamate 126m

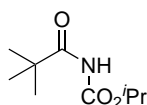
Purification by column chromatography (10%-50% EtOAc/Petrol) yielded ethyl (4-fluorobenzoyl)carbamate as a white solid (152 mg, 0.720 mmol, 72%). m.p. 87-90 °C; ¹H NMR (600 MHz, CDCl₃) δ 8.60 (br s, NH, 1H), 7.93-7.89 (m, 2H), 7.15-7.11 (m, 2H), 4.25 (q, *J* = 7.1 Hz, 2H) 1.29 (t, *J* = 7.1 Hz, 3H); ¹³C NMR (150 MHz, CDCl₃) δ 165.7 (d, *J*_{C-F} = 254.5 Hz, C), 164.4 (C), 151.5 (C), 130.6 (d, *J*_{C-F} = 9.3 Hz, CH), 129.2 (d, *J*_{C-F} = 3.0 Hz, C), 116.1 (d, *J*_{C-F} = 22.1 Hz, CH), 62.6 (CH₂), 14.3 (CH₃); IR (solid) 3274, 2983, 2938, 1751, 1686, 1602, 1525 cm⁻¹; LRMS (ESI) 212 (100, [M+H]⁺); HRMS (ESI) calcd for C₁₀H₁₁FNO₄ [M+H]⁺ 212.0717; observed 212.0717.

***tert*-Butyl (4-fluorobenzoyl)carbamate 126n**

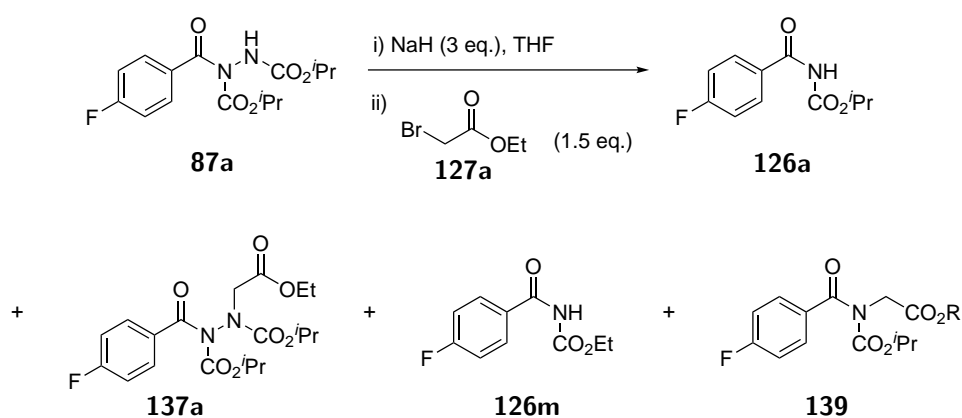
Purification by column chromatography (10%-50% EtOAc/Petrol) yielded *tert*-butyl (4-fluorobenzoyl)carbamate as a white solid (177 mg, 0.740 mmol, 74%). m.p. 116-118 °C; ¹H NMR (600 MHz, CDCl₃) δ 7.92-7.74 (m, 3H), 7.18-7.13 (m, 2H), 1.54 (s, 9H); ¹³C NMR (150 MHz, CDCl₃) δ 166.4 (d, *J*_{C-F} = 254.4 Hz, C), 164.4 (C), 149.6 (C), 130.3 (d, *J*_{C-F} = 9.3 Hz, CH), 129.6 (d, *J*_{C-F} = 3.0 Hz, C), 116.1 (d, *J*_{C-F} = 22.1 Hz, CH), 83.2 (C) 28.1 (CH₃); IR (solid) 3268, 2980, 2931, 1748, 1682, 1603, 1526, 1501 cm⁻¹. LRMS (ESI) 240 (25, [M+H]⁺), 262 (100, [M+Na]⁺); HRMS (ESI) calcd for C₁₂H₁₅FNO₃ [M+H]⁺ 240.1030; observed 240.1032.

Benzyl (4-fluorobenzoyl)carbamate **126o**

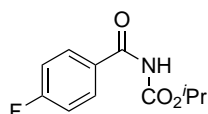
Purification by column chromatography (10%-50% EtOAc/Petrol) yielded benzyl (4-fluorobenzoyl)carbamate as a white solid (189 mg, 0.690 mmol, 69%). m.p. 125-130 °C; ^1H NMR (600 MHz, CDCl_3) δ 9.04 (br s, NH, 1H), 7.94-7.89 (m, 2H), 7.33-7.26 (m, 5H), 7.10-7.05 (m, 2H), 5.12 (s, 2H); ^{13}C NMR (150 MHz, CDCl_3) δ 165.7 (d, $J_{\text{C-F}} = 254.3$ Hz, C), 164.7 (C), 151.5 (C), 135.1 (C), 130.9 (d, $J_{\text{C-F}} = 9.3$ Hz, CH), 129.2 (d, $J_{\text{C-F}} = 2.9$ Hz, C), 128.7 (CH), 128.7 (CH), 115.9 (d, $J_{\text{C-F}} = 22.1$ Hz, CH), 67.9 (CH_2); IR (solid) 3273, 2982, 2937, 1761, 1736, 1681, 1599, 1582, 1508 cm^{-1} . LRMS (ESI) 274 (100, $[\text{M}+\text{H}]^+$), 291 (35, $[\text{M}+\text{NH}_4]^+$); HRMS (ESI) calcd for $\text{C}_{15}\text{H}_{13}\text{FNO}_3$ $[\text{M}+\text{H}]^+$ 274.0874; observed 274.0875.

Isopropyl pivaloylcarbamate **126r**

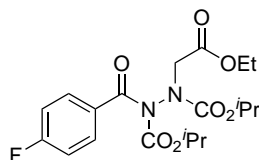
Purification by column chromatography (10%-50% EtOAc/Petrol) afforded isopropyl pivaloylcarbamate as a white solid (152 mg, 0.810 mmol, 81%). m.p. 80-84 °C; ^1H NMR (600 MHz, CDCl_3) δ 7.51 (br s, NH, 1H), 5.03 (septet, $J = 6.3$ Hz, 1H), 1.30 (d, $J = 6.3$ Hz, 6H), 1.24 (s, 9H); ^{13}C NMR (150 MHz, CDCl_3) δ 175.8 (C), 150.5 (C), 70.2 (CH), 40.3 (C), 27.2 (CH_3), 22.2 (CH_3), 21.9 (CH_3); IR (solid) 3267, 3193, 2979, 2937, 1771, 1758, 1509 cm^{-1} . LRMS (ESI) 188 (100, $[\text{M}+\text{H}]^+$), 210 (60, $[\text{M}+\text{Na}]^+$); HRMS (ESI) calcd for $\text{C}_9\text{H}_{18}\text{NO}_3$ $[\text{M}+\text{H}]^+$ 188.1281; observed 188.1279.



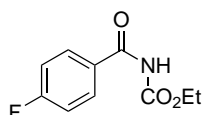
To a stirring solution of sodium hydride (60% mineral oil dispersion, 120 mg, 3.00 mmol, 3 eq.) in anhydrous THF (0.5 mL) was added dropwise a solution of diisopropyl 1-(4-fluorobenzoyl)hydrazine-1,2-dicarboxylate **87a** (326 mg, 1.00 mmol, 1 eq.) in anhydrous THF (1.5 mL) under an atmosphere of argon and the reaction mixture stirred for 5 minutes. After this time, to the reaction mixture was added dropwise ethyl bromoacetate **127a** (167 μ L, 1.50 mmol, 1.5 eq.) pre-dissolved in anhydrous THF (0.5 mL). The reaction was stirred at 25 $^{\circ}$ C for 16 h and poured over stirring saturated, aqueous NH_4Cl (10 mL). The resulting solution was extracted with EtOAc (3 \times 15 mL). The combined extracts were dried (MgSO_4), filtered and the solvent was evaporated *in vacuo*. Purification by column chromatography (10%-50% EtOAc/Petrol) yielded isopropyl (4-fluorobenzoyl)carbamate **126a** as a white solid (56.0 mg, 0.250 mmol, 25%); diisopropyl 1 (2-ethoxy-2-oxoethyl)-2-(4-fluorobenzoyl)hydrazine-1,2-dicarboxylate **137a** as a colourless oil (157 mg, 0.380 mmol, 38%); ethyl (4-fluorobenzoyl)carbamate **126m** as a white solid (34.0 mg, 0.160 mmol, 16%) and ethyl *N*-(4-fluorobenzoyl)-*N*-(isopropoxycarbonyl)glycinate **139** as a colourless oil (34.0 mg, 0.110 mmol, 11%).



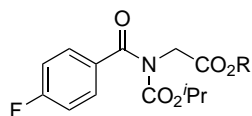
Data for isopropyl (4-fluorobenzoyl)carbamate **126a** matched that given above.

Diisopropyl 1-(2-ethoxy-2-oxoethyl)-2-(4-fluorobenzoyl)hydrazine-1,2-dicarboxylate

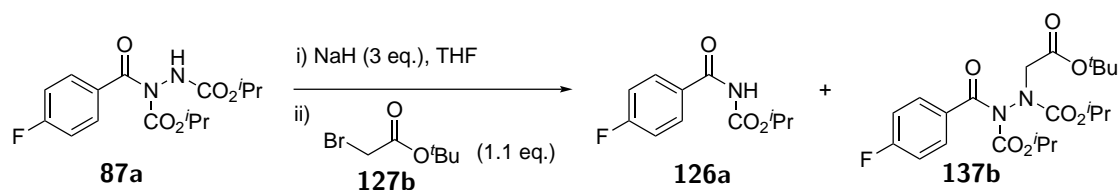
^1H NMR (600 MHz, CDCl_3) δ 7.71-7.69 (m, 2H), 7.10-7.05 (m, 2H), 5.01-4.95 (m, 1H), 4.90-4.84 (m, 1H), 4.41-4.29 (m, 2H), 4.17-4.12 (m, 2H), 1.29-1.06 (m, 15H); ^{13}C NMR (150 MHz, CDCl_3) δ 169.4 (C), 168.8 (C), 168.0 (C), 167.9 (C), 165.4 (d, $J_{\text{C-F}} = 253.3$ Hz, C), 164.8 (d, $J_{\text{C-F}} = 253.3$ Hz, C), 154.8 (C), 154.6 (C), 152.9 (C), 152.7 (C), 131.5 (d, $J_{\text{C-F}} = 3.2$ Hz, C), 131.3 (d, $J_{\text{C-F}} = 3.2$ Hz, C), 131.0 (d, $J_{\text{C-F}} = 9.1$ Hz, CH), 130.8 (d, $J_{\text{C-F}} = 9.1$ Hz, CH), 115.5 (d, $J_{\text{C-F}} = 22.1$ Hz, CH), 115.4 (d, $J_{\text{C-F}} = 22.1$ Hz, CH), 72.6 (CH), 72.5 (CH), 71.8 (CH), 71.4 (CH), 61.4 (CH_2), 61.4 (CH_2), 52.5 (CH_2), 51.3 (CH_2), 22.1 (CH_3), 22.1 (CH_3), 22.0 (CH_3), 22.0 (CH_3), 21.6 (CH_3), 21.5 (CH_3), 21.5 (CH_3), 21.4 (CH_3), 14.2 (CH_3), 14.1 (CH_3); IR (thin film) 2984, 2939, 1753, 1725, 1603, 1508 cm^{-1} ; LRMS (ESI) 413 (100, $[\text{M}+\text{H}]^+$); HRMS (ESI) calcd for $\text{C}_{19}\text{H}_{26}\text{N}_2\text{O}_7\text{F}$ $[\text{M}+\text{H}]^+$ 413.1724; observed 413.1726.



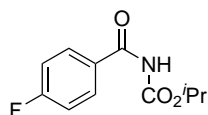
Data for ethyl (4-fluorobenzoyl)carbamate **126m** matched that given above.

Ethyl *N*-(4-fluorobenzoyl)-*N*-(isopropoxycarbonyl)glycinate

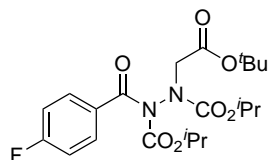
^1H NMR (600 MHz, CDCl_3) δ 7.75-7.57 (m, 2H), 7.17-7.04 (m, 2H), 4.85 (septet, $J = 6.2$ Hz, 1H), 4.55 (s, 2H), 4.25 (q, $J = 7.1$ Hz, 2H), 1.30 (t, $J = 7.1$ Hz, 3H), 1.03 (d, $J = 6.3$ Hz, 6H); ^{13}C NMR (150 MHz, CDCl_3) δ 171.8 (C), 168.9 (C), 164.8 (d, $J_{\text{C-F}} = 252.2$ Hz, C), 153.7 (C), 132.9 (d, $J_{\text{C-F}} = 3.3$ Hz, C), 130.4 (d, $J_{\text{C-F}} = 9.0$ Hz, CH), 115.3 (d, $J_{\text{C-F}} = 22.2$ Hz, CH), 71.9 (CH), 61.7 (CH_2), 46.7 (CH_2), 21.4 (CH_3), 14.3 (CH_3); IR (thin film) 2982, 2939, 1732, 1678, 1602, 1508 cm^{-1} ; LRMS (ESI) 312 (100, $[\text{M}+\text{H}]^+$); HRMS (ESI) calcd for $\text{C}_{15}\text{H}_{19}\text{FNO}_5$ $[\text{M}+\text{H}]^+$ 312.1242; observed 312.1241.



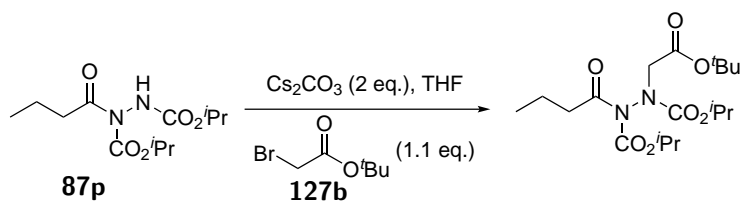
To a stirring solution of sodium hydride (60% mineral oil dispersion, 120 mg, 3.00 mmol, 3 eq.) in anhydrous THF (0.5 mL) was added dropwise a solution of diisopropyl 1-(4-fluorobenzoyl)hydrazine-1,2-dicarboxylate **87a** (326 mg, 1.00 mmol, 1 eq.) in anhydrous THF (1.5 mL) under an atmosphere of argon and the reaction mixture stirred for 5 minutes. After this time, to the reaction mixture was added dropwise *tert*-butyl bromoacetate **127b** (162 μ L, 1.10 mmol, 1.1 eq.) pre-dissolved in anhydrous THF (0.5 mL). The reaction was stirred at 25 °C for 16 h and poured over stirring saturated, aqueous NH_4Cl (10 mL). The resulting solution was extracted with EtOAc (3 \times 15 mL). The combined extracts were dried (MgSO_4), filtered and the solvent was evaporated *in vacuo*. Purification by column chromatography (10%-50% EtOAc/Petrol) yielded isopropyl (4-fluorobenzoyl)carbamate **126a** as a white solid (131 mg, 0.580 mmol, 58%) and diisopropyl 1-(2-(*tert*-butoxy)-2-oxoethyl)-2-(4-fluorobenzoyl)hydrazine-1,2-dicarboxylate **137b** as a colourless oil (110 mg, 0.250 mmol, 25%).



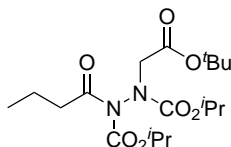
Data for isopropyl (4-fluorobenzoyl)carbamate **126a** matched that given above.

Diisopropyl 1-(2-(*tert*-butoxy)-2-oxoethyl)-2-(4-fluorobenzoyl)hydrazine-1,2-dicarboxylate 137b

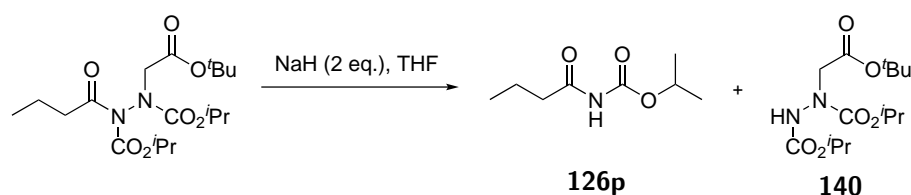
^1H NMR (600 MHz, CDCl_3) δ 7.75-7.64 (m, 2H), 7.13-7.07 (m, 2H), 5.05-4.96 (m, 1H), 4.93-4.85 (m, 1H), 4.40-4.17 (m, 2H), 1.47-1.41 (m, 9H), 1.33-1.23 (m, 6H), 1.18-1.07 (m, 6H); ^{13}C NMR (150 MHz, CDCl_3) δ 169.4 (C), 168.7 (C), 167.1 (C), 166.9 (C), 165.1 (d, $J_{\text{C-F}} = 253.3$ Hz, C), 165.1 (d, $J_{\text{C-F}} = 253.0$ Hz, C), 154.9 (C), 154.8 (C), 153.0 (C), 152.8 (C), 131.7 (d, $J_{\text{C-F}} = 3.2$ Hz, C), 131.5 (d, $J_{\text{C-F}} = 3.2$ Hz, C), 131.0 (d, $J_{\text{C-F}} = 9.1$ Hz, CH), 130.8 (d, $J_{\text{C-F}} = 9.1$ Hz, CH), 115.5 (d, $J_{\text{C-F}} = 22.2$ Hz, CH), 115.4 (d, $J_{\text{C-F}} = 22.2$ Hz, CH), 82.1 (C), 82.0 (C), 72.5 (CH), 72.5 (CH), 71.6 (CH), 71.2 (CH), 53.4 (CH_2), 52.0 (CH_2), 28.1 (CH_3), 28.1 (CH_3), 28.1 (CH_3), 22.2 (CH_3), 22.1 (CH_3), 22.1 (CH_3), 22.0 (CH_3), 21.6 (CH_3), 21.5 (CH_3), 21.5 (CH_3), 21.5 (CH_3); IR (thin film) 2978, 2933, 2876, 1748, 1720, 1601, 1506 cm^{-1} ; LRMS (ESI) 441 (100, $[\text{M}+\text{H}]^+$); HRMS (ESI) calcd for $\text{C}_{21}\text{H}_{30}\text{FN}_2\text{O}_7$ $[\text{M}+\text{H}]^+$ 441.2032; observed 441.2031.



To a stirring solution of cesium carbonate (652 mg, 2.00 mmol, 2 eq.) in anhydrous THF (0.5 mL) was added dropwise a solution of diisopropyl 1-butylhydrazine-1,2-dicarboxylate **87p** (274 mg, 1.00 mmol) in anhydrous THF (1.5 mL) under an atmosphere of argon and the reaction mixture stirred for 5 minutes. After this time, to the reaction mixture was added dropwise *tert*-butyl bromoacetate **127b** (162 μL , 1.10 mmol, 1.1 eq.) pre-dissolved in anhydrous THF (0.5 mL). The reaction was stirred at 25 °C for 16 h and poured over stirring saturated, aqueous NH_4Cl (10 mL). The resulting solution was extracted with EtOAc (3×15 mL). The combined extracts were dried (MgSO_4), filtered and the solvent was removed *in vacuo*.

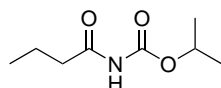
Diisopropyl 1-(2-(*tert*-butoxy)-2-oxoethyl)-2-butyrylhydrazine-1,2-dicarboxylate

Purification by column chromatography (10%-50% EtOAc/Petrol) afforded diisopropyl 1-(2-(*tert*-butoxy)-2-oxoethyl)-2-butyrylhydrazine-1,2-dicarboxylate as a colourless oil (357 mg, 0.920 mmol, 92%). ^1H NMR (600 MHz, CDCl_3) δ 4.94-4.87 (m, 1H), 4.85-4.77 (m, 1H), 4.08-3.82 (m, 2H), 2.84-2.76 (m, 1H), 2.67-2.57 (m, 1H), 1.61-1.49 (m, 2H), 1.35-1.31 (m, 9H), 1.21-1.04 (m, 12H), 0.86-0.81 (m, 3H); ^{13}C NMR (150 MHz, CDCl_3) δ 173.1 (C), 172.9 (C), 166.6 (C), 166.5 (C), 154.7 (C), 154.3 (C), 152.4 (C), 152.4 (C), 81.5 (C), 81.4 (C), 71.9 (CH), 71.9 (CH), 71.1 (CH), 70.6 (CH), 53.5 (CH_2), 52.3 (CH_2), 38.4 (CH_2), 38.3 (CH_2), 27.9 (CH_3), 21.9 (CH_3), 21.9 (CH_3), 21.8 (CH_3), 21.7 (CH_3), 21.6 (CH_3), 21.6 (CH_3), 21.5 (CH_3), 18.1 (CH_2), 17.9 (CH_2), 13.6 (CH_3) 13.6 (CH_3); IR (solid) 3023, 2981, 2937, 1790, 1725 cm^{-1} . LRMS (ESI) 389 (75, $[\text{M}+\text{H}]^+$), 411 (100, $[\text{M}+\text{Na}]^+$); HRMS (ESI) calcd for $\text{C}_{18}\text{H}_{33}\text{N}_2\text{O}_7$ $[\text{M}+\text{H}]^+$ 389.2282; observed 389.2281.

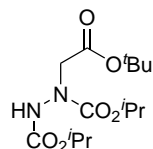


To a stirring solution of sodium hydride (60% mineral oil dispersion, 73.6 mg, 1.84 mmol, 2 eq.) in anhydrous THF (0.5 mL) was added dropwise a solution of diisopropyl 1-(2-(*tert*-butoxy)-2-oxoethyl)-2-butyrylhydrazine-1,2-dicarboxylate (357 mg, 0.920 mmol, 1 eq.) pre-dissolved in anhydrous THF (1.5 mL) under an atmosphere of argon. The reaction was stirred at 25 °C for 16 h and poured over stirring saturated, aqueous NH₄Cl (10 mL). The resulting solution was extracted with EtOAc (3 × 15 mL). The combined extracts were dried (MgSO₄), filtered and the solvent was evaporated in vacuo. Purification by column chromatography (10%-50% EtOAc/Petrol) afforded isopropyl butyrylcarbamate **126p** as a white solid (90.0 mg, 0.520 mmol, 56%) and diisopropyl 1-(2-(*tert*-butoxy)-2-oxoethyl)hydrazine-1,2-dicarboxylate **140** as a white solid (118 mg, 0.370 mmol, 40%).

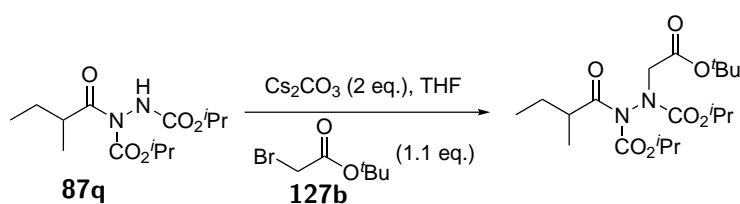
Isopropyl butyrylcarbamate **126p**



m.p. 65-67 °C; ¹H NMR (600 MHz, CDCl₃) δ 7.60 (br s, NH, 1H), 4.96 (septet, *J* = 6.3 Hz, 1H), 2.71 (t, *J* = 7.4 Hz, 2H), 1.67 (sextet, *J* = 7.4 Hz, 2H), 1.27 (d, *J* = 6.3 Hz, 6H), 0.96 (t, *J* = 7.4 Hz, 3H); ¹³C NMR (150 MHz, CDCl₃) δ 174.8 (C), 151.4 (C), 70.2 (CH), 38.1 (CH₂), 21.9 (CH₃), 17.8 (CH₂), (CH₃); IR (thin film) 3275, 2966, 2936, 2876, 1756, 1697 cm⁻¹; LRMS (ESI) 196 (100, [M+Na]⁺), 174 (90, [M+H]⁺); HRMS (ESI) calcd for C₈H₁₆NO₃ [M+H]⁺ 174.1130; observed 174.1134.

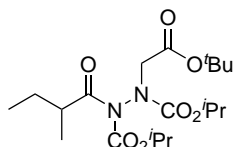
Diisopropyl 1-(2-(*tert*-butoxy)-2-oxoethyl)hydrazine-1,2-dicarboxylate 140

m.p. 100-105 °C; ^1H NMR (600 MHz, CDCl_3) δ 6.85-6.50 (m, NH, 1H), 5.00-4.87 (m, 2H), 4.22-4.06 (m, 2H), 1.45 (s, 9H), 1.26-1.22 (m, 12H); ^{13}C NMR (150 MHz, CDCl_3) δ 168.9 (C), 155.9 (C), 155.3 (C), 82.4 (C), 71.1 (CH), 71.0 (CH), 70.7 (CH), 70.0 (CH), 69.7 (CH), 53.4 (CH_2), 51.9 (CH_2), 28.2 (CH_3), 28.2 (CH_3), 27.8 (CH_3), 22.1 (CH_3), 21.8 (CH_3); IR (solid) 3321, 2981, 2937, 1726 cm^{-1} . LRMS (ESI) 319 (75, $[\text{M}+\text{H}]^+$), 341 (100, $[\text{M}+\text{Na}]^+$); HRMS (ESI) calcd for $\text{C}_{14}\text{H}_{27}\text{N}_2\text{O}_6$ $[\text{M}+\text{H}]^+$ 319.1864; observed 319.1865.

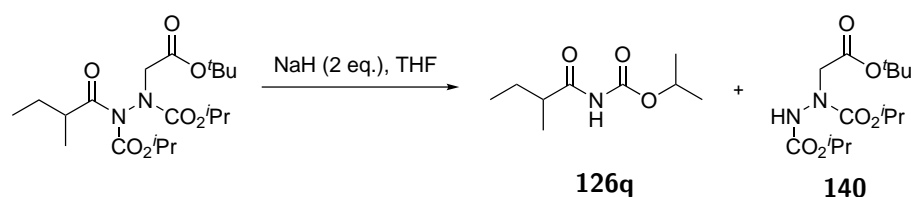


To a stirring solution of cesium carbonate (652 mg, 2.00 mmol, 2 eq.) in anhydrous THF (0.5 mL) was added dropwise a solution of diisopropyl 1-(2-methylbutanoyl)hydrazine-1,2-dicarboxylate **87q** (288 mg, 1.00 mmol) in anhydrous THF (1.5 mL) under an atmosphere of argon and the reaction mixture stirred for 5 minutes. After this time, to the reaction mixture was added dropwise *tert*-butyl bromoacetate **127b** (162 μ L, 1.10 mmol, 1.1 eq.) pre-dissolved in anhydrous THF (0.5 mL). The reaction was stirred at 25 $^{\circ}$ C for 16 h and poured over stirring saturated, aqueous NH_4Cl (10 mL). The resulting solution was extracted with EtOAc (3×15 mL). The combined extracts were dried (MgSO_4), filtered and the solvent was removed *in vacuo*.

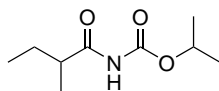
Diisopropyl 1-(2-(*tert*-butoxy)-2-oxoethyl)-2-(2-methylbutanoyl)hydrazine-1,2-dicarboxylate



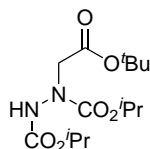
Purification by column chromatography (10%-50% EtOAc/Petrol) afforded diisopropyl 1-(2-(*tert*-butoxy)-2-oxoethyl)-2-(2-methylbutanoyl)hydrazine-1,2-dicarboxylate as a colourless oil (322 mg, 0.800 mmol, 80%). ^1H NMR (600 MHz, CDCl_3) δ 5.03-4.96 (m, 1H), 4.93-4.85 (m, 1H), 4.24-3.84 (m, 2H), 3.53-3.41 (m, 1H), 1.80-1.68 (m, 1H), 1.44-1.34 (m, 10H), 1.29-1.09 (m, 15H), 0.90-0.84 (m, 3H); ^{13}C NMR (150 MHz, CDCl_3) δ 177.3 (C), 177.2 (C), 176.9 (C), 176.8 (C), 166.7 (C), 166.6 (C), 166.6 (C), 154.9 (C), 154.4 (C), 154.4 (C), 152.7 (C), 152.6 (C), 152.6 (C), 81.9 (C), 81.6 (C), 81.6 (C), 81.5 (C), 72.1 (CH), 72.0 (CH), 71.1 (CH), 70.7 (CH), 70.7 (CH), 68.5 (CH), 53.6 (CH_2), 53.6 (CH_2), 52.4 (CH_2), 52.4 (CH_2), 40.7 (CH), 40.6 (CH), 40.4 (CH), 40.3 (CH), 28.1 (CH_3), 28.1 (CH_3), 27.1 (CH_2), 27.0 (CH_2), 27.0 (CH_2), 26.9 (CH_2), 22.0 (CH_3), 22.0 (CH_3), 21.9 (CH_3), 21.9 (CH_3), 21.8 (CH_3), 21.8 (CH_3), 21.7 (CH_3), 21.7 (CH_3), 21.7 (CH_3), 21.6 (CH_3), 17.0 (CH_3), 16.9 (CH_3), 16.8 (CH_3), 11.8 (CH_3), 11.7 (CH_3), 11.7 (CH_3), 11.6 (CH_3); IR (thin film) 3021, 2982, 2937, 1784, 1722 cm^{-1} . LRMS (ESI) 389 (80, $[\text{M}+\text{H}]^+$), 411 (100, $[\text{M}+\text{Na}]^+$); HRMS (ESI) calcd for $\text{C}_{18}\text{H}_{33}\text{N}_2\text{O}_7$ $[\text{M}+\text{H}]^+$ 389.2282; observed 389.2281.



To a stirring solution of sodium hydride (60% mineral oil dispersion, 64.0 mg, 1.60 mmol, 2 eq.) in anhydrous THF (0.5 mL) was added dropwise a solution of diisopropyl 1-(2-(*tert*-butoxy)-2-oxoethyl)-2-(2-methylbutanoyl)hydrazine-1,2-dicarboxylate (322 mg, 0.800 mmol, 1 eq.) pre-dissolved in anhydrous THF (1.5 mL) under an atmosphere of argon. The reaction was stirred at 25 °C for 16 h and poured over stirring saturated, aqueous NH₄Cl (10 mL). The resulting solution was extracted with EtOAc (3 × 15 mL). The combined extracts were dried (MgSO₄), filtered and the solvent was removed *in vacuo*. Purification by column chromatography (10%-50% EtOAc/Petrol) afforded isopropyl (2-methylbutanoyl)carbamate as a white solid **126q** (101 mg, 0.540 mmol, 67%) and diisopropyl 1-(2-(*tert*-butoxy)-2-oxoethyl)hydrazine-1,2-dicarboxylate **140** as a white solid (51.0 mg, 0.160 mmol, 20%).

Isopropyl (2-methylbutanoyl)carbamate 126q

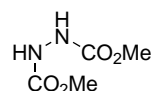
m.p. 73-77 °C; ^1H NMR (600 MHz, CDCl_3) δ 7.54 (br s, NH, 1H), 4.97 (septet, $J = 6.3$ Hz, 1H), 3.03 (m, 1H), 1.73 (septet, $J = 6.9$ Hz, 1H), 1.43 (septet, $J = 6.9$ Hz, 1H), 1.27 (d, $J = 6.3$ Hz, 6H), 1.15 (d, $J = 6.9$ Hz, 3H), 0.92 (t, $J = 7.4$ Hz, 3H); ^{13}C NMR (150 MHz, CDCl_3) δ 177.7 (C), 151.0 (C), 70.2 (CH), 41.2 (CH), 26.7 (CH_2), 21.9 (CH_3), 16.6 (CH_3), 11.7 (CH_3); IR (solid) 3271, 3198, 2973, 2936, 2877, 1772, 1752, 1525 cm^{-1} . LRMS (ESI) 188 (100, $[\text{M}+\text{H}]^+$), 210 (30, $[\text{M}+\text{Na}]^+$); HRMS (ESI) calcd for $\text{C}_9\text{H}_{18}\text{NO}_3$ $[\text{M}+\text{H}]^+$ 188.1281; observed 188.1278.



Data for diisopropyl 1-(2-(*tert*-butoxy)-2-oxoethyl)hydrazine-1,2-dicarboxylate **140** matched that given above.

6.3 Experimental for Chapter 4

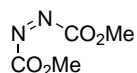
Dimethyl hydrazine-1,2-dicarboxylate¹⁶⁶ 149



To a solution of methyl carbazate (901 mg, 10.0 mmol) and sodium carbonate (1.06 g, 10.0 mmol) in DCM (15 mL) at -78 °C was added methyl chloroformate (923 μL , 12.0 mmol). The reaction mixture was allowed to stir for 16 h and warm to room temperature. The reaction mixture was then filtered through a pad of Celite® and the solvent removed *in vacuo* to afford dimethyl hydrazine-1,2-dicarboxylate as a white solid (815 mg, 5.50 mmol, 55%).

¹H NMR (600 MHz, CDCl₃) δ 6.62 (br s, 2H), 3.77 (s, 6H); ¹³C NMR (150 MHz, CDCl₃) δ 157.3 (C), 55.3 (CH₃); IR (thin film) 3279, 3048, 2958, 1743, 1707, 1536 cm⁻¹.

Dimethyl azodicarboxylate¹⁶⁶ 63c



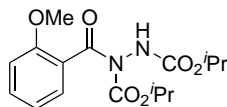
To a solution of dimethyl hydrazine-1,2-dicarboxylate (645 mg, 4.35 mmol) and pyridine (348 μL , 4.35 mmol) in DCM (11 mL) was added NBS (774 mg, 4.35 mmol). The reaction mixture was allowed to stir for 20 mins and warm to room temperature. The reaction mixture was then diluted with DCM (20 mL) and washed with H₂O (2 \times 20 mL), aq. sat. NaHCO₃ (2 \times 20 mL) and aq. sat. NaCl (20 mL). The solution was then dried (MgSO₄), filtered and the solvent removed *in vacuo* affording an orange-red oil (617 mg, 4.23 mmol, 97%).

¹H NMR (600 MHz, CDCl₃) δ 4.08 (s, 6H); ¹³C NMR (150 MHz, CDCl₃) δ 160.8 (C), 55.7 (CH₃); IR (thin film) 3055, 3017, 2963, 1774 cm⁻¹.

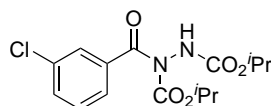
General experimental for the formation of acyl hydrazides

The following molecules were synthesised based on literature procedures described by Caddick *et al.*⁸¹

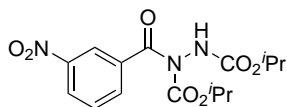
To a solution of azodicarboxylate (6.00 mmol) on H₂O (1 mL) was added aldehyde (5.00 mmol). The reaction mixture stirred at 21 °C for 48 h. The resulting solution was extracted with EtOAc (3 × 15 mL). The combined extracts were dried (MgSO₄), filtered and the solvent was removed *in vacuo*. The resultant crude residue was purified as described below.

Diisopropyl 1-(2-methoxybenzoyl)hydrazine-1,2-dicarboxylate 87s

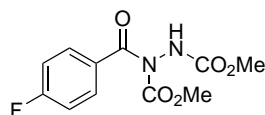
Purification by column chromatography (10%-50% EtOAc/Petrol) afforded diisopropyl 1-(2-methoxybenzoyl)hydrazine-1,2-dicarboxylate as a clear oil (1.08 g, 3.20 mmol, 64%). ^1H NMR (600 MHz, CDCl_3) δ 7.44-7.11 (m, NH, 1H), 7.33-7.27 (m, 2H), 6.87 (t, $J = 7.5$ Hz, 1H), 6.79 (d, $J = 8.3$ Hz, 1H), 4.88 (septet, $J = 6.3$ Hz, 1H), 4.84-4.74 (m, 1H), 3.70 (s, 3H), 1.15 (d, $J = 6.8$ Hz, 6H), 1.10-0.92 (m, 6H); ^{13}C NMR (150 MHz, CDCl_3) δ 168.4 (C), 156.2 (C), 155.3 (C), 152.4 (C), 131.9 (CH), 128.8 (CH), 125.7 (C), 110.8 (CH), 72.1 (CH), 70.2 (CH), 55.7 (CH_3), 21.9 (CH_3), 21.4 (CH_3); IR (thin film) 3308, 2970, 2932, 1731, 1699, 1601, 1517 cm^{-1} ; LRMS (ESI) 361 (25, $[\text{M}+\text{Na}]^+$), 339 (100, $[\text{M}+\text{H}]^+$), 135 (70, $[\text{M}-\text{C}_8\text{H}_{15}\text{N}_2\text{O}_4+\text{H}]^+$); HRMS (ESI) calcd for $\text{C}_{16}\text{H}_{23}\text{N}_2\text{O}_6$ $[\text{M}+\text{H}]^+$ 339.1551; observed 339.1554.

Diisopropyl 1-(3-chlorobenzoyl)hydrazine-1,2-dicarboxylate¹⁶⁵ 87t

Purification by column chromatography (10%-50% EtOAc/Petrol) afforded diisopropyl 1-(3-chlorobenzoyl)hydrazine-1,2-dicarboxylate as a white solid (1.35 g, 3.95 mmol, 79%). ^1H NMR (700 MHz, CDCl_3) δ 7.76-7.50 (m, 2H), 7.48 (d, $J = 7.9$ Hz, 1H), 7.36 (d, $J = 7.9$ Hz, 1H), 6.96-6.75 (m, NH, 1H), 5.01 (septet, $J = 6.2$ Hz, 1H), 4.91 (septet, $J = 5.6$ Hz, 1H), 1.29 (d, $J = 5.8$ Hz, 6H), 1.14-1.08 (m, 6H); ^{13}C NMR (175 MHz, CDCl_3) δ 170.0 (C), 155.3 (C), 152.7 (C), 137.0 (C), 134.4 (CH), 131.9 (CH), 129.6 (CH), 128.2 (CH), 126.3 (C), 73.0 (CH), 71.0 (CH), 22.0 (CH_3), 21.5 (CH_3); IR (solid) 3287, 2981, 2940, 2921, 1710, 1560 cm^{-1} .

Diisopropyl 1-(3-nitrobenzoyl)hydrazine-1,2-dicarboxylate 87u

Purification by column chromatography (10%-50% EtOAc/Petrol) afforded diisopropyl 1-(3-nitrobenzoyl)hydrazine-1,2-dicarboxylate as a white solid (1.01 g, 2.85 mmol, 57%). m.p. 114-116 °C; ^1H NMR (600 MHz, CDCl_3) δ 8.54-8.43 (m, 1H), 8.40-8.36 (m, 1H), 8.05-7.91 (m, 1H), 7.65-7.60 (m, 1H), 6.87-6.62 (br s, NH, 1H), 5.08-4.99 (m, 1H), 4.98-4.91 (m, 1H), 1.34-1.12 (m, 12H); ^{13}C NMR (150 MHz, CDCl_3) δ 169.0 (C), 155.2 (C), 152.5 (C), 148.0 (C), 136.9 (C), 133.9 (CH), 129.5 (CH), 126.3 (CH), 123.2 (CH), 73.3 (CH), 71.3 (CH), 22.0 (CH_3), 21.6 (CH_3); IR (thin film) 3310, 2984, 1715, 1534, 1350, 1258, 1102 cm^{-1} ; LRMS (ESI) 354 (100, $[\text{M}+\text{H}]^+$); HRMS (ESI) calcd for $\text{C}_{15}\text{H}_{20}\text{N}_3\text{O}_7$ $[\text{M}+\text{H}]^+$ 354.1301, observed 354.1319.

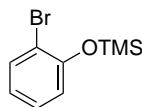
Dimethyl 1-(4-fluorobenzoyl)hydrazine-1,2-dicarboxylate 87v

Purification by column chromatography (10%-40% EtOAc/Petrol) afforded dimethyl 1-(4-fluorobenzoyl)hydrazine-1,2-dicarboxylate as a white solid (918 mg, 3.40 mmol, 68%). m.p. 148-152 °C; ^1H NMR (600 MHz, CDCl_3) δ 7.77-7.62 (m, 2H), 7.30 (br s, 1H), 7.10 (t, $J = 8.6$ Hz, 2H), 3.80 (s, 3H) 3.75 (s, 3H); ^{13}C NMR (150 MHz, CDCl_3) δ 170.0 (C), 165.5 (d, $J_{\text{C-F}} = 253.9$ Hz, C), 156.2 (C), 154.1 (C), 131.2 (d, $J_{\text{C-F}} = 23.5$ Hz, CH), 130.4 (C), 115.7 (d, $J_{\text{C-F}} = 9.1$ Hz, CH), 54.7 (CH_3), 53.6 (CH_3); IR (thin film) 3271, 3070, 3023, 2959, 1748, 1718, 1699, 1602, 1559 cm^{-1} . LRMS (ESI) 293 (65, $[\text{M}+\text{Na}]^+$), 271 (20, $[\text{M}+\text{H}]^+$); HRMS (ESI) calcd for $\text{C}_{11}\text{H}_{12}\text{FN}_2\text{O}_5$ $[\text{M}+\text{H}]^+$ 271.0725; observed 271.0728.

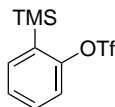
Synthesis of benzyne precursor

The following molecules were synthesised based on literature procedures described by Liu *et al.*¹⁶⁷

(2-Bromophenoxy)trimethylsilane¹⁶⁷ 146



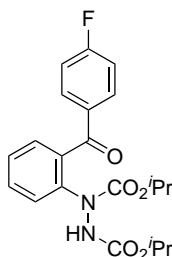
To a solution of 2-bromophenol (603 μL , 5.70 mmol) in THF (10 mL) was added hexamethyldisilazane (1.57 mL, 7.50 mmol). The solution was refluxed for 2 h and then allowed to cool to room temperature. The solvent was then removed *in vacuo* to afford (2-bromophenoxy)trimethylsilane as an orange oil (1.24 g, 5.10 mmol, 89%). ^1H NMR (600 MHz, CDCl_3) δ 7.53 (dd, $J = 7.9, 1.6$ Hz, 1H), 7.18 (td, $J = 8.0, 1.6$ Hz, 1H), 6.88 (dd, $J = 8.0, 1.5$ Hz, 1H), 6.85 (td, $J = 7.8, 1.5$ Hz, 1H), 0.31 (s, 9H); ^{13}C NMR (150 MHz, CDCl_3) δ 152.6 (C), 133.4 (CH), 128.4 (CH), 122.8 (CH), 120.9 (CH), 115.7 (C), -0.5 (CH_3); IR (thin film) 3056, 2986, 1584 cm^{-1} .

2-(Trimethylsilyl)phenyl trifluoromethanesulfonate¹⁶⁷ 144

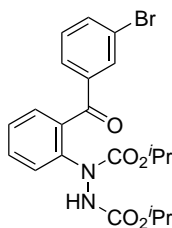
To a solution of (2-bromophenoxy)trimethylsilane (2.00 g, 8.60 mmol) in THF (20 mL) at 78 °C was added dropwise n-BuLi (2.5 M, 3.91 mL, 12.2 mmol). The reaction mixture was stirred for 20 mins. After this time, to the solution was added dropwise Tf₂O (1.90 mL, 12.2 mmol). The reaction was allowed to warm slowly to room temperature and stirred for a further 30 mins. The solution was quenched with sat. aq. NaHCO₃ and extracted with EtOAc. The combined organic extracts were dried (MgSO₄), filtered and the solvent removed *in vacuo*. Purification by column chromatography (10%-80% EtOAc/Petrol) afforded 2-(trimethylsilyl)phenyl trifluoromethanesulfonate as a yellow oil (1.46 g, 4.90 mmol, 57%). ¹H NMR (600 MHz, CDCl₃) δ 7.54 (d, *J* = 7.3 Hz, 1H), 7.45 (td, *J* = 7.8, 1.5 Hz, 1H), 7.36 7.33 (m, 2H), 0.37 (s, 9H); ¹³C NMR (150 MHz, CDCl₃) δ 155.2 (C), 136.4 (CH), 132.7 (CH), 131.4 (CH), 127.6 (CH), 119.6 (CH), 118.6 (q, *J*_{C-F} = 319.9 Hz, C), -0.7 (CH₃); IR (thin film) 3054, 2987 cm⁻¹.

General experimental for the formation of 2-hydrazobenzophenones

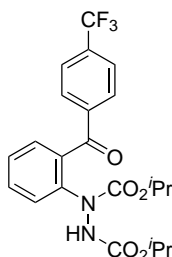
To a solution of acyl hydrazide (0.500 mmol) and TBAT (1.00 mmol) in toluene (6 mL) was added 2-(trimethylsilyl)phenyl trifluoromethanesulfonate (0.750 mmol). The reaction mixture was stirred at 50 °C for 16 h. The resulting solution was allowed to cool to room temperature and the solvent removed *in vacuo*. The resultant crude residue was purified as described below.

Diisopropyl 1-(2-(4-fluorobenzoyl)phenyl)hydrazine-1,2-dicarboxylate 141a

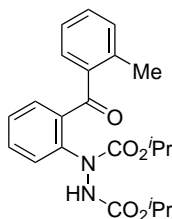
Purification by column chromatography (10%-50% EtOAc/Petrol) afforded diisopropyl 1-(2-(4-fluorobenzoyl)phenyl)hydrazine-1,2-dicarboxylate as a pale-yellow oil (173 mg, 430 μmol , 86%). ^1H NMR (700 MHz, CDCl_3) δ 7.83-7.81 (m, 2H), 7.77-7.76 (m, 1H), 7.57-7.54 (m, 1H), 7.42-7.35 (m, 2H), 7.12 (t, $J = 7.6$ Hz, 2H), 7.12 (br s, 1H, NH), 5.00-4.93 (m, 1H), 4.79 (septet, $J = 6.1$ Hz, 1H), 1.31-1.22 (m, 6H), 1.16-0.90 (m, 6H); ^{13}C NMR (175 MHz, CDCl_3) δ 195.1 (C), 194.5 (C), 166.1 (d, $J_{\text{C-F}} = 253.8$ Hz, C), 165.9 (d, $J_{\text{C-F}} = 253.7$ Hz, C), 156.1 (C), 155.8 (C), 155.0 (C), 154.5 (C), 141.0 (C), 135.4 (C), 133.5 (C), 133.4 (C), 133.1 (CH), 132.4 (CH), 130.1 (CH), 129.8 (CH), 129.4 (CH), 128.9 (CH), 127.7 (CH), 127.4 (CH), 115.7 (d, $J_{\text{C-F}} = 21.7$ Hz), 71.2 (CH), 70.8 (CH), 70.0 (CH), 22.1 (CH_3), 22.0 (CH_3), 21.8 (CH_3); IR (thin film) 3323, 2921, 2834, 1711, 1666, 1622, 1599, 1574 cm^{-1} ; LRMS (ESI) 403 (100, $[\text{M}+\text{H}]^+$); HRMS (ESI) calcd for $\text{C}_{21}\text{H}_{24}\text{FN}_2\text{O}_5$ $[\text{M}+\text{H}]^+$ 403.1664; observed 403.1658.

Diisopropyl 1-(2-(3-bromobenzoyl)phenyl)hydrazine-1,2-dicarboxylate 141b

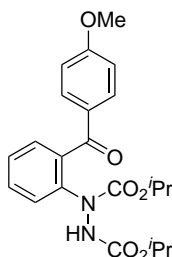
Purification by column chromatography (10%-50% EtOAc/Petrol) afforded diisopropyl 1-(2-(3-bromobenzoyl)phenyl)hydrazine-1,2-dicarboxylate as a clear oil (183 mg, 395 μmol , 79%). ^1H NMR (600 MHz, CDCl_3) δ 8.08-7.09 (m, 8H), 7.08-6.65 (m, NH, 1H), 5.06-4.77 (m, 2H), 3.96-3.93 (m, 3H), 1.31-0.94 (m, 12H); ^{13}C NMR (150 MHz, CDCl_3) δ 195.0 (C), 194.6 (C), 156.2 (C), 155.8 (C), 154.9 (C), 154.5 (C), 142.0 (C), 141.1 (C), 139.1 (C), 136.4 (CH), 136.1 (CH), 134.8 (CH), 133.3 (CH), 132.7 (CH), 130.1 (CH), 128.9 (CH), 128.7 (CH), 127.7 (CH), 127.4 (CH), 126.1 (C), 122.8 (C), 71.3 (CH), 71.0 (CH), 70.1 (CH), 22.2 (CH_3), 22.1 (CH_3), 22.0 (CH_3), 21.8 (CH_3); IR (thin film) 3312, 2980, 2880, 1715, 1660, 1622, 1595, 1575 cm^{-1} ; LRMS (ESI) 487 (30, $[\text{M}^{81}\text{Br}+\text{Na}]^+$), 485 (31, $[\text{M}^{79}\text{Br}+\text{Na}]^+$), 465 (100, $[\text{M}^{79}\text{Br}+\text{H}]^+$), 463 (98, $[\text{M}^{79}\text{Br}+\text{H}]^+$); HRMS (ESI) calcd for $\text{C}_{21}\text{H}_{24}\text{BrN}_2\text{O}_5$ $[\text{M}^{79}\text{Br}+\text{H}]^+$ 463.0863; observed 463.0858.

Diisopropyl 1-(2-(4-(trifluoromethyl)benzoyl)phenyl)hydrazine-1,2-dicarboxylate 141c

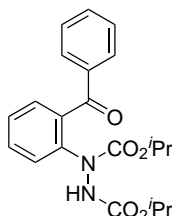
Purification by column chromatography (10%-50% EtOAc/Petrol) afforded diisopropyl 1-(2-(4-(trifluoromethyl)benzoyl)phenyl)hydrazine-1,2-dicarboxylate as a clear oil (161 mg, 355 μmol , 71%). ^1H NMR (600 MHz, CDCl_3) δ 7.94-7.85 (m, 2H), 7.83-7.63 (m, 3H), 7.62-7.57 (m, 1H), 7.42-7.34 (m, 2H), 7.09-6.84 (m, NH, 1H), 5.03-4.94 (m, 1H), 4.85-4.75 (m, 1H), 1.30-1.23 (m, 6H), 1.18-0.92 (m, 6H); ^{13}C NMR (150 MHz, CDCl_3) δ 195.4 (C), 194.9 (C), 155.9 (C), 154.9 (C), 141.1 (C), 140.2 (C), 134.7 (C), 132.9 (CH), 130.6 (CH), 130.0 (CH), 129.9 (CH), 129.2 (CH), 128.7 (CH), 127.7 (CH), 127.4 (CH), 125.6 (CH), 123.7 (q, $J_{\text{C-F}} = 272.2$ Hz, C), 119.0 (CH), 71.3 (CH), 71.0 (CH), 70.1 (CH), 22.1 (CH_3), 21.9 (CH_3); IR (thin film) 3323, 2921, 2834, 1711, 1666, 1622, 1599, 1574 cm^{-1} ; LRMS (ESI) 453 (100, $[\text{M}+\text{H}]^+$); HRMS (ESI) calcd for $\text{C}_{22}\text{H}_{24}\text{F}_3\text{N}_2\text{O}_5$ $[\text{M}+\text{H}]^+$ 453.1632; observed 453.1630.

Diisopropyl 1-(2-(2-methylbenzoyl)phenyl)hydrazine-1,2-dicarboxylate 141d

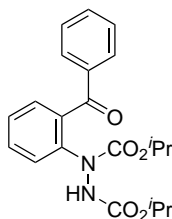
Purification by column chromatography (10%-50% EtOAc/Petrol) afforded diisopropyl 1-(2-(2-methylbenzoyl)phenyl)hydrazine-1,2-dicarboxylate as a clear oil (104 mg, 260 μmol , 52%). ^1H NMR (600 MHz, CDCl_3) δ 7.79-7.19 (m, 9H), 5.14-4.77 (m, 2H), 2.55-2.33 (m, 3H), 1.33-1.01 (m, 12H); ^{13}C NMR (150 MHz, CDCl_3) δ 198.8 (C), 198.3 (C), 156.0 (C), 155.8 (C), 155.1 (C), 154.7 (C), 140.9 (C), 140.9 (C), 138.9 (C), 138.3 (CH), 138.1 (CH), 137.6 (C), 136.2 (CH), 135.6 (CH), 133.0 (CH), 131.4 (CH), 130.6 (CH), 128.0 (CH), 125.5 (CH), 125.3 (CH), 109.2 (C), 71.1 (CH), 70.8 (CH), 69.9 (CH), 69.7 (CH), 24.0 (CH_3), 22.1 (CH_3), 21.9 (CH_3), 20.7 (CH_3), 20.5 (CH_3); IR (thin film) 3314, 2924, 2830, 1710, 1656, 1621, 1599, 1573 cm^{-1} ; LRMS (ESI) 421 (20, $[\text{M}+\text{Na}]^+$), 399 (100, $[\text{M}+\text{H}]^+$); HRMS (ESI) calcd for $\text{C}_{22}\text{H}_{27}\text{N}_2\text{O}_5$ $[\text{M}+\text{H}]^+$ 399.1914; observed 399.1910.

Diisopropyl 1-(2-(4-methoxybenzoyl)phenyl)hydrazine-1,2-dicarboxylate 141e

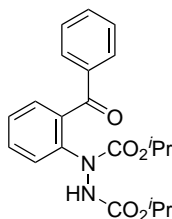
Purification by column chromatography (10%-50% EtOAc/Petrol) afforded diisopropyl 1-(2-(4-methoxybenzoyl)phenyl)hydrazine-1,2-dicarboxylate as a pale brown oil (151 mg, 365 μmol , 73%). ^1H NMR (700 MHz, CDCl_3) δ 7.77-7.57 (m, 3H), 7.57 (t, $J = 7.5$ Hz, 1H), 7.41-7.35 (m, 2H), 7.17-7.04 (m, 1H, NH), 6.92 (d, $J = 8.6$ Hz, 1H), 5.02-4.93 (m, 1H), 4.90-4.75 (m, 1H), 3.87-3.82 (m, 3H), 1.31-1.20 (m, 6H), 1.16-0.90 (m, 6H); ^{13}C NMR (175 MHz, CDCl_3) δ 195.4 (C), 194.7 (C), 164.0 (C), 163.9 (C), 163.1 (C), 156.0 (C), 156.1 (C), 155.7 (C), 155.0 (C), 154.6 (C), 140.8 (C), 136.3 (C), 132.9 (C), 131.9 (CH), 131.1 (CH), 131.1 (CH), 129.8 (CH), 129.6 (CH), 128.9 (CH), 127.6 (CH), 127.4 (CH), 120.8 (CH), 113.8 (CH), 113.5 (CH), 72.6 (CH), 72.3 (CH), 70.7 (CH), 70.6 (CH), 69.9 (CH), 55.7 (CH_3), 55.6 (CH_3), 55.6 (CH_3), 22.1 (CH_3), 22.1 (CH_3), 22.0 (CH_3), 21.7 (CH_3), 21.6 (CH_3); IR (thin film) 3302, 2981, 2937, 2842, 1717, 1652, 1597, 1577 cm^{-1} ; LRMS (ESI) 437 (30, $[\text{M}+\text{Na}]^+$), 415 (100, $[\text{M}+\text{H}]^+$); HRMS (ESI) calcd for $\text{C}_{22}\text{H}_{27}\text{N}_2\text{O}_6$ $[\text{M}+\text{H}]^+$ 415.1864; observed 415.1862.

Diisopropyl 1-(2-benzoylphenyl)hydrazine-1,2-dicarboxylate 141f

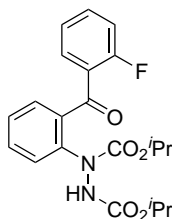
Purification by column chromatography (10%-50% EtOAc/Petrol) afforded diisopropyl 1-(2-benzoylphenyl)hydrazine-1,2-dicarboxylate as a pale brown oil (161 mg, 420 μmol , 84%). ^1H NMR (700 MHz, CDCl_3) δ 7.83-7.81 (m, 2H), 7.80-7.49 (m, 5H), 7.46-7.35 (m, 4H), 7.10-6.87 (m, 1H, NH), 5.06-4.92 (m, 1H), 4.92-4.76 (m, 1H), 1.32-1.22 (m, 6H), 1.18-0.92 (m, 6H); ^{13}C NMR (175 MHz, CDCl_3) δ 196.7 (C), 196.1 (C), 156.1 (C), 155.8 (C), 154.9 (C), 154.5 (C), 153.0 (C), 141.0 (C), 137.3 (C), 137.1 (C), 135.6 (C), 133.6 (CH), 133.2 (C), 132.3 (CH), 132.0 (CH), 130.4 (CH), 130.3 (CH), 129.7 (CH), 129.5 (CH), 128.5 (CH), 128.3 (CH), 127.6 (CH), 127.4 (CH), 120.8 (CH), 72.6 (CH), 71.2 (CH), 70.8 (CH), 70.0 (CH), 69.9 (CH), 22.1 (CH_3), 22.1 (CH_3), 22.0 (CH_3), 21.7 (CH_3), 21.5 (CH_3); IR (thin film) 3301, 2981, 2937, 1883, 1716, 1659, 1598, 1579 cm^{-1} ; LRMS (ESI) 385 (100, $[\text{M}+\text{H}]^+$); HRMS (ESI) calcd for $\text{C}_{21}\text{H}_{25}\text{N}_2\text{O}_5$ $[\text{M}+\text{H}]^+$ 385.1758; observed 385.1755.

Diisopropyl 1-(2-(4-iodobenzoyl)phenyl)hydrazine-1,2-dicarboxylate 141g

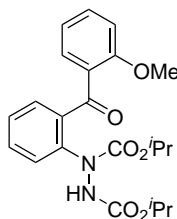
Purification by column chromatography (10%-50% EtOAc/Petrol) afforded diisopropyl 1-(2-(4-iodobenzoyl)phenyl)hydrazine-1,2-dicarboxylate as a clear oil (189 mg, 370 μmol , 74%). ^1H NMR (600 MHz, CDCl_3) δ 7.88-7.73 (m, 2H), 7.58 (t, J = 7.2 Hz, 1H), 7.55-7.29 (m, 4H), 7.25-6.94 (m, 1H), 5.04-4.79 (m, 2H), 1.29-0.94 (m, 12H); ^{13}C NMR (150 MHz, CDCl_3) δ 195.9 (C), 195.3 (C), 155.9 (C), 154.9 (C), 152.2 (C), 150.1 (C), 141.1 (C), 137.9 (CH), 136.5 (C), 135.1 (CH), 132.6 (CH), 131.7 (CH), 129.9 (CH), 128.7 (CH), 127.7 (CH), 127.4 (CH), 120.8 (CH), 101.3 (C), 71.2 (CH), 71.1 (CH), 70.2 (CH), 70.1 (CH), 22.8 (CH_3), 21.1 (CH_3), 22.0 (CH_3) 21.9 (CH_3); IR (thin film) 3314, 2919, 2835, 1709, 1666, 1620, 1599 cm^{-1} ; LRMS (ESI) 511 (100, $[\text{M}+\text{H}]^+$); HRMS (ESI) calcd for $\text{C}_{21}\text{H}_{24}\text{IN}_2\text{O}_5$ $[\text{M}+\text{H}]^+$ 511.0724; observed 511.0719.

Diisopropyl 1-(2-(4-(methoxycarbonyl)benzoyl)phenyl)hydrazine-1,2-dicarboxylate 141h

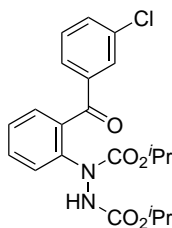
Purification by column chromatography (10%-50% EtOAc/Petrol) afforded diisopropyl 1-(2-(4-(methoxycarbonyl)benzoyl)phenyl)hydrazine-1,2-dicarboxylate as a clear oil (150 mg, 340 μmol , 68%). ^1H NMR (600 MHz, CDCl_3) δ 8.11 (d, $J = 8.3, 1.5$ Hz, 2H), 7.98-7.65 (m, 3H), 7.59 (td, $J = 7.9, 2.0$ Hz, 1H), 7.53-7.27 (m, 2H), 7.09-6.62 (m, NH, 1H), 5.03-4.76 (m, 2H), 3.96-3.93 (m, 3H), 1.31-0.94 (m, 12H); ^{13}C NMR (150 MHz, CDCl_3) δ 195.9 (C), 195.4 (C), 168.6 (C), 166.2 (C), 155.9 (C), 154.7 (C), 151.4 (C), 141.1 (C), 140.9 (C), 140.5 (C), 138.8 (C), 134.9 (C), 134.2 (CH), 133.9 (CH), 133.1 (CH), 132.8 (CH), 130.1 (CH), 129.7 (CH), 129.6 (CH), 128.0 (CH), 127.7 (CH), 127.4 (CH), 120.8 (CH), 73.5 (CH), 71.0 (CH), 70.1 (CH), 52.6 (CH_3), 52.6 (CH_3), 22.1 (CH_3), 21.8 (CH_3), 21.4 (CH_3); IR (thin film) 3302, 2910, 2836, 1723, 1660, 1620, 1602, 1570 cm^{-1} ; LRMS (ESI) 465 (25, $[\text{M}+\text{Na}]^+$), 443 (100, $[\text{M}+\text{H}]^+$); HRMS (ESI) calcd for $\text{C}_{23}\text{H}_{27}\text{N}_2\text{O}_7$ $[\text{M}+\text{H}]^+$ 443.1813; observed 443.1809.

Diisopropyl 1-(2-(2-fluorobenzoyl)phenyl)hydrazine-1,2-dicarboxylate 141j

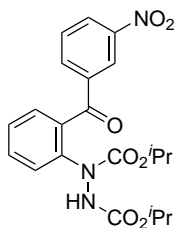
Purification by column chromatography (10%-50% EtOAc/Petrol) afforded diisopropyl 1-(2-(2-fluorobenzoyl)phenyl)hydrazine-1,2-dicarboxylate as a clear oil (141 mg, 350 μmol , 70%). ^1H NMR (600 MHz, CDCl_3) δ 7.85-7.13 (m, 8H), 5.02-4.83 (m, 2H), 1.28-1.03 (m, 12H); ^{13}C NMR (150 MHz, CDCl_3) δ 193.4 (C), 193.0 (C), 166.2 (C), 166.2 (C), 160.9 (d, $J = 253.2$ Hz, C), 159.1 (d, $J_{\text{C-F}} = 253.2$ Hz, C), 156.1 (C), 155.8 (C), 155.2 (C), 155.0 (C), 154.6 (C), 140.6 (C), 135.4 (C), 140.6 (C), 135.4 (CH), 134.6 (CH), 133.0 (CH), 131.7 (CH), 130.7 (CH), 129.7 (CH), 128.0 (C), 127.8 (C), 126.6 (d, $J_{\text{C-F}} = 10.8$ Hz, CH), 124.5 (CH), 124.3 (CH), 116.7 (d, $J_{\text{C-F}} = 20.8$ Hz, CH), 115.6 (C), 73.5 (CH), 71.0 (CH), 70.1 (CH), 52.6 (CH_3), 52.6 (CH_3), 22.1 (CH_3), 21.8 (CH_3), 21.4 (CH_3); IR (thin film) 3320, 2919, 2835, 1711, 1667, 1620, 1602, 1570 cm^{-1} ; LRMS (ESI) 425 (25, $[\text{M}+\text{Na}]^+$), 403 (100, $[\text{M}+\text{H}]^+$); HRMS (ESI) calcd for $\text{C}_{21}\text{H}_{24}\text{FN}_2\text{O}_5$ $[\text{M}+\text{H}]^+$ 403.1664; observed 403.1661.

Diisopropyl 1-(2-(2-methoxybenzoyl)phenyl)hydrazine-1,2-dicarboxylate 141s

Purification by column chromatography (10%-50% EtOAc/Petrol) afforded diisopropyl 1-(2-(2-methoxybenzoyl)phenyl)hydrazine-1,2-dicarboxylate as a clear oil (99.5 mg, 240 μmol , 48%). ^1H NMR (600 MHz, CDCl_3) δ 7.75-6.76 (m, 8H), 5.03-4.83 (m, 2H), 3.83-3.71 (m, 3H), 1.30-1.03 (m, 12H); ^{13}C NMR (150 MHz, CDCl_3) δ 196.5 (C), 195.9 (C), 168.4 (C), 158.4 (C), 156.1 (C), 155.2 (C), 152.3 (C), 140.6 (C), 133.5 (CH), 133.2 (CH), 132.9 (CH), 132.7 (CH), 132.0 (CH), 131.6 (C), 131.3 (C), 130.9 (CH), 130.3 (CH), 130.2 (CH), 129.6 (CH), 129.0 (CH), 128.5 (C), 127.8 (CH), 125.7 (C), 120.8 (CH), 120.4 (CH), 111.9 (CH), 111.8 (CH), 100.8 (CH), 72.2 (CH), 70.8 (CH), 70.6 (CH), 70.5 (CH), 70.0 (CH), 69.8 (CH), 69.6 (CH), 55.9 (CH_3), 55.8 (CH_3), 55.7 (CH_3), 22.1 (CH_3), 22.0 (CH_3), 21.9 (CH_3), 21.5 (CH_3); IR (thin film) 3300, 2979, 2937, 2912, 2845, 1721, 1650, 1591 cm^{-1} ; LRMS (ESI) 415 (100, $[\text{M}+\text{H}]^+$), 339 (95, $[\text{M}+\text{H}]^+$); HRMS (ESI) calcd for $\text{C}_{22}\text{H}_{27}\text{N}_2\text{O}_6$ $[\text{M}+\text{H}]^+$ 415.1864; observed 415.1863.

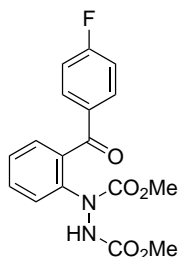
Diisopropyl 1-(2-(3-chlorobenzoyl)phenyl)hydrazine-1,2-dicarboxylate 141t

Purification by column chromatography (10%-50% EtOAc/Petrol) afforded diisopropyl 1-(2-(3-chlorobenzoyl)phenyl)hydrazine-1,2-dicarboxylate as a pale-yellow oil (170 mg, 405 μmol , 81%). ^1H NMR (700 MHz, CDCl_3) δ 8.00-7.11 (m, 8H), 7.10-6.73 (m, 1H, NH), 5.07-4.80 (m, 2H), 1.30-0.94 (m, 12H); ^{13}C NMR (175 MHz, CDCl_3) δ 195.1 (C), 194.7 (C), 156.2 (C), 156.1 (C), 155.9 (C), 154.9 (C), 154.5 (C), 142.0 (C), 141.0 (C), 138.9 (C), 138.7 (C), 134.8 (C), 133.5 (CH), 133.2 (CH), 132.7 (CH), 130.4 (CH), 130.0 (CH), 129.9 (CH), 129.2 (CH), 128.7 (CH), 128.4 (CH), 127.8 (CH), 127.4 (CH), 126.2 (CH), 120.8 (CH), 71.3 (CH), 71.0 (CH), 70.1 (CH), 22.1 (CH_3), 22.1 (CH_3), 22.0 (CH_3), 22.0 (CH_3), 21.8 (CH_3); IR (thin film) 3305, 2985, 2884, 1718, 1658, 1619, 1599, 1580 cm^{-1} ; LRMS (ESI) 443 (8, $[\text{M}^{37}\text{Cl}+\text{Na}]^+$), 441 (25, $[\text{M}^{35}\text{Cl}+\text{Na}]^+$), 421 (30, $[\text{M}^{37}\text{Cl}+\text{H}]^+$), 419 (100, $[\text{M}^{35}\text{Cl}+\text{H}]^+$); HRMS (ESI) calcd for $\text{C}_{21}\text{H}_{24}\text{ClN}_2\text{O}_5$ $[\text{M}^{35}\text{Cl}+\text{H}]^+$ 419.1368; observed 419.1367.

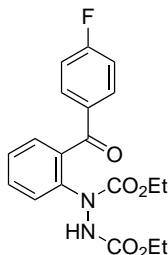
Diisopropyl 1-(2-(3-nitrobenzoyl)phenyl)hydrazine-1,2-dicarboxylate 141u

Purification by column chromatography (10%-50% EtOAc/Petrol) afforded diisopropyl 1-(2-(3-nitrobenzoyl)phenyl)hydrazine-1,2-dicarboxylate as a yellow oil (155 mg, 360 μ mol, 72%). ^1H NMR (600 MHz, CDCl_3) δ 8.70-8.34 (m, 2H), 8.18-7.97 (m, 1H), 7.96-7.28 (m, 4H), 7.12-6.78 (m, NH, 1H), 5.08-4.76 (m, 2H), 3.96-3.93 (m, 3H), 1.31-0.95 (m, 12H); ^{13}C NMR (150 MHz, CDCl_3) δ 195.6 (C), 193.8 (C), 156.5 (C), 156.0 (C), 155.3 (C), 152.5 (C), 148.4 (C), 147.9 (C), 141.1 (C), 138.6 (C), 136.9 (C), 135.8 (C), 133.8 (C), 133.0 (C), 129.7 (CH), 127.9 (CH), 127.4 (CH), 126.2 (CH), 125.0 (CH), 123.2 (CH), 73.2 (CH), 71.1 (CH), 70.2 (CH), 22.1 (CH_3), 22.0 (CH_3), 22.0 (CH_3), 21.6 (CH_3); IR (thin film) 3313, 2914, 2830, 1715, 1664, 1619, 1593, 1574 cm^{-1} ; LRMS (ESI) 452 (30, $[\text{M}+\text{Na}]^+$), 430 (100, $[\text{M}+\text{H}]^+$); HRMS (ESI) calcd for $\text{C}_{21}\text{H}_{24}\text{N}_3\text{O}_7$ $[\text{M}+\text{H}]^+$ 430.1609; observed 430.1606.

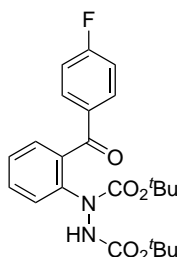
Dimethyl 1-(2-(4-fluorobenzoyl)phenyl)hydrazine-1,2-dicarboxylate 141v



Purification by column chromatography (10%-30% EtOAc/Petrol) afforded dimethyl 1-(2-(4-fluorobenzoyl)phenyl)hydrazine-1,2-dicarboxylate as a brown-orange oil (45.0 mg, 130 μ mol, 26%). ^1H NMR (600 MHz, CDCl_3) δ 7.84-7.82 (m, 2H), 7.63-7.54 (m, 1H), 7.44-7.38 (m, 2H), 7.37-7.33 (m, 1H), 7.12 (t, $J = 7.6$ Hz, 2H), 3.83-3.45 (m, 6H); ^{13}C NMR (150 MHz, CDCl_3) δ 195.5 (C), 194.6 (C), 166.9 (d, $J_{\text{C-F}} = 255.8$ Hz, C), 164.1 (d, $J_{\text{C-F}} = 255.8$ Hz, C), 156.8 (C), 156.3 (C), 156.1 (C), 155.3 (C), 140.6 (C), 135.5 (C), 133.1 (C), 132.8 (CH), 132.5 (CH), 131.5 (d, $J_{\text{C-F}} = 8.6$ Hz, CH), 130.4 (CH), 130.2 (CH), 130.1 (d, $J_{\text{C-F}} = 8.6$ Hz, CH), 129.7 (CH), 129.2 (CH), 128.9 (CH), 127.9 (CH), 127.4 (C), 115.8 (d, $J_{\text{C-F}} = 22.2$ Hz), 115.3 (d, $J_{\text{C-F}} = 21.9$ Hz), 54.0 (CH_3), 53.7 (CH_3), 53.1 (CH_3); IR (thin film) 3308, 3020, 2957, 1722, 1659, 1598 cm^{-1} ; LRMS (ESI) 347 (100, $[\text{M}+\text{H}]^+$); HRMS (ESI) calcd for $\text{C}_{17}\text{H}_{16}\text{FN}_2\text{O}_5$ $[\text{M}+\text{H}]^+$ 347.1038; observed 347.1043.

Diethyl 1-(2-(4-fluorobenzoyl)phenyl)hydrazine-1,2-dicarboxylate 141m

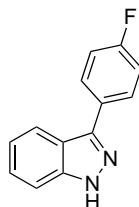
Purification by column chromatography (10%-30% EtOAc/Petrol) afforded diethyl 1-(2-(4-fluorobenzoyl)phenyl)hydrazine-1,2-dicarboxylate as a brown-orange oil (77.0 mg, 210 μ mol, 41%). ¹H NMR (600 MHz, CDCl₃) δ 7.84-7.76 (m, 2H), 7.60-7.55 (m, 1H), 7.44-7.38 (m, 2H), 7.33-7.22 (m, 1H), 7.15-7.05 (m, 2H), 4.26-3.94 (m, 4H), 1.30-0.91 (m, 6H); ¹³C NMR (150 MHz, CDCl₃) δ 195.4 (C), 194.6 (C), 166.0 (d, J_{C-F} = 254.5 Hz, C), 156.4 (C), 156.0 (C), 155.5 (C), 154.9 (C), 153.3 (C), 141.8 (C), 140.8 (C), 135.4 (C), 133.1 (d, J_{C-F} = 8.6 Hz, CH), 132.4 (CH), 131.1 (CH), 131.0 (CH), 130.1 (CH), 129.8 (CH), 127.8 (CH), 127.6 (CH), 115.8 (d, J_{C-F} = 21.8 Hz), 64.2 (CH₂), 63.1 (CH₂), 62.8 (CH₂), 62.4 (CH₂), 62.2 (CH₂), 14.6 (CH₃), 14.5 (CH₃), 14.5 (CH₃), 14.3 (CH₃); IR (thin film) 3310, 3019, 2984, 1720, 1659, 1598 cm⁻¹; LRMS (ESI) 375 (100, [M+H]⁺); HRMS (ESI) calcd for C₁₉H₂₀FN₂O₅ [M+H]⁺ 375.1351; observed 375.1345.

Di-*tert*-butyl 1-(2-(4-fluorobenzoyl)phenyl)hydrazine-1,2-dicarboxylate 141n

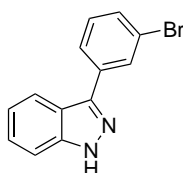
Purification by column chromatography (10%-25% EtOAc/Petrol) afforded di-*tert*-butyl 1-(2-(4-fluorobenzoyl)phenyl)hydrazine-1,2-dicarboxylate as a brown-orange oil (140 mg, 330 μmol , 65%). ^1H NMR (600 MHz, CDCl_3) δ 7.85-7.82 (m, 2H), 7.77-7.72 (m, 1H), 7.56 (td, $J = 7.7, 1.6$ Hz, 1H), 7.43-7.36 (m, 2H), 7.15-7.07 (m, 2H), 6.88-6.75 (br s, NH, 1H), 1.54-1.44 (m, 9H), 1.36-1.20 (m, 9H); ^{13}C NMR (150 MHz, CDCl_3) δ 195.2 (C), 194.2 (C), 165.8 (d, $J_{\text{C-F}} = 254.1$ Hz, C), 155.2 (C), 154.3 (C), 141.2 (C), 140.8 (C), 135.5 (C), 133.4 (C), 133.0 (d, $J_{\text{C-F}} = 9.1$ Hz, CH), 132.2 (CH), 131.9 (CH), 129.5 (CH), 129.2 (CH), 128.5 (CH), 127.3 (CH), 127.1 (CH), 115.6 (d, $J_{\text{C-F}} = 20.4$ Hz), 82.3 (C), 81.3 (C), 28.3 (CH_3), 28.0 (CH_3); IR (thin film) 3307, 2981, 2932, 1716, 1661, 1505 cm^{-1} ; LRMS (ESI) 431 (100, $[\text{M}+\text{H}]^+$); HRMS (ESI) calcd for $\text{C}_{19}\text{H}_{20}\text{FN}_2\text{O}_5$ $[\text{M}+\text{H}]^+$ 431.1977; observed 431.1968.

General experimental for the formation of 1*H*-indazoles

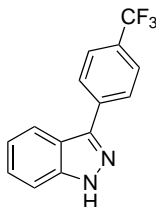
To a stirring solution of 2-hydrazobenzophenone (250 μmol , 1 eq.) in dimethylacetamide (5 mL) was added KOH (56.1 mg, 1.00 mmol, 4 eq.) pre-dissolved in distilled H_2O (3 mL) under an atmosphere of argon. The reaction mixture was stirred at 60 $^\circ\text{C}$ for 16 h and then poured over distilled H_2O (20 mL). The resulting mixture was extracted with EtOAc (3×15 mL). The combined extracts were then dried (MgSO_4), filtered and the solvent removed *in vacuo*. The resultant crude residue was purified as described below.

3-(4-Fluorophenyl)-1*H*-indazole¹⁶⁸ 163a

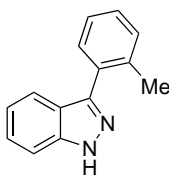
Purification by column chromatography (10%-50% EtOAc/Petrol) afforded 3-(4-fluorophenyl)-1*H*-indazole as a white solid (48.8 mg, 0.230 mmol, 92%). m.p. 116-118 °C; ¹H NMR (600 MHz, CDCl₃) δ 8.01-7.95 (m, 3H), 7.45-7.38 (m, 2H), 7.27 7.21 (m, 3H); ¹³C NMR (150 MHz, CDCl₃) δ 162.9 (d, *J*_{C-F} = 247.5 Hz, C), 145.0 (C), 141.8 (C), 129.8 (d, *J*_{C-F} = 3.3 Hz, C), 129.4 (d, *J*_{C-F} = 8.1 Hz, CH), 127.1 (CH), 121.7 (CH), 121.0 (CH), 121.0 (C), 116.0 (d, *J*_{C-F} = 21.6 Hz, CH), 110.2 (CH); IR (thin film) 3420, 3098, 2918, 2858, 1590 cm⁻¹; LRMS (ESI) 213 (100, [M+H]⁺); HRMS (ESI) calcd for C₁₃H₁₀FN₂ [M+H]⁺ 213.0823; observed 213.0822.

3-(3-Bromophenyl)-1*H*-indazole¹⁶⁹ 163b

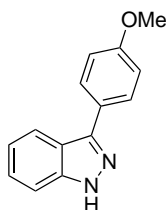
Purification by column chromatography (10%-50% EtOAc/Petrol) afforded 3-(3-bromophenyl)-1*H*-indazole as a white solid (57.4 mg, 0.210 mmol, 84%). m.p. 125-128 °C; ¹H NMR (700 MHz, CDCl₃) δ 10.17 (br s, NH, 1H), 8.15 (s, 1H), 8.02 (d, *J* = 8.2 Hz, 1H), 7.92 (d, *J* = 7.7 Hz, 1H), 7.54 (t, *J* = 8.0 Hz, 2H), 7.45 (t, *J* = 7.6 Hz, 1H), 7.39 (t, *J* = 8.0 Hz, 1H) 7.28 (t, *J* = 7.5 Hz, 1H); ¹³C NMR (175 MHz, CDCl₃) δ 144.5 (C), 141.8 (C), 133.7 (C), 131.2 (CH), 130.5 (CH), 130.5 (CH), 127.2 (CH), 126.1 (CH), 123.1 (C), 122.0 (CH), 121.0 (CH), 121.0 (C), 110.2 (CH); IR (solid) 3120, 2938, 1619 cm⁻¹; LRMS (ESI) 275 (96, [M⁸¹Br+H]⁺) 273 (100, [M⁷⁹Br+H]⁺); HRMS (ESI) calcd for C₁₃H₁₀BrN₂ [M⁷⁹Br+H]⁺ 273.0022; observed 273.0025.

3-(4-(Trifluoromethyl)phenyl)-1*H*-indazole¹⁷⁰ 163c

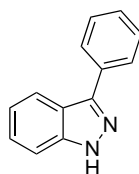
Purification by column chromatography (10%-50% EtOAc/Petrol) afforded 3-(4-(trifluoromethyl)phenyl)-1*H*-indazole as a white solid (54.4 mg, 0.208 mmol, 83%). m.p. 82-84 °C; ¹H NMR (600 MHz, CDCl₃) δ 10.51 (br s, NH, 1H), 8.12 (d, *J* = 8.1 Hz, 2H), 8.03 (d, *J* = 8.2 Hz, 1H), 7.78 (d, *J* = 8.2 Hz, 2H), 7.52 7.48 (m, 1H), 7.47 7.43 (m, 1H), 7.28 (ddd, *J* = 7.8, 6.8, 0.8 Hz, 1H); ¹³C NMR (150 MHz, CDCl₃) δ 144.5 (C), 141.8 (C), 137.2 (C), 130.1 (q, *J*_{C-F} = 32.9 Hz, C), 127.8 (CH), 127.3 (CH), 125.9 (q, *J*_{C-F} = 3.5 Hz, CH), 124.4 (q, *J*_{C-F} = 271.9 Hz, C), 122.1 (CH), 121.1 (C), 120.9 (CH), 110.3 (CH); IR (solid) 3468, 3242, 2943, 1619 cm⁻¹; LRMS (ESI) 263 (100, [M+H]⁺); HRMS (ESI) calcd for C₁₄H₁₀F₃N₂ [M+H]⁺ 263.0791; observed 263.0795.

3-(*o*-Tolyl)-1*H*-indazole¹⁷⁰ 163d

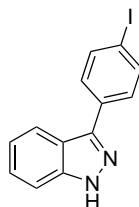
Compound prepared according to general method except reaction temperature was 100 °C. Purification by column chromatography (10%-50% EtOAc/Petrol) afforded 3-(*o*-tolyl)-1*H*-indazole as a white solid (44.3 mg, 0.213 mmol, 85%). m.p. 89-92 °C; ¹H NMR (600 MHz, CDCl₃) δ 10.35 (br s, NH, 1H), 7.67 (d, *J* = 8.1 Hz, 1H), 7.54 (d, *J* = 7.4 Hz, 1H), 7.47 (d, *J* = 8.4 Hz, 1H), 7.41 (t, *J* = 7.6 Hz, 1H), 7.38-7.35 (m, 2H), 7.32 (t, *J* = 7.1 Hz, 1H), 7.19 (t, *J* = 7.4 Hz, 1H); ¹³C NMR (150 MHz, CDCl₃) δ 146.6 (C), 141.0 (C), 137.5 (C), 133.2 (CH), 130.9 (CH), 130.6 (CH), 128.4 (CH), 126.9 (CH), 125.8 (CH), 122.6 (C), 121.4 (C), 121.2 (CH), 110.0 (CH); IR (solid) 3420, 3103, 2949, 1616 cm⁻¹; LRMS (ESI) 209 (100, [M+H]⁺); HRMS (ESI) calcd for C₁₄H₁₃N₂ [M+H]⁺ 209.1073; observed 209.1074.

3-(4-Methoxyphenyl)-1*H*-indazole¹⁵⁴ 163e

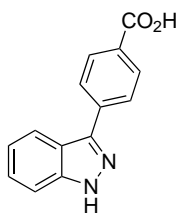
Compound prepared according to general method except reaction temperature was 100 °C. Purification by column chromatography (10%-50% EtOAc/Petrol) afforded 3-(4-methoxyphenyl)-1*H*-indazole as a white solid (44.9 mg, 0.200 mmol, 80%). m.p. 84-86 °C; ¹H NMR (600 MHz, CDCl₃) δ 8.01 (dt, *J* = 8.2, 0.9 Hz, 1H), 7.94-7.91 (m, 2H), 7.45 (dt, *J* = 8.4, 0.9 Hz, 1H), 7.42-7.39 (m, 1H), 7.22 (ddd, *J* = 7.9, 6.7, 1.0 Hz, 1H), 7.07-7.04 (m, 2H), 3.89 (s, 3H); ¹³C NMR (150 MHz, CDCl₃) δ 159.8 (C), 145.7 (C), 141.8 (C), 129.0 (CH), 127.0 (CH), 126.2 (C), 121.4 (CH), 121.4 (CH), 121.0 (C), 114.5 (CH), 110.2 (CH), 55.5 (CH₃) ; IR (solid) 3454, 3163, 2940, 1614 cm⁻¹; LRMS (ESI) 225 (100, [M+H]⁺); HRMS (ESI) calcd for C₁₄H₁₃N₂O [M+H]⁺ 225.1022; observed 225.1024.

3-Phenyl-1*H*-indazole¹⁵⁴ 163f

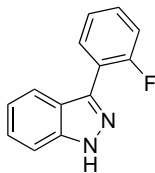
Purification by column chromatography (10%-50% EtOAc/Petrol) afforded 3-phenyl-1*H*-indazole as a white solid (42.7 mg, 0.220 mmol, 88%). m.p. 113-115 °C; ¹H NMR (600 MHz, CDCl₃) δ 8.05 (dt, *J* = 8.2, 0.8 Hz, 1H), 8.01-7.98 (m, 2H), 7.53 (tt, *J* = 7.7, 1.6 Hz, 2H), 7.48 7.45 (m, 1H), 7.45 7.40 (m, 2H), 7.24 (ddd, *J* = 7.9, 6.8, 1.0 Hz, 1H); ¹³C NMR (150 MHz, CDCl₃) δ 146.0 (C), 141.8 (C), 133.6 (C), 129.0 (CH), 128.3 (CH), 127.7 (CH), 127.0 (CH), 121.6 (CH), 121.4 (C), 121.2 (C), 110.2 (CH); IR (solid) 3150, 2935, 1622 cm⁻¹; LRMS (ESI) 195 (100, [M+H]⁺); HRMS (ESI) calcd for C₁₃H₁₁N₂ [M+H]⁺ 195.0917; observed 195.0916.

3-(4-Iodophenyl)-1*H*-indazole 163g

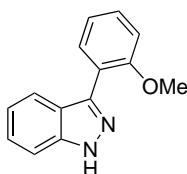
Purification by column chromatography (10%-50% EtOAc/Petrol) afforded 3-(4-iodophenyl)-1*H*-indazole as a white solid (66.4 mg, 0.208 mmol, 83%). m.p. 154-157 °C; ¹H NMR (600 MHz, CDCl₃) δ 10.17 (br s, NH, 1H), 7.99 (d, *J* = 8.2 Hz, 1H), 7.86-7.83 (m, 2H), 7.75-7.71 (m, 2H), 7.52 (d, *J* = 8.4, 1H), 7.45-7.43 (m, 1H), 7.27-7.25 (m, 1H); ¹³C NMR (150 MHz, CDCl₃) δ 145.0 (C), 141.8 (C), 138.1 (CH), 133.2 (C), 129.3 (CH), 128.7 (CH), 127.2 (CH), 121.9 (CH), 121.1 (C), 110.2 (CH), 94.0 (C); 3425, 3179, 2922, 1621 cm⁻¹; LRMS (ESI) 321 (100, [M+H]⁺); HRMS (ESI) calcd for C₁₃H₁₀IN₂ [M+H]⁺ 320.9883; observed 320.9887.

4-(1*H*-Indazol-3-yl)benzoic acid 163h

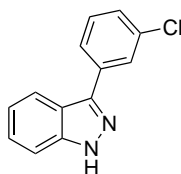
Compound prepared according to general method except that the reaction was poured over HCl (1 M, 20 mL) prior to extraction with EtOAc. Purification by column chromatography (10%-50% EtOAc/Petrol) afforded 4-(1*H*-indazol-3-yl)benzoic acid as a white solid (47.7 mg, 0.200 mmol, 80%). m.p. 196-202 °C; ¹H NMR (600 MHz, DMSO-d₆) δ 13.44 (br s, NH, 1H), 13.00 (br s, CO₂H, 1H), 8.16-8.14 (m, 3H), 8.10-8.07 (m, 2H), 7.63 (dt, *J* = 8.4, 0.8 Hz, 1H), 7.44 (ddd, *J* = 7.6, 6.8, 1.0 Hz, 1H), 7.26 (ddd, *J* = 7.6, 6.8, 1.0 Hz, 1H); ¹³C NMR (150 MHz, DMSO-d₆) δ 167.2 (C), 142.1 (C), 141.7 (C), 138.0 (C), 130.0 (CH), 129.6 (C), 126.6 (CH), 126.3 (CH), 121.5 (CH), 120.6 (C), 120.2 (CH), 110.9 (CH); IR (solid) 3470, 3223, 2970, 2799, 1737, 1565 cm⁻¹; LRMS (ESI) 239 (100, [M+H]⁺); HRMS (ESI) calcd for C₁₄H₁₁N₂O₂ [M+H]⁺ 239.0815; observed 239.0815.

3-(2-fluorophenyl)-1*H*-indazole 163i

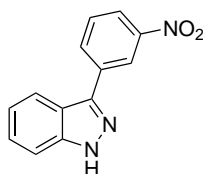
Purification by column chromatography (10%-50% EtOAc/Petrol) afforded 3-(2-fluorophenyl)-1*H*-indazole as a white solid (41.4 mg, 0.195 mmol, 78%). m.p. 114-116 °C; ¹H NMR (600 MHz, CDCl₃) δ 7.88-7.83 (m, 2H), 7.46-7.38 (m, 3H), 7.32-7.26 (m, 2H), 7.24-7.20 (m, 1H); ¹³C NMR (150 MHz, CDCl₃) δ 160.3 (d, J_{C-F} = 249.6 Hz, C), 141.5 (C), 141.3 (C), 131.3 (d, J_{C-F} = 4.1 Hz, CH), 130.2 (d, J_{C-F} = 8.1 Hz, C), 127.1 (CH), 124.6 (d, J_{C-F} = 3.3 Hz, C), 122.0 (C), 121.7 (d, J_{C-F} = 6.2 Hz, C), 121.5 (CH), 121.2 (d, J_{C-F} = 14.3 Hz, C), 116.4 (d, J_{C-F} = 22.0 Hz, C), 110.1 (CH); 3418, 3054, 2926, 2870, 1594 cm⁻¹; LRMS (ESI) 213 (100, [M+H]⁺); HRMS (ESI) calcd for C₁₃H₁₀FN₂ [M+H]⁺ 213.0823; observed 213.0822.

3-(2-Methoxyphenyl)-1*H*-indazole¹⁷⁰ 163j

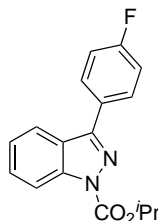
Compound prepared according to general method except reaction temperature was at 100 °C. Purification by column chromatography (10%-50% EtOAc/Petrol) afforded 3-(2-methoxyphenyl)-1*H*-indazole as a white solid (44.3 mg, 0.198 mmol, 79%). m.p. 78-80 °C; ¹H NMR (600 MHz, CDCl₃) δ 7.78 (d, J = 8.2 Hz, 1H), 7.69 (dd, J = 8.2, 1.7 Hz, 1H), 7.45-7.42 (m, 2H), 7.39-7.36 (m, 1H), 7.18-7.15 (m, 1H), 7.13-7.06 (m, 2H); ¹³C NMR (150 MHz, CDCl₃) δ 157.4 (C), 143.5 (C), 131.5 (C), 129.9 (CH), 126.7 (CH), 122.4 (CH), 122.2 (C), 121.0 (CH), 120.9 (CH), 111.5 (CH), 110.4 (CH); IR (solid) 3454, 3163, 2940, 1614 cm⁻¹; LRMS (ESI) 225 (100, [M+H]⁺); HRMS (ESI) calcd for C₁₄H₁₃N₂O [M+H]⁺ 225.1022; observed 225.1022.

3-(3-Chlorophenyl)-1*H*-indazole¹⁷¹ 163k

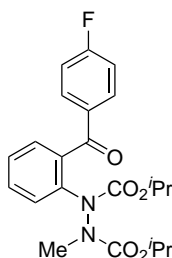
Purification by column chromatography (10%-50% EtOAc/Petrol) afforded 3-(3-chlorophenyl)-1*H*-indazole as a white solid (48.6 mg, 0.213 mmol, 85%). m.p. 136-137 °C; ¹H NMR (600 MHz, CDCl₃) δ 8.02 (dt, *J* = 8.2, 0.9 Hz, 1H), 7.99 (t, *J* = 1.8 Hz, 1H), 7.88 (ddd, *J* = 7.7, 1.5, 1.2 Hz, 1H), 7.52 (dt, *J* = 8.4, 0.9 Hz, 1H), 7.46 7.43 (m, 2H), 7.39 (ddd, *J* = 8.0, 2.1, 1.1 Hz, 1H) 7.29-7.26 (m, 1H); ¹³C NMR (150 MHz, CDCl₃) δ 144.6 (C), 141.8 (C), 133.5 (C), 134.9 (C), 130.2 (CH), 128.3 (CH), 127.7 (CH), 127.6 (CH), 127.2 (CH), 125.7 (CH), 121.9 (CH), 121.0 (C), 110.2 (CH); IR (solid) 3425, 3179, 2922, 1621 cm⁻¹; LRMS (ESI) 231 (30, [M³⁷Cl+H]⁺), 229 (100, [M³⁵Cl+H]⁺); HRMS (ESI) calcd for C₁₃H₁₀ClN₂ [M³⁵Cl+H]⁺ 229.0527; observed 229.0528.

3-(3-Nitrophenyl)-1*H*-indazole¹⁵⁴ 163l

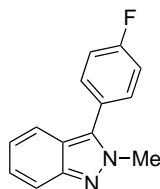
Purification by column chromatography (10%-50% EtOAc/Petrol) afforded 3-(3-nitrophenyl)-1*H*-indazole as a white solid (11.4 mg, 0.0475 mmol, 19%). m.p. 182-185 °C; ¹H NMR (700 MHz, CDCl₃) δ 10.31 (br s, NH, 1H), 8.87 (t, *J* = 1.9 Hz, 1H), 8.35 (ddd, *J* = 7.7, 1.6, 1.1 Hz, 1H), 8.26 (ddd, *J* = 8.2, 2.3, 1.0 Hz, 1H), 8.08-8.06 (m, 1H), 7.71-7.66 (m, 1H), 7.57 (d, *J* = 8.4, 0.9 Hz, 1H), 7.48 (ddd, *J* = 8.4, 6.9, 1.0 Hz, 1H), 7.34-7.30 (m, 1H); ¹³C NMR (175 MHz, CDCl₃) δ 146.0 (C), 143.5 (C), 141.9 (C), 135.5 (C), 133.2, 129.9 (CH), 127.4 (CH), 122.8 (CH), 122.4 (CH), 122.3 (CH), 120.9 (C), 120.7 (CH), 110.4 (CH); IR (solid) 3419, 3120, 2941, 1621 cm⁻¹; LRMS (ESI) 240 (100, [M+H]⁺); HRMS (ESI) calcd for C₁₃H₁₀N₃O₂ [M+H]⁺ 240.0768; observed 240.0768.

Formation of carbamate-protected 1*H*-indazoleIsopropyl 3-(4-fluorophenyl)-1*H*-indazole-1-carboxylate **152**

To a solution of diisopropyl 1-(2-(4-fluorobenzoyl)phenyl)hydrazine-1,2-dicarboxylate **141a** (163 mg, 0.400 mmol) in EtOAc (2.4 mL) was added HCl (3 M, 0.5 mL). The reaction mixture was refluxed for 16 h. The resulting solution was allowed to cool to room temperature before distilled H₂O (15 mL) was added. The organic layer was then extracted with EtOAc (3 × 15 mL), dried (MgSO₄), filtered and the solvent removed *in vacuo*. Purification of the crude residue by column chromatography (10%-40% EtOAc/Petrol) afforded isopropyl 3-(4-fluorophenyl)-1*H*-indazole-1-carboxylate **152** as a clear oil (74.2 mg, 0.260 mmol, 65%). ¹H NMR (600 MHz, CDCl₃) δ 8.27 (d, *J* = 8.4 Hz, 1H), 7.99-7.97 (m, 2H), 7.93 (d, *J* = 8.1 Hz, 1H), 7.59 (ddd, *J* = 8.3, 7.1, 1.0 Hz, 1H), 7.41-7.38 (m, 1H), 7.41-7.21 (m, 2H), 5.40 (septet, *J* = 6.3 Hz, 1H), 1.54 (d, *J* = 6.3 Hz, 6H); ¹³C NMR (150 MHz, CDCl₃) δ 163.6 (d, *J*_{C-F} = 249.2 Hz, C), 150.6 (C), 149.5 (C), 141.3 (C), 130.4 (d, *J*_{C-F} = 8.4 Hz, CH), 129.2 (CH), 128.1 (d, *J*_{C-F} = 3.3 Hz, C), 124.3 (CH), 124.3 (C), 121.3 (CH), 116.1 (d, *J*_{C-F} = 21.8 Hz, C), 115.1 (CH), 72.7 (CH), 22.1 (CH₃); IR (thin film) 3077, 2983, 2937, 1754, 1731, 1608, 1529 cm⁻¹; LRMS (ESI) 597 (60, [2M+H]⁺), 299 (100, [M+H]⁺); HRMS (ESI) calcd for C₁₇H₁₆FN₂O₂ [M+H]⁺ 299.1190; observed 299.1188.

Synthesis of 2*H*-indazolesDiisopropyl 1-(2-(4-fluorobenzoyl)phenyl)-2-methylhydrazine-1,2-dicarboxylate **153**

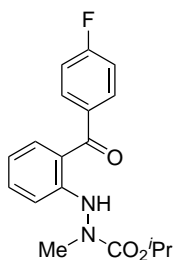
To a solution of diisopropyl 1-(2-(4-fluorobenzoyl)phenyl)hydrazine-1,2-dicarboxylate **141a** (201 mg, 0.500 mmol, 1 eq.) in DMF (20 mL) were added caesium carbonate (179 mg, 0.55 mmol, 1.1 eq.) and iodomethane (34.0 μ L, 0.550 mmol, 1.1 eq.). The heterogeneous mixture was stirred at 21 °C for 24 h. After this time, DMF was removed *in vacuo* with toluene co-evaporation (3 \times 50 mL as an azeotrope). The crude reaction mixture was then dissolved in ethyl acetate (50 mL), and then washed with H₂O (3 \times 15 mL) and sat. aq. LiCl solution (3 \times 15 mL). The organic layer was dried (MgSO₄), filtered and concentrated *in vacuo*. Purification by column chromatography (10%-30% EtOAc/Petrol) afforded diisopropyl 1-(2-(4-fluorobenzoyl)phenyl)-2-methylhydrazine-1,2-dicarboxylate **153** as a clear oil (192 mg, 0.460 mmol, 92%). ¹H NMR (600 MHz, CDCl₃) δ 7.98-7.72 (m, 2H), 7.72 7.35 (m, 2H), 7.34 7.21 (m, 2H), 7.18-7.06 (m, 2H), 5.09-4.98 (m, 1H), 4.86-4.68 (m, 2H), 3.21 (s, 3H), 1.34 1.23 (m, 6H), 1.19-0.63 (m, 6H); ¹³C NMR (150 MHz, CDCl₃) δ 194.1 (C), 193.6 (C), 165.7 (d, J_{C-F} = 253.2 Hz, C), 157.1 (C), 156.4 (C), 153.9 (C), 139.1 (C), 138.7 (C), 134.8 (C), 134.5 (C), 133.4 (CH), 133.2 (CH), 133.1 (d, J_{C-F} = 8.9 Hz, C), 131.6 (CH), 131.5 (CH), 129.1 (CH), 128.7 (C), 125.9 (CH), 125.8 (CH), 125.0 (CH), 115.5 (d, J_{C-F} = 21.8 Hz, CH), 72.4 (CH), 71.5 (CH), 70.9 (CH), 70.4 (CH), 36.6 (CH₃), 35.5 (CH₃), 22.4 (CH₃), 22.3 (CH₃) 22.3 (CH₃), 22.1 (CH₃), 22.1 (CH₃); IR (thin film) 3008, 2957, 1712, 1660, 1597 cm⁻¹; LRMS (ESI) 439 (40, [M+Na]⁺), 417 (100, [M+H]⁺); HRMS (ESI) calcd for C₂₂H₂₆FN₂O₅ [M+H]⁺ 417.1820; observed 417.1817.

3-(4-Fluorophenyl)-2-methyl-2*H*-indazole 143a

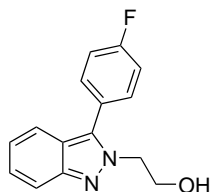
A solution of diisopropyl 1-(2-(4-fluorobenzoyl)phenyl)-2-methylhydrazine-1,2-dicarboxylate **153** (104 mg, 250 μmol) in concentrated HCl (35%, 5 mL) was refluxed for 24 h and then poured over sat. aq. NaHCO_3 (20 mL). The resulting mixture was then extracted with EtOAc (3 \times 15 mL). The combined extracts were dried (MgSO_4), filtered and the solvent evaporated *in vacuo*. Purification by column chromatography (10%-50% EtOAc/Petrol) afforded 3-(4-fluorophenyl)-2-methyl-2*H*-indazole **143a** as a pale yellow oil (94.7 mg, 228 μmol , 91%). ^1H NMR (600 MHz, CDCl_3) δ 7.71 (td, $J = 8.7, 0.9$ Hz, 1H), 7.55-7.49 (m, 3H), 7.31 (ddd, $J = 8.7, 6.6, 1.1$ Hz, 1H), 7.29-7.24 (m, 2H), 7.09 (ddd, $J = 8.4, 6.6, 0.8$ Hz, 1H), 4.16 (s, 3H); ^{13}C NMR (150 MHz, CDCl_3) δ 163.9 (d, $J_{\text{C-F}} = 249.4$ Hz, C), 148.1 (C), 135.1 (C), 131.6 (d, $J_{\text{C-F}} = 8.0$ Hz, CH), 126.5 (CH), 125.9 (d, $J_{\text{C-F}} = 3.3$ Hz, C), 122.1 (CH), 121.4 (CH), 120.0 (CH), 117.2 (CH), 116.4 (d, $J_{\text{C-F}} = 21.8$ Hz, CH), 38.6 (CH_3); IR (thin film) 3087, 2935, 2902, 2858, 1600 cm^{-1} ; LRMS (ESI) 227 (100, $[\text{M}+\text{H}]^+$); HRMS (ESI) calcd for $\text{C}_{14}\text{H}_{12}\text{FN}_2$ $[\text{M}+\text{H}]^+$ 227.0979; observed 227.0980.

Isopropyl 2-(2-(4-fluorobenzoyl)phenyl)-1-methylhydrazine-1-carboxylate

154

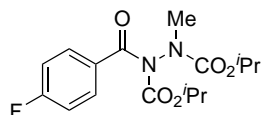


A solution of diisopropyl 1-(2-(4-fluorobenzoyl)phenyl)-2-methylhydrazine-1,2-dicarboxylate **153** (104 mg, 250 μmol) in AcOH (5 mL) was refluxed for 24 h and then poured over sat. aq. NaHCO_3 (20 mL). The resulting mixture was extracted with EtOAc (3×15 mL). The combined extracts were dried (MgSO_4), filtered and the solvent evaporated *in vacuo*. Purification by column chromatography (10%-30% EtOAc/Petrol) afforded isopropyl 2-(2-(4-fluorobenzoyl)phenyl)-1-methylhydrazine-1-carboxylate as a lime-green oil (57.8 mg, 175 μmol , 70%). ^1H NMR (600 MHz, CDCl_3) δ 9.43 (br s, NH, 1H), 7.71-7.66 (m, 2H), 7.49 (dd, $J = 7.9, 1.5$ Hz, 1H), 7.46-7.41 (m, 1H), 7.17-7.12 (m, 2H), 6.88 (d, $J = 8.4$ Hz, 1H), 6.78-6.74 (m, 1H), 4.92-4.90 (m, 1H), 3.27 (s, 3H), 1.28-1.05 (m, 6H); ^{13}C NMR (150 MHz, CDCl_3) δ 197.5 (C), 164.9 (d, $J_{\text{C-F}} = 252.9$ Hz, C), 156.6 (C), 150.9 (C), 135.9 (d, $J_{\text{C-F}} = 3.2$ Hz, C), 134.9 (CH), 134.5 (CH), 132.0 (d, $J_{\text{C-F}} = 8.9$ Hz, CH), 118.9 (C), 117.5 (CH), 115.4 (d, $J_{\text{C-F}} = 21.6$ Hz, CH), 112.3 (CH), 70.0 (CH), 37.7 (CH_3), 22.2 (CH_3); IR (thin film) 3401, 2989, 2946, 1720, 1651, 1580 cm^{-1} ; LRMS (ESI) 331 (100, $[\text{M}+\text{H}]^+$); HRMS (ESI) calcd for $\text{C}_{18}\text{H}_{20}\text{FN}_2\text{O}_3$ $[\text{M}+\text{H}]^+$ 331.1452; observed 331.1457.

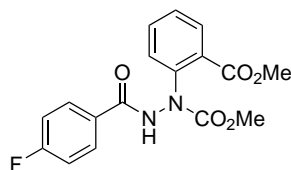
2-(3-(4-Fluorophenyl)-2H-indazol-2-yl)ethan-1-ol 143b

To a solution of diisopropyl 1-(2-(4-fluorobenzoyl)phenyl)hydrazine-1,2-dicarboxylate **141a** (201 mg, 0.500 mmol, 1 eq.) in DMF (20 mL) were added caesium carbonate (179 mg, 0.550 mmol, 1.1 eq.) and 2-bromoethanol (39.0 μ L, 0.550 mmol, 1.1 eq.). The heterogeneous mixture was stirred at 21 °C for 24 h. After this time, DMF was removed in vacuo with toluene co-evaporation (3 \times 50 mL as an azeotrope). The crude reaction mixture was then dissolved in ethyl acetate (50 mL), and then washed with distilled H₂O (3 \times 15 mL) and sat. aq. LiCl solution (3 \times 15 mL). The organic layer was dried (MgSO₄), filtered and concentrated *in vacuo*. To the resultant crude residue was then added concentrated HCl (35%, 5 mL). The reaction mixture was refluxed for 24 h and then poured over sat. aq. NaHCO₃ (20 mL) and the resulting mixture was extracted with EtOAc (3 \times 15 mL). The combined extracts were dried (MgSO₄), filtered and the solvent evaporated *in vacuo*. Purification by column chromatography (10%-70% EtOAc/Petrol) afforded 2-(3-(4-fluorophenyl)-2H-indazol-2-yl)ethan-1-ol **143b** (101 mg, 395 μ mol, 79%) as a pale yellow oil. ¹H NMR (600 MHz, CDCl₃) δ 7.71 (d, J = 8.8 Hz, 1H), 7.56-7.51 (m, 3H), 7.35 (ddd, J = 8.7, 6.6, 1.0 Hz, 1H), 7.29-7.24 (m, 2H), 7.11 (ddd, J = 8.4, 6.6, 0.7 Hz, 1H) 4.49 (dd, J = 5.3, 4.2 Hz, 2H), 4.14-4.11 (m, 2H); ¹³C NMR (150 MHz, CDCl₃) δ 163.2 (d, J_{C-F} = 250.1 Hz, C), 148.3 (C), 135.9 (C), 132.0 (d, J_{C-F} = 8.3 Hz, C), 127.0 (CH), 125.5 (d, J_{C-F} = 3.5 Hz, C), 122.3 (CH), 121.2 (C), 120.2 (CH), 117.2 (C), 116.5 (d, J_{C-F} = 21.8 Hz, CH), 62.0 (CH₂), 52.1 (CH₂); IR (thin film) 3201, 2921, 2905, 2834, 1641, 1569 cm⁻¹. LRMS (ESI) 257 (100, [M+H]⁺).

Mechanistic Study

Diisopropyl 1-(4-fluorobenzoyl)-2-methylhydrazine-1,2-dicarboxylate **155**

To a solution of diisopropyl 1-(4-fluorobenzoyl)hydrazine-1,2-dicarboxylate **87a** (163 mg, 0.500 mmol) and TBAT (594 mg, 0.550 mmol) in toluene (6 mL) was added iodomethane (31.0 μ L, 0.500 mmol) and the reaction mixture stirred at 60 $^{\circ}$ C for 16 h. After this time, to the crude reaction mixture was added distilled H₂O (15 mL). The organic layer was then extracted with EtOAc (3 \times 15 mL), dried (MgSO₄), filtered and the solvent removed *in vacuo*. Purification by column chromatography (10%-40% EtOAc/Petrol) afforded diisopropyl 1-(4-fluorobenzoyl)-2-methylhydrazine-1,2-dicarboxylate **155** as a clear oil (153 mg, 0.450 mmol, 90%). ¹H NMR (600 MHz, CDCl₃) δ 7.71-7.60 (m, 2H), 7.10-7.06 (m, 2H), 4.96-4.89 (m, 2H), 3.25-3.21 (m, 3H), 1.30-1.09 (m, 12H); ¹³C NMR (150 MHz, CDCl₃) δ 169.7 (C), 169.0 (C), 165.0 (d, J_{C-F} = 253.2 Hz, C), 155.4 (C), 155.0 (C), 152.4 (C), 152.3 (C), 131.7 (d, J_{C-F} = 3.3 Hz, CH), 131.4 (d, J_{C-F} = 3.2 Hz, CH), 130.7 (d, J_{C-F} = 9.5 Hz, CH), 130.5 (d, J_{C-F} = 8.9 Hz, CH), 115.5 (d, J_{C-F} = 22.2 Hz, CH), 115.4 (d, J_{C-F} = 22.2 Hz, CH), 72.5 (CH), 72.4 (CH), 71.0 (CH), 71.0 (CH), 70.6 (CH), 70.6 (CH), 37.5 (CH), 36.7 (CH), 22.2 (CH₃), 22.2 (CH₃), 22.1 (CH₃), 21.6 (CH₃); IR (thin film) 2983, 2937, 1744, 1599 cm⁻¹; LRMS (ESI) 341 (100, [M+H]⁺); HRMS (ESI) calcd for C₁₆H₂₂FN₂O₅ [M+H]⁺ 341.1507; observed 341.1503.

By-product formed upon aryl anion attack on carbamate-carbonyl**Methyl 2-(4-fluorobenzoyl)-1-(2-(methoxycarbonyl)phenyl)hydrazine-1-carboxylate 151**

Compound observed upon general method for formation of 2-hydrazobenzophenones using dimethyl 1-(4-fluorobenzoyl)hydrazine-1,2-dicarboxylate **141v** as acyl hydrazide starting material. Purification by column chromatography (10%-30% EtOAc/Petrol) afforded methyl 2-(4-fluorobenzoyl)-1-(2-(methoxycarbonyl)phenyl)hydrazine-1-carboxylate as a brown-orange oil (85.0 mg, 0.250 mmol, 49%). ^1H NMR (600 MHz, CDCl_3) δ 9.25-8.97 (m, NH, 1H), 8.03 (t, $J = 6.2$ Hz, 1H), 7.90-7.81 (m, 3H), 7.67-7.61 (m, 1H), 7.45 (t, $J = 6.6$ Hz, 1H), 7.12 (q, $J = 8.1$ Hz, 2H), 3.97-3.93 (m, 3H), 3.83-3.69 (m, 3H); ^{13}C NMR (150 MHz, CDCl_3) δ 166.9 (C), 166.5 (C), 165.4 (C), 165.3 (d, $J_{\text{C-F}} = 254.5$ Hz, C), 164.6 (C), 156.0 (C), 155.4 (C), 141.1 (C), 140.8 (C), 134.2 (CH), 134.0 (CH), 132.0 (CH), 131.7 (CH), 131.5 (CH), 131.3 (CH), 130.0 (d, $J_{\text{C-F}} = 9.0$ Hz, CH), 129.9 (d, $J_{\text{C-F}} = 9.0$ Hz, CH), 128.8 (CH), 128.5 (C), 126.9 (C), 126.7 (C), 116.0 (d, $J_{\text{C-F}} = 22.0$ Hz), 115.9 (d, $J_{\text{C-F}} = 22.0$ Hz), 54.0 (CH_3), 54.0 (CH_3), 52.8 (CH_3), 52.7 (CH_3); IR (thin film) 3295, 2957, 1718, 1602 cm^{-1} ; LRMS (ESI) 347 (100, $[\text{M}+\text{H}]^+$); HRMS (ESI) calcd for $\text{C}_{17}\text{H}_{16}\text{FN}_2\text{O}_5$ $[\text{M}+\text{H}]^+$ 347.1042; observed 347.1038.

References

- (1) M. Gomberg, *J. Am. Chem. Soc.*, 1900, **22**, 757–771.
- (2) H. Lankamp, W. Nauta and C. MacLean, *Tetrahedron Lett.*, 1968, **9**, 249–254.
- (3) F. Paneth and W. Hofeditz, *Ber.*, 1929, **62**, 1335–1347.
- (4) D. H. Hey, *J. Chem. Soc.*, 1934, 1966–1969.
- (5) M. Julia, *Acc. Chem. Res.*, 1971, **4**, 386–392.
- (6) J. F. Ogilvie, *Spectrosc. Lett.*, 1976, **9**, 203–210.
- (7) P. J. Krusic and P. Meakin, *J. Am. Chem. Soc.*, 1976, **98**, 228–230.
- (8) S. J. Blanksby and G. B. Ellison, *Acc. Chem. Res.*, 2003, **36**, 255–263.
- (9) A. Székely and M. Klussmann, *Chem. - An Asian J.*, 2019, **14**, 105–115.
- (10) T. A. Scott, B. A. Ooro, D. J. Collins, M. Shatruk, A. Yakovenko, K. R. Dunbar and H.-C. Zhou, *Chem. Commun.*, 2009, 65–67.
- (11) R. Çahşkan, N. Nohut, Ö. Yılmaz, E. Sahin and M. Balci, *Tetrahedron*, 2017, **73**, 291–297.
- (12) S. W. Benson, *Can. J. Chem.*, 1983, **61**, 881–887.
- (13) M. J. Gibian and R. C. Corley, *Chem. Rev.*, 1973, **73**, 441–464.
- (14) E. Nakamura, T. Inubushi, S. Aoki and D. Machii, *J. Am. Chem. Soc.*, 1991, **113**, 8980–8982.
- (15) Z. Yang, C. M. Gonzalez, T. K. Purkait, M. Iqbal, A. Meldrum and J. G. C. Veinot, *Langmuir*, 2015, **31**, 10540–10548.
- (16) M. S. Kharasch and F. R. Mayo, *J. Am. Chem. Soc.*, 1933, **55**, 2468–2496.
- (17) C. Walling, *Tetrahedron*, 1985, **41**, 3887–3900.
- (18) N. V. Steere, *J. Chem. Edu.*, 1964, **41**, A445.
- (19) E. Nakamura, D. Machii and T. Inubushi, *J. Am. Chem. Soc.*, 1989, **111**, 6849–6850.
- (20) B. Giese and J. Dupuis, *Tetrahedron Lett.*, 1984, **25**, 1349–1352.
- (21) D. H. R. Barton, *Aldrichimica Acta*, 1990, **23**, 3–10.
- (22) D. P. Curran, *Synthesis*, 1988, 417–437.
- (23) B. Giese, *Angew. Chem., Int. Ed.*, 1985, **24**, 553–565.
- (24) F. Agapito, B. J. Costa Cabral and J. A. Martinho Simões, *J. Mol. Struct. THEOCHEM*, 2005, **719**, 109–114.

- (25) V. Tumanov, *Pet. Chem.*, 2005, **45**, 350–363.
- (26) T. Yoshimitsu, Y. Arano and H. Nagaoka, *J. Org. Chem.*, 2005, **70**, 2342–2345.
- (27) S. Han and S. Z. Zard, *Tetrahedron*, 2016, **72**, 7859–7865.
- (28) S. Kamijo, T. Hoshikawa and M. Inoue, *Org. Lett.*, 2011, **13**, 5928–5931.
- (29) C. Chatgililoglu, D. Crich, M. Komatsu and I. Ryu, *Chem. Rev.*, 1999, **99**, 1991–2070.
- (30) Z. B. Alfassi and D. M. Golden, *J. Am. Chem. Soc.*, 1973, **95**, 319–323.
- (31) R. K. Solly and S. W. Benson, *J. Am. Chem. Soc.*, 1971, **93**, 1592–1595.
- (32) J. T. Niiranen and D. Gutman, *J. Phys. Chem.*, 1992, **96**, 5881–5886.
- (33) Y. Feng, H. Huang, L. Liu and Q. X. Guo, *Phys. Chem. Chem. Phys.*, 2003, **5**, 685–690.
- (34) C. E. Brown, A. G. Neville, D. M. Rayner, K. U. Ingold and J. Lusztyk, *Aust. J. Chem.*, 1995, **48**, 363–379.
- (35) I. Ryu, K. Kusano, A. Ogawa, N. Kambe and N. Sonoda, *J. Am. Chem. Soc.*, 1990, **112**, 1295–1297.
- (36) I. Ryu, M. Hasegawa, A. Kurihara, A. Ogawa, S. Tsunoi and N. Sonoda, *Synlett*, 1993, 143–145.
- (37) V. Gupta and D. Kahne, *Tetrahedron Lett.*, 1992, **34**, 591–594.
- (38) N. Petragnani and H. A. Stefani, *Tetrahedron*, 2005, **61**, 1613–1679.
- (39) J. H. Penn and F. Liu, *J. Org. Chem.*, 1994, **59**, 2608–2612.
- (40) D. L. Boger and R. J. Mathvink, *J. Org. Chem.*, 1988, **53**, 3377–3379.
- (41) D. L. Boger and R. J. Mathvink, *J. Org. Chem.*, 1992, **57**, 1429–1443.
- (42) M. Ballestri, C. Chatgililoglu, N. Cardi and A. Sommazzi, *Tetrahedron Lett.*, 1992, **33**, 1787–1790.
- (43) W. T. Borden, R. Hoffmann, T. Stuyver and B. Chen, *J. Am. Chem. Soc.*, 2017, **139**, 9010–9018.
- (44) C. S. Foote and E. L. Clennan, *Properties and Reactions of Singlet Dioxygen*, 1995, pp. 105–140.
- (45) C. S. Foote, *Acc. Chem. Res.*, 1968, **1**, 104–110.
- (46) D. G. Bradley and D. B. Min, *Crit. Rev. Food Sci. Nutr.*, 1992, **31**, 211–236.
- (47) P. R. Ogilby, *Chem. Soc. Rev.*, 2010, **39**, 3181–3209.
- (48) P. P. Fu, Q. Xia, X. Sun and H. Yu, *J. Environ. Sci. Heal. - Part C Environ. Carcinog. Ecotoxicol. Rev.*, 2012, **30**, 1–41.
- (49) A. Shamsabadi and V. Chudasama, *Org. Biomol. Chem.*, 2019, **17**, 2865–2872.
- (50) A. Sagadevan, K. C. Hwang and M. D. Su, *Nat. Commun.*, 2017, **8**, 1–8.
- (51) J. R. McNesby and C. A. Heller, *Chem. Rev.*, 1954, **54**, 325–346.
- (52) B. A. Arndtsen, R. G. Bergman, T. A. Mobley and T. H. Peterson, *Acc. Chem. Res.*, 1995, **28**, 154–162.
- (53) H. M. Davies and D. Morton, *ACS Cent. Sci.*, 2017, **3**, 936–943.

- (54) K. Godula and D. Sames, *Science*, 2006, **312**, 67–72.
- (55) E. J. E. Caro-Diaz, M. Urbano, D. J. Buzard and R. M. Jones, *Bioorganic Med. Chem. Lett.*, 2016, **26**, 5378–5383.
- (56) M. C. Bryan, P. J. Dunn, D. Entwistle, F. Gallou, S. G. Koenig, J. D. Hayler, M. R. Hickey, S. Hughes, M. E. Kopach, G. Moine, P. Richardson, F. Roschangar, A. Steven and F. J. Weiberth, *Green Chem.*, 2018, **20**, 5082–5103.
- (57) R. Shang, L. Ilies and E. Nakamura, *Chem. Rev.*, 2017, **117**, 9086–9139.
- (58) X. X. Guo, D. W. Gu, Z. Wu and W. Zhang, *Chem. Rev.*, 2015, **115**, 1622–1651.
- (59) M. A. Légaré, M. A. Courtemanche, É. Rochette and F. G. Fontaine, *Science*, 2015, **349**, 513–516.
- (60) M. Usman, X.-W. Zhang, D. Wu, Z.-H. Guan and W.-B. Liu, *Org. Chem. Front.*, 2019, **6**, 1905–1928.
- (61) O. Mitsunobu, M. Yamada and T. Mukaiyama, *Bull. Chem. Soc. Jpn.*, 1967, **40**, 935–939.
- (62) W. Y. Yu, N. S. Wing, K. M. Lai, Z. Zhou and A. S. Chan, *J. Am. Chem. Soc.*, 2008, **130**, 3304–3306.
- (63) Y. Huang, G. Li, J. Huang and J. You, *Org. Chem. Front.*, 2014, **1**, 347–350.
- (64) N. Xu, D. Li, Y. Zhang and L. Wang, *Org. Biomol. Chem.*, 2015, **13**, 9083–9092.
- (65) G. R. Morais and R. A. Falconer, *Tetrahedron Lett.*, 2007, **48**, 7637–7641.
- (66) H. T. Cao and R. Grée, *Tetrahedron Lett.*, 2009, **50**, 1493–1494.
- (67) F. D. Marsh and M. E. Hermes, *J. Am. Chem. Soc.*, 1965, **87**, 1819–1820.
- (68) M. S. Goh, L. Rintoul, M. C. Pfrunder, J. C. McMurtrie and D. P. Arnold, *J. Mol. Struct.*, 2015, **1098**, 298–305.
- (69) B. Han, X.-L. Yang, R. Fang, W. Yu, C. Wang, X.-Y. Duan and S. Liu, *Angew. Chem., Int. Ed.*, 2012, **51**, 8816–8820.
- (70) X.-Y. Duan, X.-L. Yang, R. Fang, X.-X. Peng, W. Yu and B. Han, *J. Org. Chem.*, 2013, **78**, 10692–10704.
- (71) R. Guo, K.-N. Li, B. Liu, H.-J. Zhu, Y.-M. Fan and L.-Z. Gong, *Chem. Commun.*, 2014, **50**, 5451–5454.
- (72) J. Nan, J. Liu, H. Zheng, Z. Zuo, L. Hou, H. Hu, Y. Wang and X. Luan, *Angew. Chem., Int. Ed.*, 2015, **54**, 2356–2360.
- (73) Q.-Z. Li, X.-H. Wang, S.-H. Hou, Y.-Y. Ma, D.-G. Zhao, S.-Y. Zhang, H.-Y. Bai and T.-M. Ding, *Synthesis*, 2019, **51**, 2697–2704.
- (74) D. Wang, W. Liu, M. Tang, N. Yu and X. Yang, *iScience*, 2019, **22**, 195–205.
- (75) L. A. Trimble and J. C. Vederas, *J. Am. Chem. Soc.*, 1986, **108**, 6397–6399.
- (76) B. List, *J. Am. Chem. Soc.*, 2002, **124**, 5656–5657.
- (77) R. J. Fitzmaurice, J. M. Ahern and S. Caddick, *Org. Biomol. Chem.*, 2009, **7**, 235–237.
- (78) V. Chudasama, R. J. Fitzmaurice, J. M. Ahern and S. Caddick, *Chem. Commun.*, 2010, **46**, 133–135.
- (79) V. Chudasama, R. J. Fitzmaurice and S. Caddick, *Nat. Chem.*, 2010, **2**, 592–596.

- (80) V. Chudasama, J. M. Ahern, R. J. Fitzmaurice and S. Caddick, *Tetrahedron Lett.*, 2011, **52**, 1067–1069.
- (81) V. Chudasama, J. M. Ahern, D. V. Dhokia, R. J. Fitzmaurice and S. Caddick, *Chem. Commun.*, 2011, **47**, 3269–3271.
- (82) V. Chudasama, A. R. Akhbar, K. A. Bahou, R. J. Fitzmaurice and S. Caddick, *Org. Biomol. Chem.*, 2013, **11**, 7301–7317.
- (83) R. K. Dieter, *Tetrahedron*, 1999, **55**, 4177–4236.
- (84) S. Balasubramaniam and I. S. Aidhen, *Synthesis*, 2008, 3707–3738.
- (85) A. R. Akhbar, V. Chudasama, R. J. Fitzmaurice, L. Powell and S. Caddick, *Chem. Commun.*, 2014, **50**, 743–746.
- (86) A. Maruani, M. T. W. Lee, G. Watkins, A. R. Akhbar, H. Baggs, A. Shamsabadi, D. A. Richards and V. Chudasama, *RSC Adv.*, 2016, **6**, 3372–3376.
- (87) G. N. Papadopoulos and C. G. Kokotos, *Chem. Eur. J.*, 2016, **22**, 6964–6967.
- (88) G. N. Papadopoulos, D. Limnios and C. G. Kokotos, *Chem. Eur. J.*, 2014, **20**, 13811–13814.
- (89) Y. J. Kim and D. Lee, *Org. Lett.*, 2004, **6**, 4351–4353.
- (90) A. V. Kalinin, É. T. Apasov, S. V. Bugaeva, S. L. Ioffe and V. A. Tartakovskii, *Bull. Acad. Sci. USSR, Div. Chem. Sci. (English Transl.)*, 1983, **32**, 1282–1284.
- (91) E. Vitaku, D. T. Smith and J. T. Njardarson, *J. Med. Chem.*, 2014, **57**, 10257–10274.
- (92) D. Hazelard, P. A. Nocquet and P. Compain, *Org. Chem. Front.*, 2017, **4**, 2500–2521.
- (93) R. Dorel, C. P. Grugel and A. M. Haydl, *Angew. Chem., Int. Ed.*, 2019, **58**, 17118–17129.
- (94) C. Sambigioglio, D. Schönbauer, R. Blicke, T. Dao-Huy, G. Pototschnig, P. Schaaf, T. Wiesinger, M. F. Zia, J. Wencel-Delord, T. Besset, B. U. Maes and M. Schnürch, *Chem. Soc. Rev.*, 2018, **47**, 6603–6743.
- (95) M. Zhang, Y. Zhang, X. Jie, H. Zhao, G. Li and W. Su, *Org. Chem. Front.*, 2014, **1**, 843–895.
- (96) J. C. Chu and T. Rovis, *Angew. Chem., Int. Ed.*, 2018, **57**, 62–101.
- (97) D. Mu, X. Wang, G. Chen and G. He, *J. Org. Chem.*, 2017, **82**, 4497–4503.
- (98) J. Peng, Z. Xie, M. Chen, J. Wang and Q. Zhu, *Org. Lett.*, 2014, **16**, 4702–4705.
- (99) R. Giri, B.-F. Shi, K. M. Engle, N. Maugel and J.-Q. Yu, *Chem. Soc. Rev.*, 2009, **38**, 3242–3272.
- (100) D. Basu, S. Kumar, S. Sudhir and R. Bandichhor, *J. Chem. Sci.*, 2018, **130**, DOI: 10.1007/s12039-018-1468-6.
- (101) A. Shamsabadi and V. Chudasama, *Org. Biomol. Chem.*, 2017, **15**, 17–33.
- (102) R. Askani, *Chem. Ber.*, 1965, **98**, 2551–2555.
- (103) Y. Amaoka, S. Kamijo, T. Hoshikawa and M. Inoue, *J. Org. Chem.*, 2012, **77**, 9959–9969.

- (104) I. Colomer, A. E. Chamberlain, M. B. Haughey and T. J. Donohoe, *Nat. Rev. Chem.*, 2017, **1**, 1–12.
- (105) M. H. Abraham, P. L. Grellier, D. V. Prior, P. P. Duce, J. J. Morris and P. J. Taylor, *J. Chem. Soc., Perkin Trans. 2*, 1989, 699–711.
- (106) G. Ahlgren, *Tetrahedron Lett.*, 1974, **15**, 2779–2782.
- (107) M. J. Kamlet, J. L. M. Abboud, M. H. Abraham and R. W. Taft, *J. Org. Chem.*, 1983, **48**, 2877–2887.
- (108) H. Matsubara, S. Suzuki and S. Hirano, *Org. Biomol. Chem.*, 2015, **13**, 4686–4692.
- (109) H. K. Aldridge, X. Liu, M. C. Lin and C. F. Melius, *Int. J. Chem. Kinet.*, 1991, **23**, 947–956.
- (110) <http://supramolecular.org>.
- (111) D. Brynn Hibbert and P. Thordarson, *Chem. Commun.*, 2016, **52**, 12792–12805.
- (112) A. Shamsabadi, J. Ren and V. Chudasama, *RSC Adv.*, 2017, **7**, 27608–27611.
- (113) J. A. Howard and S. Korcek, *Can. J. Chem.*, 1971, **49**, 2178–2182.
- (114) V. K. Thulam, S. C. B. Kotte, H. Sanjay Kumar, P. M. Murali, K. Mukkanti and P. S. Mainker, *J. Pharm. Res.*, 2013, **7**, 195–199.
- (115) J. Fraser, P. G. Clinch and R. C. Reay, *J. Sci. Food. Agr.*, 1965, **16**, 615–618.
- (116) C. Davidovich, A. Bashan, T. Auerbach-Nevo, R. D. Yaggie, R. R. Gontarek and A. Yonath, *Proc. Natl. Acad. Sci. U. S. A.*, 2007, **104**, 4291–4296.
- (117) A. H. Kahns and H. Bundgaard, *Int. J. Pharm.*, 1991, **71**, 31–43.
- (118) S. Shaw-Ponter, G. Mills, M. Robertson, R. D. Bostwick, G. W. Hardy and R. J. Young, *Tetrahedron Lett.*, 1996, **37**, 1867–1870.
- (119) R. J. Young, S. Shaw-Ponter, G. W. Hardy and G. Mills, *Tetrahedron Lett.*, 1994, **35**, 8687–8690.
- (120) P. Bourbon, Q. Peng, G. Ferraudi, C. Stauffacher, O. Wiest and P. Helquist, *Bioorganic Med. Chem. Lett.*, 2013, **23**, 6321–6324.
- (121) P. Sinha, C. C. Kofink and P. Knochel, *Org. Lett.*, 2006, **8**, 3741–3744.
- (122) A. Bach, N. Stuhr-Hansen, T. S. Thorsen, N. Bork, I. S. Moreira, K. Frydenvang, S. Padrah, S. B. Christensen, K. L. Madsen, H. Weinstein, U. Gether and K. Strømgaard, *Org. Biomol. Chem.*, 2010, **8**, 4281–4288.
- (123) K. Li, X. Cheng and K. K. Hii, *European J. Org. Chem.*, 2004, 959–964.
- (124) P. A. Jacobi and M. J. Martinelli, *J. Am. Chem. Soc.*, 1984, **106**, 5594–5598.
- (125) M. A. Brimble and C. H. Heathcock, *J. Org. Chem.*, 1993, **58**, 5261–5263.
- (126) H. Ding and G. K. Friestad, *Org. Lett.*, 2004, **6**, 637–640.
- (127) P. Magnus, N. Garizi, K. A. Seibert and A. Ornholt, *Org. Lett.*, 2009, **11**, 5646–5648.
- (128) P. Magnus and A. J. Brozell, *Org. Lett.*, 2012, **14**, 3952–3954.
- (129) I. Denya, S. F. Malan and J. Joubert, *Expert Opin. Ther. Pat.*, 2018, **28**, 441–453.

- (130) A. Guglielmotti, A. C. de Joannon, N. Cazzolla, M. Marchetti, L. Soldo, G. Cavallo and M. Pinza, *Pharmacol. Res.*, 1995, **32**, 369–373.
- (131) M. J. Clarke, *Coord. Chem. Rev.*, 2003, **236**, 209–233.
- (132) A. Shrivastava, A. K. Chakraborty, N. Upmanyu and Singh A., *Austin J. Anal. Pharm. Chem.*, 2016, **3**, 1–23.
- (133) J.-H. Sun, C. A. Teleha, J.-S. Yan, J. D. Rodgers and D. A. Nugiel, *J. Org. Chem.*, 1997, **62**, 5627–5629.
- (134) K. W. Woods, J. P. Fischer, A. Claiborne, T. Li, S. A. Thomas, G.-D. Zhu, R. B. Diebold, X. Liu, Y. Shi, V. Klinghofer, E. K. Han, R. Guan, S. R. Magnone, E. F. Johnson, J. J. Bouska, A. M. Olson, R. de Jong, T. Oltersdorf, Y. Luo, S. H. Rosenberg, V. L. Giranda and Q. Li, *Bioorganic Med. Chem.*, 2006, **14**, 6832–6846.
- (135) M. Patel, J. D. Rodgers, R. J. McHugh, B. L. Johnson, B. C. Cordova, R. M. Klabe, L. T. Bacheler, S. Erickson-Viitanen and S. S. Ko, *Bioorganic Med. Chem. Lett.*, 1999, **9**, 3217–3220.
- (136) N. T. Tzvetkov, S. Hinz, P. Küppers, M. Gastreich and C. E. Müller, *J. Med. Chem.*, 2014, **57**, 6679–6703.
- (137) A. Mousnier, A. S. Bell, D. P. Swieboda, J. Morales-Sanfrutos, I. Pérez-Dorado, J. A. Brannigan, J. Newman, M. Ritzefeld, J. A. Hutton, A. Guedán, A. S. Asfor, S. W. Robinson, I. Hopkins-Navratilova, A. J. Wilkinson, S. L. Johnston, R. J. Leatherbarrow, T. J. Tuthill, R. Solari and E. W. Tate, *Nat. Chem.*, 2018, **10**, 599–606.
- (138) E. Robinson, E. Knight, N. Smoktunowicz, R. C. Chambers, G. G. Inglis, V. Chudasama and S. Caddick, *Org. Biomol. Chem.*, 2016, **14**, 3198–3201.
- (139) X. Xiong, Y. Jiang and D. Ma, *Org. Lett.*, 2012, **14**, 2552–2555.
- (140) K. Lukin, M. C. Hsu, D. Fernando and M. R. Leanna, *J. Org. Chem.*, 2006, **71**, 8166–8172.
- (141) C. S. Cho, D. K. Lim, N. H. Heo, T.-J. Kim and S. C. Shim, *Chem. Commun.*, 2004, 104–105.
- (142) Y. Himeshima, T. Sonoda and H. Kobayashi, *Chem. Lett.*, 1983, **12**, 1211–1214.
- (143) F. I. M. Idiris, C. E. Majesté, G. B. Craven and C. R. Jones, *Chem. Sci.*, 2018, **9**, 2873–2878.
- (144) P. M. Tadross and B. M. Stoltz, *Chem. Rev.*, 2012, **112**, 3550–3577.
- (145) J. Shi, Y. Li and Y. Li, *Chem. Soc. Rev.*, 2017, **46**, 1707–1719.
- (146) R. W. Hoffmann and K. Suzuki, *Angew. Chem., Int. Ed.*, 2013, **52**, 2655–2656.
- (147) J.-A. García-López and M. F. Greaney, *Chem. Soc. Rev.*, 2016, **45**, 6766–6798.
- (148) S. S. Bhojgude, A. Bhunia and A. T. Biju, *Acc. Chem. Res.*, 2016, **49**, 1658–1670.
- (149) C. Holden and M. F. Greaney, *Angew. Chem., Int. Ed.*, 2014, **53**, 5746–5749.
- (150) F. I. M. Idiris and C. R. Jones, *Org. Biomol. Chem.*, 2017, **15**, 9044–9056.
- (151) J. Shi, D. Qiu, J. Wang, H. Xu and Y. Li, *J. Am. Chem. Soc.*, 2015, **137**, 5670–5673.
- (152) H. Yoshida and K. Takaki, *Heterocycles*, 2012, **85**, 1333–1349.

- (153) A. V. Dubrovskiy, N. A. Markina and R. C. Larock, *Org. Biomol. Chem.*, 2013, **11**, 191–218.
- (154) P. Li, J. Zhao, C. Wu, R. C. Larock and F. Shi, *Org. Lett.*, 2011, **13**, 3340–3343.
- (155) C. Spiteri, S. Keeling and J. E. Moses, *Org. Lett.*, 2010, **12**, 3368–3371.
- (156) P.-F. Wang, Y.-S. Feng, Z.-F. Cheng, Q.-M. Wu, G.-Y. Wang, L.-L. Liu, J.-J. Dai, J. Xu and H.-J. Xu, *J. Org. Chem.*, 2015, **80**, 9314–9320.
- (157) D. Peña, A. Cobas, D. Pérez and E. Guitián, *Synthesis*, 2002, 1454–1458.
- (158) N. Ahmed, A. Shamsabadi and V. Chudasama, *ACS Omega*, 2019, **4**, 22601–22612.
- (159) S. Cortez-Maya, E. Cortes Cortes, S. Hernández-Ortega, T. R. Apan and M. Martínez-García, *Synth. Commun.*, 2012, **42**, 46–54.
- (160) I. Ryu, A. Tani, T. Fukuyama, D. Ravelli, S. Montanaro and M. Fagnoni, *Org. Lett.*, 2013, **15**, 2554–2557.
- (161) D. Lee and R. D. Otte, *J. Org. Chem.*, 2004, **69**, 3569–3571.
- (162) S. M. Inamdar, V. K. More and S. K. Mandal, *Chem. Lett.*, 2012, **41**, 1484–1486.
- (163) Y. Qin, Q. Peng, J. Song and D. Zhou, *Tetrahedron Lett.*, 2011, **52**, 5880–5883.
- (164) O. Sugimoto, T. Arakaki, H. Kamio and K.-i. Tanji, *Chem. Commun.*, 2014, **50**, 7314–7317.
- (165) A. Mariappan, K. Rajaguru, S. Muthusubramanian and N. Bhuvanesh, *Tetrahedron Lett.*, 2015, **56**, 338–341.
- (166) M. Fetizon, M. Golfier, R. Milcent and I. Papadakis, *Tetrahedron*, 1975, **31**, 165–170.
- (167) B. S. Shaibu, R. K. Kawade and R.-S. Liu, *Org. Biomol. Chem.*, 2012, **10**, 6834–6839.
- (168) C. M. Counciller, C. C. Eichman, B. C. Wray and J. P. Stambuli, *Org. Lett.*, 2008, **10**, 1021–1023.
- (169) H. L. Barlow, P. T. Rabet, A. Durie, T. Evans and M. F. Greaney, *Org. Lett.*, 2019, **21**, 9033–9035.
- (170) W. Youngsaye, C. L. Hartland, B. J. Morgan, A. Ting, P. P. Nag, B. Vincent, C. A. Mosher, J. A. Bittker, S. Dandapani, M. Palmer, L. Whitesell, S. Lindquist, S. L. Schreiber and B. Munoz, *Beilstein J. Org. Chem.*, 2013, **9**, 1501–1507.
- (171) S. Paul, S. Panda and D. Manna, *Tetrahedron Lett.*, 2014, **55**, 2480–2483.